BIREFRINGENT DEVICES

NAS8-20570

Final Report

8 March 1967

E. O. Ammann

J. M. Yarborough

SYLVANIA ELECTRONIC SYSTEMS
Government Systems Management
for GENERAL TELEPHONE & ELECTRONICS

SYLVANIA ELECTRONIC SYSTEMS - WESTERN OPERATION
Post Office Box 205
Mountain View, California 94040

BIREFRINGENT DEVICES

Final Report

NAS8-20570

8 March 1967

Authors:

E. O. Ammann
J. M. Yarborough

APPROVED BY: Dr. D. E. Caddes, Manager
Quantum Electronic Techniques
Department

Prepared for

National Aeronautics and Space Administration
Huntsville, Alabama

FOREWORD

This is the final report prepared under NASA Contract NAS8-20570, "Birefringent Devices". This report describes work performed on a one-year program whose goal was to advance the state of the art of optical birefringent devices. The work described here was performed in the Quantum Electronic Techniques Department of the Advanced Technology Laboratory of Sylvania Electronic Systems - Western Operation in Mountain View, California, during the period 8 March 1966 through 8 March 1967. The project leader was Dr. E. O. Ammann; another principal contributor was Mr. J. M. Yarborough. The experimental phases of the program received expert technical assistance from Mr. E. J. Sleep.

All work on this contract was under the direction of the Astronautics Laboratory at George C. Marshall Space Flight Center, Huntsville, Alabama. Dr. J. L. Randall was the technical representative for this program, and Messrs. C. Wyman and C. Q. Lee were alternate technical representatives. Their guidance on this program is gratefully acknowledged.

ABSTRACT

This report summarizes the results of a one-year program whose goal was to advance the state of the art of optical birefringent devices. Both theory and experiments were performed and are reported.

Theoretical work was performed in several areas. A generalization of the original birefringent network synthesis procedure of Harris, Ammann, and Chang [1] is given which allows the synthesis of networks having asymmetric transmittances. This new procedure increases the versatility of birefringent networks considerably at no expense in network complexity. In addition, a double-pass technique is described which can be used in connection with the new synthesis procedure. This technique reduces by a factor of two the number of network components needed to realize most transmittances. Finally, procedures are given for synthesizing optical amplitude modulators having less distortion than conventional modulators.

Experiments were performed on both single-pass and double-pass naturally birefringent networks. The results of these experiments provide the first direct verification of the single- and double-pass birefringent network synthesis procedures. In addition, distortion measurements were made on one- and three-stage amplitude modulators to verify the calculations mentioned above.

TABLE OF CONTENTS

TABLE OF CONTENTS (Continued)

LIST OF ILLUSTRATIONS

LIST OF ILLUSTRATIONS (Continued)

LIST OF ILLUSTRATIONS (Continued)

I. INTRODUCTION

This report presents the results of a one-year applied research program on optical birefringent devices. The object of this program was to perform theoretical and experimental studies which would advance the state of the art of birefringent devices.

In this report, we use the term "birefringent devices" to denote optical devices consisting of polarizers and birefringent crystals. The birefringence of the crystals can be either natural or electrically-induced. Networks containing naturally-birefringent crystals will be called naturally-birefringent networks, while networks containing electro-optic crystals will be called electro-optic networks. Much of the previous birefringent network theory, in addition to the theory developed on this program, is applicable to both types of network.

A brief resumé of birefringent networks is perhaps appropriate here to put the contributions of the present program into proper perspective. The first birefringent devices used in optical systems were the Lyot and Solc filters. The Lyot filter was discovered in 1933, while the Solc filter followed some 20 years later. Both these devices are narrow-band filters capable of very narrow passbands. In fact, the major attraction of birefringent devices is their capability of producing bandwidths the order of Angstroms or less.

The Lyot and Solc filters are both particular crystal-polarizer configurations giving particular transmission characteristics. Hence the use of birefringent devices to produce other types of characteristics awaited the development of a synthesis procedure. This important development occurred in 1964 when Harris, Ammann, and Chang found two procedures [1,2] for synthesizing birefringent networks whose transmittance could be arbitrarily specified. These procedures opened the possibility of using birefringent networks to realize a variety of devices for optical and laser systems.

Shortly thereafter, Ammann [3,4] found a method for reducing (by a factor of two) the number of network components needed to realize a desired transmittance. The technique involved passage of the light through the birefringent network twice and hence was called a "double-pass" procedure. This discovery was followed closely by the realization [5] that the techniques which had been developed for naturally-birefringent networks could also be applied to electro-optic networks. This opened the way for synthesis of electro-optic shutters, modulators, and so on.

It was with this background that the present program was begun. The object of this program was to further extend the theory of birefringent devices, and in addition, to carry out an experimental program. There were at least three broad goals for the theoretical portion of the work. First, it was desired to find still more general or powerful synthesis techniques in order to increase the versatility and usefulness of birefringent devices. The synthesis procedure of Section II-A and Appendix A is an example of a result which succeeds along these lines. Second, we wished to find modifications of existing procedures or completely new procedures which would result in simplification of the form of the resulting birefringent networks. The goal here, of course, is to obtain the simplest possible practical form for the devices which are obtained. The work of Section II-B and Appendix B is an example of work which has accomplished this goal. Finally, the third goal was to apply the synthesis procedures to particular devices of special importance. The results of Section II-C and Appendix C on the synthesis of amplitude-modulators are typical of this goal.

The experimental portion of the work was expected to yield much valuable information, for although substantial progress had occurred in the past few years in the theory of birefringent devices, experimentation had not kept pace. Hence much work remained to be done in verifying the recently developed theory, and for providing guidance in establishing problem areas for future study. In addition to verifying the theory, the experimental program would also yield some useful devices, of course.

This report is organized in the following manner. Section II gives the theory performed on the program, while Section III reports the experimental results. The conclusions reached and recommendations for future work are given in Section IV. The research contributions resulting from the work of this program are summarized in Section V, while Section VI lists the journal publications and papers presented at conferences. References are listed in Section VII and several appendices are given at the end of the report.

II. THEORY OF BIREFRINGENT NETWORKS

In this section, we discuss the theoretical work which was performed during the program. This work has resulted in several significant advances in the theory of optical birefringent networks. The first of these is a generalization of the earlier procedure of Harris, et al. [1] which allows the synthesis of birefringent networks with asymmetric amplitude-transmittances. This has resulted in an entire new class of birefringent networks with very versatile characteristics. The second accomplishment is the discovery of double-pass procedures which are applicable to this new class of network. These two topics are discussed in greater detail in Parts A and B of this Section, and in Appendices A and B. A third accomplishment concerns the synthesis of electro-optic amplitude modulators. Methods were found for synthesizing amplitude modulators having less distortion than present conventional modulators. These are fully described in Part C of this Section and in Appendix C.

In addition to the above problems which were successfully solved, several additional topics were studied with only limited success. These are mentioned in Parts D and E of this section.

A. SYNTHESIS OF LOSSLESS NETWORKS CONTAINING EQUAL-LENGTH CRYSTALS AND COMPENSATORS

Harris, Ammann, and Chang [1] have given a procedure for synthesizing birefringent networks whose amplitude transmittance could be specified. The work described here is a generalization of that procedure which provides still greater flexibility in the synthesis of birefringent networks. We will not go into the mechanics of the procedure in this section since they are given in Appendix A. Instead we will describe here what can be accomplished with the new procedure.

The procedure of Harris, et al. [1] allows the realization of a birefringent network whose amplitude transmittance $C(\omega)$ is of the form,

$$C(\omega) = C_0 + C_1 e^{-ia\omega} + C_2 e^{-i2a\omega} + \dots + C_n e^{-ina\omega} . \tag{2.1}$$

The number of terms employed in $C(\omega)$ is finite but arbitrary. The choice of the term coefficients (the C_i) is also arbitrary as long as each C_i is real. The form of the network obtained from this synthesis procedure is shown in Figure 1 of Appendix A. The network consists of a series of identical cascaded birefringent crystals between and input and output polarizer. The network may be thought of as composed of several stages, with each stage consisting of one birefringent crystal. A network containing n stages is required for a $C(\omega)$ having $n+1$ terms. Once $C(\omega)$ has been chosen, the rotation angles (the ϕ_i) of the crystals and the output polarizer can be calculated from the synthesis procedure.

The synthesis procedure of this section allows greater freedom in the choice of $C(\omega)$ and results in a network whose basic form is shown in Figure 2 of Appendix A. The desired amplitude transmittance $C(\omega)$ is still written in the form of Equation (2.1), but the C_i may now be complex. An n-stage network is again required to realize a $C(\omega)$ having $n+1$ terms, but each stage now consists of an optical compensator and birefringent crystal. The synthesis procedure determines the rotation angle of each crystal, the retardation introduced by each compensator, and the rotation angle of the output polarizer.

The flexibility obtained by dealing with complex C_i instead of real C_i may be explained as follows. If one is limited to real C_i, one is limited to amplitude transmittances whose real part has even symmetry and whose imaginary part has odd symmetry. When complex C_i can be used, the real and imaginary portions of the transmittance may have any symmetry whatsoever. Finally, it should be mentioned that this technique can be used (as can all the previous techniques) on both naturally-birefringent and electro-optic networks.

A detailed description of the synthesis procedure is given along with an example in Appendix A.

B. ADDITIONAL TECHNIQUES FOR THE SYNTHESIS OF LOSSLESS DOUBLE-PASS NETWORKS

It was mentioned in the introduction that Ammann has found a procedure [4] which, under certain circumstances, reduced by a factor of two the number of network components necessary to give a certain transmittance. That procedure was applicable to the type of network described in Reference [1], i.e., when the C_i of Equation (2.1) are real. A logical question arises then as to whether a double-pass procedure can be found for use with the more general synthesis procedure of Section II-A, i.e., when the C_i of (2.1) are complex. This Section and Appendix B give the successful solution to that question.

Let us briefly review the essence of the double-pass procedure of Reference [4]. For a certain class of amplitude transmittances $C(\omega)$, the birefringent network which results from using the synthesis procedure of Reference [1] has a particular symmetry. Because of this symmetry, the last half of the birefringent network can be replaced by a mirror which reflects the light back through the first half of the network. In Appendix B, it is shown that networks obtained using the synthesis procedure of Section II-A can be made to have this symmetry. Having done this, the techniques of Reference [4] can then be used directly.

The details are given in Appendix B which is a copy of the paper accepted for publication in the Journal of the Optical Society of America.

C. SYNTHESIS OF ELECTRO-OPTIC MODULATORS FOR AMPLITUDE MODULATION OF LIGHT

A technique has been found for synthesizing electro-optic amplitude modulators having arbitrary modulation characteristics. The technique is an adaptation of the procedure of Appendix A for synthesizing naturally-birefringent networks. The desired amplitude-transmission vs. applied voltage function $K(v)$ of the modulator is written as an exponential series containing a finite number of terms. The resulting modulator consists of a series of stages between an input and output polarizer, with each stage consisting of an electro-optic element and optical compensator. The induced birefringence of the electro-optic medium is assumed to be directly proportional to the applied modulating voltage v. The question of how $K(v)$ should be chosen was also investigated. Two cases were considered:

(a) an amplitude modulator to be used with an envelope detector, and (b) an amplitude modulator to be used with a square-law detector. For each case, the ideal $K(v)$ and several methods of approximating it were found. It was found that the manner in which $K(v)$ is chosen is of great importance. Best results were obtained when the term coefficients (the C_1) of $K(v)$ were chosen to directly optimize the modulator property (or properties) deemed most important. Modulator designs corresponding to several useful $K(v)$ were tabulated.

The details of this procedure are given in the paper of Appendix C which will be submitted for publication.

D. SELECTION OF C(ω) BY CHOOSING ITS ZEROS

In this section, a discussion is given of the relationship between the zeros of $C(\omega)$ and the behavior of $C(\omega)$ over one period. This work was undertaken in the hope that it might prove feasible to determine $C(\omega)$ by choosing its zeros. (The transmittance $C(\omega)$ is usually chosen now by writing a Fourier series approximation to the ideal function and truncating it.) It appears however that only in certain limited circumstances can an acceptance $C(\omega)$ be found from selection of its zeros. Nonetheless it is felt that this technique is sufficiently illuminating to merit a short discussion here.

The transmittance $C(\omega)$ is normally written as in Equation (2.1). We can consider $C(\omega)$ to be a polynomial in $e^{-ia\omega}$, and therefore rewrite (2.1) as

$$C(\omega) = C_n\left[(C_0/C_n) + (C_1/C_n)e^{-ia\omega} + \dots + e^{-ina\omega}\right]$$

$$= C_n(-z_1 + e^{-ia\omega})(-z_2 + e^{-ia\omega}) \dots (-z_n + e^{-ia\omega}),$$

where the z's are the zeros of the polynomial. These zeros are, in general, complex and can be plotted on the "complex $e^{-ia\omega}$ plane" as shown in Figure 2.1.

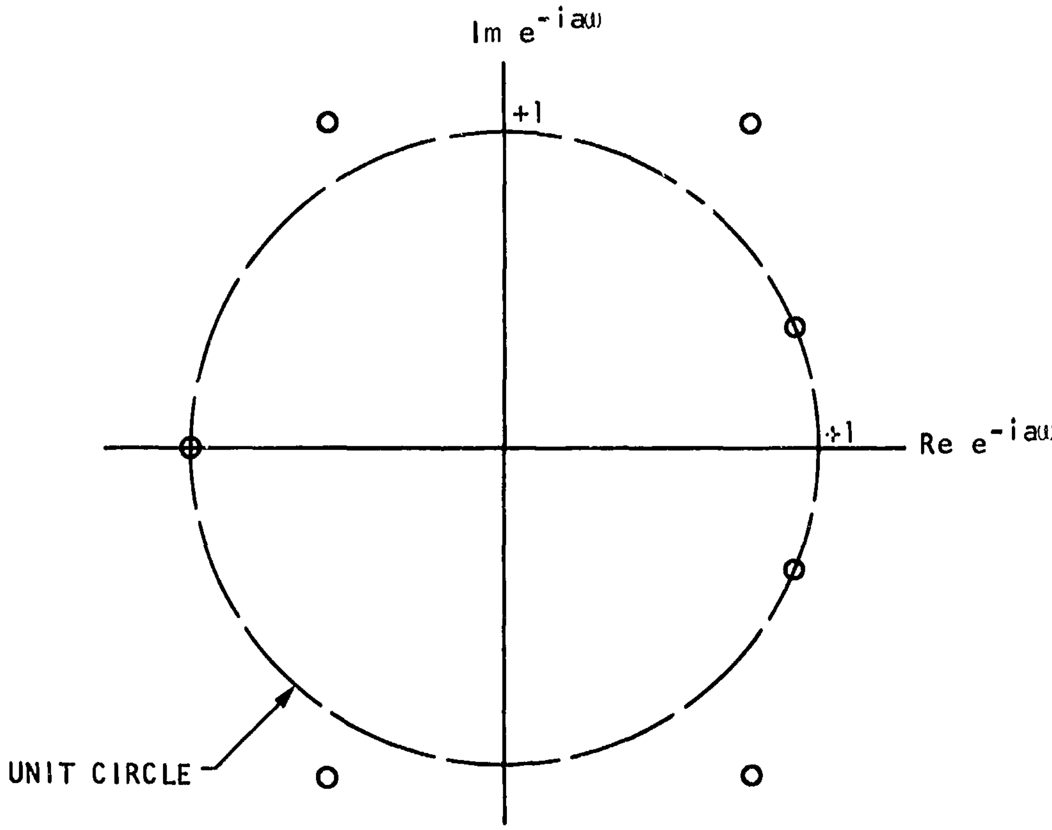

Figure 2.1 Typical set of zeros for $C(\omega)$

Figure 2.1 has the imaginary part of $e^{-ia\omega}$ plotted along the y axis and the real part of $e^{-ia\omega}$ plotted along the x axis. Let us now consider what path is traced out on the $e^{-ia\omega}$ plane when ω is changed sufficiently to cover one period of the characteristic.

The quantity $e^{-ia\omega}$ always has a magnitude of unity and hence must always lie on the unit circle. The phase of $e^{-ia\omega}$ is linearly proportional to ω. Thus as ω increases, the quantity $e^{-ia\omega}$ uniformly traces out the unit circle. If one of the zeros of $C(\omega)$ lies on the unit circle, $C(\omega)$ will be zero when the value of ω is reached which causes $e^{-ia\omega}$ to equal that root. If several zeros lie on the unit circle, then $C(\omega)$ will be zero a corresponding number of times.

Thus the number and spacing of the nulls of $C(\omega)$ can be controlled by properly choosing its zeros. The difficulty with this procedure is that even though the nulls of $C(\omega)$ can be precisely controlled, $C(\omega)$ will often have unacceptable behavior between its nulls. Hence unless the nulls of $C(\omega)$ are the major properties of interest (as they might be, for example, in the design of a band-stop filter), this technique will probably not prove satisfactory.

As an illustration, let us consider a Lyot filter having n = 15. The amplitude-transmittance of such a filter is given by

$$C(\omega) = \frac{1}{16}\,(1 + e^{-ia\omega} + e^{-i2a\omega} + e^{-i3a\omega} + e^{-i4a\omega} + e^{-i5a\omega} + e^{-i6a\omega}$$

$$+ e^{-i7a\omega} + e^{-i8a\omega} + e^{-i9a\omega} + e^{-i10a\omega} + e^{-i11a\omega} + e^{-i12a\omega}$$

$$+ e^{-i13a\omega} + e^{-i14a\omega} + e^{-i15a\omega}).$$

The zeros of $C(\omega)$, written in polar form, are $1\underline{/22.5^\circ}$, $1\underline{/45^\circ}$, $1\underline{/67.5^\circ}$, $1\underline{/90^\circ}$, $1\underline{/112.5^\circ}$, $1\underline{/135^\circ}$, $1\underline{/157.5^\circ}$, $1\underline{/180^\circ}$, $1\underline{/202.5^\circ}$, $1\underline{/225^\circ}$, $1\underline{/247.5^\circ}$, $1\underline{/270^\circ}$, $1\underline{/292.5^\circ}$, $1\underline{/315^\circ}$, and $1\underline{/337.5^\circ}$. These zeros are shown in Figure 2.2. We see that all the zeros lie on the unit circle and hence $C(\omega)$ is forced to zero many times during

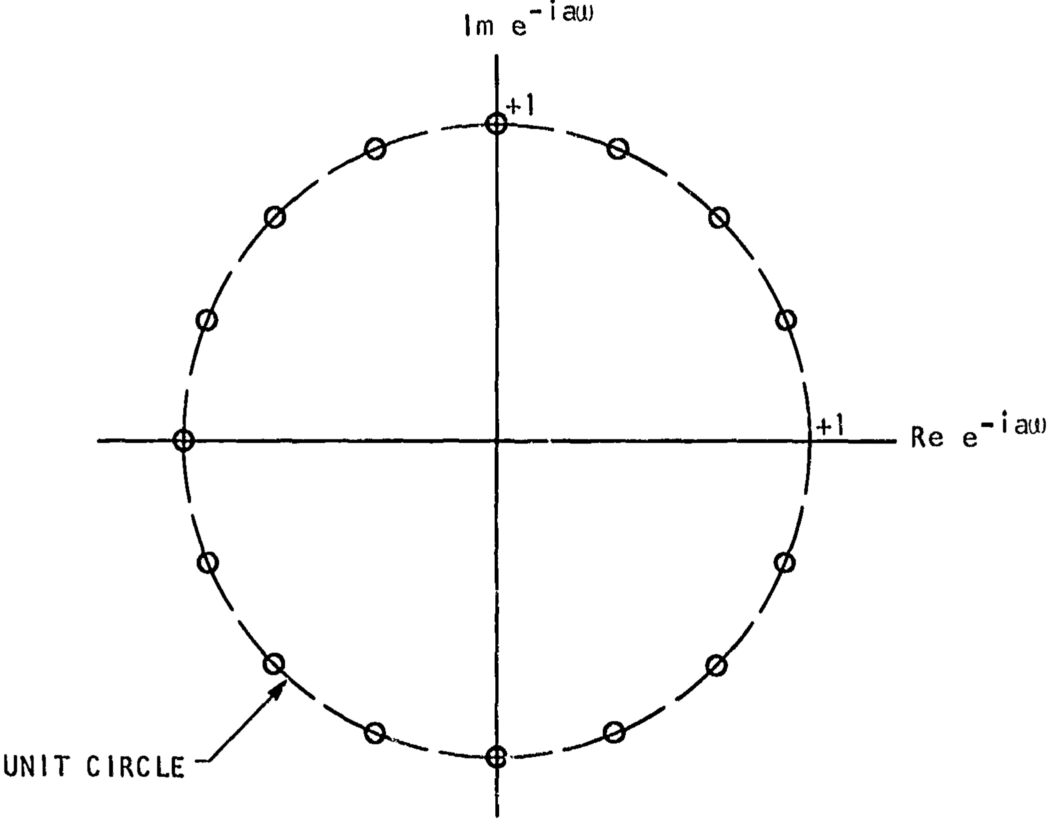

Figure 2.2 Zeros of C(ω) for Lyot filter with n = 15

each period. In addition, we see that the zeros are uniformly spaced around the unit circle except that one is missing at the point $1\underline{/0^\circ}$. This suggests that the filter passband occurs when ω has a value which makes $e^{-ia\omega} = 1$. This is indeed so as seen from Figure 2.3 which is a plot of the amplitude-transmittance of the Lyot filter.

E. OTHER TOPICS

During this program, work was performed on two other theoretical problems for which successful solutions were not found. The first of these was the problem of obtaining a procedure which could be used for synthesizing single-sideband modulators. None of the birefringent network synthesis procedures developed to date are appropriate for designing a single-sideband modulator. It can be shown that all electro-optic devices designed from existing procedures will have symmetric output spectra, but a single-sideband modulator by its very definition has an asymmetric output spectrum (e.g., the first upper sideband should be absent). Hence it is necessary to develop a basically different procedure in order to synthesize single-sideband modulators.

An attempt was made to find a procedure which would produce a network of the form shown in Figure 2.4. This network is different from previous network forms in that driving voltages to the various crystals are not identical. The phases of the driving voltages were allowed to be different and were to be calculated from the synthesis procedure. In addition, the rotation angles of the various stages were to be calculated. The network of Figure 2.4 is capable of producing an asymmetric spectrum as required. However, the very thing which distinguishes the network of Figure 2.4 from previous networks also eliminates the possibility of obtaining a synthesis procedure by generalizing or modifying previous results. For the key requirement of existing procedures has been <u>identical birefringent crystals</u> and this is violated by the network of Figure 2.4. The result is that a general synthesis procedure is substantially more difficult to formulate when non-identical birefringent stages compose the network. The complexity of the problem has thwarted attempts thus far to find a synthesis procedure for the general case.

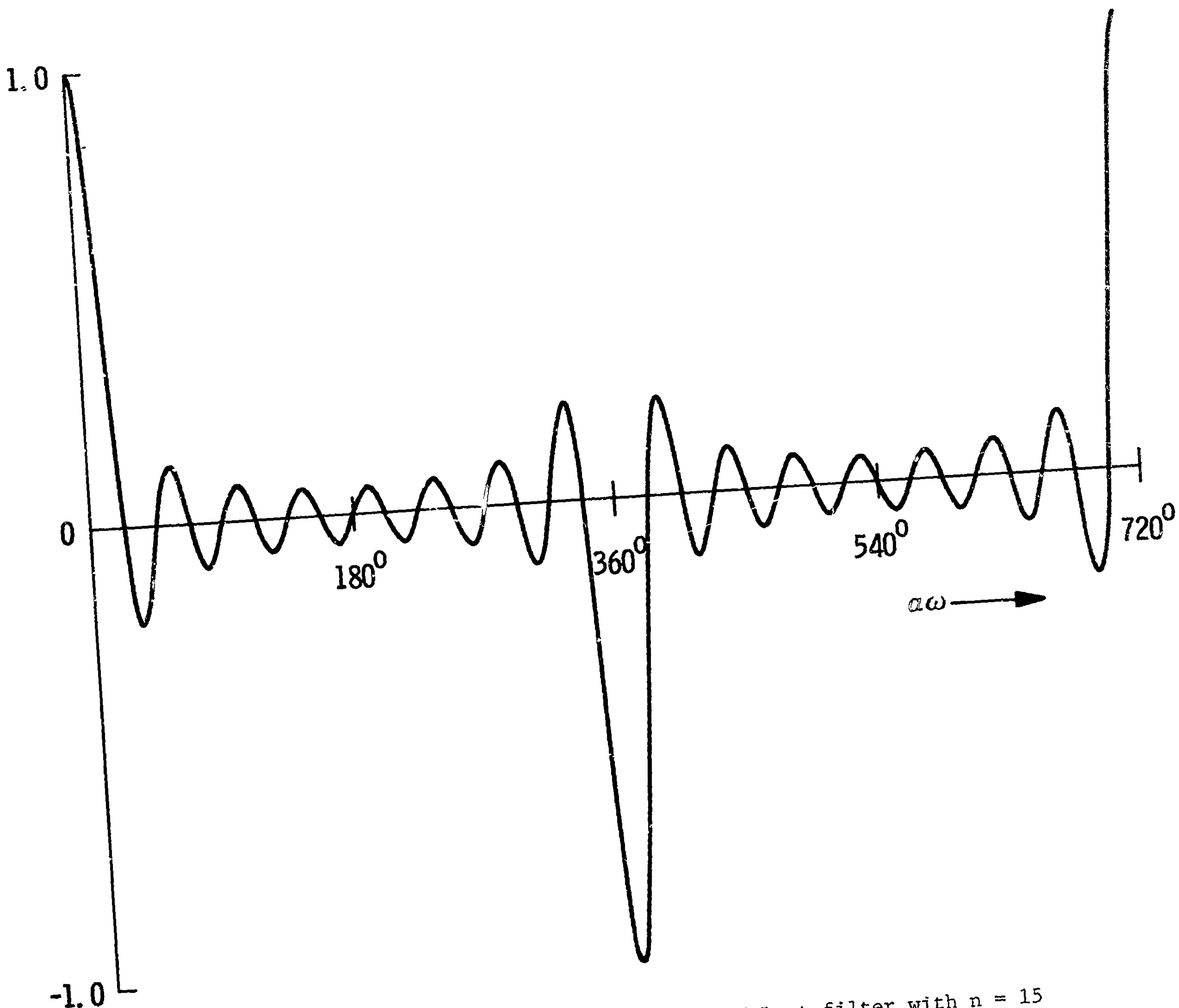

Figure 2.3 Amplitude-transmittance of Lyot filter with n = 15

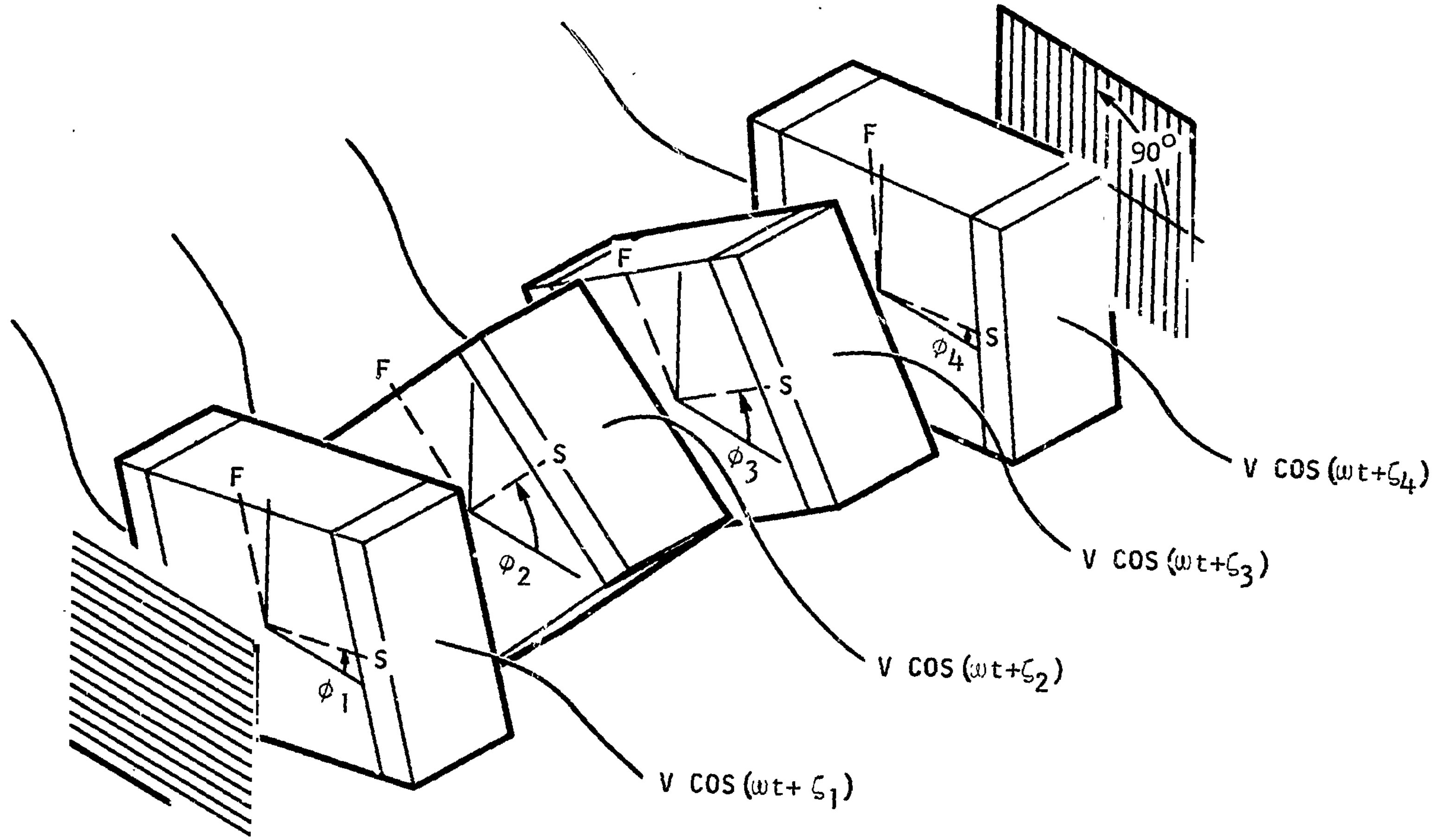

Figure 2.4 Electro-optic network with non-identical driving voltages

It is proposed that one possible alternate approach to obtaining a single-sideband modulator synthesis procedure might be to begin with a more modest problem. For example, instead of allowing the driving voltage of each stage to have a different phase, the phases might be restricted to be either 0° or 90°. Perhaps a synthesis procedure could then be found for this simpler network. This solution to the simplified problem might then give insight into how the general problem should be approached. It appears in any case that the task of devising a synthesis procedure for single-sideband modulators is a very difficult one.

Another general problem area which was studied during the program was that of synthesizing lossless birefringent networks composed of unequal-length crystals. This important problem was approached through the synthesis procedure of Harris, et al. [1] in the following way. The general form of the network resulting from that procedure is shown in Figure 1 of Appendix A. Suppose now that two consecutive crystals are rotated to the same angle. This would be equivalent to a single crystal which is twice as long. Hence the problem under consideration may be restated as, "What must be true about $C(\omega)$ in order to cause two or more consecutive crystals to be rotated to the same angle?"

Again this quest has resulted in little success. Studies were made to detect possible relationships between the C_i which would cause several crystals to be rotated to the same angle. Some relations were found among the C_i, but they were sufficiently complex so as to be of little or no practical value. In addition, relations were sought among the zeros of $C(\omega)$, but again unsuccessfully. Thus no set of restrictions has been found which is simple enough to be practical. This problem is an important one, however; its solution would contribute considerably to the practicality of birefringent networks.

III. EXPERIMENTAL RESULTS

In this section, the results of the experimental program are given. The experiments may be conveniently divided into two parts: (a) those performed on naturally-birefringent networks and (b) those performed on electro-optic networks. The experimental program had several goals among which were verification of the various theories, illumination of practical problem areas, and the realization of actual devices.

A. NATURALLY-BIREFRINGENT NETWORKS

A major goal of these experiments was to verify the synthesis procedures of References [1] and [4]. The optical network involved consists of a series of naturally-birefringent crystals between input and output polarizers (see Figure 1 of Appendix A). Such a network was built and tested in order to compare actual and predicted performance. The details of the construction of the network are discussed below.

1. Physical Considerations

a. Crystal material and sizes

Many materials are suitable for use as the "basic building blocks" of a naturally-birefringent network. One must consider the frequency range of interest and the desired basic periodicity of the network in order to choose an appropriate material. The material must be transparent to the optical frequency band of interest and should be of good optical quality. Having determined the material to be used, the lengths of the crystals can then be chosen to give the periodicity desired for the network's transmittance. A useful graph for determining the periodicity is given in Figure 7 of Reference [1].

For the present experiments, we elected to use an optical wavelength of 6328 Å (from a He-Ne gas laser), and to use calcite crystals with a length of 2 cm. This gives a periodicity of about 100 GHz. Calcite was chosen primarily because of its availability, large birefringence, and good optical quality. The cross section of the crystals was chosen to be 1 cm by 1 cm. Calcite is a negative crystal, and hence the optic axis is the slow axis.

The crystals were cut with the optic axis in the planes of the end faces, as shown in Figure 3.1.

b. Crystal tolerances and compensators

The synthesis of optical birefringent networks requires the use of "identical" crystals. This means that each crystal must have exactly the same retardation. The following calculation points out the difficulty in making identical crystals.

We shall calculate the number of "retardation waves" in a calcite crystal 2 cm long. By retardation waves, we mean the number of optical wavelengths the slow (S) component of an incident impulse of light is retarded compared to the fast (F) component. The indices of refraction of calcite at 6328 Å are approximately $\eta_o = 1.654$ and $\eta_e = 1.485$. Then the number of optical waves along the F axis is L/λ_e or $L\eta_e/\lambda_v$, while the number of optical waves along the S axis is L/λ_o or $L\eta_o/\lambda_v$, where $\lambda_v = 6328$ Å. The difference is then

$$\text{Retardation} = \frac{L\eta_e}{\lambda_v} - \frac{L\eta_o}{\lambda_v} = \frac{L\eta_e - L\eta_o}{\lambda_v} = \frac{L(\Delta\eta)}{\lambda_v}$$

$$= \frac{(2)(.169)}{(6328 \times 10^{-8})} = 5300 \text{ waves.}$$

The problems involved in making crystals with exactly the same number of retardation waves are obvious. Even if all crystals were perfectly homogeneous, the lengths would have to be the same to within, say, 1/360 of a retardation wave. This requires a length tolerance of $\frac{2}{(360) \times (5300)}$ = .01 micron.

The crystals can be made to all have an <u>integral</u> number of waves retardation (although not necessarily the same integer in each case) by adding thin "trimmer" plates (compensators) with just enough birefringence to make the combination of crystal and compensator have an integral number of waves retardation. Thus, for example, one might have crystal-compensator combinations with delays of 5280, 5325, and 5336 waves. The percentage difference in these is small enough that the actual transmittance

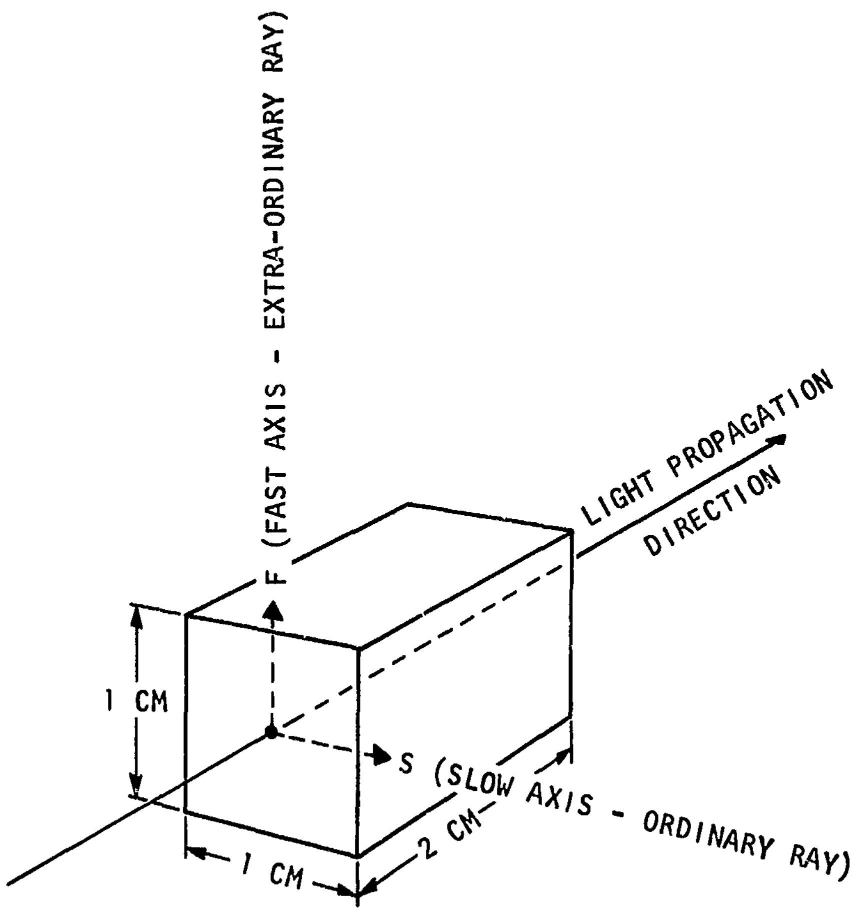

Figure 3.1 Calcite crystals used as basic unit of birefringent network

of the network will not differ significantly from the ideal transmittance over the wavelength range of interest. In our experiments, quartz crystals were used for the compensator crystals.

Due to the large number of retardation waves in the calcite crystals, the retardation varies rapidly as a ray moves off-axis. A change of only a few degrees in ray direction is sufficient to significantly deteriorate performance. In order to insure that the light travels down the propagation axis, there must be no refraction at the surfaces, which means that the end faces must be very parallel.

Another problem in preparing the crystals is in properly orienting them. If the optic axis does not lie exactly in the plane of the face, the index of the extraordinary ray is changed. Again, only slight change is necessary to deteriorate performance substantially.

The final problem in preparing the crystals is flatness of the faces. If there is much variation, again the retardation will change significantly.

All of the above considerations apply also to the quartz compensators, although the requirements are not quite so stringent in this case. The only critical item concerning the compensators is parallelism. Again the faces must be very parallel in order to avoid refraction. Other factors are not as critical since the compensators have many fewer retardation waves delay.

For quartz, $\eta_o = 1.542$, $\eta_e = 1.551$. Thus, for a 2 mm quartz crystal,

$$\text{Retardation} = \frac{L(\Delta\eta)}{\lambda} = \frac{(.2)(.009)}{6328 \times 10^{-8}} = 28 \text{ waves.}$$

c. Temperature effects

All of the above discussion assumes a constant temperature, for birefringence in general varies with temperature. In calcite crystals as long as the ones being used, the retardation thus varies substantially with temperature. Accordingly, all compensators must be matched to their crystal at a particular temperature.

Actually, the retardation of the compensators also varies with temperature. However, since the compensators are thin (2 mm) compared to the crystals and made of a much less birefringent material (quartz), they do not vary nearly as rapidly and hence are satisfactory over several waves change in the calcite. The temperature dependence of the networks is discussed in more detail later.

In the present experiments, advantage was taken of the temperature-dependent birefringence to sweep the transmittance of the networks through several cycles. This method proved to be quite successful, and at the same time provided valuable data on the temperature behavior of optical networks. To our knowledge, this technique has not been used previously to measure the transmittance of birefringent devices.

d. Selection of a reference crystal and matching of crystals and compensators

From the above discussion, it is clear that all crystal-compensator combinations must have an integral number of waves delay at some fixed temperature. This temperature is arbitrary, but certain practical considerations set limits on the range into which it must fall. In order to make the temperature-control system as simple as possible, it is desirable to keep the oven above room temperature so that no cooling system is needed. Room temperature is normally 20 to 25°C, so that one would like to pick a reference temperature at least 10°C above this. The most convenient choice is to put a calcite crystal into the oven and note the temperature at which it is an integral number of waves long. Then if all compensators are matched to crystals at this reference temperature (T_{ref}) , the reference crystal will not need a compensator. Using one crystal (which we shall call crystal #1) as a reference, T_{ref} was determined to be 36.264°C. One could, of course, use a higher temperature for the reference temperature since the crystal's transmittance is periodic, but this temperature was deemed adequate for the present experiments. Having established this temperature, compensators were then matched to the remaining crystals (#2, 3, and 4). A one-cm calcite crystal was also cut and matched with a compensator for use in the double-pass experiments. This crystal will be called #5 henceforth.

e. Alignment

A very convenient way to aligning the calcite crystals is to use the characteristic isogyre pattern, which may be observed by placing the crystal in diverging or converging light between crossed polarizers. When light propagates at right angles to the optic axis of a uni-axial crystal, as is the case here, the isogyre pattern is a family of hyperbolae as indicated in the sketch of Figure 3.2a. A photograph of the observed pattern of one of the crystals is shown in Figure 3.2b. Each crystal was carefully aligned so that the laser beam hit exactly in the middle of the pattern. After the crystals were thus aligned, they were placed in the oven and compensators were matched to them.

2. Experimental Apparatus

a. Oven

Of central importance to the experiments with naturally birefringent networks are the oven and temperature control unit (to be discussed below). It has already been pointed out that an oven is necessary to select a reference temperature and to match compensators to crystals. Preliminary calculations suggested that a change in temperature of .01°C would change the retardation of a crystal by 1°. After investigating commercially available units, it was decided to build an oven. A photograph of the oven constructed is shown in Figure 3.3. It was made of aluminum with glass end windows to allow passage of the laser beam. A "V" block (shown in Figure 3.5a) was bolted to the bottom to hold the crystal holders (to be described later). The oven was made long enough to hold five crystals, and was made watertight so it could be filled with an index matching oil to reduce reflection losses. The oven was wrapped with a heating coil and insulated on all sides by 2" of styrofoam. The oven was equipped with adjustable feet which could be mounted on an optical bench.

b. Temperature control unit

As mentioned above, it was decided to build a temperature controller rather than buying one. A schematic of the unit built, as well as the oven, is shown in Figure 3.4. The circuit consists basically of a bridge

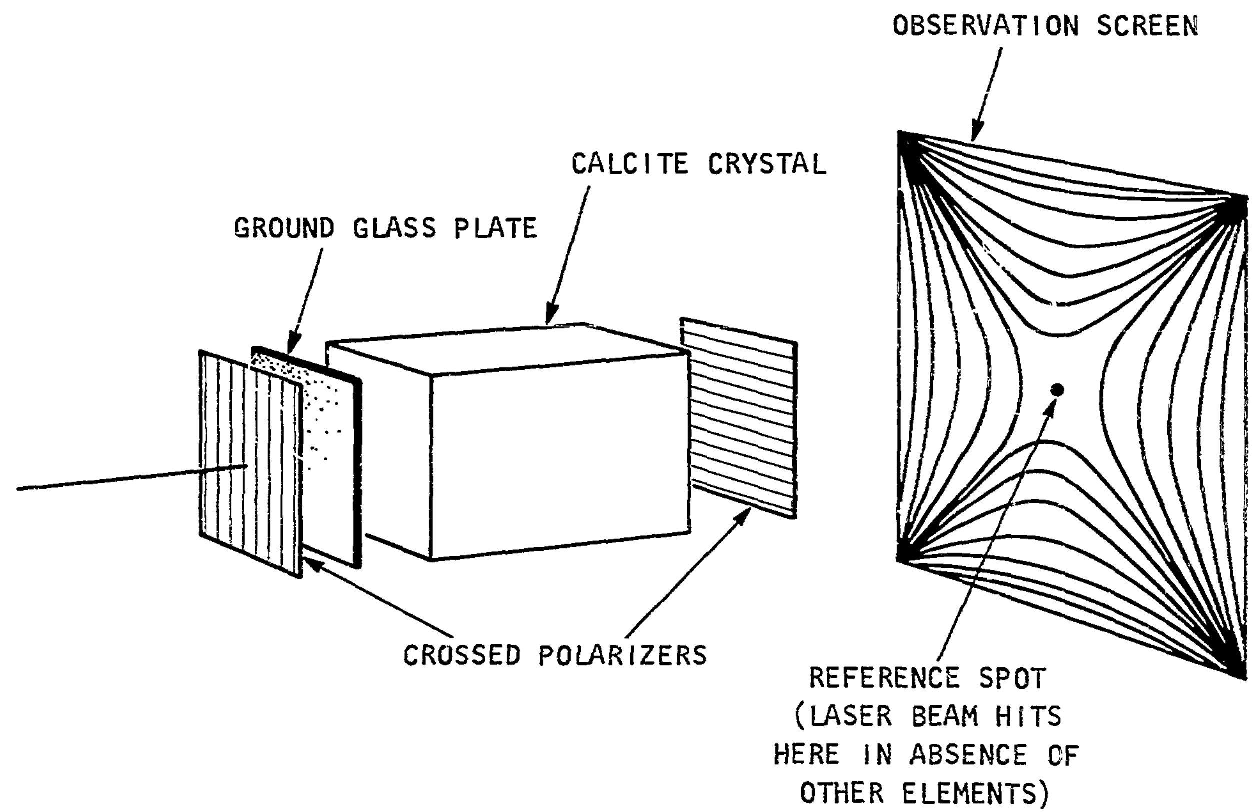

Figure 3.2a Experimental setup for aligning calcite crystals

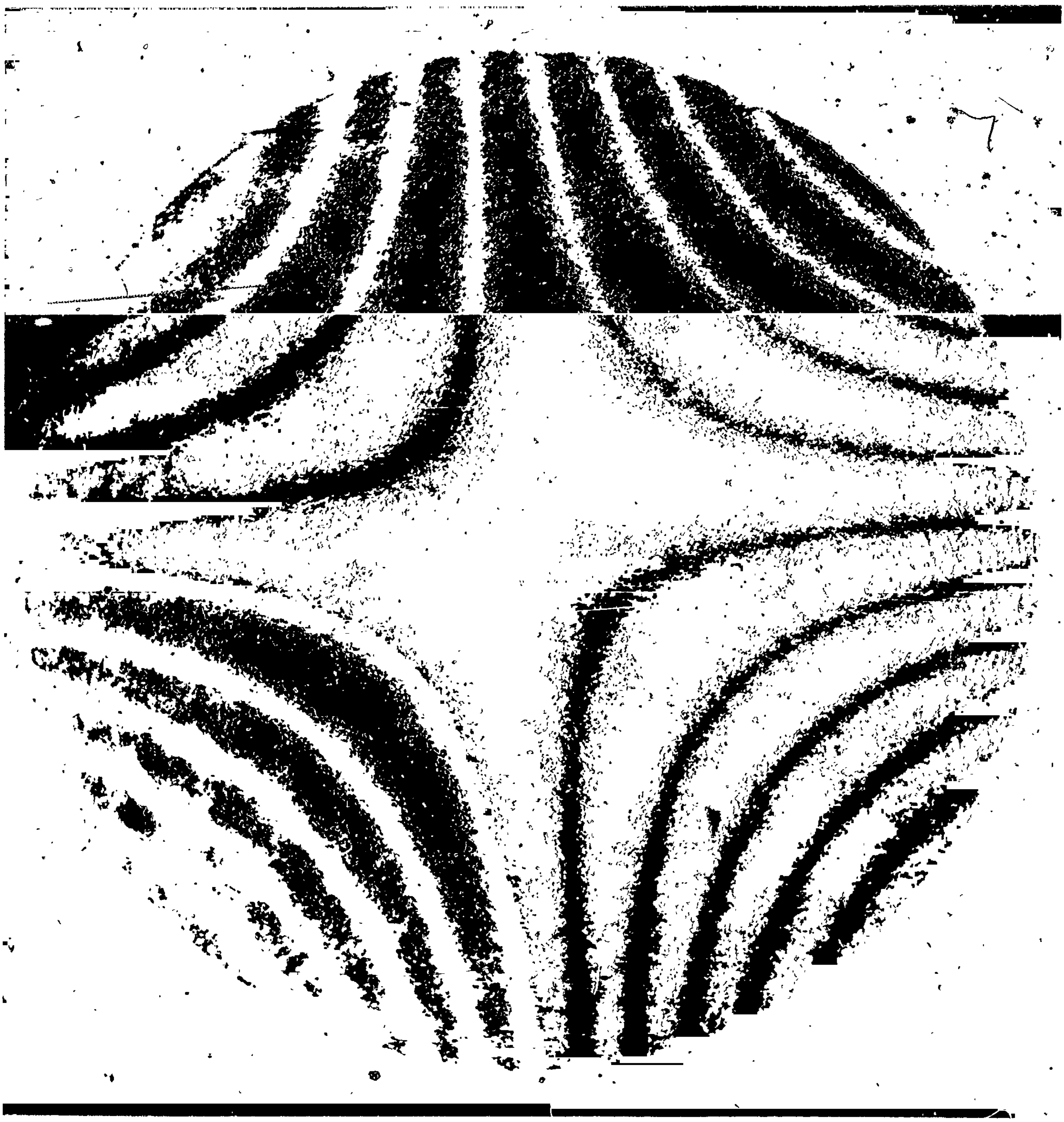

Figure 3.2b Typical isogyre pattern for calcite

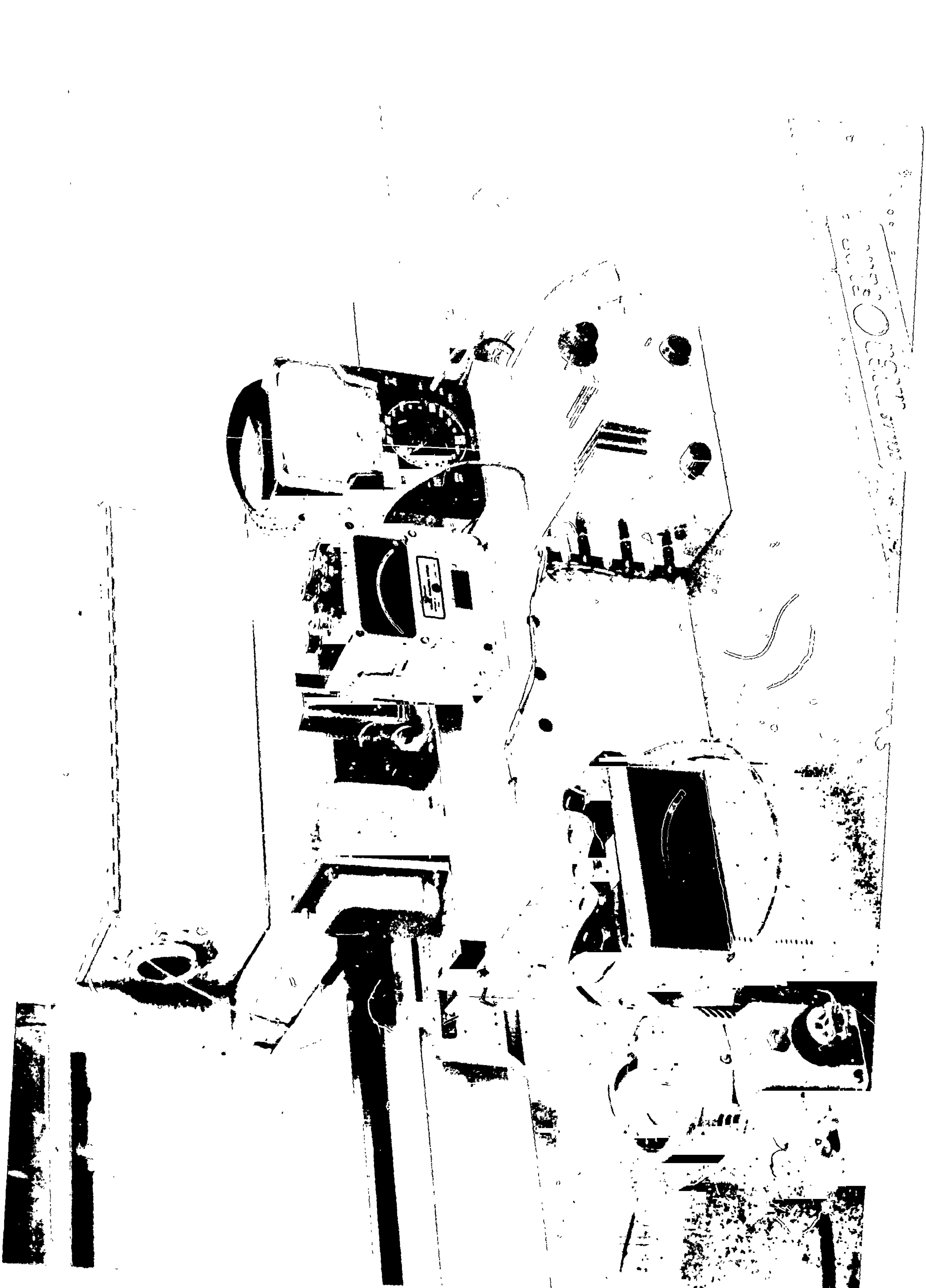

Figure 3.3 Oven used in birefringent network experiments

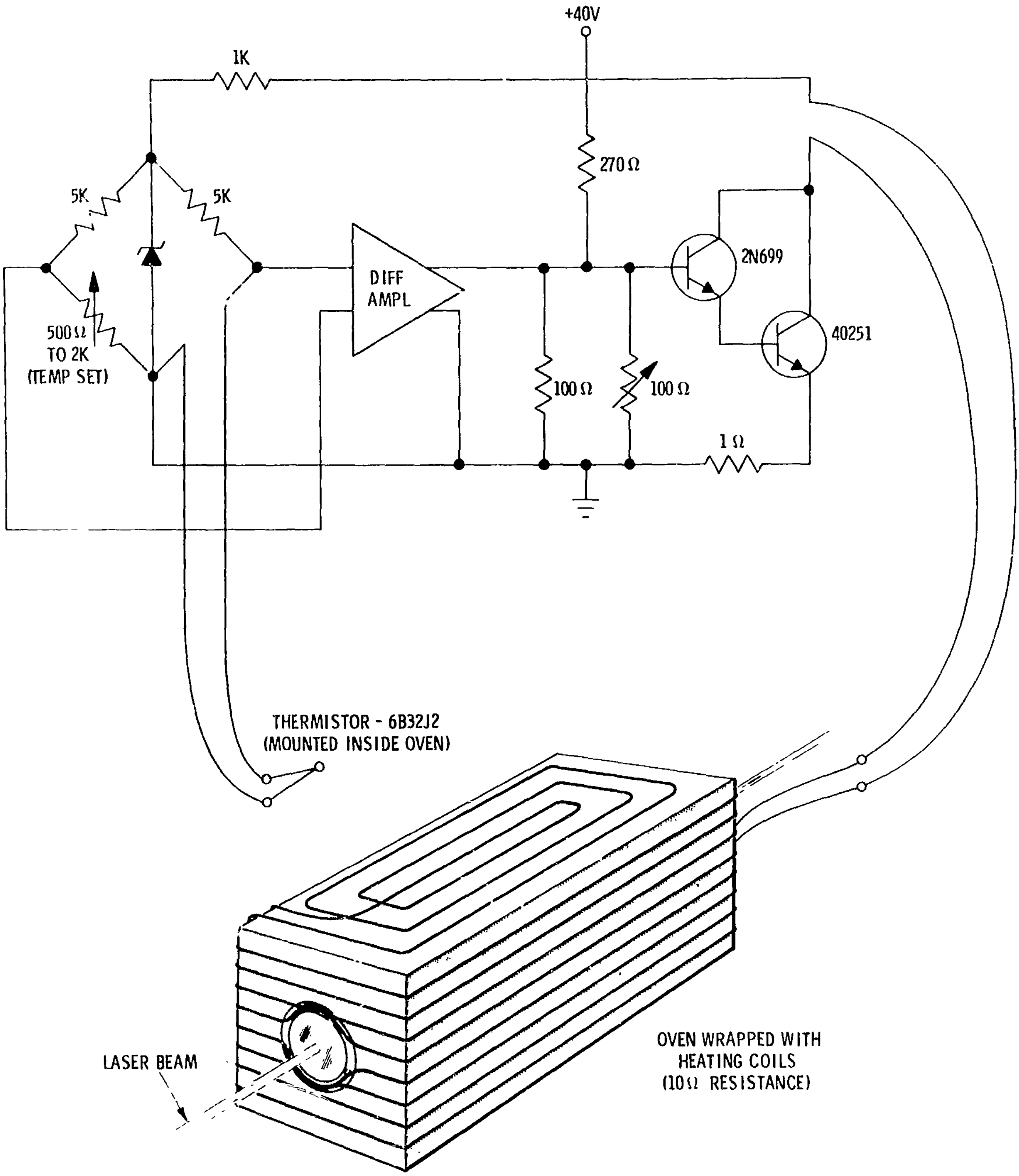

Figure 3.4 Temperature control unit for oven

circuit and a differential amplifier. The power device is a power transistor. The unit runs from an un-regulated power supply. This unit turned out to do an extremely good job of controlling temperature in the oven. It has been verified by direct measurement that the unit maintains the oven temperature constant to within .005°C over 24-hour periods.

c. Crystal holders

The crystal holders were constructed as shown in Figures 3.5a and 3.5b. The calcite crystals were mounted in rectangular aluminum holders which, in turn, were spring mounted in steel cylinders to allow adjustment of the crystals. The compensators were placed in brass plugs which were inserted in the back of the aluminum crystal holders. The circumference of the steel cylinder was graduated in 1° increments in order to allow precise rotation of the crystals. The steel cylinders were placed in the cylindrical block on the bottom of the oven. With this arrangement, it was thus possible to use the same crystals to synthesize different networks simply by rotating them to new angles.

d. Thermometer

In order to work within the tight temperature tolerances mentioned above, it is obviously desirable to be able to measure temperatures very accurately. To do this, a Hewlett-Packard Model 2801A quartz thermometer was used. This instrument has two temperature sensors and is capable of reading temperatures to within .0001°C. The digital temperature output was converted to an analog signal by a digital-to-analog converter and used to drive the x axis of an x-y recorder.

e. Detector

The detector used in these experiments was an ordinary silicon solar cell. Since this device is a square-law detector, the square of the amplitude-transmission characteristic will be detected. The detected signal was applied to the y axis of the x-y recorder.

f. Experimental setup

The components mentioned above were used to record the transmission curves of the various networks. For each experiment, the crystals were

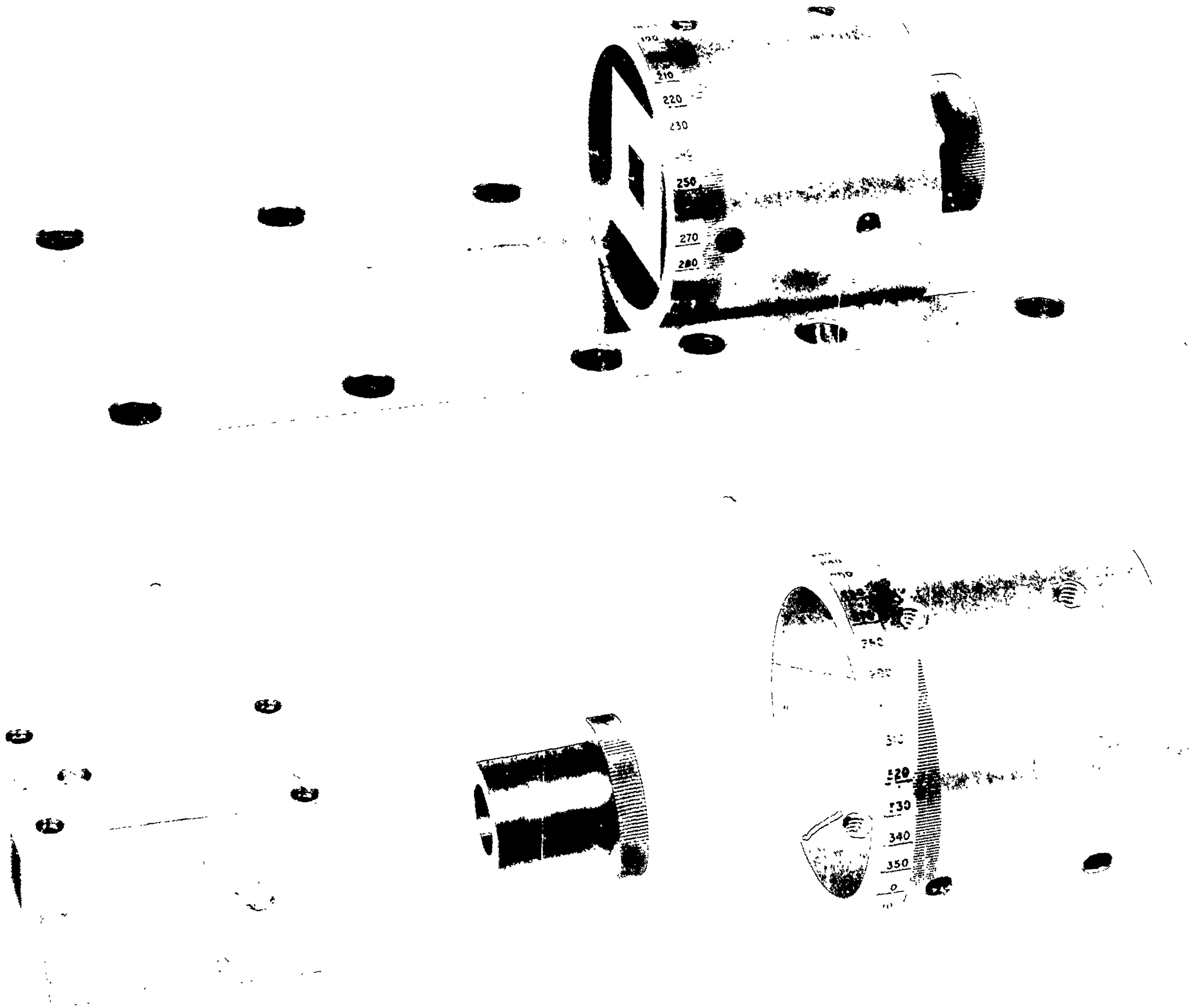

Figure 3.5a Holders in which the calcite crystals are mounted

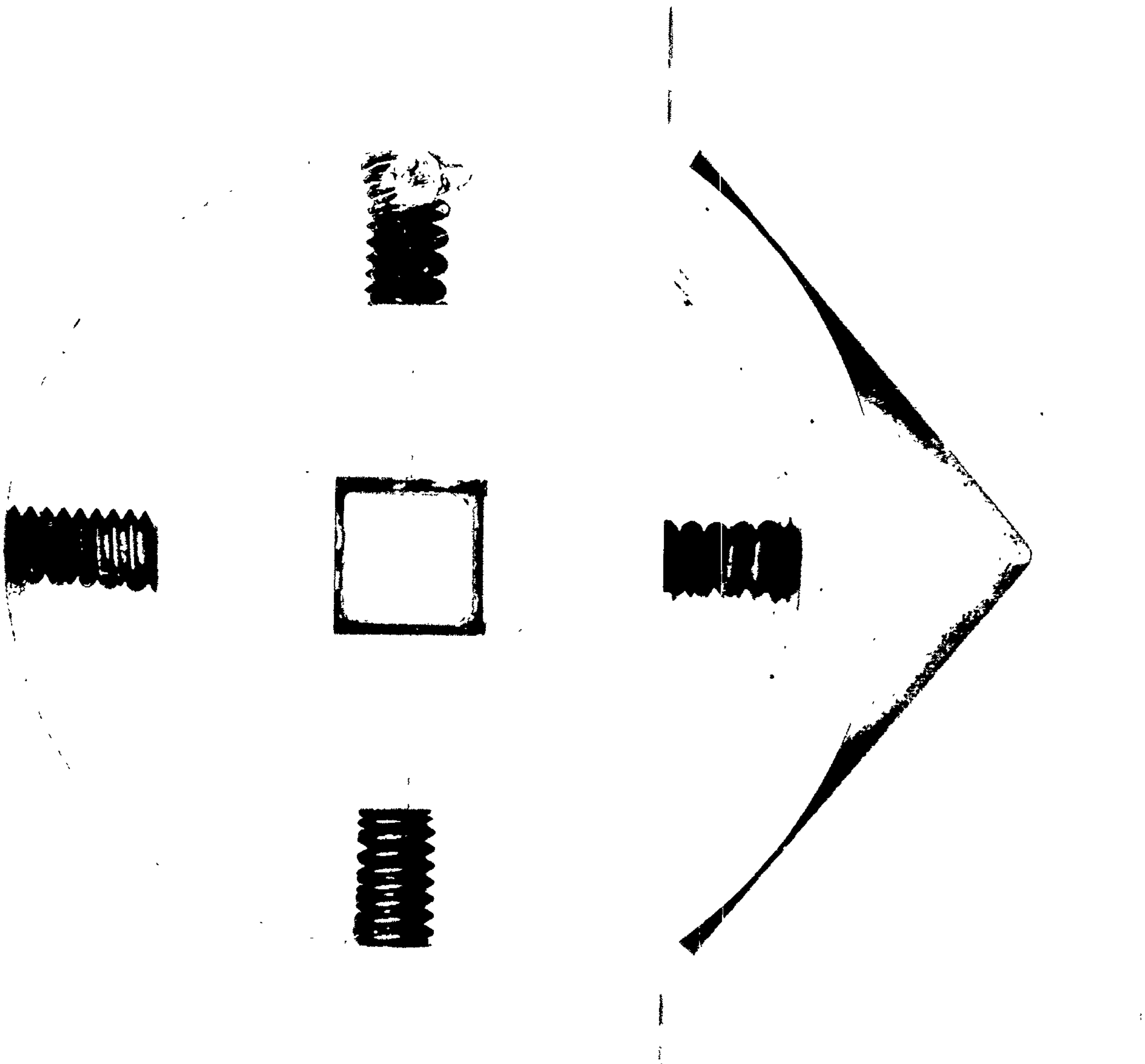

Figure 3.5b End view of calcite crystal holder

rotated to the prescribed angles, and the oven was heated to about 50°C. The power to the oven was turned off and the oven allowed to slowly cool. The oven cooled at a rate of about 0.001°C/sec. Plots of the optical network's transmittance were obtained by the thermometer driving the x-axis and the silicon solar cell driving the y-axis of an x-y recorder. These traces were taken in the temperature range from about 39°C to 33°C, so that the reference temperature fell about in the middle of the graphs.

3. Data

a. Single-pass experiments

We now give the experimental results obtained for the single-pass birefringent networks. All single-pass experiments were performed on three-stage networks (n = 3) consisting of three appropriately rotated calcite crystals and an input and output polarizer. In each case, a four-term $C(\omega)$ was found (using Fourier techniques) which approximated the ideal characteristic in question. The synthesis procedure of Reference [1] was then used to calculate the rotation angles (the θ_i) for the network stages. The θ_i used for the various characteristics are summarized in Table I. Three different ideal transmittances were used in these experiments. They were the triangular wave of Figure 3.6a, the rectangular wave of Figure 3.6b, and the square wave of Figure 3.6c.

A photograph and schematic of the experimental setup used for the single-pass experiments are shown in Figures 3.7a and 3.7b. On each of the following graphs, the recorder trace shows the measured value of $|C(\omega)|^2$ while the circles show the calculated values of $|C(\omega)|^2$.

(1) Triangular wave (n = 3)

The first characteristic was a three-crystal approximation to a triangular wave. Crystals #1, #2, and #3 were used. The ideal function in this case is the triangular wave sketched in Figure 3.6a. With three crystals we can achieve a four-term Fourier series approximation to the ideal function. The trace from the x-y recorder is shown in Figure 3.8, with the theoretical points denoted by circles. Agreement with theory is very good. Note that the

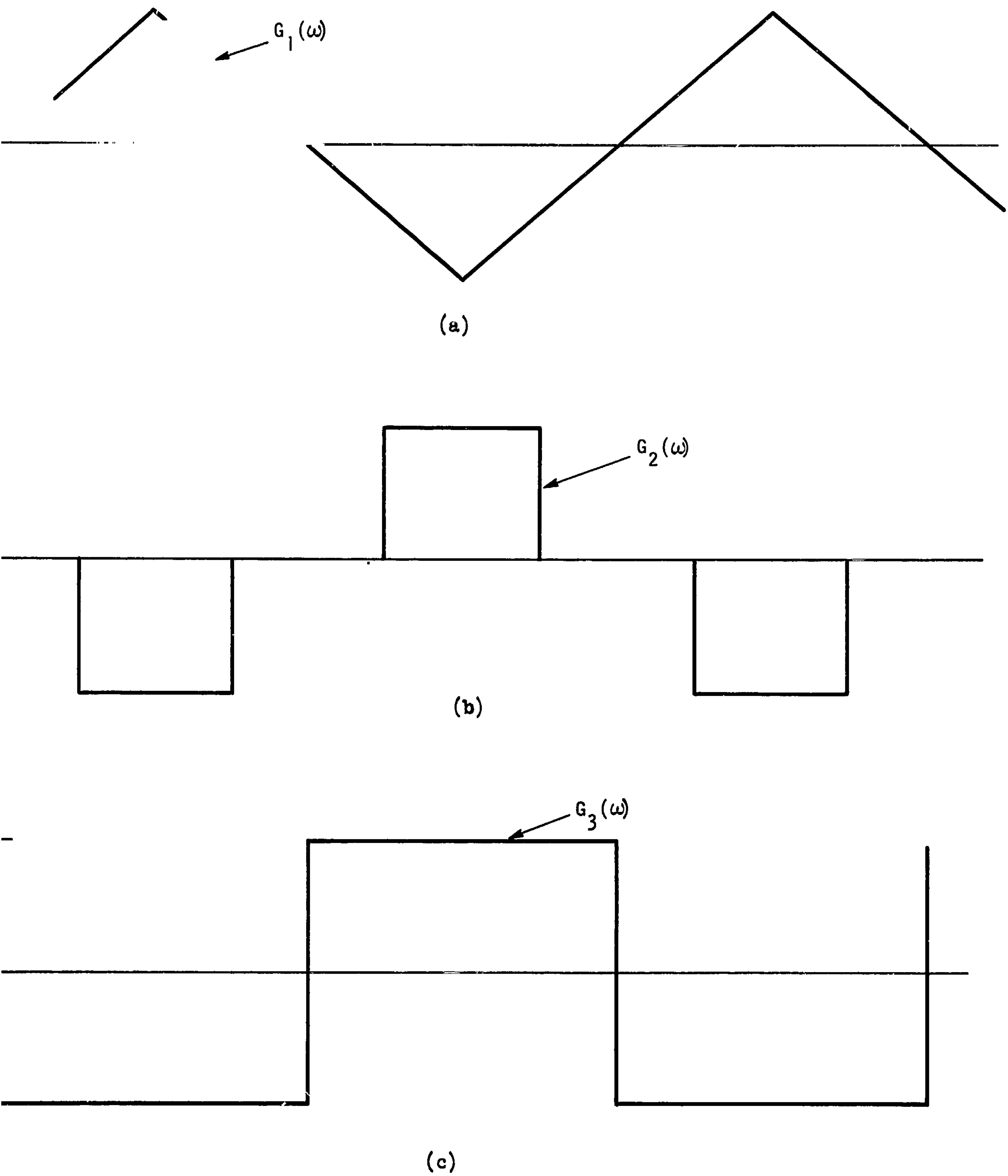

Figure 3.6 Ideal transmittances used for the naturally-birefringent network experiments: (a) triangular wave, (b) rectangular wave, (c) square wave.

SINGLE-PASS NETWORKS

Ideal Characteristic	n	θ_1	θ_2	θ_3	θ_p
Triangular Wave	3	- 4°35'	-37°45'	-37°45'	85°25'
Rectangular Wave	3	-17°10'	-33°31'	-33°31'	72°50'
Square Wave	3	-27°27'	49°23'	49°23'	62°33'

DOUBLE-PASS NETWORKS

Ideal Characteristic	n	θ_1	θ_2	θ_3	θ_4
Triangular Wave	3	- 4°35'	37°45'	-	-
Rectangular Wave	3	-17°10'	33°31'	-	-
Square Wave	3	-27°27'	-49°23'	-	-
Triangular Wave	5	1°28'	- 4°56'	34°34'	-
Rectangular Wave	5	3°50'	-14°04'	23°04'	-
Triangular Wave	7	0°43'	- 1°48'	5°00'	-33°28'
Rectangular Wave	7	3°09'	2°44'	-14°57'	26°26'

Table I

Rotation Angles Used in Single-Pass and Double-Pass
Birefringent Network Experiments

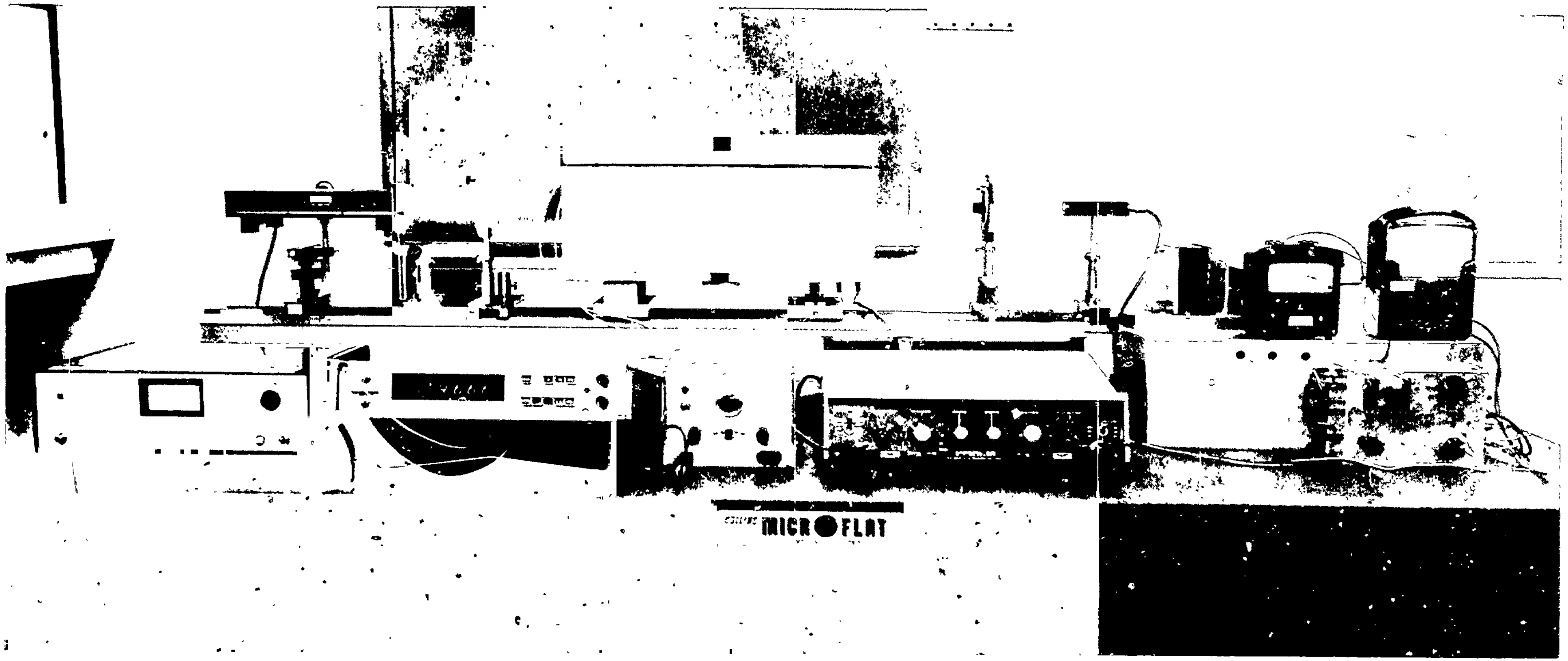

Figure 3.7a Experimental setup used for the single-pass birefringent network experiments

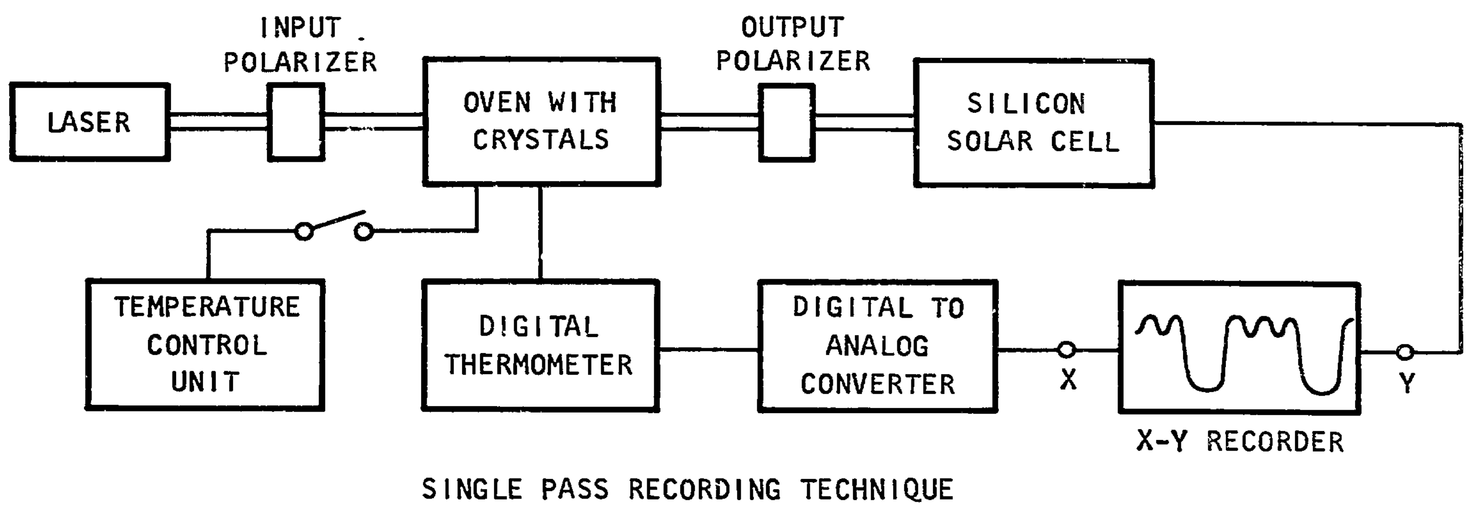

Figure 3.7b Schematic of experimental setup used for the single-pass birefringent network experiments

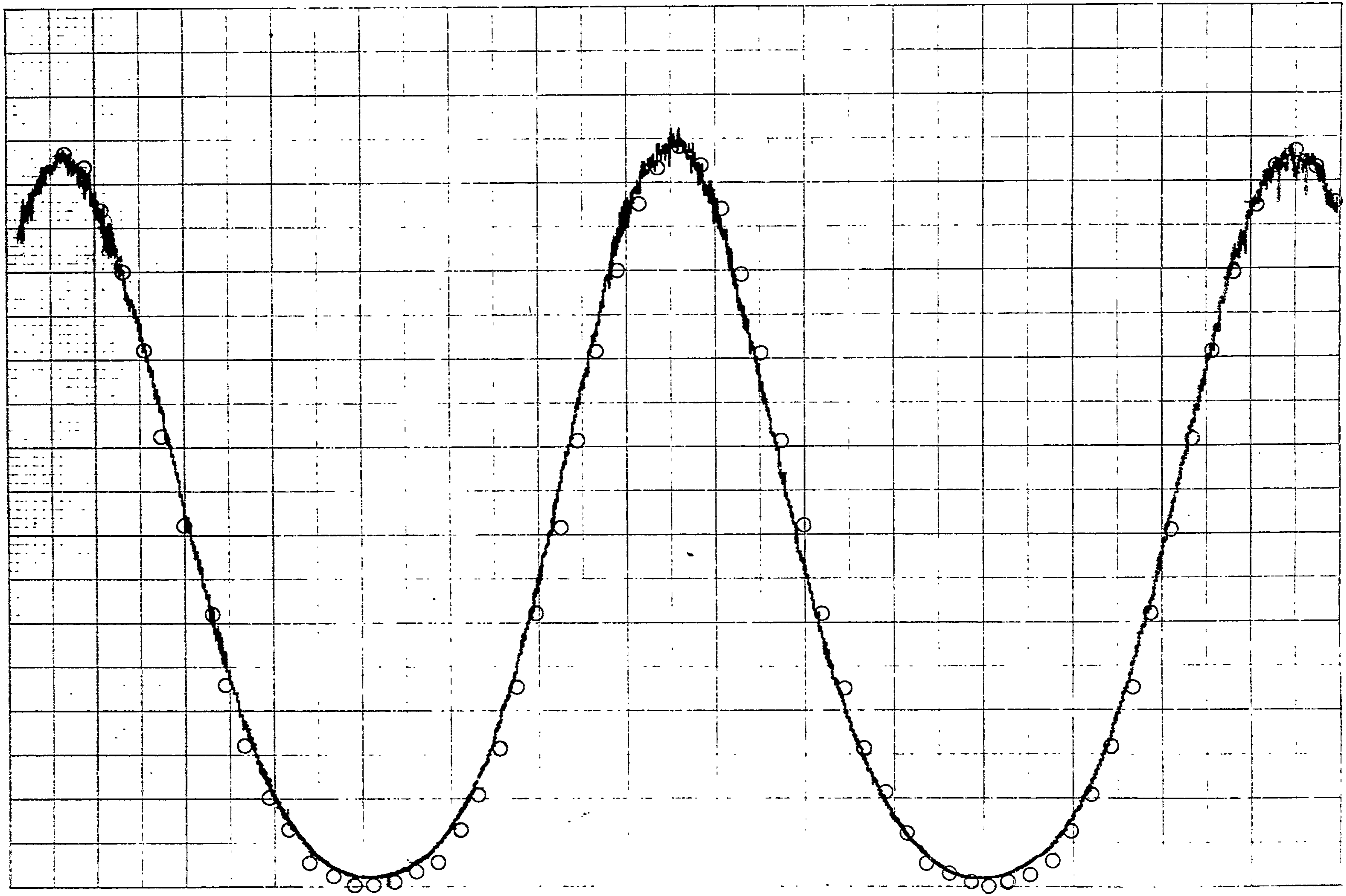

Figure 3.8 Experimental and calculated results for single-pass birefringent network (triangular wave approximation) with n = 3. The figure shows transmitted optical power vs. network temperature (which is equivalent to transmitted optical power vs. optical frequency).

detected curve is the square of the approximation curve, since a square-law detector was used. The trace was taken by cooling the oven slowly from approximately 39°C to 33°C (which took about five hours). The small irregularities in the trace, as well as succeeding traces, are due to laser power fluctuations.

(2) Rectangular wave ($n = 3$)

The second characteristic synthesized was a rectangular wave, whose ideal characteristic is shown in Figure 3.6b. The actual experimental trace is shown in Figure 3.9, with the theoretical points again superimposed as circles. Again three crystals were used, and agreement with theory found to be very good.

(3) Square wave ($n = 3$)

The final characteristic chosen to be synthesized is sketched in Figure 3.6c. The experimental curve is shown in Figure 3.10. Again agreement with theory is very good.

b. Double-pass experiments

We next give the results of experiments performed on double-pass birefringent networks. Recall that with the double-pass technique [4], the optical signal passes through the birefringent network twice. As a result, a given $C(\omega)$ can be obtained using only half the number of stages required by the synthesis procedure of Reference [1]. Thus a $C(\omega)$ with $n = 3$ can be realized by a 1 1/2-stage birefringent network (one full-length calcite crystal and one half-length calcite crystal) while $n = 5$ can be realized by a 2 1/2-stage network, and so forth.

Double-pass experiments were performed for $n = 3$, 5, and 7. The experimental arrangement is shown in the sketch of Figure 3.11 and in the photograph of Figure 3.12. As seen in those figures, a mirror reflects the light back through the birefringent network for the second pass, and a prism deflects the returning beam to the detector.

For these experiments, four-term ($n = 3$), six-term ($n = 5$), and eight-term ($n = 7$) $C(\omega)$'s were found using Fourier techniques which approximated

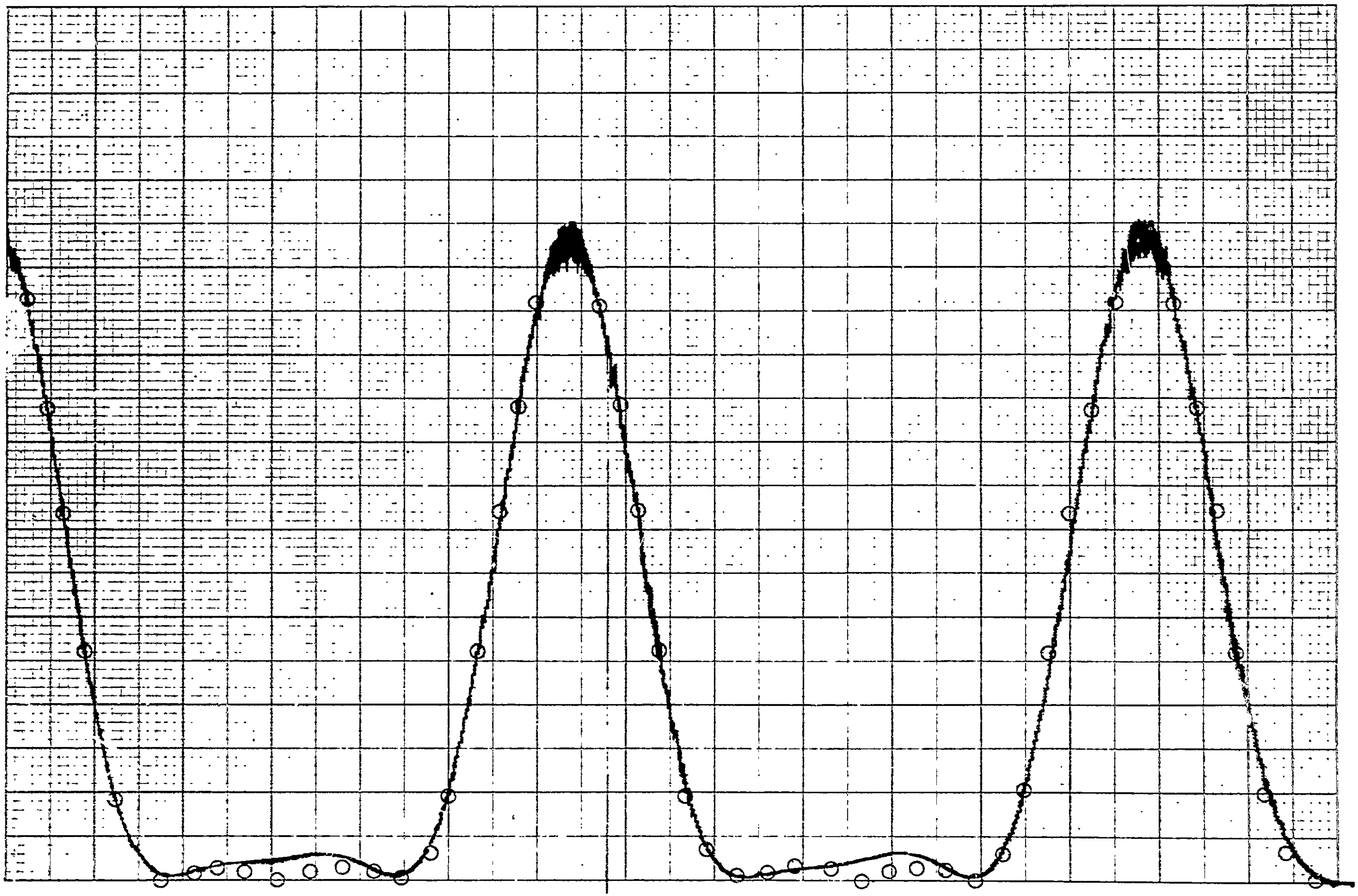

Figure 3.9 Experimental and calculated results for single-pass birefringent network (rectangular wave approximation) with n = 3. The figure shows transmitted optical power vs. network temperature (which is equivalent to transmitted optical power vs. optical frequency).

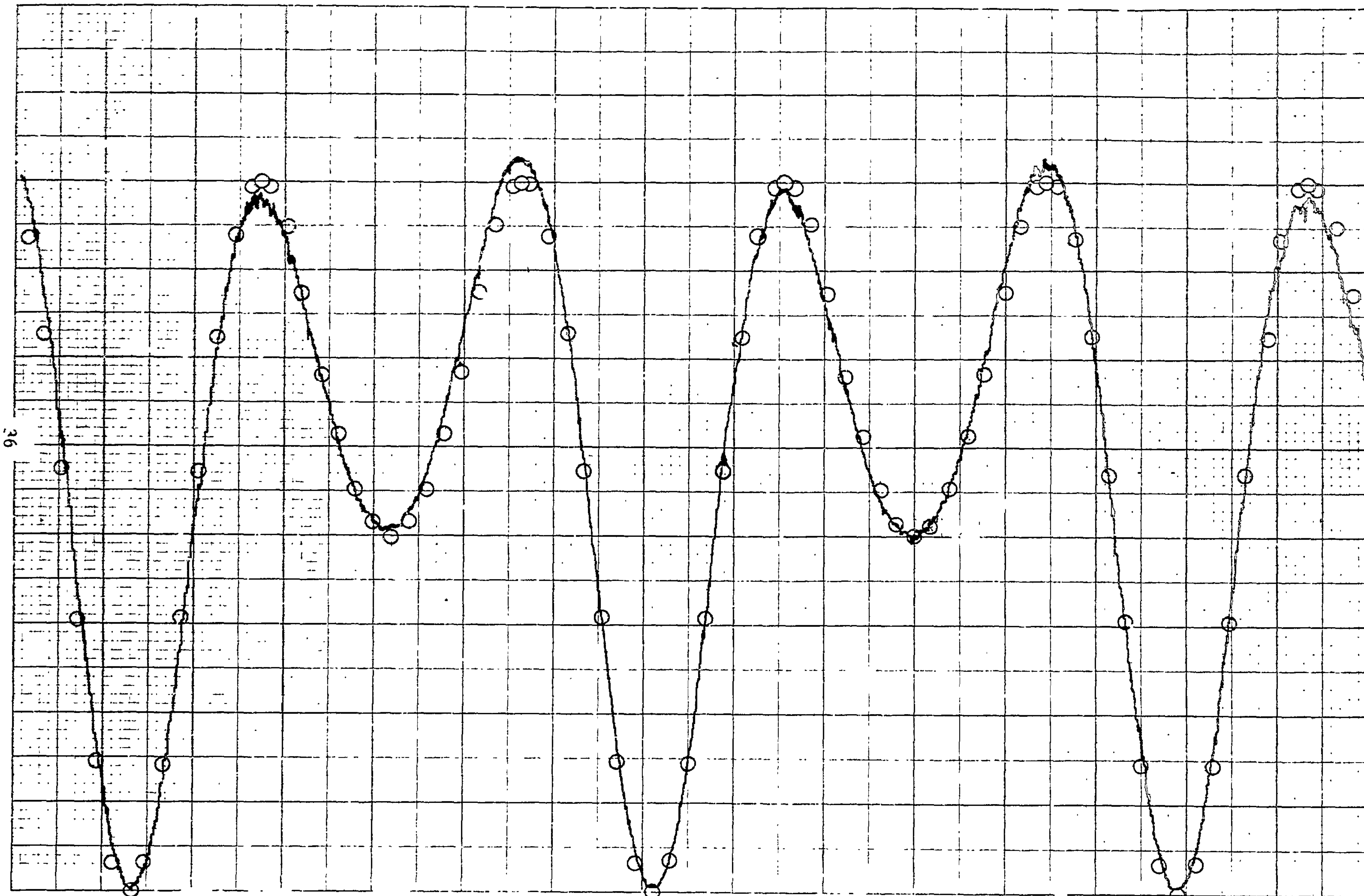

Figure 3.10 Experimental and calculated results for single-pass birefringent network (square wave approximation) with n = 3. The figure shows transmitted optical power vs. network temperature (which is equivalent to transmitted optical power vs. optical frequency).

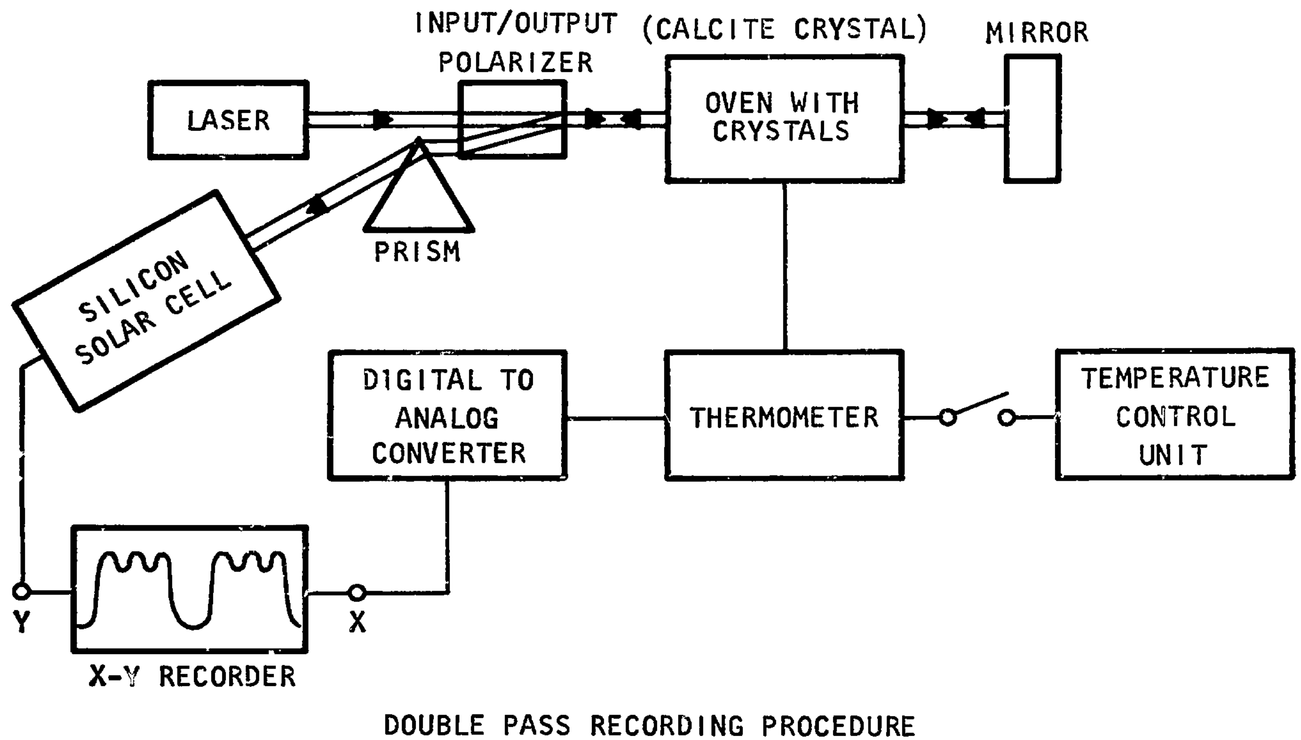

Figure 3.11 Schematic diagram of setup used for double-pass birefringent network experiments.

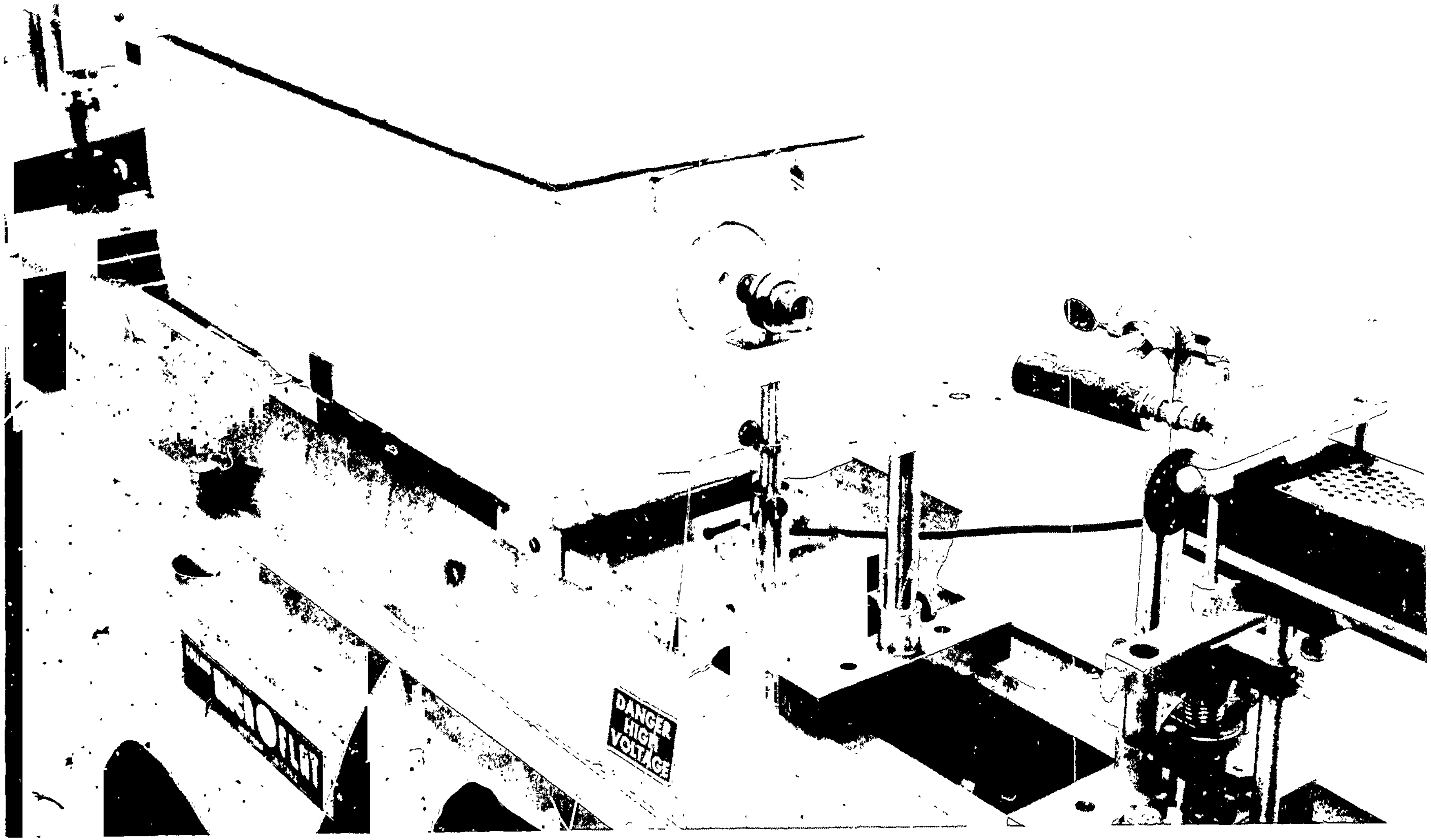

Figure 3.12 Setup used for double-pass birefringent network experiments

the various ideal functions of Figure 3.6. The synthesis procedure of Reference [1] was then used to calculate the rotation angles (the θ_i) for the stages of the corresponding <u>single-pass</u> networks. These single-pass networks were each symmetric about their midpoint. Hence they could be converted to double-pass networks by replacing the last half of the network by a mirror, and by replacing the input polarizer by a polarizing beam splitter. The rotation angles used for the double-pass network stages are summarized in Table I. The following graphs again show measured and calculated values of $|C(\omega)|^2$.

<u>(1) Triangular wave (n = 3, 5, and 7)</u>

The double-pass experimental results for the triangular wave characteristic of Figure 3.6a are shown in Figures 3.13, 3.14, and 3.15. These figures show the cases of n = 3, n = 5, and n = 7, respectively. It can be seen that the agreement between theory and experimental results is very good for all cases. It was apparent, however, that greater care must be taken in aligning the crystals as one goes to larger values of n . Even so, no particular difficulty was encountered in obtaining any of the three traces of Figures 3.13, 3.14, and 3.15.

<u>(2) Rectangular wave (n = 3, 5, and 7)</u>

Double-pass experimental results for the rectangular wave characteristic of Figure 3.6b are shown in Figures 3.16, 3.17, and 3.18 for the cases of n = 3, 5, and 7, respectively. The agreement between experiment and theory is again seen to be very good for each of the values of n . It is worth noting that adjacent passbands of these characteristics are separated by approximately 1 Angstrom. Thus these birefringent networks are actually band-pass filters having bandwidths of about 1/3 Å and a periodicity of about 1 Å. One might wonder perhaps why the width of the passband does not decrease greatly in going from n = 3 to n = 5 to n = 7. This happens because we are approximating the same ideal function of Figure 3.6b in each of these cases. If we had wished, we could have approximated successively narrower "rectangular functions" as we went to larger values of n , and then the bandwidth could have indeed been reduced. However, our object here was

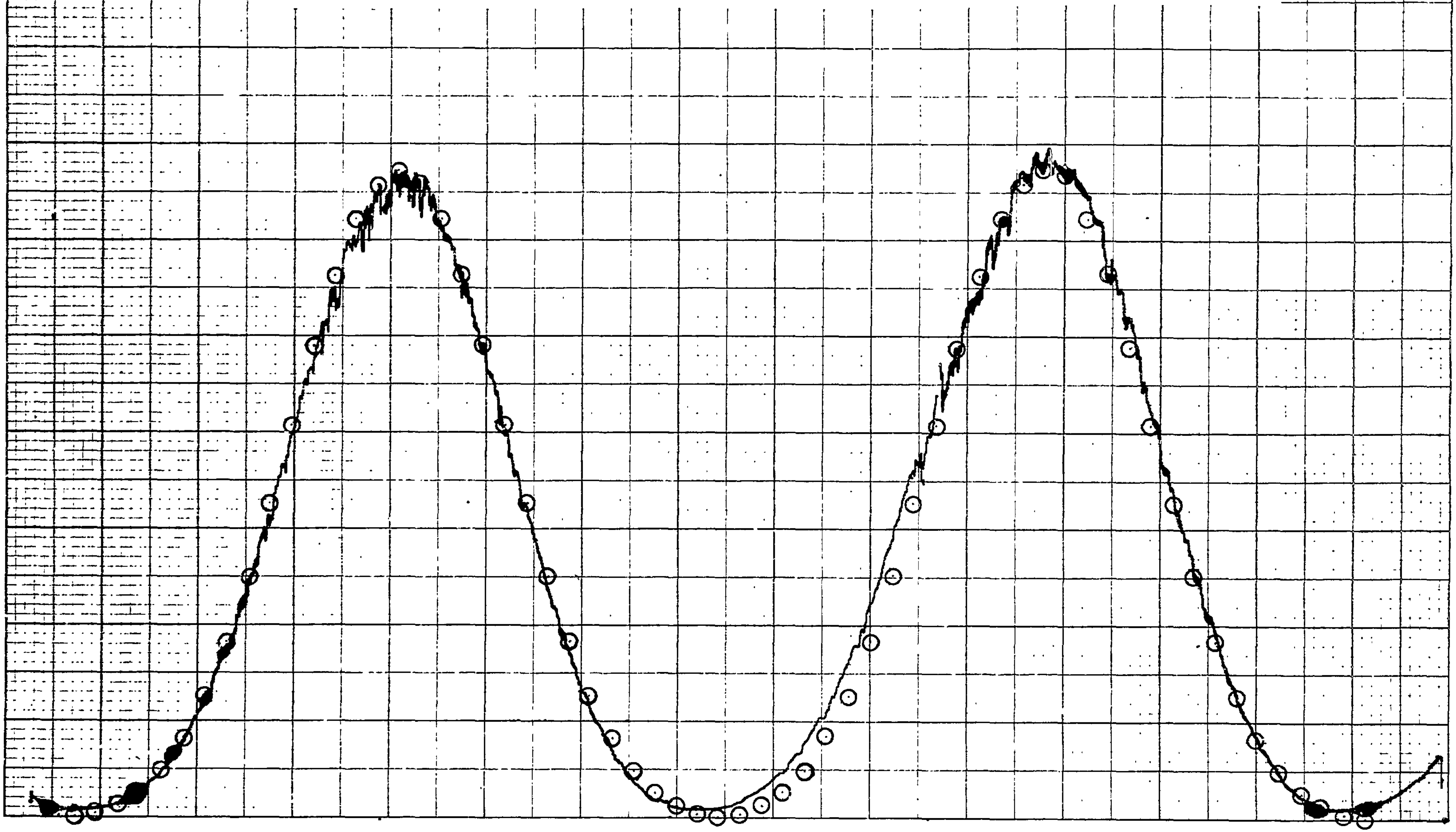

Figure 3.13 Experimental and calculated results for double-pass birefringent network (triangular wave approximation) with n = 3. The figure shows transmitted optical power vs. network temperature (which is equivalent to transmitted optical power vs. optical frequency).

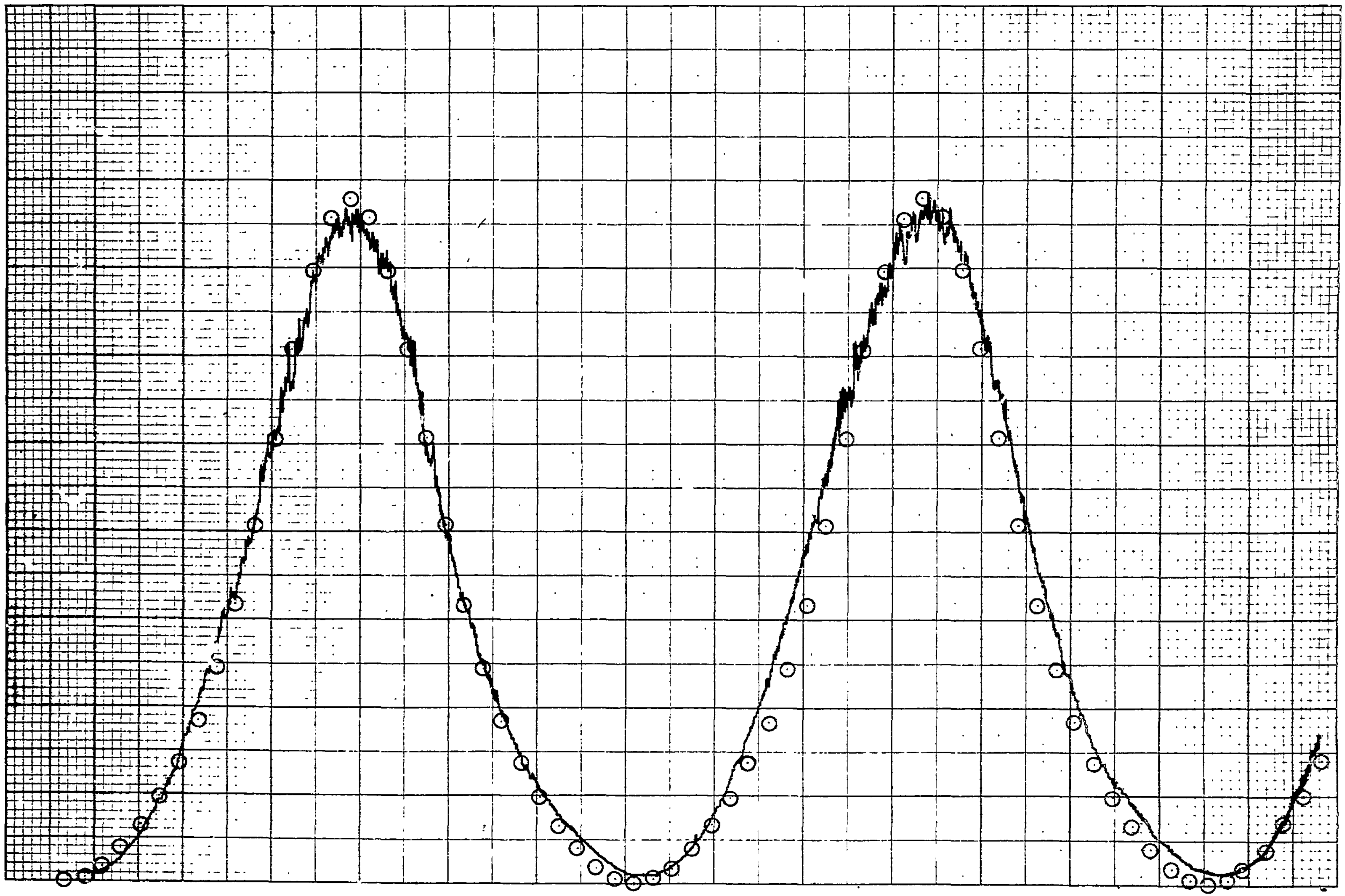

Figure 3.14 Experimental and calculated results for double-pass birefringent network (triangular wave approximation) with n = 5. The figure shows transmitted optical power vs. network temperature (which is equivalent to transmitted optical power vs. optical frequency).

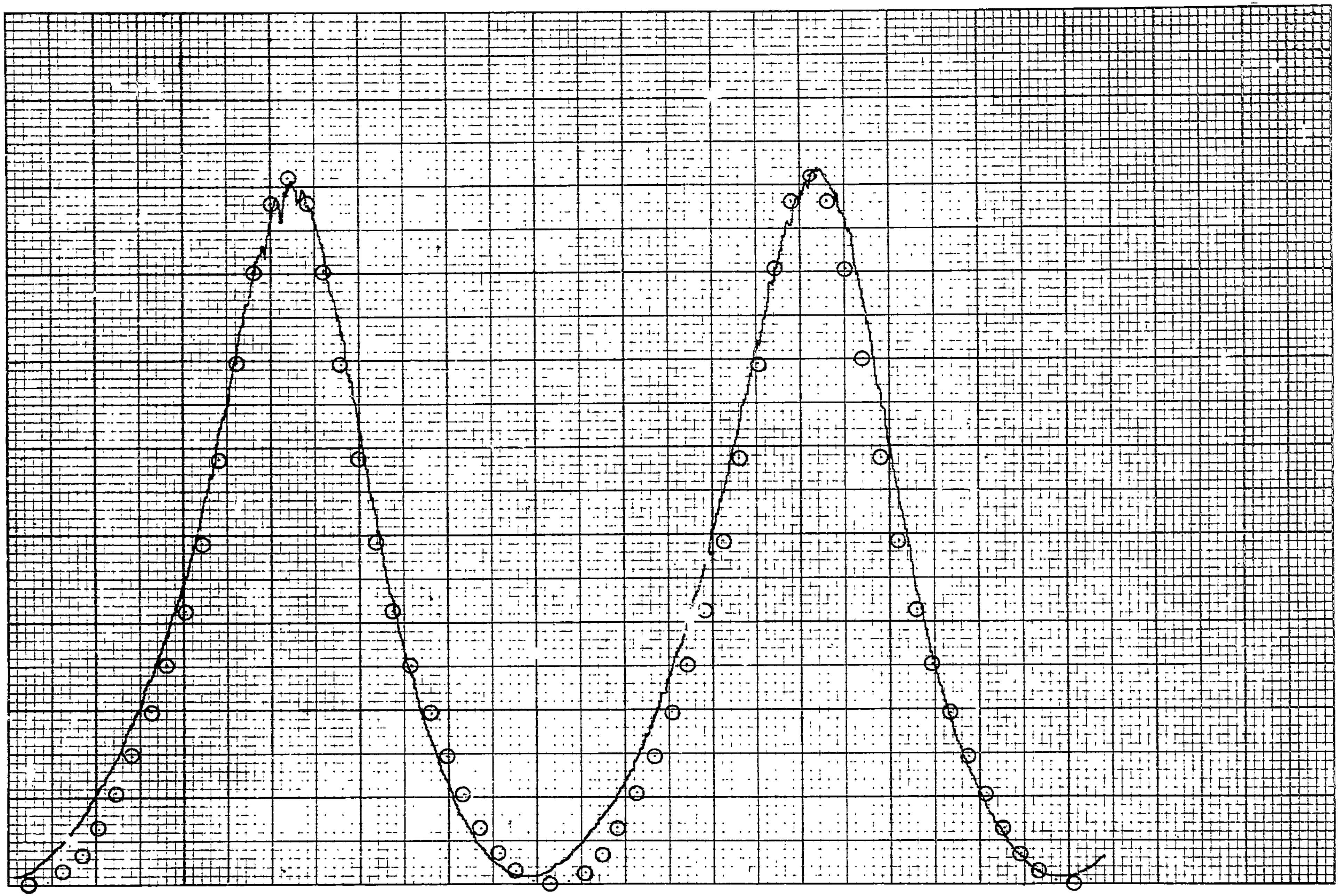

Figure 3.15 Experimental and calculated results for double-pass birefringent network (triangular wave approximation) with n = 7. The figure shows transmitted optical power vs. network temperature (which is equivalent to transmitted optical power vs. optical frequency).

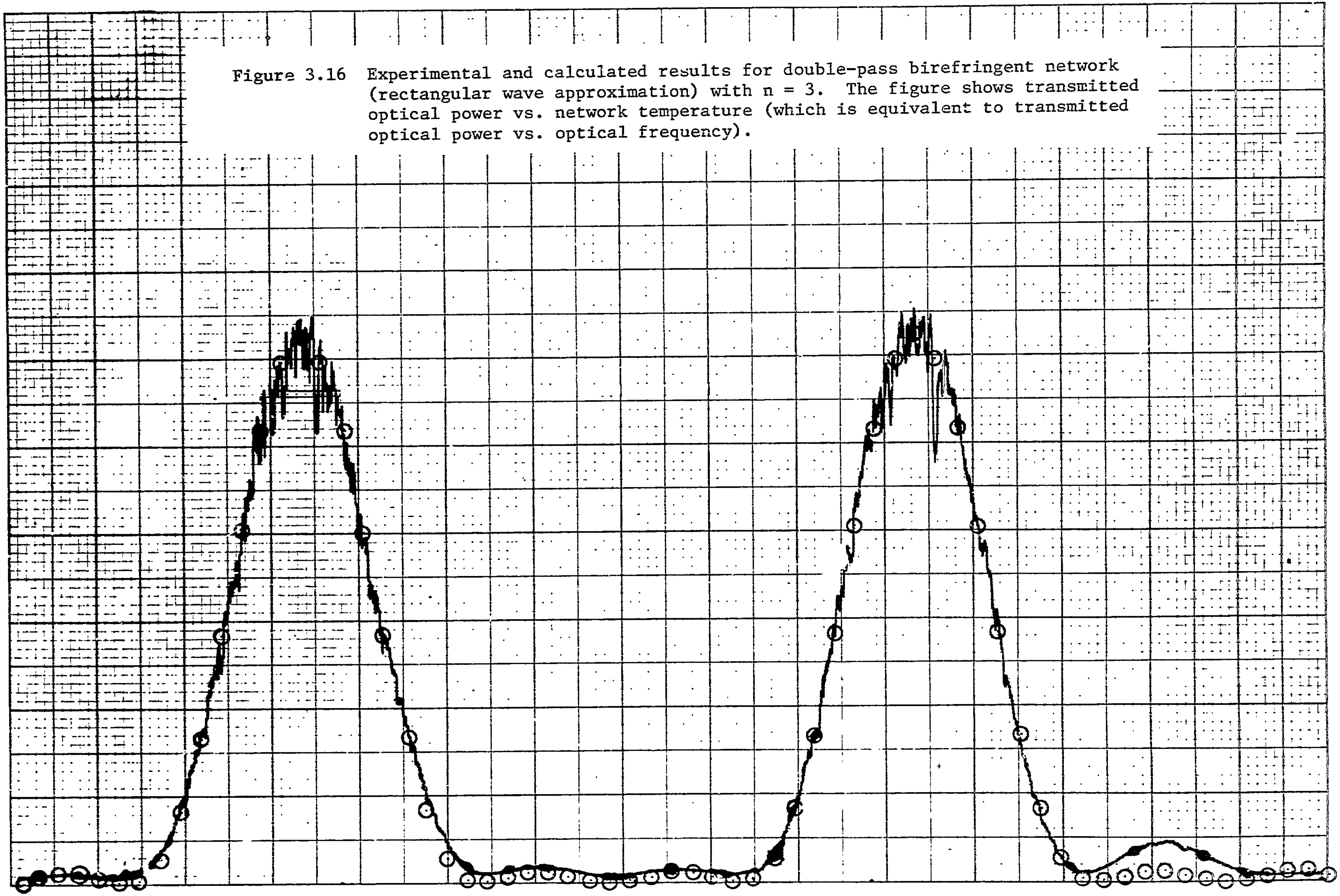

Figure 3.16 Experimental and calculated results for double-pass birefringent network (rectangular wave approximation) with n = 3. The figure shows transmitted optical power vs. network temperature (which is equivalent to transmitted optical power vs. optical frequency).

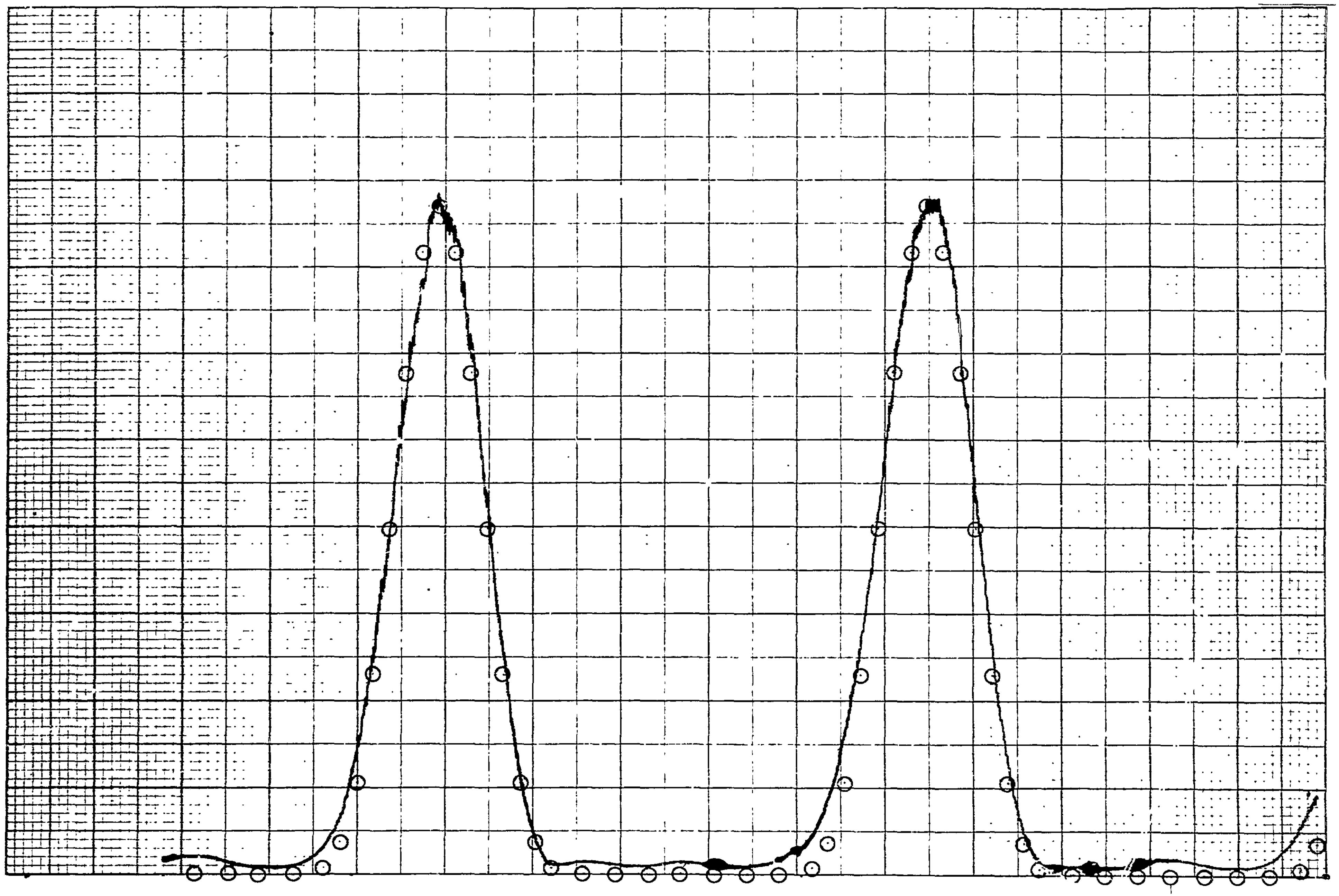

Figure 3.17 Experimental and calculated results for double-pass birefringent network (rectangular wave approximation) with n=5. The figure shows transmitted optical power vs. network temperature (which is equivalent to transmitted optical power vs. optical frequency).

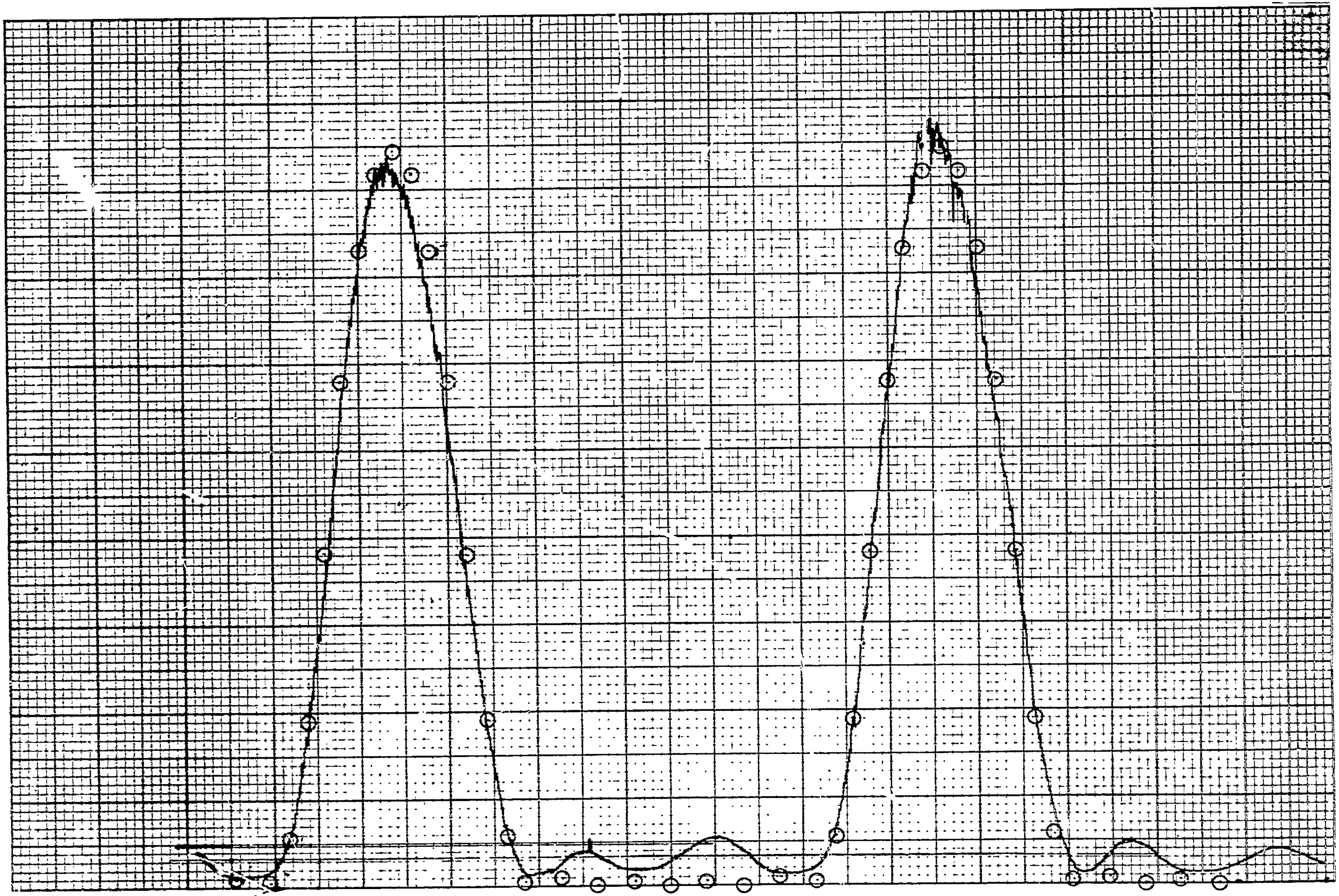

Figure 3.18 Experimental and calculated results for double-pass birefringent network (rectangular wave approximation) with n=7. The figure shows transmitted optical power vs. network temperature (which is equivalent to transmitted optical power vs. optical frequency).

simply to compare experimental results with theory, rather than to obtain the narrowest possible pass-band from a given birefringent network.

(3) Square wave (n = 3)

The experimental results for the square-wave characteristic of Figure 3.7c are given in Figure 3.19 for n = 3. For the n = 3 case, theory and experimental results have failed thus far to show good agreement with theory. This is believed to be due to one of two possible causes: (a) Perhaps this particular characteristic is particularly susceptible to crystal misalignment, or (b) the possibility exists that a mistake is present in our calculations of the angles for the stages of the network. We are presently checking both possibilities but, due to time limitations, have not yet succeeded in pinpointing the problem.

4. Discussion of Results

a. Single-pass experiments

As has been pointed out earlier, quantitative agreement of the n = 3 single-pass experiments with theory is virtually exact. Thus the theory of Reference [1] has been demonstrated to be sufficient for synthesizing arbitrary amplitude-transmission characteristics. Three dissimilar characteristics were synthesized with equally good results. While it is true that none of these characteristics required the more complicated synthesis procedure of Appendix A, nevertheless the two types of network are essentially the same in practical form, and hence there is no reason to believe that new difficulties would arise. In addition, the results from the amplitude modulator experiments to be presented later substantiate the generalized synthesis procedure of Appendix A since this procedure was used to calculate the rotation angles and retardations.

b. Double-pass experiments

The data presented in the previous section substantiates the theory of double-pass networks of Reference [4]. Again agreement with theory is very good. We believe the development of this new technique and its demonstration to be a significant technical advance, and that double-pass techniques should be used whenever possible. The use of more than two passes becomes an attractive possiblity which we believe should be investigated further, for

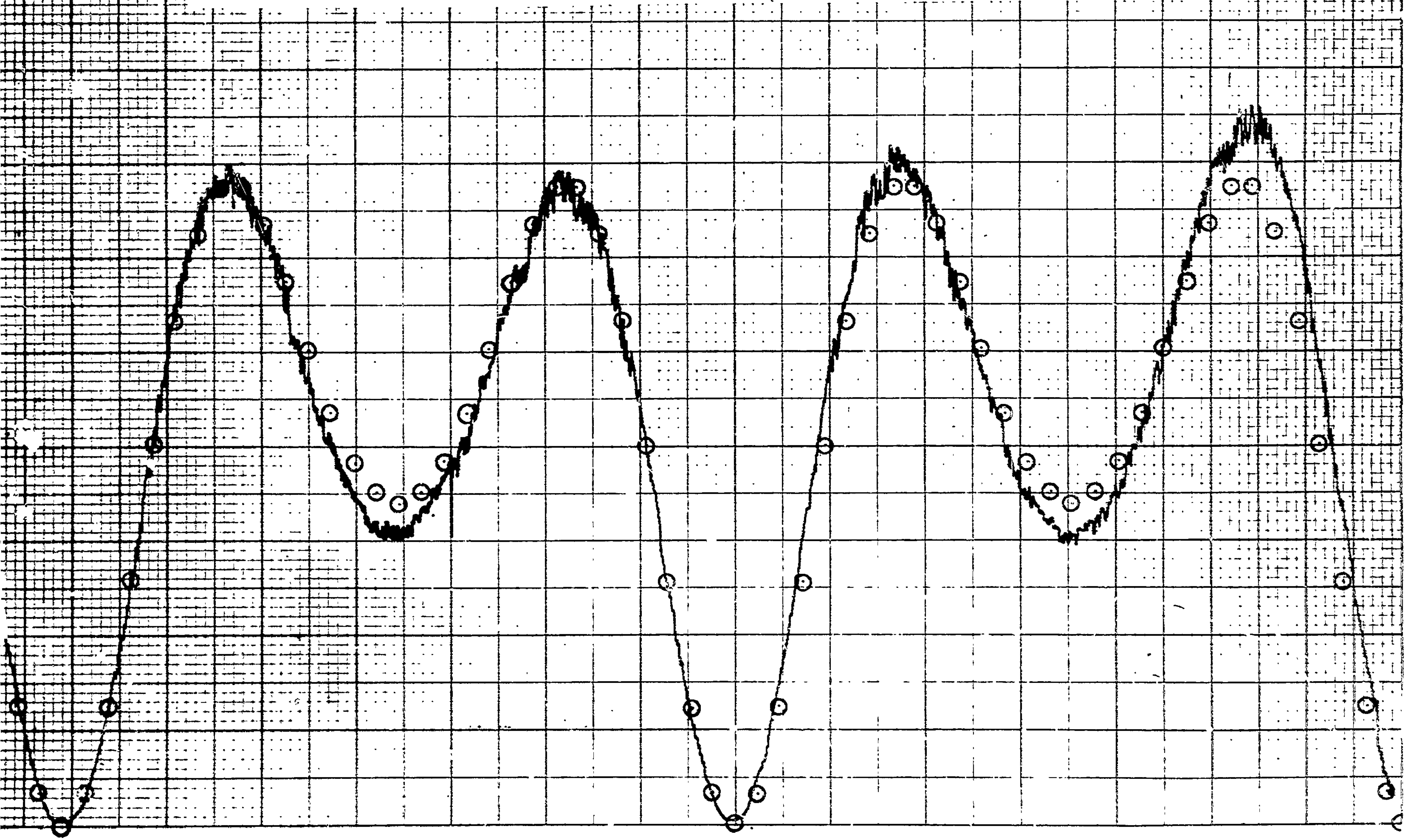

Figure 3.19 Experimental and calculated results for double-pass birefringent network (square wave approximation) with n = 3. The figure shows transmitted optical power vs. network temperature (which is equivalent to transmitted optical power vs. optical frequency).

the advantages of such a system are obvious. The double-pass experiments for n = 3, 5, and 7 have also demonstrated that greater care in crystal alignment must be used for increasing values of n, as might be expected.

B. ELECTRO-OPTIC NETWORKS: AMPLITUDE MODULATOR

We now discuss the results of experiments which were performed on electro-optic networks. The set of experiments carried out had an object of verifying the amplitude-modulator theory of Appendix C. A three-stage amplitude modulator was designed (using that theory) and tested, and the measured distortion compared with the predicted distortion. In addition, a conventional (one-stage) modulator was tested and its measured and calculated distortion compared. The factors which influenced the design of our amplitude modulator will now be discussed.

1. Physical Considerations

a. Crystal material and size

As in the naturally birefringent case, many materials are suitable for use as the basic "building blocks" of these networks. One must consider the optical frequency of interest, the optical quality of the material, the electro-optic coefficients and many others.

In the present experiments, it was decided to use KDP as the electro-optic material. In order to avoid the problem of natural birefringence of KDP, the crystals were oriented so that the light propagated along the optic axis. (An oven would have been required to stabilize the temperature if the light propagated at right angles to the optic axis, for KDP is birefringent in that orientation.) Again the crystals were chosen to be 1 cm by 1 cm in cross section, while the length was chosen to be 4 cm. A sketch of the crystal size and orientation is given in Figure 3.20.

b. Crystal tolerances and compensators

The crystal tolerances are less severe in this case than for calcite since the lengths do not have to be kept exactly the same. This is because the half-wave retardation voltage of KDP is independent of length in the orientation being used. The parallelism requirement of the end faces is also less stringent.

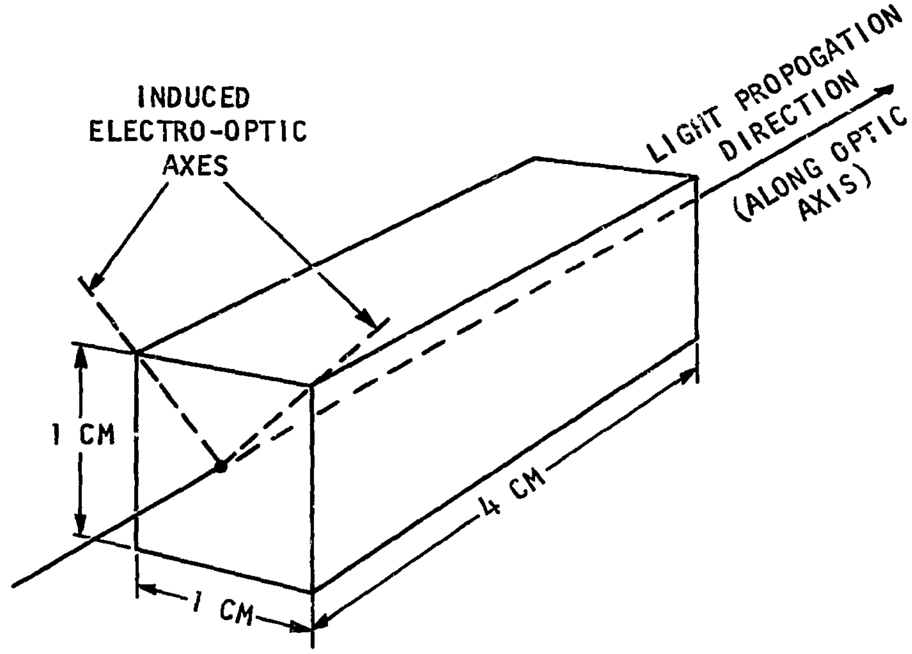

Figure 3.20 KDP crystal used as basic unit of three-stage amplitude modulator.

Again it was decided to use quartz compensators. In this case, each compensator was ground and polished to the precise retardation required by the theory.

c. Temperature effects

Since light propagates along the optic axis of the KDP crystals, the only effect of a change in temperature is to change the retardation of the compensators. It has been pointed out previously that the retardation of the quartz compensators changes by about 1° per °C. Thus fluctuations of a few degrees Centigrade are not harmful.

d. Alignment

The isogyre pattern was again used to align the crystals. In this case, one sees the characteristic "bull's eye" pattern obtained by shining diverging or converging light through a crystal between crossed polarizers. The alignment procedure is indicated schematically in Figure 3.21a, and a photograph of the observed pattern is given in Figure 3.21b. Each crystal was carefully aligned so the laser beam hit in exactly the middle of the pattern.

e. Method of applying modulating voltage to KDP

Large electric fields are required to modulate KDP when the orientation of Figure 3.20 is used. These large fields may be achieved in either of two ways. The first is to use a resonant cavity of high Q in which the KDP is placed, while the second possibility is to apply a large voltage to a nonresonant circuit. The first method has the advantage of requiring a lower applied voltage, but suffers from at least one serious disadvantage. It would be necessary for each resonant circuit of the modulator to be tuned precisely to the same frequency. If the resonant circuits were not tuned precisely to the same frequency, the voltage applied to the various stages would differ in amplitude and phase thereby causing error in the results. To avoid this problem, we chose to use nonresonant circuits driven by an amplifier capable of producing a large voltage swing. With this arrangement, a voltage of about 7500 volts (zero to peak) was necessary in order to obtain 100% amplitude modulation.

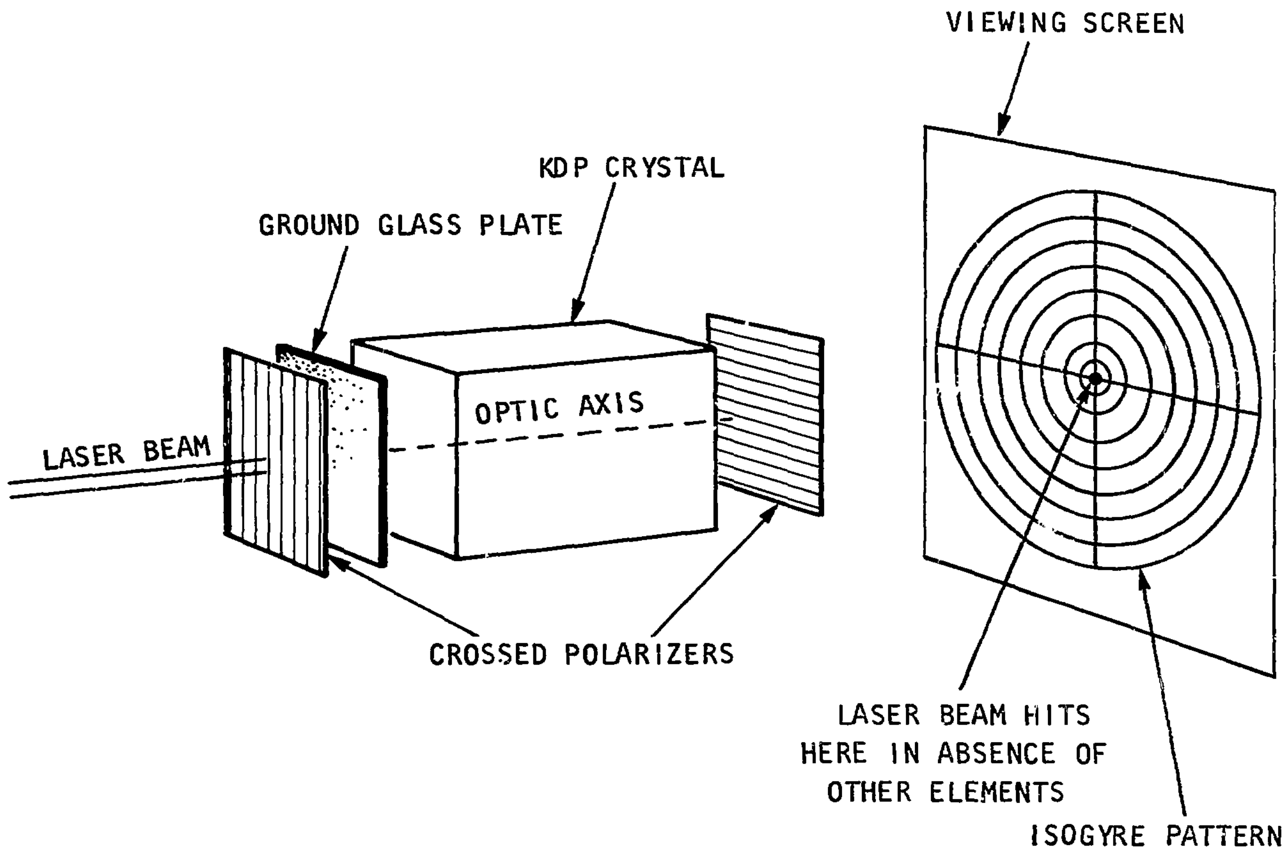

Figure 3.21a Experimental setup for aligning KDP crystals

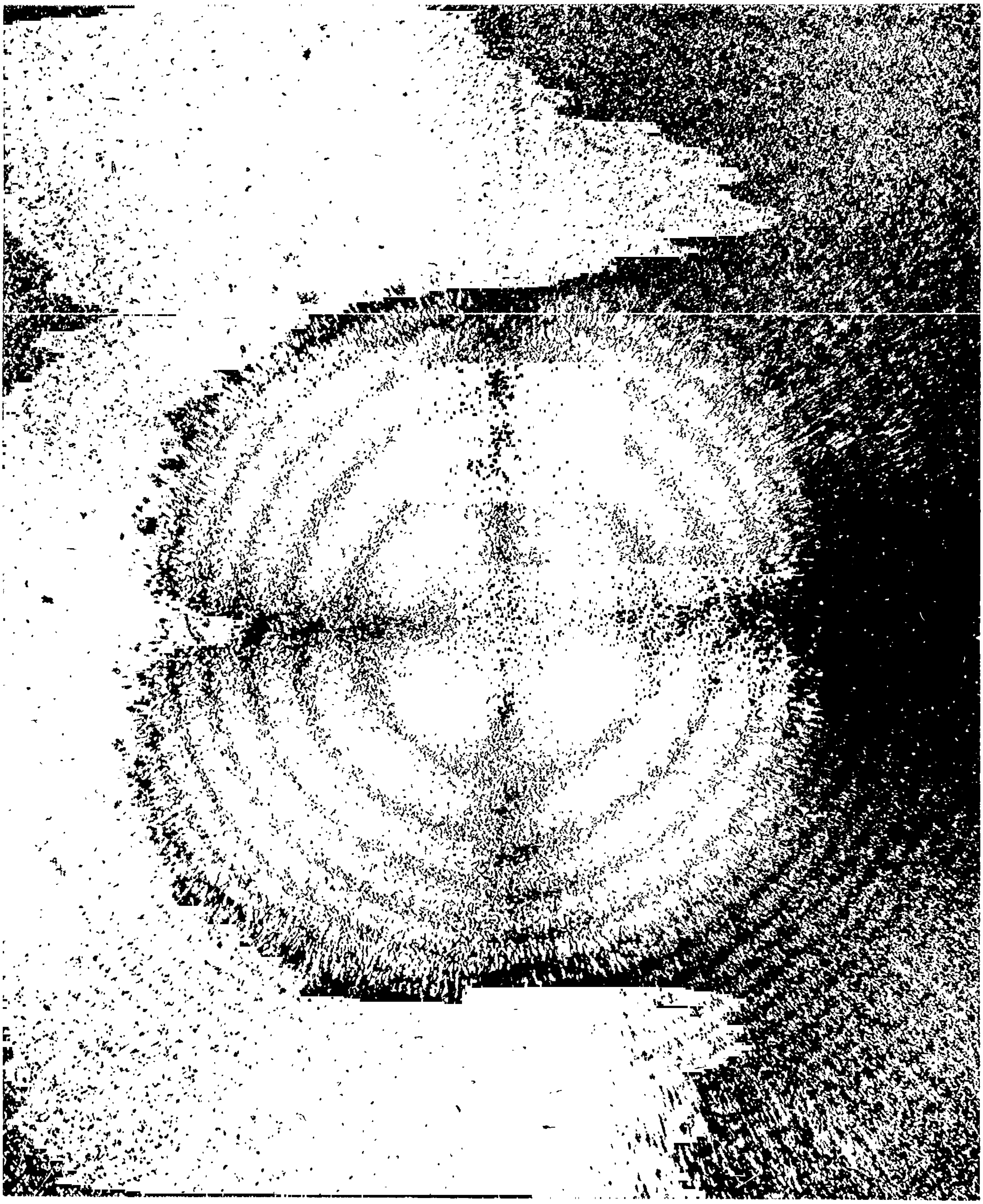

Figure 3.21b Typical isogyre pattern for KDP

2. Experimental Apparatus

a. Crystal holders

The KDP crystal holders were constructed as in Figures 3.22a and 3.22b. The KDP crystals were mounted in Rexolite rectangular blocks which were in turn supported in aluminum cylinders by nylon screws. Copper electrodes with holes drilled to allow passage of the laser beam were mounted at each end of the crystal, with one electrode grouned to the cylinder and the other connected to the high voltage. The compensators were placed in brass holders which were slipped in behind the rear electrode.

Early experiments showed that the KDP was strained, causing slight natural birefringence. To cancel this natural birefringence, additional compensators were used with each stage. These compensators were mounted in the same brass holders which contain the compensators required by theory.

b. Plexiglass box

A plexiglass box with an aluminum "V" block at the bottom was constructed to hold the crystals. This apparatus is shown in Figure 3.23. A high-voltage bus runs the length of the box, and the crystal electrodes are connected to it.

c. High-voltage amplifier

It was found that a high-voltage amplifier with a peak-to-peak voltage swing of 15,000 volts was needed to obtain 100% modulation. Such a device was constructed using a high-voltage beam tetrode tube, with feedback to reduce distortion. A schematic of the amplifier is shown in Figure 3.24. The experiments were all run at a modulating frequency of 1000 Hz. The amplifier was driven by a signal generator.

d. Detector

An RCA 931A phototube was used as a detector.

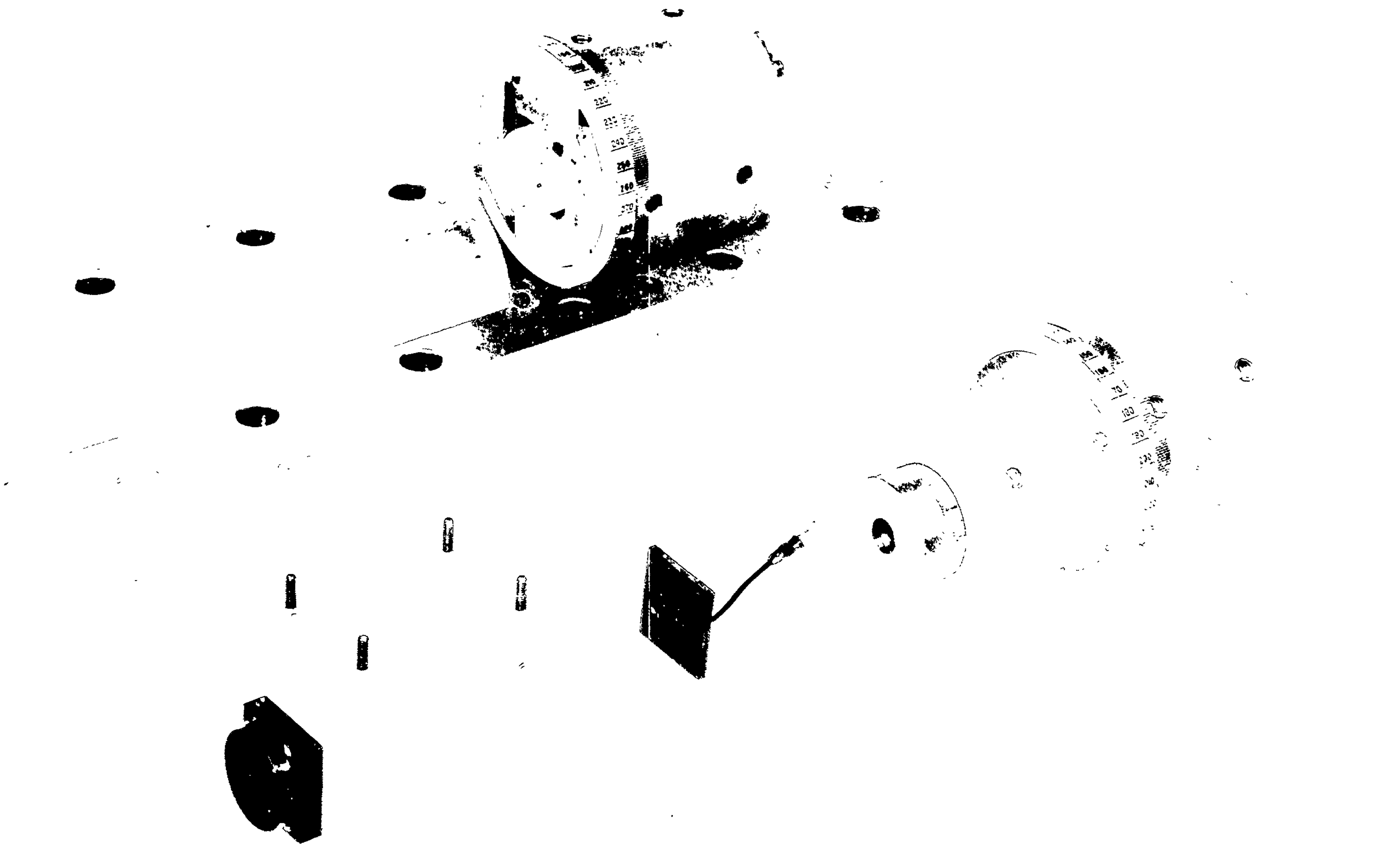

Figure 3.22a Holder in which KDP crystals are mounted

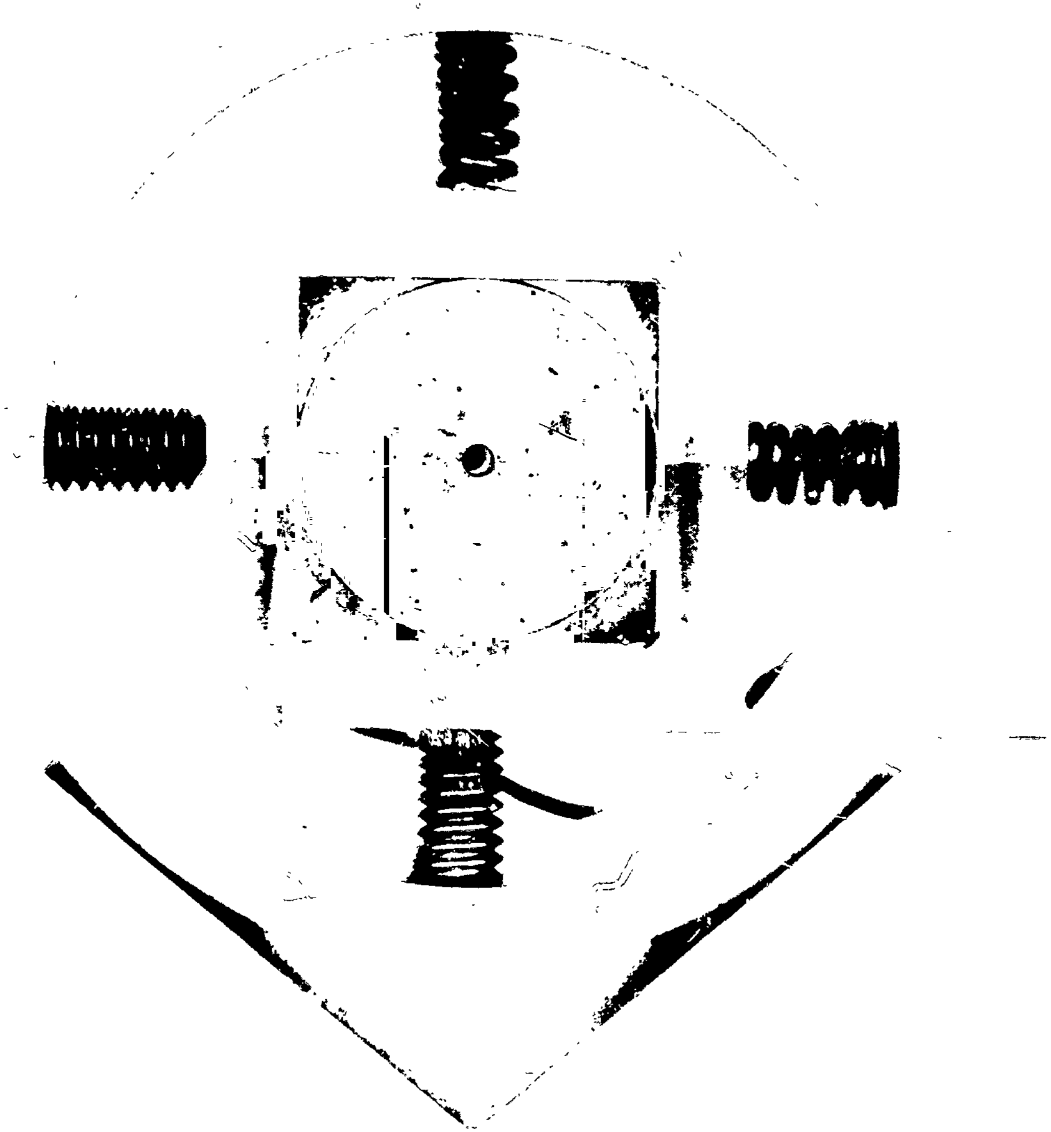

Figure 3.22b End view of KDP crystal holder

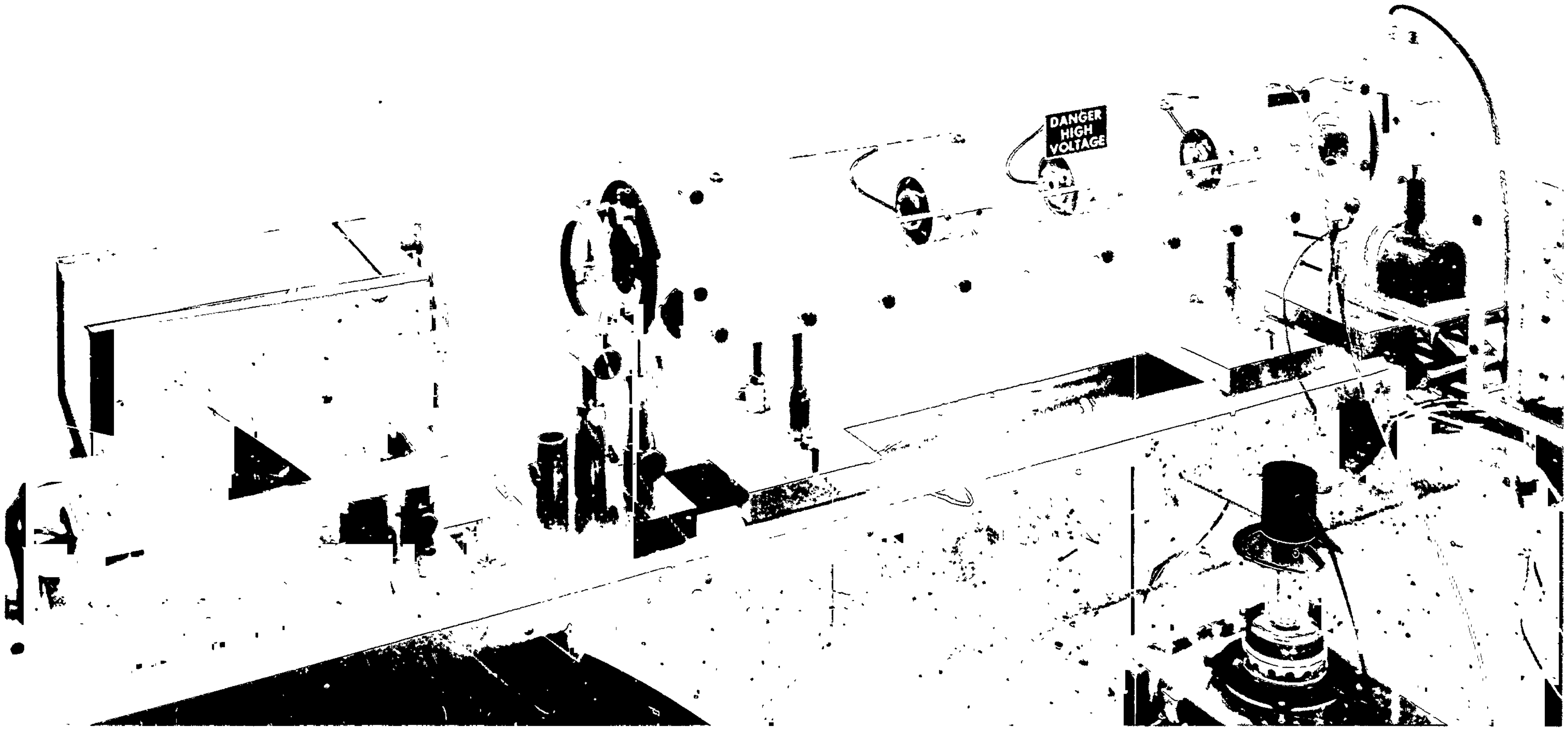

Figure 3.23 Three-stage amplitude modulator

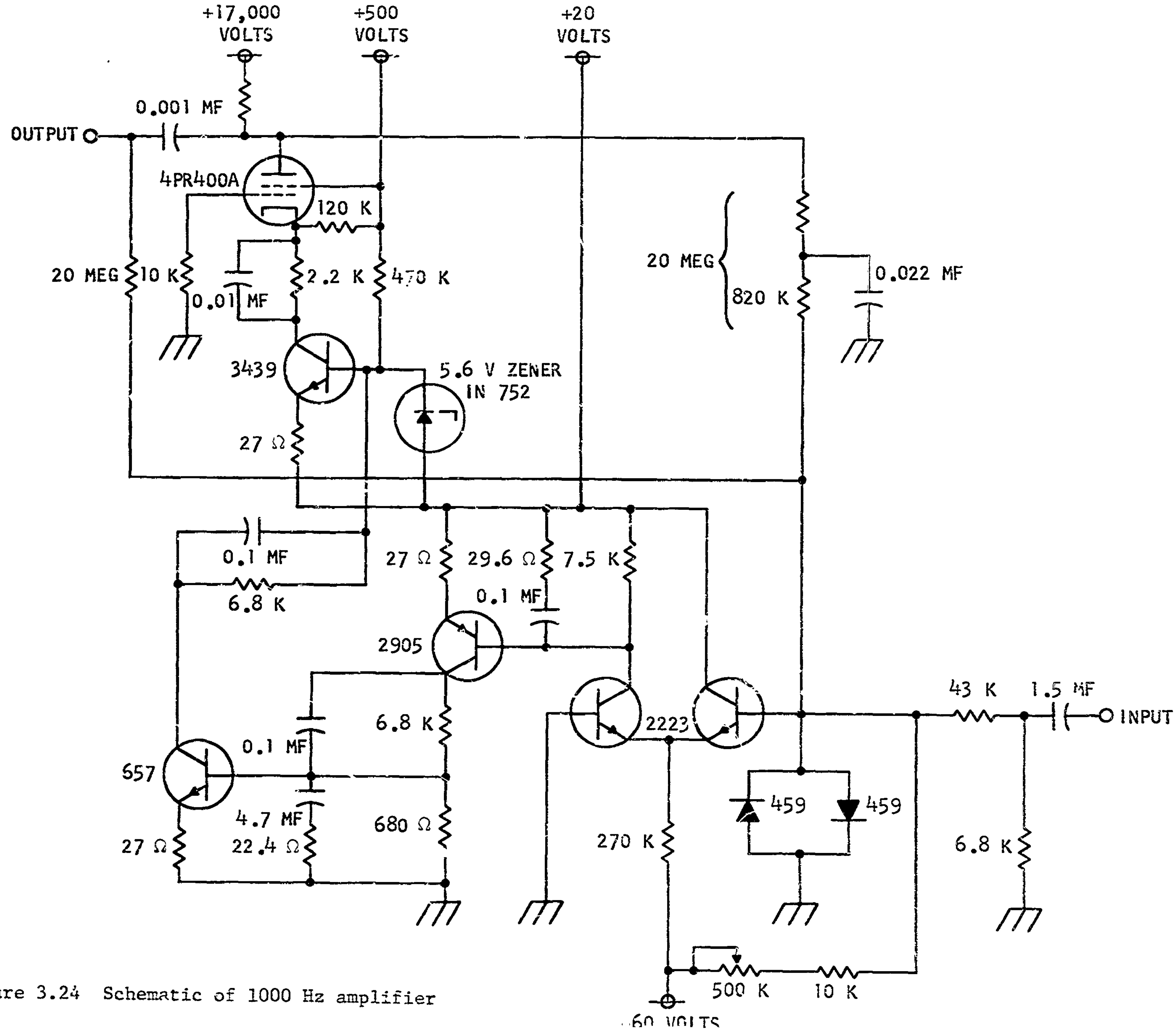

Figure 3.24 Schematic of 1000 Hz amplifier

e. Experimental setup

The components described above were set up as shown in Figure 3.25. The crystals were rotated to the angles prescribed by the synthesis procedure of Appendix C, and a wave analyzer was used to measure the amplitude of fundamental and harmonics as a function of the drive voltage.

3. Data

The data obtained from the experiment is shown in Figures 3.26a, 3.26b, and 3.26c, where fundamental, second harmonic, and third harmonic amplitudes are plotted as a function of normalized modulating voltage. Solid curves represent theoretical values, with the experimental points plotted as circles for $n = 1$ and as squares for $n = 3$. It will be noted that the fundamental and third harmonic curves fit rather well for both $n = 1$ and $n = 3$, while the second harmonic curve is somewhat more irregular. Particularly conspicuous is the notch in the second harmonic curve for the three-crystal case. It was found that this notch could be moved by slightly rotating one of the crystals. Later tests revealed that one of the crystals was modulating to only 85% the depth of the other two, and it is felt that making all crystals modulate equally will remove the notch.

Also of note is that the $n = 1$ modulator, while theoretically producing no second harmonic modulation, actually had more than the three-crystal modulator. The reason for this has not been determined, but its presence makes the three-crystal modulator even more valuable.

4. Discussion of Results

The experimental data presented in the preceding section agree quite well with the theory of Appendix C. As pointed out earlier, one of the three crystals used in the modulator differed from the other two by 15% in electro-optic effect. We are presently modifying the crystal holders in an attempt to equalize the modulation of the three crystals. It will not be possible, however, to give these results in this report. However, the fact that reasonably good results were obtained in spite of this problem is very encouraging, for it appears that such modulators are not overly sensitive to crystal differences.

n	θ_1	b_1 (rad)	θ_2	b_2 (rad)	θ_3	b_3 (rad)	θ_p
1	$45^\circ 00'$	1.57	--	-----	--	-----	-45°
3	$4^\circ 40'$	2.95	$49^\circ 32'$	4.52	$49^\circ 32'$	6.09	$85^\circ 20'$

Table II

Rotation Angles and Compensator Delays for One- and Three-Stage Amplitude Modulators Used in Experiment

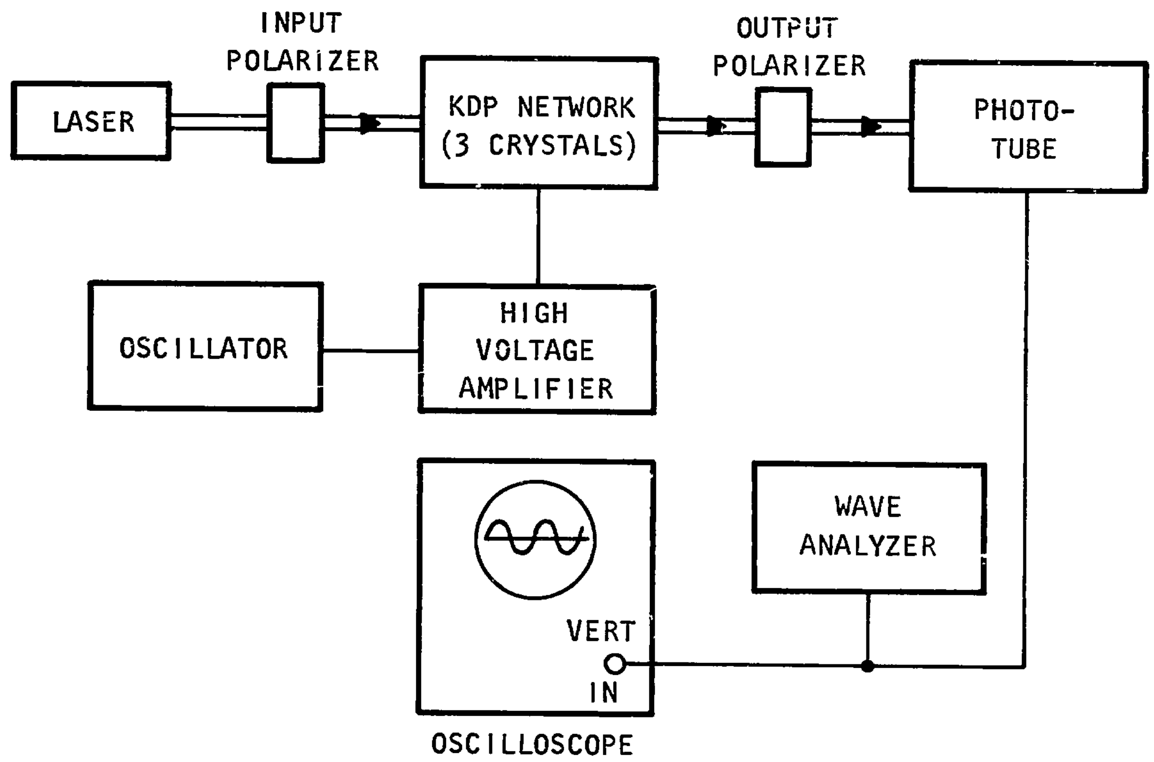

Figure 3.25 Experimental setup used to measure the performance of one- and three-stage amplitude modulators.

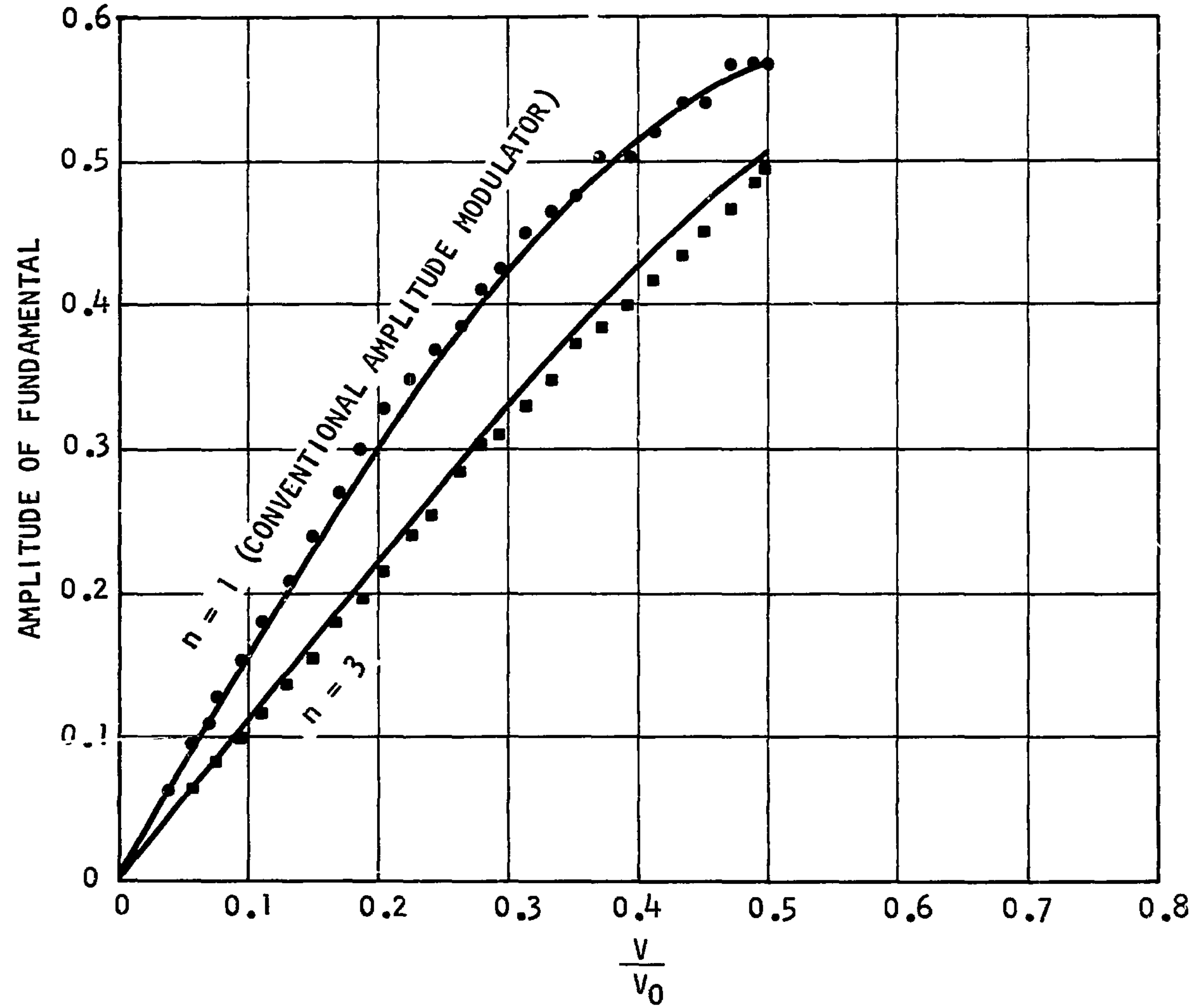

Figure 3.26a Measured and calculated amplitude of fundamental vs. V/V_0 for the one- and three-stage modulators of Table II.

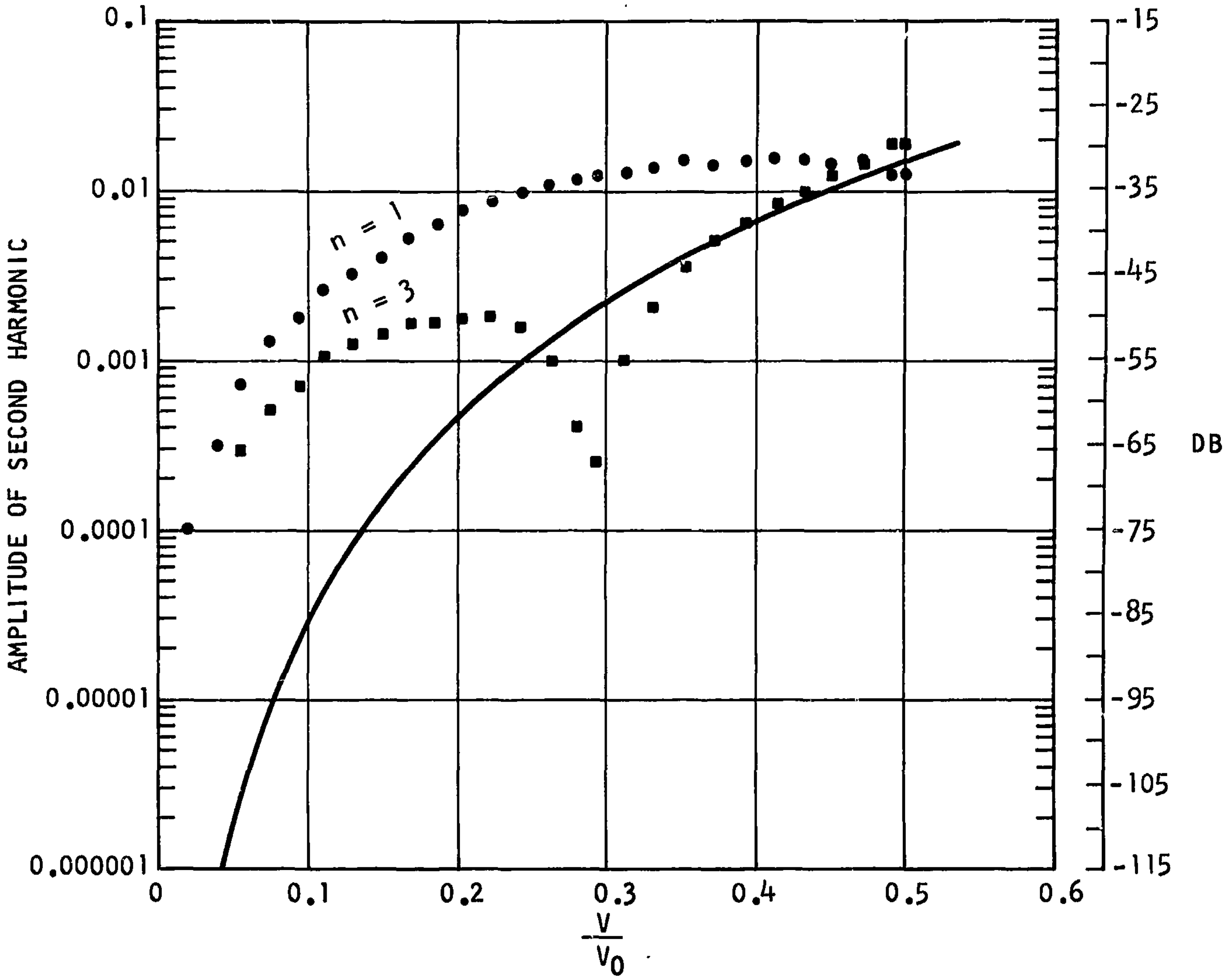

Figure 3.26b Measured and calculated amplitude of the second harmonic vs. V/V_0 for the one- and three-stage modulators of Table II. The calculated amplitude of the second harmonic for a one-stage modulator is zero.

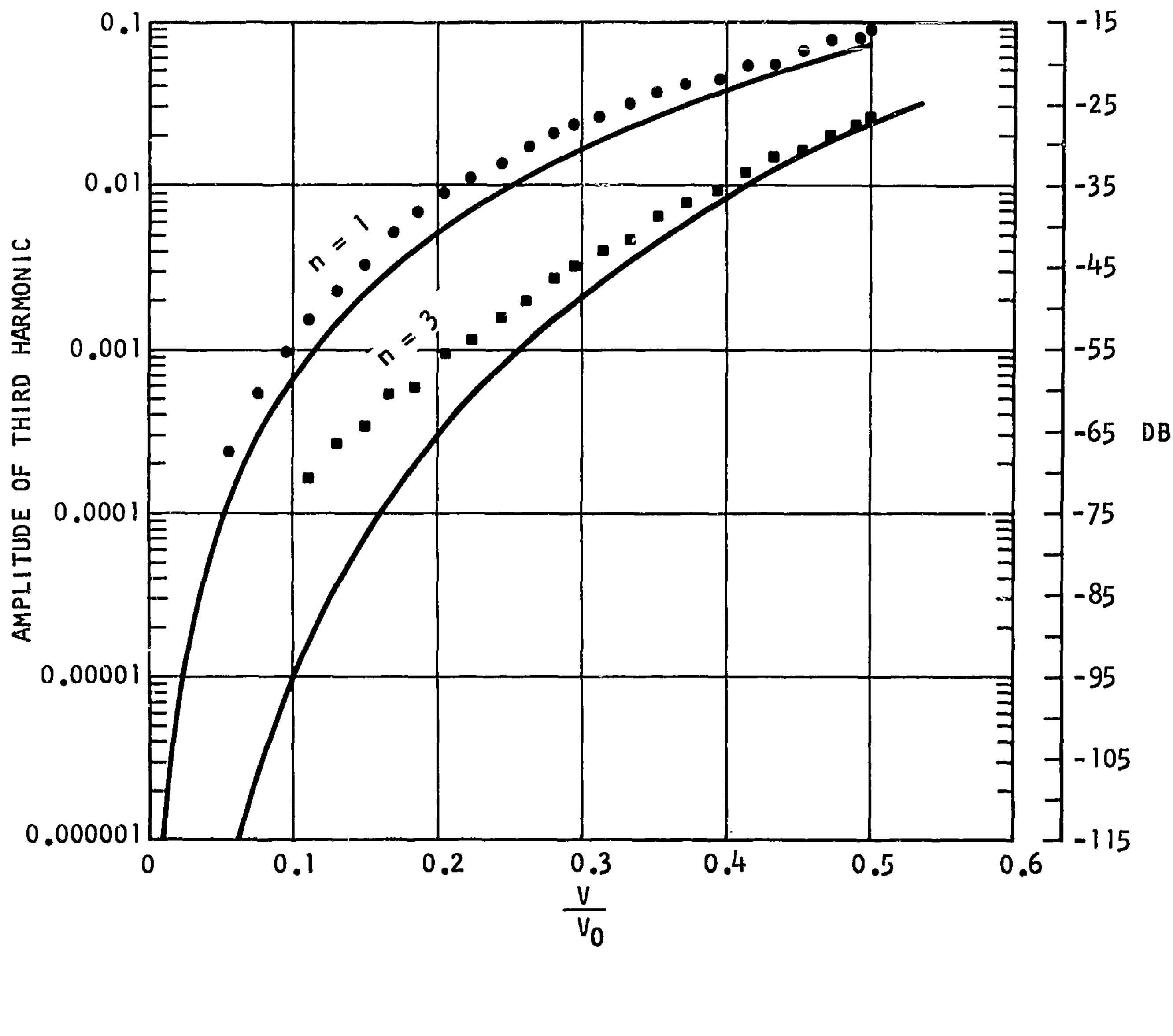

Figure 3.26c Measured and calculated amplitude of the third harmonic vs. V/V_0 for the one- and three-stage modulators of Table II.

We feel that this experimental data verifies the theory reasonably well. Thus it indeed appears possible to synthesize improved amplitude modulators using the techniques of Appendix C.

IV. CONCLUSIONS AND RECOMMENDATIONS

The goal of this program was to advance the state of the art of optical birefringent devices. Progress in both theory and experimentation was made and has been reported. The advances in theory have resulted in (1) the availability of more general and versatile synthesis techniques; (2) a simplification in the practical form of many birefringent devices; and (3) some detailed analyses of certain particularly important birefringent devices.

Experiments were performed which verify much of the theory and, in addition, demonstrate the practicality of the type of devices under study. These experiments included tests on three-stage single-pass birefringent networks and tests on three-, five-, and seven-stage double-pass networks. The results of these experiments agree very well with predicted results.

Under the conditions of this program, three devices are to be delivered to NASA. These devices will be a single-pass birefringent network having $n = 3$, a double-pass network (derived from the single-pass network) having $n = 7$, and a three-stage electro-optic amplitude modulator.

Both the theory and experiments indicate that the birefringent networks have become sufficiently well understood to consider the design and realization of particular devices. The device which would probably be of greatest interest at present is a very narrow-band band-pass filter.

Several unsolved theoretical problems remain which are quite important. First, any techniques which could be found for increasing (or even analyzing) the angular aperture of birefringent networks would be most welcome. Second, double-pass techniques developed on this and previous programs have substantially simplified the practical form of birefringent networks. Any techniques which allow still more passes through the network would give still further simplification. Third, the synthesis of networks composed of unequal-length crystals is of extreme importance since that would yield networks composed of fewer, but longer crystals. Still other topics come to mind, but these are probably the most significant.

V. SUMMARY OF RESEARCH CONTRIBUTIONS ON BIREFRINGENT DEVICES

The major research achievements of this program on optical birefringent devices are summarized below:

(1) A generalization of the original birefringent network synthesis procedure of Harris, et al. [1] was found which permits the synthesis of networks having asymmetric transmittances. This new procedure substantially increases the versatility of birefringent networks at no expense in network complexity. The new procedure is applicable both to naturally-birefringent networks and electro-optic networks, but will probably be most important in connection with the latter.

(2) A double-pass technique was developed which could be used with the new synthesis procedure mentioned above. The double-pass technique reduces by a factor of two the number of network components needed to realize a given asymmetric transmittance. A double-pass network is approximately one-half the size of the corresponding single-pass network.

(3) Techniques were developed for synthesizing multi-stage amplitude modulators having less distortion than conventional (single-stage) modulators. Two cases were considered: (a) the synthesis of modulators to be used with a linear detector, and (b) the synthesis of modulators to be used with a square-law detector. Designs for 1-, 2-, 3-, 4-, 5-, 6-, 7-, 8-, 9-, and 10-stage modulators were tabulated.

(4) Single-pass and double-pass experiments were performed on naturally-birefringent networks using calcite as the birefringent material. The results of these experiments provide the first experimental confirmation of the synthesis techniques involved. Single-pass experiments were performed on networks with $n = 3$, while double-pass experiments were performed on networks with $n = 3, 5$, and 7.

(5) Experiments were performed to verify the calculations on the synthesis of amplitude modulators. Distortion measurements made on one- and three-stage amplitude modulators agreed reasonably well with predicted results.

VI. PUBLICATIONS AND ORAL PRESENTATIONS

Full support from this contract was acknowledged in each of the following publications and oral presentations.

Journal Publications

1. E. O. Ammann and J. M. Yarborough, "Optical Network Synthesis Using Birefringent Crystals. V. Synthesis of Lossless Networks Containing Equal-Length Crystals and Compensators," J. Opt. Soc. Am., vol. 56, pp. 1746-1754, December 1966.

2. E. O. Ammann and J. M. Yarborough, "Optical Network Synthesis Using Birefringent Crystals. VI. Additional Techniques for the Synthesis of Lossless Double-Pass Networks," (accepted for publication), J. Opt. Soc. Am.

3. E. O. Ammann and J. M. Yarborough, "Synthesis of Electro-Optic Modulators for Amplitude Modulation of Light," (submitted for publication).

4. J. M. Yarborough and E. O. Ammann, "Experiments on Single-Pass and Double-Pass Lossless Birefringent Networks," (to be submitted for publication).

5. J. M. Yarborough and E. O. Ammann, "Experiments on One- and Three-Stage Electro-Optic Light Modulators," (to be submitted for publication).

Oral Presentations

1. E. O. Ammann and J. M. Yarborough, "Optical Network Synthesis Using Birefringent Crystals. V. Synthesis of Lossless Networks Containing Equal-Length Crystals and Compensators," presented at the 1966 Fall Meeting of the Optical Society of America.

2. E. O. Ammann and J. M. Yarborough, "Synthesis of Electro-Optic Modulators for Amplitude Modulation of Light," (to be submitted for presentation).

3. E. C. Ammann and J. M. Yarborough, "Experiments on Single-Pass and Double-Pass Lossless Birefringent Networks," (to be submitted for presentation at the 1967 Fall Meeting of the Optical Society of America).

VII. REFERENCES

1. S. E. Harris, E. O. Ammann, and I. C. Chang, "Optical Network Synthesis Using Birefringent Crystals. I. Synthesis of Lossless Networks of Equal-Length Crystals," J. Opt. Soc. Am., vol. 54, pp. 1267-1279, October 1964.

2. E. O. Ammann and I. C. Chang, "Optical Network Synthesis Using Birefringent Crystals. II. Synthesis of Networks Containing One Crystal, Optical Compensator, and Polarizer per Stage," J. Opt. Soc. Am., vol. 55, pp. 835-841, July 1965.

3. E. O. Ammann, "Optical Network Synthesis Using Birefringent Crystals. III. Some General Properties of Lossless Birefringent Networks," J. Opt. Soc. Am., vol. 56, pp. 943-951, July 1966.

4. E. O. Ammann, "Optical Network Synthesis Using Birefringent Crystals. IV. Synthesis of Lossless Double-Pass Networks," J. Opt. Soc. Am., vol. 56, pp. 952-955, July 1966.

5. E. O. Ammann, "Synthesis of Electro-Optic Shutters having a Prescribed Transmission vs. Voltage Characteristic," J. Opt. Soc. Am., vol. 56 pp. 1081-1088, August 1966.

Appendix A

N 67-20523

OPTICAL NETWORK SYNTHESIS USING BIREFRINGENT CRYSTALS.

V. SYNTHESIS OF LOSSLESS NETWORKS CONTAINING EQUAL-LENGTH CRYSTALS AND COMPENSATORS

E. O. Ammann and J. M. Yarborough
Electronic Defense Laboratories
Sylvania Electronic Systems - Western Operation
Mountain View, California

published in
Journal of the Optical Society of America
vol. 56, pages 1746-1754
December 1966

Optical Network Synthesis Using Birefringent Crystals. V. Synthesis of Lossless Networks Containing Equal-Length Crystals and Compensators*

E. O. AMMANN AND J. M. YARBOROUGH
Electronic Defense Laboratories, Sylvania Electronic Systems, Mountain View, California 94040
(Received 23 June 1966)

Part I of this series reported a procedure for synthesizing birefringent networks having a prescribed amplitude transmittance. The desired transmittance $C(\omega)$ was written as $C(\omega)=C_0+C_1e^{-ia\omega}+C_2e^{-i2a\omega}+\cdots+C_ne^{-ina\omega}$, where the C_i could be arbitrarily chosen as long as each was real. The synthesis procedure of this paper is a generalization of the procedure of Part I and allows for the realization of $C(\omega)$ having complex C_i. The resulting network consists of n stages between an input and output polarizer, with each stage containing a birefringent crystal and (achromatic) optical compensator. The form of this network is essentially the same as the practical form of the network obtained from Part I, and hence the additional versatility is obtained at no extra cost in network complexity.
INDEX HEADINGS: Polarization; Crystals; Filters; Birefringence.

I. INTRODUCTION

PART I of this series[1] described a procedure for synthesizing birefringent networks whose amplitude transmittance could be specified. The purpose of this paper is to describe a generalization of that procedure which provides still greater flexibility in the synthesis of birefringent networks.

The procedure of Part I allows the realization of a birefringent network whose amplitude transmittance $C(\omega)$ is of the form,

$$C(\omega)=C_0+C_1e^{-ia\omega}+C_2e^{-i2a\omega}+\cdots+C_ne^{-ina\omega}. \quad (1)$$

The number of terms employed in $C(\omega)$ is finite but arbitrary. The choice of the coefficients (the C_i) is also arbitrary as long as each C_i is real. The form of the network obtained from the synthesis procedure of Part 1 is shown in Fig. 1. The network consists of a series of identical cascaded birefringent crystals between an input and output polarizer. The network may be thought of as composed of several stages, with each stage consisting of one birefringent crystal. A network containing n stages is required for a $C(\omega)$ having $n+1$ terms. Once $C(\omega)$ has been chosen, the rotation angles (the ϕ_i) of the crystals and the output polarizer can be calculated from the synthesis procedure.

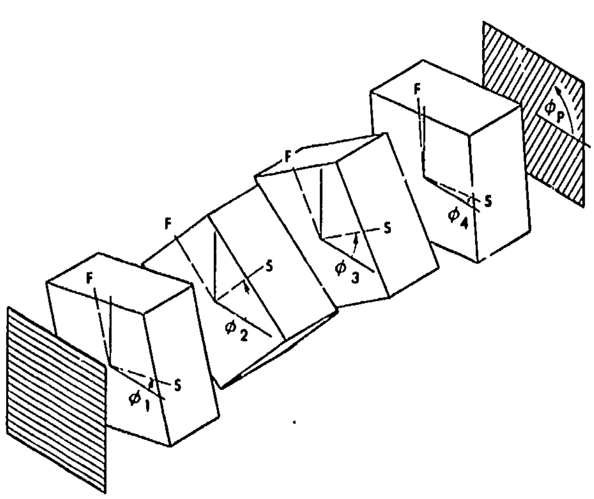

FIG. 1. Basic configuration of birefringent network (4 stages) obtained from the synthesis procedure of Part I. F and S denote the "fast" and "slow" axes of the birefringent crystals.

The synthesis procedure of this paper allows greater freedom in the choice of $C(\omega)$ and results in a network whose basic form is shown in Fig. 2. The desired amplitude transmittance $C(\omega)$ is still written in the form of Eq. (1), but the C_i may now be complex. An n-stage network is again required to realize a $C(\omega)$ having $n+1$ terms, but each stage now consists of an optical compensator[2] and a birefringent crystal. The synthesis procedure determines the rotation angle of each crystal, the retardation introduced by each compensator, and the rotation angle of the output polarizer.

The networks of Part I have been termed lossless birefringent networks since there are no energy-dissipating components between the input and output polarizers. The networks of this paper are lossless in the same sense, since no internal polarizers are required.

The following sections contain a description of the synthesis procedure and give an example of its application.

II. SYNTHESIS PROCEDURE

A. General

The object of the synthesis procedure is to find the n birefringent-crystal angles, the retardations of the $n+1$ optical compensators, and the output-polarizer angle which result in the desired amplitude transmittance $C(\omega)$. For a given $C(\omega)$, $2n+2$ network parameters are to be determined. This matches the number of quantities in $C(\omega)$ which we are free to choose, for we may specify the real and imaginary parts of the $n+1$ coefficients C_i. The length L of the crystals (all crystals have the same length) is determined by the periodicity of the desired amplitude transmittance.

* Work supported by the National Aeronautics and Space Administration under Contract NAS8-20570.
[1] S. E. Harris, E. O. Ammann, and I. C. Chang, J. Opt. Soc. Am. 54, 1267 (1964).
[2] H. G. Jerrard, J. Opt. Soc. Am. 38, 35 (1948).

The notation, conventions, and approaches used here follow closely those used in Part I. Hence for brevity it is assumed that the reader is familiar with that reference, and much of the information contained therein is not repeated here. Because of this, an understanding of Part I is important to the understanding of this paper.

In this paper, optical compensators play an important role. A compensator is used with each crystal of the network and with the output polarizer. Since compensators were not required (in theory) in Part I and hence were not discussed, we briefly describe their operation and analysis. Optical compensators behave essentially the same as very short birefringent crystals. A compensator introduces a phase difference of b radians (where $0<b<2\pi$) between slow-axis (S) and fast-axis (F) components. It is assumed that this phase difference is independent of ω, an assumption which is approximately valid for most cases of interest. If this assumption is valid, light passing through the compensator polarized in the S direction is operated upon by e^{-ib}, while light polarized in the F direction is operated upon by unity.

We assume in this paper (as in Part I) that the birefringent crystals and optical compensators of the network are lossless. This means that energy must be conserved at all points within the network between the input and output polarizers. Energy conservation places certain important restrictions on the F_i and S_i, and on the C_i and D_i. These restrictions are derived and listed in Appendix B.

As in Part I, it is convenient to deal with relative angles (θ_i) of the stages instead of absolute angles (ϕ_i). By relative angle, we mean the additional angle of rotation measured from the preceding stage. The relative angles are given in terms of the ϕ_i of Fig. 2 by

$$\begin{aligned}\theta_1&=\phi_1,\\ \theta_2&=\phi_2-\phi_1,\\ &\vdots\\ \theta_n&=\phi_n-\phi_{n-1},\\ \theta_p&=\phi_p-\phi_n.\end{aligned}$$

B. Procedure

As mentioned in Part I, a useful approach to the synthesis problem is to consider the impulse response of the network. Since the inverse Fourier transform of the amplitude transmittance of a network yields its impulse response, we obtain, by taking the inverse Fourier transform of Eq. (1), the impulse response of the network of Fig. 2:

$$C(t)=C_0\delta(t)+C_1\delta(t-a)+C_2\delta(t-2a)+\cdots+C_n\delta(t-na). \quad (2)$$

Thus the impulse response of our network consists of a series of equally spaced impulses whose areas are given by the C_i. Since the C_i are complex, the impulse response

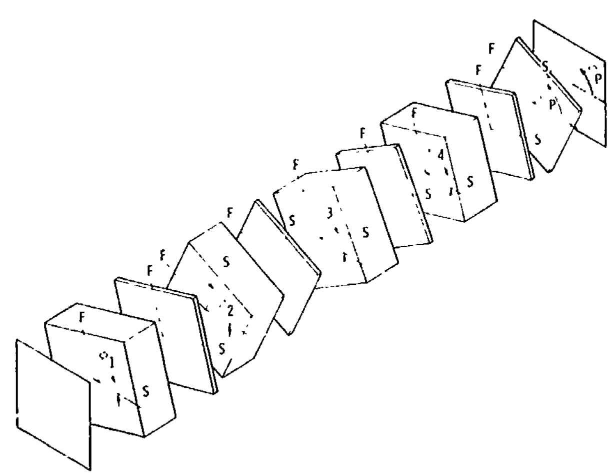

Fig. 2. Basic configuration of birefringent network (4 stages) obtained from the synthesis procedure of this paper.

is also complex. The explanation of this apparent paradox and its significance is given in Sec. III.

In the synthesis, we begin with the desired $C(\omega)$ as given by Eq. (1). This is equivalent to prescribing the impulse reponse $C(t)$ of the network. We next proceed from the last component of the network (the output polarizer) back to the first (the input polarizer), calculating the impulse trains which exist at all intermediate points. The areas of the individual impulses of these trains are denoted by the F_i^j and S_i^j of Fig. 3, where the F_i^j impulses are polarized along the fast axis of the preceding (jth) crystal and the S_i^j impulses along the slow axis. In the course of calculating these impulse trains, the crystal angles, compensator delays, and output polarizer angle are determined.

Assume that $C(\omega)$ and therefore the desired C_i of Eqs. (1) and (2) have been chosen. We must next find the signal $D(\omega)$ which is polarized perpendicular to $C(\omega)$ and therefore is stopped by the output polarizer. Since the network is lossless (between the input and output polarizers), the signal energy entering the first crystal must equal the sum of the energies in the $C(\omega)$ and $D(\omega)$ outputs. In equation form, this gives[3]

$$C(\omega)C^*(\omega)+D(\omega)D^*(\omega)=(I_0^0)^2, \quad (3a)$$

where I_0^0 is the area of the impulse which is incident upon the first crystal. Rewriting this, we have

$$D(\omega)D^*(\omega)=(I_0^0)^2-C(\omega)C^*(\omega). \quad (3b)$$

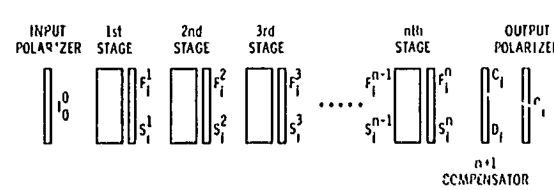

Fig. 3. n-stage network. Each stage contains a birefringent crystal and optical compensator.

[3] Asterisks are used in this paper to denote the complex conjugate of a quantity.

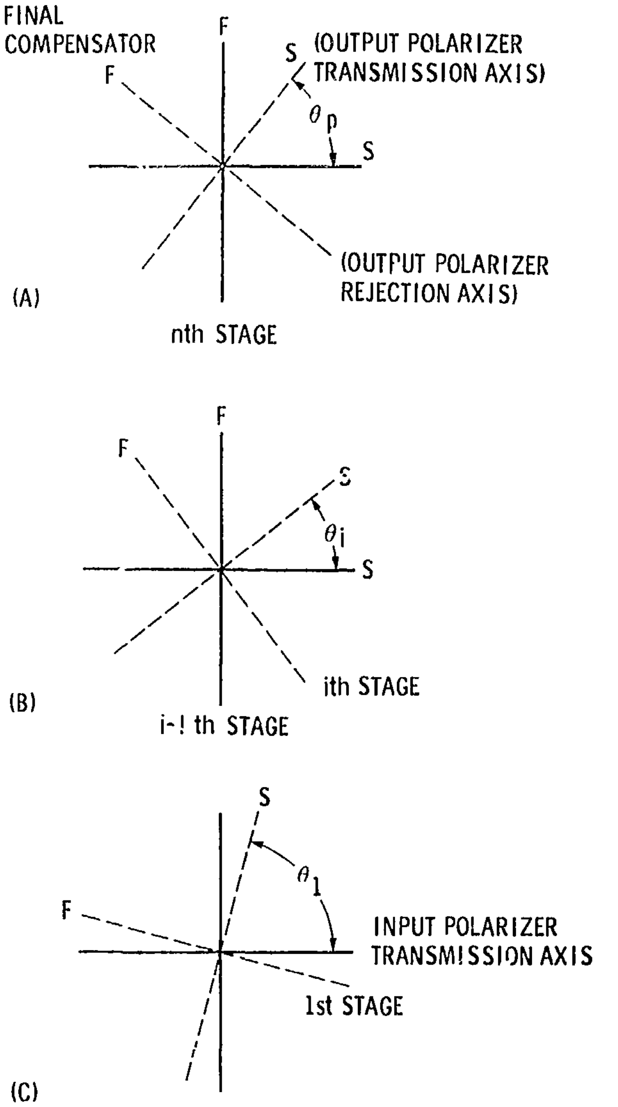

FIG. 4. Angle conventions used in the synthesis procedure: (a) final compensator (and output polarizer); (b) ith stage; (c) input polarizer.

We are now ready to choose a value for I_0^0. The left side of (3b) must be nonnegative for all frequencies; thus $(I_0^0)^2$ must be chosen greater than, or equal to, the maximum value of $C(\omega)C^*(\omega)$. Having chosen I_0^0, we can calculate $D(\omega)$ from $D(\omega)D^*(\omega)$ using the method given in Appendix A.

Doing this, we obtain $D(\omega)$ in the form

$$D(\omega)=D_0'+D_1'e^{-ia\omega}+D_2'e^{-i2a\omega}+\cdots+D_n'e^{-ina\omega},$$

where the D_i' are in general complex. It is important to note, however, that if $D(\omega)$ is a solution of Eq. (3b), then $e^{i\mu}D(\omega)$ is also a solution. Hence a more general solution for $D(\omega)$ is

$$\begin{aligned} D(\omega)&=e^{i\mu}[D_0'+D_1'e^{-ia\omega}+D_2'e^{-i2a\omega}+\cdots \\ &\qquad +D_n'e^{-ina\omega}] \\ &=D_0+D_1e^{-ia\omega}+D_2e^{-i2a\omega}+\cdots+D_ne^{-ina\omega}. \end{aligned} \quad (4)$$

Although the method of Appendix A gives us the values of the D_i', it does not determine a value for μ. The quantity μ must be determined from other considerations and, as is described shortly, has a value which is fixed by the manner in which the synthesis is formulated.

Let us now relate the inputs (the F_i^n and S_i^n) and outputs (the C_i and D_i) of the final compensator. It should be remembered that the F_i^n and S_i^n are components along the fast and slow axes of the preceding (nth) stage while the C_i and D_i are components along the slow and fast axes of the compensator. With the aid of Fig. 4(a), we find

$$\begin{bmatrix} F_i^n \\ S_i^n \end{bmatrix} = \begin{bmatrix} \exp(ib_p)\cdot\sin\theta_p & -\cos\theta_p \\ \exp(ib_p)\cdot\cos\theta_p & \sin\theta_p \end{bmatrix} \begin{bmatrix} C_i \\ e^{i\mu}D_i' \end{bmatrix}, \quad (5)$$

where θ_p is the relative angle of the final compensator (and hence also of the output polarizer), and b_p is the compensator delay.

We must next determine the quantities μ, θ_p, and b_p. To do this, we derive and solve three simultaneous equations. The first of these equations is obtained by noting that the first impulse to leave the nth stage must have a real area. This is equivalent to stating that F_0^n must be real. This condition arises from our convention of Sec. IIA which states that light passing through a compensator polarized in the S direction is operated upon by e^{-ib} while light polarized in the F direction is operated upon by unity. Since the first impulse to leave the nth stage must have been polarized along the F axis of each preceding stage, this impulse will have been operated upon by unity in each compensator and will therefore be real. From Eq. (5) we obtain for F_0^n

$$F_0^n=\exp(ib_p)\cdot(\sin\theta_p)\cdot C_0-e^{i\mu}\cdot(\cos\theta_p)\cdot D_0'.$$

Equating the imaginary parts of the left- and right-hand sides of this equation, we obtain the first of our three desired equations,

$$\begin{aligned} 0=\sin\theta_p[\mathrm{Im}(C_0)\cos b_p+\mathrm{Re}(C_0)\sin b_p] \\ -\cos\theta_p[\mathrm{Im}(D_0')\cos\mu+\mathrm{Re}(D_0')\sin\mu], \end{aligned} \quad (6a)$$

where Im and Re denote the imaginary and real parts of the quantity in question. The remaining two equations result because the first and last impulses leaving the nth stage must have been polarized along its fast and slow axes, respectively. This means that

$$F_n^n=S_0^n=0,$$

which, with (5), gives

$$\exp[i(b_p-\mu)]\cdot\tan\theta_p=D_n'/C_n \quad (6b)$$

and

$$\exp[-i(b_p-\mu)]\cdot\tan\theta_p=C_0/D_0'. \quad (6c)$$

Taking the complex conjugate of both sides of Eq. (6c), we obtain

$$\exp[i(b_p-\mu)]\cdot\tan\theta_p=-(C_0^*/D_0'^*).$$

Combining this equation with Eq. (6b), we obtain

$$C_0^*C_n+D_0'^*D_n'=0, \tag{7a}$$

the relation which must be true if Eqs. (6b) and (6c) are to be satisfied simultaneously. Noting that $D_i'=e^{-i\mu}D_i$, we can rewrite (7a) as

$$C_0^*C_n+D_0^*D_n=0. \tag{7b}$$

But Eq. (7b) is automatically satisfied from conservation of energy since it is identical to Eq. (B9) of Appendix B.

Since the C_i and D_i' are complex, we can rewrite (6b) in the form

$$\exp[i(b_p-\mu)]\cdot\tan\theta_p=|D_n'/C_n|\exp(i\alpha_p), \tag{8}$$

where in (8) we have expressed (D_n'/C_n) as a magnitude and phase angle. It is apparent from (8) that the rotation angle θ_p of the polarizer and compensator should be chosen to be

$$\tan\theta_p=|D_n'/C_n|. \tag{9}$$

By further manipulations of Eqs. (6a), (6b), and (6c), we obtain

$$\tan b_p=-\mathrm{Im}(C_0)/\mathrm{Re}(C_0) \tag{10}$$

and

$$\mu=b_p-\alpha_p. \tag{11}$$

Having determined α_p, b_p, and μ, we can substitute these values into (5) to obtain F_i^n and S_i^n, the outputs along the fast and slow axes of the nth stage. We must next find the rotation angles and compensator delays of the n stages of the network.

To do this, we write expressions relating the input and output of each stage. With the help of Figs. 4(b) and 4(c), we obtain

First Stage

$$\begin{bmatrix}F_0^1\\ S_1^1\end{bmatrix}=\begin{bmatrix}-\sin\theta_1\\ \exp(-ib_1)\cdot\cos\theta_1\end{bmatrix}[I_0^0], \tag{12a}$$

Second Stage

$$\begin{bmatrix}F_0^2\\ F_1^2\\ S_1^2\\ S_2^2\end{bmatrix}=\begin{bmatrix}\cos\theta_2 & 0\\ 0 & -\sin\theta_2\\ \exp(-ib_2)\cdot\sin\theta_2 & 0\\ 0 & \exp(-ib_2)\cdot\cos\theta_2\end{bmatrix}\begin{bmatrix}F_0^1\\ S_1^1\end{bmatrix} \tag{12b}$$

Third Stage

$$\begin{bmatrix}F_0^3\\ F_1^3\\ F_2^3\\ S_1^3\\ S_2^3\\ S_3^3\end{bmatrix}=\begin{bmatrix}\cos\theta_3 & 0 & 0 & 0\\ 0 & \cos\theta_3 & -\sin\theta_3 & 0\\ 0 & 0 & 0 & -\sin\theta_3\\ \exp(-ib_3)\cdot\sin\theta_3 & 0 & 0 & 0\\ 0 & \exp(-ib_3)\cdot\sin\theta_3 & \exp(-ib_3)\cdot\cos\theta_3 & 0\\ 0 & 0 & 0 & \exp(-ib_3)\cdot\cos\theta_3\end{bmatrix}\begin{bmatrix}F_0^2\\ F_1^2\\ S_1^2\\ S_2^2\end{bmatrix}, \tag{12c}$$

and in general,

jth Stage

$$\begin{bmatrix}F_0^j\\ F_1^j\\ F_2^j\\ \vdots\\ F_{j-3}^j\\ F_{j-2}^j\\ F_{j-1}^j\\ S_1^j\\ S_2^j\\ S_3^j\\ \vdots\\ S_{j-2}^j\\ S_{j-1}^j\\ S_j^j\end{bmatrix}=\begin{bmatrix}\cos\theta_j & 0 & 0 & \cdots & 0 & 0 & 0\\ 0 & \cos\theta_j & 0 & \cdots & 0 & 0 & 0\\ 0 & 0 & \cos\theta_j & \cdots & 0 & 0 & 0\\ \vdots & \vdots & \vdots & & \vdots & \vdots & \vdots\\ 0 & 0 & 0 & \cdots & -\sin\theta_j & 0 & 0\\ 0 & 0 & 0 & \cdots & 0 & -\sin\theta_j & 0\\ 0 & 0 & 0 & \cdots & 0 & 0 & -\sin\theta_j\\ \exp(-ib_j)\cdot\sin\theta_j & 0 & 0 & \cdots & 0 & 0 & 0\\ 0 & \exp(-ib_j)\cdot\sin\theta_j & 0 & \cdots & 0 & 0 & 0\\ 0 & 0 & \exp(-ib_j)\cdot\sin\theta_j & \cdots & 0 & 0 & 0\\ \vdots & \vdots & \vdots & & \vdots & \vdots & \vdots\\ 0 & 0 & 0 & \cdots & \exp(-ib_j)\cdot\cos\theta_j & 0 & 0\\ 0 & 0 & 0 & \cdots & 0 & \exp(-ib_j)\cdot\cos\theta_j & 0\\ 0 & 0 & 0 & \cdots & 0 & 0 & \exp(-ib_j)\cdot\cos\theta_j\end{bmatrix}\begin{bmatrix}F_0^{j-1}\\ F_1^{j-1}\\ F_2^{j-1}\\ \vdots\\ F_{j-3}^{j-1}\\ F_{j-2}^{j-1}\\ S_1^{j-1}\\ S_2^{j-1}\\ S_3^{j-1}\\ \vdots\\ S_{j-2}^{j-1}\\ S_{j-1}^{j-1}\end{bmatrix}. \tag{12d}$$

Putting $j=n$ in (12d), we have the input and output relations for the nth stage. We know the output (the F_i^n and S_i^n) and wish to find θ_n, b_n, and the input. As discussed in detail in Part I, an input exists which produces our given output provided that

$$\exp(ib_n)\cdot\tan\theta_n=-F_{n-1}^n/S_n^n=|F_{n-1}^n/S_n^n|\times\exp(i\alpha_n) \tag{13a}$$

and

$$F_0^{n*}F_{n-1}^n+S_1^{n*}S_n^n=0. \tag{13b}$$

Note that α_n includes the effect of the minus sign which precedes F_{n-1}^n/S_n^n.

We can satisfy Eq. (13a) by properly choosing b_n and θ_n, while (13b) is automatically satisfied by conservation of energy. Knowing b_n and θ_n, we can then calculate the input to the nth stage from (12d). This, of course, is also the output from the $n-1$ stage; hence we can repeat the procedure just described to determine b_{n-1} and θ_{n-1}. In this fashion, we can work our way back through the entire network until all rotation angles and compensator delays have been determined. The general equations for the jth stage are

$$\exp(ib_j)\cdot\tan\theta_j = -F_{j-1}^j/S_j^j = |F_{j-1}^j/S_j^j| \times\exp(i\alpha_j), \quad (14a)$$

and

$$F_0^{j*}F_{j-1}^j + S_1^{j*}S_j^j = 0, \quad (14b)$$

which gives

$$b_j = \alpha_j \quad (15a)$$

and

$$\tan\theta_j = |F_{j-1}^j/S_j^j|. \quad (15b)$$

As seen from Appendix B, Eq. (14b) is always automatically satisfied by conservation of energy.

Note that if $\alpha_j = 0$, a compensator is not required (in theory) for that particular stage. Furthermore it is possible to eliminate the compensator from a stage which has $\alpha_j = \pi$. This is because when $\alpha_j = \pi$, an alternate solution to Eq. (14a) is

$$b_j = 0, \quad (15c)$$

and

$$\tan\theta_j = -|F_{j-1}^j/S_j^j|. \quad (15d)$$

Hence whenever $\alpha_j = \pi$, Eqs. (15c) and (15d), rather than (15a) and (15b), should be used to determine b_j and θ_j.

We now have sufficient information to synthesize a birefringent network. The procedure to be followed is summarized below.

C. Summary of Synthesis Procedure

(1) Choose the desired amplitude transmittance $C(\omega)$ and write it in the form of Eq. (1). The C_i may be complex.

(2) The required length L for all crystals is given by $L = ac/\Delta\eta$, where c is the velocity of light in a vacuum and $\Delta\eta$ is the difference between the extraordinary and ordinary indices of refraction of the crystal. The quantity a is determined by comparing $C(\omega)$ as written in step (1) to $C(\omega)$ as given by Eq. (1).

(3) Choose a (real) value for I_0^0. The choice is arbitrary as long as $(I_0^0)^2$ is greater than or equal to the maximum magnitude of $C(\omega)C^*(\omega)$.

(4) Calculate $D(\omega)D^*(\omega)$ from Eq. (3b). Use the method of Appendix A to solve for $D(\omega)$ from $D(\omega)D^*(\omega)$. This gives the D_i' of Eq. (4), but does not determine μ. Several different $D(\omega)$ result, and each of these, when used with $C(\omega)$ results in an acceptable network. The D_i' of these $D(\omega)$ are, in general, complex. The remaining steps should be carried out for each $D(\omega)$.

(5) Calculate the rotation angle θ_p of the output polarizer and final compensator from Eq. (9), the phase delay b_p of the final compensator from Eq. (10), and μ from Eq. (11).

(6) Calculate the F_i^n and S_i^n from Eq. (5).

(7) Using Eq. (15b), calculate the rotation angle θ_n of the last stage. The compensator delay b_n for that stage should be computed from (15a). Using Eqs. (C1) and (C2), calculate the input to the last stage (which is the output from the preceding stage).

(8) Repeat the procedure of step (7) on each succeeding stage until the rotation angle and compensator delay of each stage have been determined. If $\alpha_j = \pi$ for a particular stage, Eqs. (15c) and (15d) rather than (15a) and (15b) should be used to calculate b_j and θ_j.

III. DISCUSSION

We now consider the implications of being able to choose C_i which are complex. In Part I, we were limited to amplitude transmittances having all C_i real. This meant that we were limited to $C(\omega)$'s whose real parts were even and whose imaginary parts were odd. These restrictions have now been removed; the real and imaginary portions of $C(\omega)$ can now be asymmetrical.

An objection might be raised that since the C_i are complex, our network has an impulse response, given by Eq. (2), which is complex; but it is well known that the impulse response of a physical network must be real. This dilemma arises because our theory requires the use of achromatic optical compensators in the network. The theory assumes that these compensators introduce a delay which is independent of ω. Such a delay is not realizable in practice. Compensators can approximate this behavior over a limited frequency range however. Hence the response of the synthesized network closely approximates $C(\omega)$ over the frequency range for which the compensators may be considered achromatic. Outside of this frequency range, the transmittance departs from $C(\omega)$. Since birefringent networks are ordinarily designed for use over a limited frequency range, this is an acceptable situation.

Thus we see that $C(\omega)$ accurately describes the network's transmittance over only a limited spectral range. But when we take the inverse Fourier transform of (1) to obtain the impulse response given by (2), we are (incorrectly) assuming that Eq. (1) is valid for all possible values of ω. Hence it is not surprising that the result is a complex impulse response for the network. Even though (2) does not accurately give the network impulse response, the time-domain approach is very useful for visualizing and understanding the synthesis procedure.

Part II of this series[4] described a second synthesis procedure which achieved the same goal as the procedure of Part I, but via a different form of birefringent network. Moreover, the procedure of Part II can be used when complex C_i are present in $C(\omega)$. The network which results, however, contains internal polarizers and hence is not a "lossless" network. For that reason, the network of this paper is preferable to that of Part II for most applications.

The network resulting from the synthesis procedure of this paper contains an optical compensator . to

[4] E. O. Ammann and I. C. Chang, J. Opt. Soc. Am. 55, 835 (1965).

the output polarizer. In practice, it is often possible to remove this optical compensator. Suppose for example that we have synthesized a network which has a desired $C(\omega)$. If we now remove the final compensator from that network, the new transmittance is $\exp(ib_p)\cdot C(\omega)$. Thus the new transmittance differs from the desired transmittance by only a constant phase factor. Often the introduction of this phase factor is of no consequence, and hence the final compensator can be removed. Furthermore, we note from Eq. (10) that if C_0 is chosen to be real, $b_p=0$ and the need for the final compensator is automatically eliminated.

Finally, we note that (as seen in Figs. 1 and 2) the network of this paper contains a greater number of components than the network of Part I. It should be emphasized, however, that Figs. 1 and 2 show the networks predicted by theory. In practice, the network of Part I requires the use of an optical compensator with each crystal of the network to compensate for slightly incorrect crystal lengths. Thus the practical forms of the networks of this paper and of Part I are identical; the additional flexibility is obtained at no expense in actual network complexity. In this paper, each optical compensator serves the dual functions of (a) introducing the delay required by theory, and (b) compensating for incorrect crystal length.

IV. EXAMPLE

A sample calculation is performed to illustrate the synthesis procedure of Sec. II. Suppose we wish to approximate the real transfer function $G(\omega)$ shown in Fig. 5. Since $G(\omega)$ is neither even nor odd, complex coefficients are required in the approximating exponential series. For this example we use a seven-term complex Fourier series.

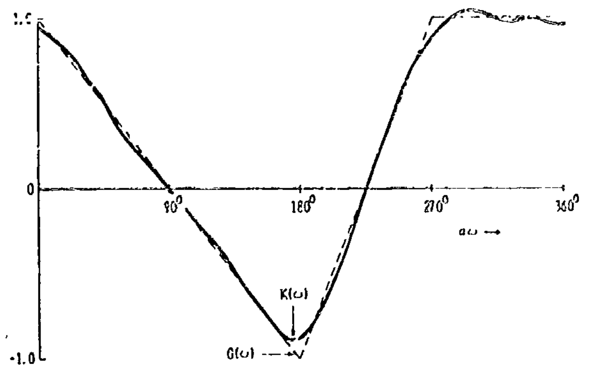

FIG. 5. Ideal and approximating amplitude transmittances of example. Ideal transmittance is shown by dotted line and approximating transmittance by solid line.

The Fourier-series approximation to the ideal transfer $G(\omega)$ is given by

$$K(\omega)=(1/\pi^2)[(4/9-i2/9)e^{i3a\omega}-e^{i2a\omega}+(4+i2)e^{ia\omega}+\pi^2/4+(4-i2)e^{-ia\omega}-e^{-i2a\omega}+(4/9+i2/9)e^{-i3a\omega}],\quad(16)$$

which is plotted in Fig. 5. Following the method of Part I, we convert this noncausal approximating function to a causal function by multiplying by $e^{-i3a\omega}$, which gives

$$C(\omega)=e^{-i3a\omega}K(\omega)=(1/\pi^2)[(4/9-i2/9)-e^{-ia\omega}+(4+i2)e^{-i2a\omega}+(\pi^2/4)e^{-i3a\omega}+(4-i2)e^{-i4a\omega}-e^{-i5a\omega}+(4/9+i2/9)e^{-i6a\omega}].\quad(17)$$

Multiplication by $e^{-i3a\omega}$ is equivalent to introducing a pure time delay in the time domain, and thus the impulse response and transfer function are essentially unchanged. Since the series contains seven terms, the synthesized network contains six stages.

We now calculate $D(\omega)$. From Eq. (3b) we have

$$\begin{aligned}|D(\omega)|^2=D(\omega)D^*(\omega)=(I_0{}^0)^2-C(\omega)C^*(\omega)=(I_0{}^0)^2-0.44257-(0.11139+i0.14695)e^{ia\omega}-(0.11139-i0.14695)e^{-ia\omega}\\-(0.09990+i0.12775)e^{i2a\omega}-(0.09990-i0.12775)e^{-i2a\omega}-(-0.05961-i0.05232)e^{i3a\omega}\\-(-0.05961+i0.05232)e^{-i3a\omega}-0.05589e^{i4a\omega}-0.05589e^{-i4a\omega}-(-0.00913+i0.00456)e^{i5a\omega}\\-(-0.00913-i0.00456)e^{-i5a\omega}-(0.00152-i0.00203)e^{i6a\omega}-(0.00152+i0.00203)e^{-i6a\omega}.\quad(18)\end{aligned}$$

The area $I_0{}^0$ of the input impulse must now be chosen in order to obtain $|D(\omega)|^2$. It may have any real value as long as $(I_0{}^0)^2$ is larger than the maximum value of $C(\omega)C^*(\omega)$. The maximum of $C(\omega)C^*(\omega)$ has been calculated to be 1.035. Thus let us choose $I_0{}^0=1.050$, which gives $(I_0{}^0)^2=1.1025$. Equation (18) then becomes, after making the substitution $x=e^{-ia\omega}$,

$$\begin{aligned}|D(\omega)|^2=-(0.00152+i0.00203)x^6-(-0.00913-i0.00456)x^5-0.05589x^4-(-0.05961+i0.05232)x^3\\-(0.09990-i0.12775)x^2-(0.11139-i0.14695)x+0.65993-(0.11139+i0.14695)x^{-1}\\-(0.09990+i0.12775)x^{-2}-(-0.05961-i0.05232)x^{-3}-0.05589x^{-4}\\-(-0.00913+i0.00456)x^{-5}-(0.00152-i0.00203)x^{-6},\quad(19)\end{aligned}$$

which is in the form of Eq. (A2). Following the procedure of Appendix A, we find the roots of (19) to be

$$\begin{aligned}
x_1&=0.06608-i0.27538, & (1/x_1)^*&=0.82394-i3.43353,\\
x_2&=-0.09690-i0.27436, & (1/x_2)^*&=-1.14455-i3.24064,\\
x_3&=-0.67656-i0.06373, & (1/x_3)^*&=-1.46526-i0.13704,\\
x_4&=0.17633+i0.17387, & (1/x_4)^*&=2.87546+i2.83537,\\
x_5&=0.57518+i0.17898, & (1/x_5)^*&=1.58510+i0.49323,\\
x_6&=0.59387+i1.30936, & (1/x_6)^*&=0.28729+i0.63342.
\end{aligned}$$

There are 128 (2^{n+1}) possible sets of D_i which can be obtained from these roots. However, sixty-four of these sets are simply negatives of the other sixty-four. We consider only the set that is formed by constructing the polynomial

$$(x-x_1)(x-x_2)(x-x_3)(x-x_4)(x-x_5)(x-x_6).$$

Performing the indicated multiplication, we obtain

$$x^6+(-0.63801-i1.04187)x^5+(0.02599-i0.29300)x^4+(0.06553+i0.44610)x^3 \\ +(-0.23903-i0.05436)x^2+(0.04871-i0.00793)x+(-0.00721+i0.00961). \quad (20)$$

As stated in Eqs. (A9), a set of D_i' is proportional to the coefficients of this polynomial. Evaluating $|q|$ using (A10), we find that

$$|q|=0.45943,$$

and so

$$D_0'=-0.00331+i0.00441,\quad D_3'=0.03011+i0.20496,\quad D_5'=-0.29312-i0.48203,$$
$$D_1'=0.02238-i0.00364,\quad D_4'=0.01194-i0.13461,\quad D_6'=0.45943.$$
$$D_2'=-0.10982-i0.02495,$$

From Eqs. (9), (10), and (11) we may now calculate θ_p, b_p, and μ. The results are

$$\theta_p=83°\,45',\quad b_p=0.46365 \text{ rad},\quad \mu=-5.35589 \text{ rad}.$$

Using Eqs. (A9), we find that

$$D_0=e^{i\mu}D_0'=-0.00552+i0,\quad D_3=e^{i\mu}D_3'=-0.14590+i0.14706,\quad D_5=e^{i\mu}D_5'=0.20976-i0.52372,$$
$$D_1=e^{i\mu}D_1'=0.01634+i0.01572,\quad D_4=e^{i\mu}D_4'=0.11485-i0.07122,\quad D_6=e^{i\mu}D_6'=0.27566+i0.36755,$$
$$D_2=e^{i\mu}D_2'=-0.04593-i0.10282,$$

and hence $D(\omega)$ is completely known. Equation (5) is now used to calculate the F_i^6 and S_i^6, giving

$$\begin{bmatrix} F_0^6\\ F_1^6\\ F_2^6\\ F_3^6\\ F_4^6\\ F_5^6 \end{bmatrix} = \begin{bmatrix} 0.05065+i0.00000\\ -0.09187-i0.04675\\ 0.27526+i0.37154\\ 0.23817+i0.09512\\ 0.43791+i0.00776\\ -0.11293+i0.01201 \end{bmatrix},\quad \begin{bmatrix} S_1^6\\ S_2^6\\ S_3^6\\ S_4^6\\ S_5^6\\ S_6^6 \end{bmatrix} = \begin{bmatrix} 0.00637+i0.01069\\ -0.01604-i0.06272\\ -0.12067+i0.15836\\ 0.16353-i0.07079\\ 0.19863-i0.52554\\ 0.27731+i0.36975 \end{bmatrix}.$$

As a check, we should note that F_0^6 must be real and that F_6^6 and S_0^6 must be zero. As a further check, we can verify that Eq. (14b) is satisfied.

We are now able to calculate θ_6 and b_6, the relative angle of the last stage and the optical compensator delay. Using (15b), we find

$$\theta_6=13°\,48'$$

and from (15a),

$$b_6=5.24997 \text{ rad}.$$

The input impulses to the sixth stage are now calculated from Eqs. (C3) and (C4). Equations (15b) and (15a) are then applied again, yielding

$$\theta_5=36°\,45'$$

and

$$b_5=6.11153 \text{ rad}.$$

By alternately applying Eqs. (C3) and (C4) and Eqs. (15a) and (15b), we obtain the remaining θ_i and b_i. The summarized results of the synthesis are

$$\begin{bmatrix} \theta_1\\ \theta_2\\ \theta_3\\ \theta_4\\ \theta_5\\ \theta_6\\ \theta_p \end{bmatrix} = \begin{bmatrix} 6°\,15'\\ 13°\,48'\\ 36°\,45'\\ 43°\,00'\\ 36°\,45'\\ 13°\,48'\\ 83°\,45' \end{bmatrix},\quad \begin{bmatrix} b_1\\ b_2\\ b_3\\ b_4\\ b_5\\ b_6\\ b_p \end{bmatrix} = \begin{bmatrix} 2.10838\\ 2.96994\\ 0.74123\\ 0.74123\\ 2.96994\\ 5.24997\\ 0.46365 \end{bmatrix} \text{ radians.}$$

The Jones calculus[5] can be used to verify that these angles and compensator delays give the desired transfer function of Eq. (17).

ACKNOWLEDGMENTS

The authors are grateful to S. Barnard for assistance in performing the calculations of Sec. IV, and to Professor S. E. Harris for a careful reading of the manuscript.

[5] R. C. Jones, J. Opt. Soc. Am. 31, 488 (1941).

APPENDIX A

We describe in this appendix a method for calculating $D(\omega)$ from $|D(\omega)|^2$. The method is similar to that given in Appendix A of Part I, but differs in its details. The differences are necessary because (a) we now begin with a $C(\omega)$ containing complex C_i, and (b) complex values of D_i can now be tolerated in $D(\omega)$.

We begin with the positive semidefinite polynomial

$$\begin{aligned}|D(\omega)|^2&=D(\omega)D^*(\omega)=(I_0^0)^2-C(\omega)C^*(\omega),\\ &=A_ne^{ina\omega}+A_{n-1}e^{i(n-1)a\omega}+\cdots+A_1e^{ia\omega}+A_0\\ &\quad+A_1^*e^{-ia\omega}+\cdots+A_{n-1}^*e^{-i(n-1)a\omega}\\ &\quad+A_n^*e^{-ina\omega}.\end{aligned}\tag{A1}$$

Letting $x=e^{-ia\omega}$ and reversing the order of the terms, Eq. (A1) becomes

$$\begin{aligned}|D(x)|^2=A_n^*x^n+A_{n-1}^*x^{n-1}+\cdots+A_1^*x+A_0\\ +A_1x^{-1}+\cdots+A_{n-1}x^{-(n-1)}+A_nx^{-n}.\end{aligned}\tag{A2}$$

Assume that x_1 is a root of Eq. (A2). Then

$$\begin{aligned}A_n^*x_1^n+A_{n-1}^*x_1^{n-1}+\cdots+A_1^*x_1+A_0+A_1x_1^{-1}+\cdots\\ +A_{n-1}x_1^{-(n-1)}+A_nx_1^{-n}=0.\end{aligned}\tag{A3}$$

If we now take the complex conjugate of Eq. (A3), we obtain

$$\begin{aligned}A_n(x_1^*)^n+A_{n-1}(x_1^*)^{n-1}+\cdots\\ +A_1x_1^*+A_0^*+A_1^*(x_1^*)^{-1}+\cdots\\ +A_{n-1}^*(x_1^*)^{-(n-1)}+A_n^*(x_1^*)^{-n}=0.\end{aligned}\tag{A4}$$

Equation (A4) can be rewritten as

$$\begin{aligned}A_n(1/x_1^*)^{-n}+A_{n-1}(1/x_1^*)^{-(n-1)}+\cdots\\ +A_1(1/x_1^*)^{-1}+A_0^*+A_1^*(1/x_1^*)+\cdots\\ +A_{n-1}^*(1/x_1^*)^{n-1}+A_n^*(1/x_1^*)^n=0.\end{aligned}\tag{A5}$$

But we now see that (A3) and (A5) have identical coefficients, with x_1 being the variable in Eq. (A3) and $(1/x_1^*)$ the variable in (A5). Thus if x_1 is a root of (A2), then $(1/x_1^*)$ is also a root. One of these two roots is associated with $D(x)$ and the other with $D^*(x)$. Hence we associate half of the roots of Eq. (A2) with $D(x)$ and half with $D^*(x)$. $D(x)$ [and hence $D(\omega)$] can then be constructed (to within a multiplicative phase factor) from a knowledge of its roots.

To summarize, begin with $|D(\omega)|^2$ written in the form of Eq. (A1). The A_i are in general complex. Form the equation

$$\begin{aligned}A_n^*x^n+A_{n-1}^*x^{n-1}+\cdots+A_1^*x+A_0+A_1x^{-1}+\cdots\\ +A_{n-1}x^{-(n-1)}+A_nx^{-n}=0.\end{aligned}\tag{A6}$$

Solve for the $2n$ roots of this equation. These roots always exist in pairs of the form

$$\begin{array}{ll}x_1, & 1/x_1^*,\\ x_2, & 1/x_2^*,\\ x_3, & 1/x_3^*,\\ \vdots & \vdots\\ x_n, & 1/x_n^*.\end{array}\tag{A7}$$

Construct all possible equations using one root from each row of (A7). One possible grouping, for example, is

$$\begin{aligned}(x-x_1)(x-x_2)(x-1/x_3^*)\cdots(x-1/x_n^*)\\ =x^n+d_{n-1}x^{n-1}+\cdots+d_2x^2+d_1x+d_0.\end{aligned}\tag{A8}$$

Each different grouping of roots results in a different $D(\omega)$.

The D_i are proportional to the d_i, where q, the constant of proportionality, is in general complex. Writing q in the form $q=|q|e^{i\mu}$, we obtain

$$\begin{aligned}D_0&=|q|e^{i\mu}d_0=e^{i\mu}D_0',\\ D_1&=|q|e^{i\mu}d_1=e^{i\mu}D_1',\\ &\vdots\\ D_n&=|q|e^{i\mu}d_n=e^{i\mu}D_n'=|q|e^{i\mu},\end{aligned}\tag{A9}$$

where

$$D_i'=|q|d_i.$$

The necessity of allowing q to be complex can be seen by noting that if $D(\omega)$ is a solution of Eq. (3b), then $e^{i\mu}D(\omega)$ is also a solution.

The quantity $|q|$ is calculated from

$$|q|^2[d_0d_0^*+d_1d_1^*+\cdots+d_{n-1}d_{n-1}^*+1]=A_0.\tag{A10}$$

In order to calculate the phase angle μ, however, additional information must be provided. The necessary information is obtained from the restriction that F_0^n must be real, a condition which results from our formulation of the synthesis procedure. With this restriction, μ is uniquely determined (see Sec. IIb) and $D(\omega)$ can be obtained.

Thus the method of this appendix allows us to find $D(\omega)$ to within a multiplicative phase factor $e^{i\mu}$. We obtain values for the D_i', where

$$\begin{aligned}D(\omega)&=e^{i\mu}[D_0'+D_1'e^{-ia\omega}+D_2'e^{-i2a\omega}+\cdots\\ &\qquad+D_{n-1}'e^{-i(n-1)a\omega}+D_n'e^{-ina\omega}],\\ &=D_0+D_1e^{-ia\omega}+D_2e^{-i2a\omega}+\cdots\\ &\qquad+D_{n-1}e^{-i(n-1)a\omega}+D_ne^{-ina\omega}.\end{aligned}\tag{A11}$$

APPENDIX B

In this appendix, the restrictions placed upon the F_i and S_i (and upon the C_i and D_i) because of conservation of energy are derived. Consider the ith stage of the network of Fig. 2. Since the network is lossless, the energy in the fast-axis output plus the energy in the slow-axis output of the ith stage must equal the energy incident upon the first stage. Stated mathematically, this gives

$$F^i(\omega)F^{i*}(\omega)+S^i(\omega)S^{i*}(\omega)=(I_0^0)^2.\tag{B1}$$

If we write out Eq. (B1) and equate the coefficients of corresponding terms, we obtain the equations

$$\begin{aligned}F_0^{i*}F_0^i+F_1^{i*}F_1^i+\cdots+F_{i-1}^{i*}F_{i-1}^i+S_1^{i*}S_1^i\\ +S_2^{i*}S_2^i+\cdots+S_i^{i*}S_i^i=(I_0^0)^2,\end{aligned}\tag{B2}$$

$$F_0^{i*}F_i^i+F_1^{i*}F_2^i+\cdots+F_{i-2}^{i*}F_{i-1}^i+S_1^{i*}S_2^i +S_2^{i*}S_3^i+\cdots+S_{i-1}^{i*}S_i^i=0, \quad \text{(B3)}$$

$$F_0^{i*}F_2^i+F_1^{i*}F_3^i+\cdots+F_{i-3}^{i*}F_{i-1}^i+S_1^{i*}S_3^i +S_2^{i*}S_4^i+\cdots+S_{i-2}^{i}S_i^i=0, \quad \text{(B4)}$$

$$\vdots$$

$$F_0^{i*}F_{i-1}^i+S_1^{i*}S_i^i=0. \quad \text{(B5)}$$

$C(\omega)$ and $D(\omega)$ must also satisfy conservation of energy, giving the following restrictions on the C_i and D_i.

$$C_0^*C_0+C_1^*C_1+\cdots+C_n^*C_n+D_0^*D_0+D_1^*D_1+\cdots +D_n^*D_n=(I_0^0)^2, \quad \text{(B6)}$$

$$C_0^*C_1+C_1^*C_2+\cdots+C_{n-1}^*C_n+D_0^*D_1+D_1^*D_2+\cdots +D_{n-1}^*D_n=0, \quad \text{(B7)}$$

$$C_0^*C_2+C_1^*C_3+\cdots+C_{n-2}^*C_n+D_0^*D_2+D_1^*D_3+\cdots +D_{n-2}^*D_n=0, \quad \text{(B8)}$$

$$\vdots$$

$$C_0^*C_n+D_0^*D_n=0. \quad \text{(B9)}$$

APPENDIX C

This appendix gives a systematic and rapid method of calculating the input to a stage, once the output is known. This is simply a formalized procedure of solving for the F^{j-1} and S^{j-1} of (12d) once the F^j and S^j are known. The expressions are similar to those of Appendix C of Part I but differ somewhat due to the complex quantities involved.

We begin by defining F_{j-1}^j and S_j^j in polar form:

$$F_{j-1}^j=|F_{j-1}^j|\exp(if_{j-1}^j) \quad \text{(C1)}$$

$$S_j^j=|S_j^j|\exp(is_j^j). \quad \text{(C2)}$$

Using these definitions, we find the expressions for the F^{j-1} and S^{j-1} in matrix form

$$\begin{bmatrix} F_0^{j-1} \\ F_1^{j-1} \\ \vdots \\ F_{j-1}^{j-1} \end{bmatrix} = \frac{\exp(-is_j^j)}{\{|F_{j-1}^j|^2+|S_j^j|^2\}^{\frac{1}{2}}} \begin{bmatrix} F_0^j & S_1^j \\ F_1^j & S_2^j \\ \vdots & \vdots \\ F_{j-1}^j & S_j^j \end{bmatrix} \begin{bmatrix} S_j^j \\ -F_{j-1}^j \end{bmatrix}. \quad \text{(C3)}$$

$$\begin{bmatrix} S_0^{j-1} \\ S_1^{j-1} \\ \vdots \\ S_{j-1}^{j-1} \end{bmatrix} = \frac{\exp(ib_j)\cdot\exp(is_j^j)}{\{|F_{j-1}^j|^2+|S_j^j|^2\}^{\frac{1}{2}}} \begin{bmatrix} F_0^j & S_1^j \\ F_1^j & S_2^j \\ \vdots & \vdots \\ F_{j-1}^j & S_j^j \end{bmatrix} \begin{bmatrix} F_{j-1}^{j*} \\ S_j^{j*} \end{bmatrix}. \quad \text{(C4)}$$

As before, the calculated values F_{j-1}^{j-1} and S_0^{j-1} should always be zero.

Appendix B

OPTICAL NETWORK SYNTHESIS USING BIREFRINGENT CRYSTALS.

VI. ADDITIONAL TECHNIQUES FOR THE SYNTHESIS OF LOSSLESS DOUBLE-PASS NETWORKS

E. O. Ammann and J. M. Yarborough
Electronic Defense Laboratories
Sylvania Electronic Systems - Western Operation
Mountain View, California

to be published in

Journal of the Optical Society of America

I. INTRODUCTION

In Part IV of this series[1], it was shown that a certain class of amplitude transmittances can be realized by birefringent networks containing only half as many crystals as normally required. The technique involved was called a double-pass synthesis procedure since the light makes two passes through the network. The purpose of this paper is to give additional double-pass procedures which are applicable, when the number of network stages is odd, to a still broader class of amplitude transmittances.

We will make use of results obtained in several previous papers of this series. Although some of this material is reviewed, familiarity with these papers is desirable. It is particularly important that the reader be acquainted with the techniques and results of Part IV[1], and to a lesser degree, with the contents of Parts I[2] and V[3].

The double-pass procedures described in Part IV are applicable to the type of birefringent network described in Part I. The first part of this paper gives additional circumstances in which a double-pass procedure can be used with that type of network. The second part of this paper deals with double-pass procedures for the more general type of birefringent network of Part V.

Let us briefly review the essence of the double-pass procedures of Part IV. For a certain class of amplitude transmittances $C(\omega)$, the birefringent network which results from using the synthesis procedure of Part I has a particular symmetry. Because of this symmetry, the last half of the birefringent network can be replaced by a mirror which reflects the light back through the first half of the network. In this paper, we show how networks obtained for still other classes of $C(\omega)$ can be made to have this symmetry. Having done this, the techniques of Part IV can then be used directly.

The forms of the networks obtained using the procedures of Part I and Part V are shown in Figs. 1 and 2 respectively. In Fig. 1, each stage of the network consists of a birefringent crystal, while in Fig. 2 each stage consists of a birefringent crystal and optical compensator (wave-plate). The network of Fig. 1 can be considered to be a special case of the network of Fig. 2 in which all optical compensators introduce zero retardation. The ϕ_i shown in Figs. 1 and 2 are the absolute rotation angles of the stages. The ϕ_i denote the angle between the slow axis of each crystal and the transmission axis of the input polarizer. It will also be useful to deal with relative angles (θ_i) of the stages, defined as the angle between the slow axis of a stage and the slow axis of the preceding stage. The θ_i are related to the ϕ_i by

$$
\begin{aligned}
\theta_1 &= \phi_1, \\
\theta_2 &= \phi_2 - \phi_1, \\
\theta_3 &= \phi_3 - \phi_2, \\
&\vdots \\
\theta_n &= \phi_n - \phi_{n-1}, \\
\theta_p &= \phi_p - \phi_n.
\end{aligned}
\tag{1}
$$

We now derive a property of these networks which will be used throughout this paper. Suppose that we alter a birefringent network by (a) for the jth stage, changing θ to $-\theta$ and adding π radians of optical compensation, and (b) for the preceding stage, adding π radians of optical compensation. The output of the new network will be identical to that of the original network.

To prove this statement, we will use the Jones calculus[4]. Figure 3 shows the jth stage of the network of Fig. 2. The u and v directions are those of the S and F

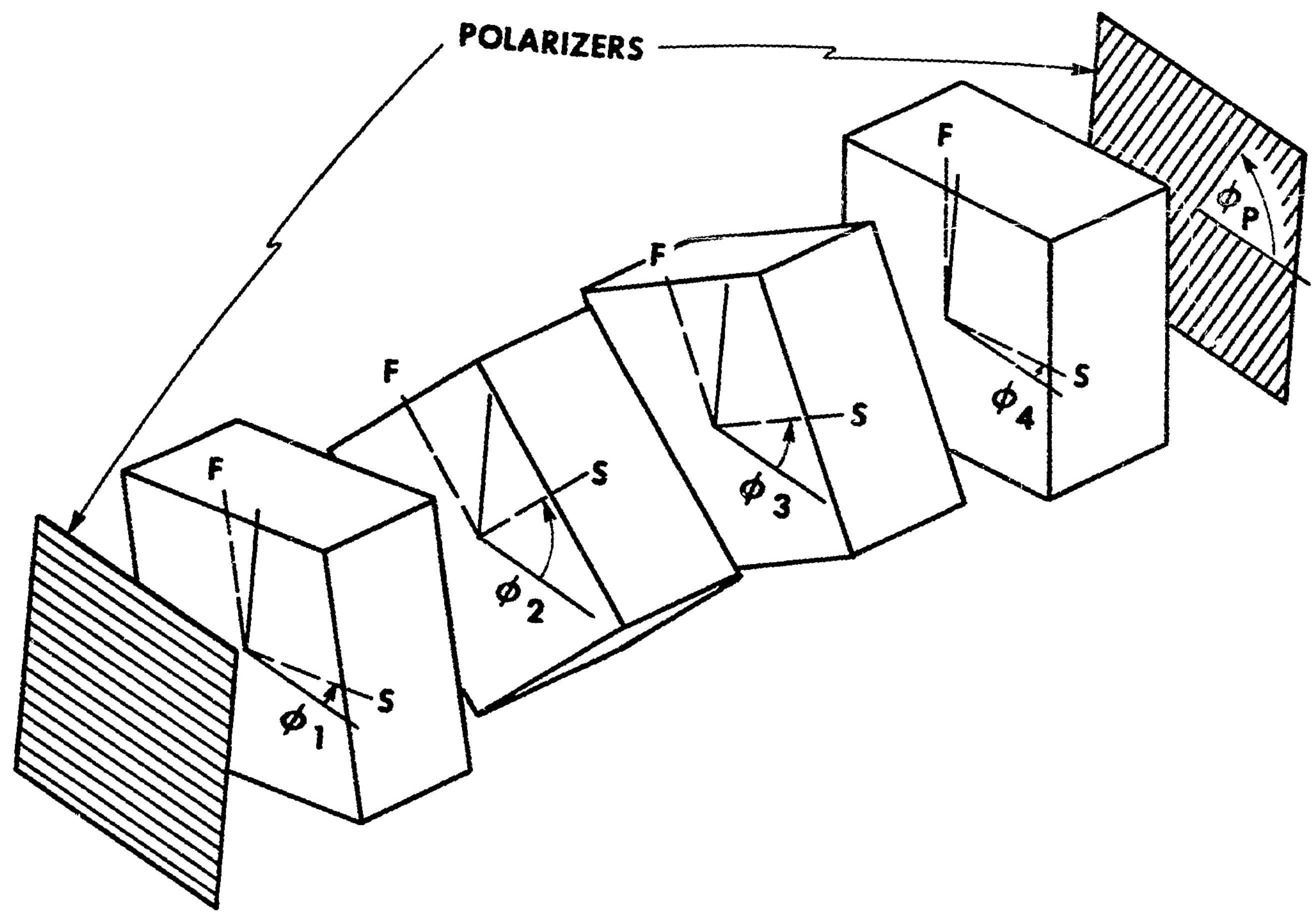

Figure 1

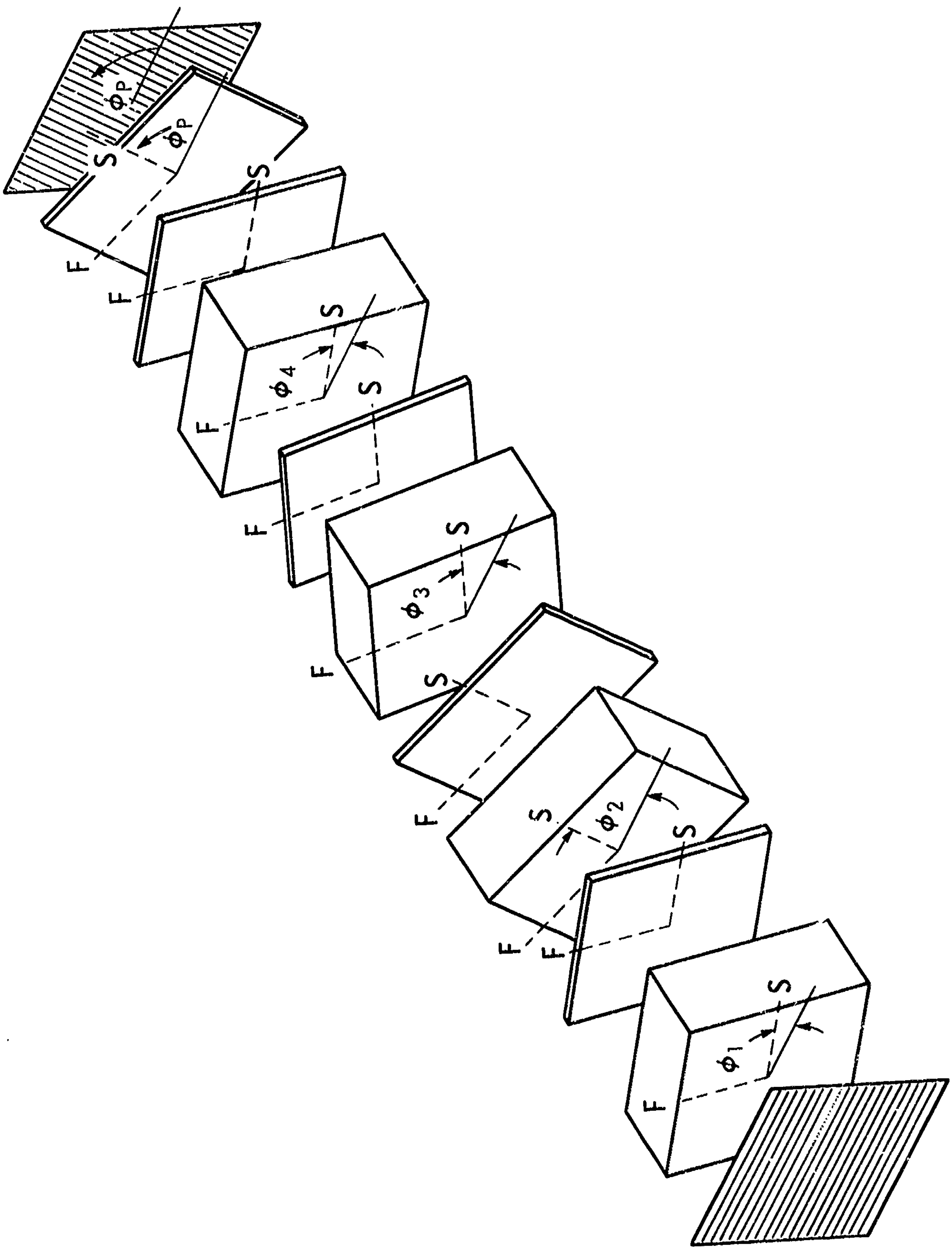

Figure 2

axes of the preceding (j-1) stage while u' and v' denote the S and F directions of the jth stage. The complex amplitudes of the E field of the incoming and outgoing light are related by

$$E' = M\,S(-\theta_j)\,E,$$

which, when written out, is

$$\begin{pmatrix} E_{u'} \\ E_{v'} \end{pmatrix} = \begin{pmatrix} e^{-ib_j} e^{-ia\omega} & 0 \\ 0 & 1 \end{pmatrix} \begin{pmatrix} \cos\theta_j & \sin\theta_j \\ -\sin\theta_j & \cos\theta_j \end{pmatrix} \begin{pmatrix} E_u \\ E_v \end{pmatrix},$$

$$= \begin{pmatrix} e^{-ib_j} e^{-ia\omega} \cos\theta_j & e^{-ib_j} e^{-ia\omega} \sin\theta_j \\ -\sin\theta_j & \cos\theta_j \end{pmatrix} \begin{pmatrix} E_u \\ E_v \end{pmatrix}. \tag{2}$$

The quantity b_j is the retardation of the compensator while $a\omega$ is the retardation of the crystal. For convenience, let us denote the 2x2 matrix of (2) by

$$\begin{pmatrix} A_j & B_j \\ C_j & D_j \end{pmatrix}. \tag{3}$$

Suppose that we now change θ_j to $-\theta_j$, and b_j to $b_j + \pi$. This causes e^{-ib_j} to become $-e^{-ib_j}$, and $\sin\theta_j$ to become $-\sin\theta_j$. The new matrix for the jth stage is thus

$$\begin{pmatrix} -A_j & B_j \\ -C_j & D_j \end{pmatrix}. \tag{4}$$

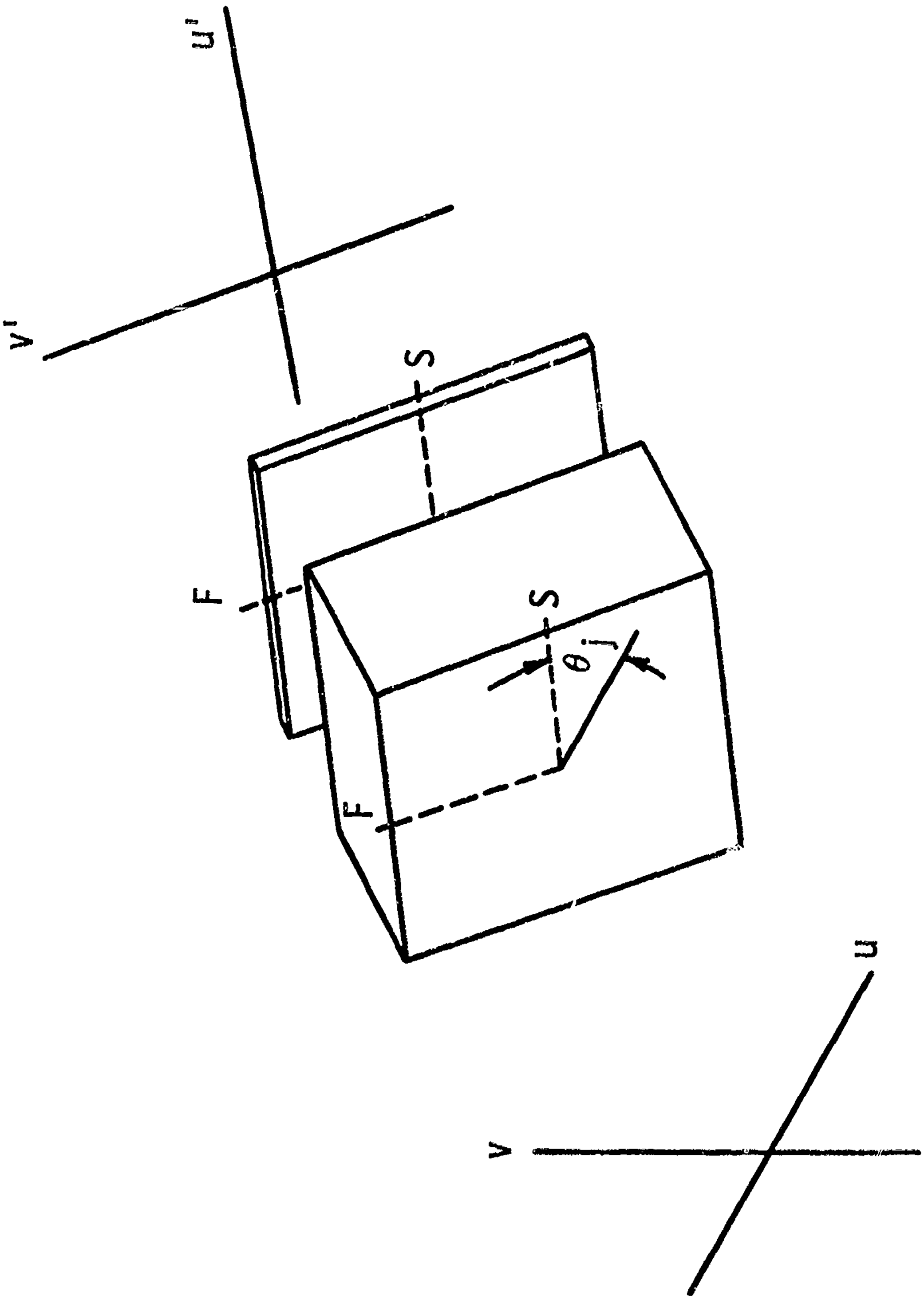

Figure 3

In addition, for the preceding stage let us change b_{j-1} to $b_{j-1} + \pi$. This means that the matrix for the (j-1)th stage is

$$\begin{pmatrix} -A_{j-1} & -B_{j-1} \\ C_{j-1} & D_{j-1} \end{pmatrix}. \tag{5}$$

The matrix for the (j-1)th and jth stages together is found by multiplying (4) and (5).

$$\begin{pmatrix} -A_j & B_j \\ -C_j & D_j \end{pmatrix} \begin{pmatrix} -A_{j-1} & -B_{j-1} \\ C_{j-1} & D_{j-1} \end{pmatrix} = \begin{pmatrix} A_jA_{j-1} + B_jC_{j-1} & A_jB_{j-1} + B_jD_{j-1} \\ C_jA_{j-1} + D_jC_{j-1} & C_jB_{j-1} + D_jD_{j-1} \end{pmatrix} \tag{6}$$

But this is identical to the matrix which would be obtained for the original (j-1)th and jth stages. Therefore in making the changes $\theta_j \rightarrow -\theta_j$, $b_j \rightarrow b_j + \pi$, and $b_{j-1} \rightarrow b_{j-1} + \pi$, we have not altered the network's behavior; the desired result has thus been proved.

We make one further observation. Suppose that we make the changes $\theta_1 \longrightarrow -\theta_1$ and $b_1 \longrightarrow b_1 + \pi$ on the first stage of a birefringent network. Since there is no preceding stage, the question arises as to how the network's performance is affected. It can be shown that such a change causes the amplitude-transmittance $C(\omega)$ of the network to become $-C(\omega)$. As noted in Part III[5], this sign change is of no practical importance.

II. TECHNIQUES WHICH ARE APPLICABLE WHEN THE C_i ARE REAL

Two basic types of lossless birefringent network are shown in Figs. 1 and 2. For both types, the amplitude transmittance $C(\omega)$ is given by

$$C(\omega) = C_0 + C_1 e^{-ia\omega} + C_2 e^{-i2a\omega} + \cdots + C_n e^{-ina\omega}. \tag{7}$$

When the C_i of (7) are real, the synthesis procedure of Part I can be used and the type of network shown in Fig. 1 results. When the C_i are complex, the procedure of Part V must be used and the type of network shown in Fig. 2 results. Part IV gave two double-pass procedures (methods A and B) and the circumstances under which they could be applied when $C(\omega)$ contained real C_i. In this section we show that for real C_i, additional circumstances exist under which double-pass procedures can be used.

In Part IV it was seen that Methods A and B are applicable to networks exhibiting the symmetry shown in Fig. 4a. In Fig. 4a, symmetry requirements are given both in terms of the φ_i and θ_i. Although optical compensators are not present in Fig. 4a, equivalent symmetry requirements can be stated for a network which contains them. These requirements are shown in Fig. 4b, where the b_i are the retardations introduced by the respective optical compensators. For both Figs. 4a and 4b, the symmetry requirements may be summarized as follows. The birefringent network (a) must have its input and output polarizers crossed, and (b) must have stages which are symmetric (both with respect to rotation angle and compensator delay) about the midpoint of the network. Satisfaction of these criteria allows methods A and B of Part IV to be applied.

Theorem 5b of Part III states that if the C_i of the desired transmittance are chosen so that $C_0 = -C_n$, $C_1 = -C_{n-1}$, $C_2 = -C_{n-2}$, $C_3 = -C_{n-3}$, $\cdots$ etc., then each of the resulting lossless birefringent networks will have $\theta_1 = -\theta_p \pm 90°$, $\theta_2 = -\theta_n$, $\theta_3 = -\theta_{n-1}$, $\theta_4 = -\theta_{n-2}$, $\cdots$ etc. As pointed out in Part IV, these angle restrictions are precisely those required for using methods A and B and hence double-pass procedures can be applied.

Suppose, however, that the C_i satisfy $C_0 = C_n$, $C_1 = C_{n-1}$, $C_2 = C_{n-2}$, $C_3 = C_{n-3}$, $\cdots$ etc. Theorem 4b of Part III states that the resulting birefringent

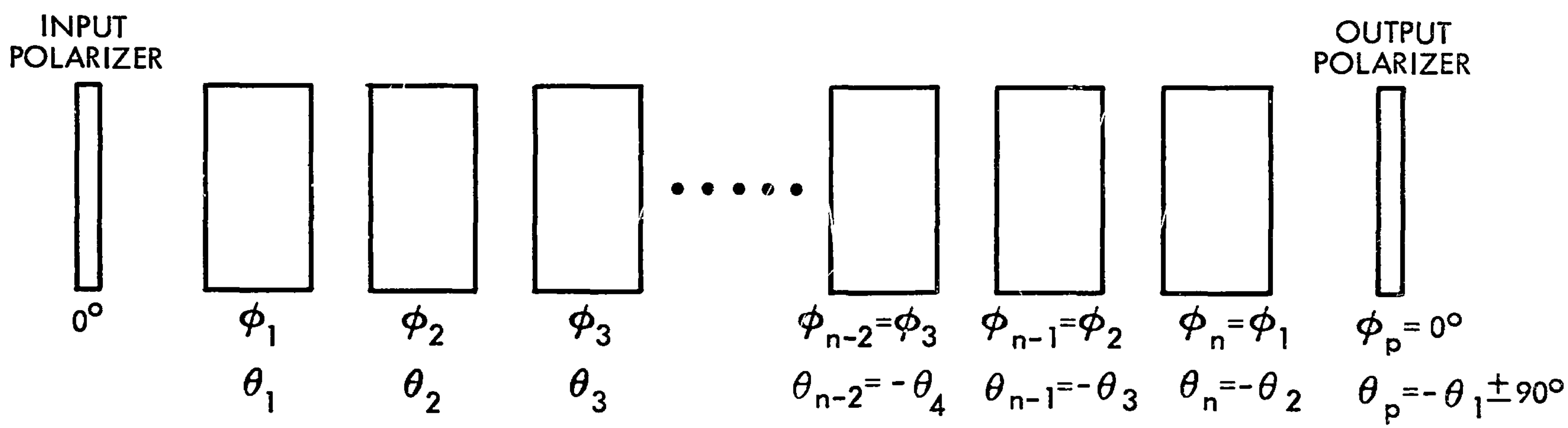
INPUT POLARIZER
0°
ϕ_1
θ_1
ϕ_2
θ_2
ϕ_3
θ_3
$\phi_{n-2}=\phi_3$
$\theta_{n-2}=-\theta_4$
$\phi_{n-1}=\phi_2$
$\theta_{n-1}=-\theta_3$
$\phi_n=\phi_1$
$\theta_n=-\theta_2$
OUTPUT POLARIZER
$\phi_p=0°$
$\theta_p=-\theta_1\pm 90°$

Figure 4a

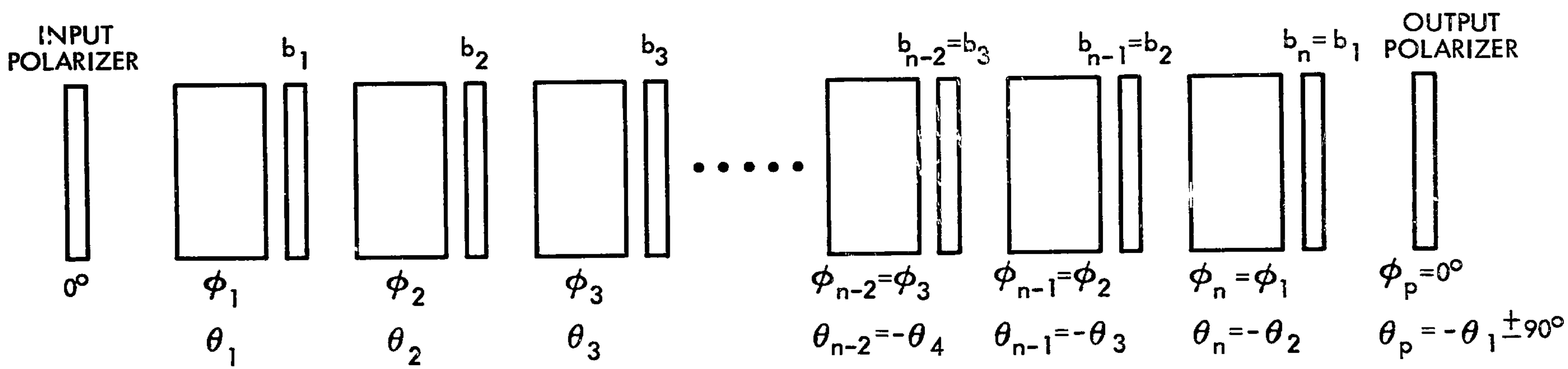
INPUT POLARIZER
0°
b_1
ϕ_1
θ_1
b_2
ϕ_2
θ_2
b_3
ϕ_3
θ_3
$b_{n-2}=b_3$
$\phi_{n-2}=\phi_3$
$\theta_{n-2}=-\theta_4$
$b_{n-1}=b_2$
$\phi_{n-1}=\phi_2$
$\theta_{n-1}=-\theta_3$
$b_n=b_1$
$\phi_n=\phi_1$
$\theta_n=-\theta_2$
OUTPUT POLARIZER
$\phi_p=0°$
$\theta_p=-\theta_1\pm 90°$

Figure 4b

networks have $\theta_1 = \theta_p \mp 90°$, $\theta_2 = \theta_n$, $\theta_3 = \theta_{n-1}$, $\cdots$ etc. This symmetry is not appropriate for double-pass techniques, but we now show how it can be made so when n is odd.

We illustrate by considering the case of $n = 9$. If $C(\omega)$ is chosen so that $C_0 = C_9$, $C_1 = C_8$, $C_2 = C_7$, $C_3 = C_6$, and $C_4 = C_5$, the networks obtained using the synthesis procedure of Part I will have the symmetry tabulated in Table I. Let us now make use of the result discussed in Section I of this paper. If we change θ_9 to $-\theta_2$, b_9 to π, and b_8 to π, the transmittance of the network is unchanged. Similarly we can change θ_7 to $-\theta_4$, b_7 to π, b_6 to π; θ_5 to $-\theta_5$, b_5 to π, b_4 to π; θ_3 to $-\theta_3$, b_3 to π, b_2 to π; and θ_1 to $-\theta_1$, b_1 to π without affecting the transmittance of the network. The network now has the symmetry shown in Table II which is the symmetry required. Hence methods A and B are directly applicable. Similar techniques apply for other odd values of n. If n is even, the use of the above procedure does not result in a symmetrical network and hence these techniques do not succeed. To date, comparable ones have not been found which apply when n is even.

In methods A and B, the symmetric network is halved by cutting it through the middle stage. For this example, the 5th stage is the middle stage and consists of a crystal of length L and compensator whose retardation is π radians. When this stage is halved, the components are a crystal of length L/2 and a compensator whose retardation is $\pi/2$ radians.

III. TECHNIQUES WHICH ARE APPLICABLE WHEN THE C_i ARE COMPLEX

Part V described a procedure for synthesizing birefringent networks whose transmittances contain complex C_i. The form of the resulting network is shown in Fig. 2. This section describes how a double-pass procedure can be obtained for use with this class of network.

STAGE	ROTATION ANGLE	COMPENSATOR RETARDATION (radians)
1	$\theta_1 = \theta_1$	$b_1 = 0$
2	$\theta_2 = \theta_2$	$b_2 = 0$
3	$\theta_3 = \theta_3$	$b_3 = 0$
4	$\theta_4 = \theta_4$	$b_4 = 0$
5	$\theta_5 = \theta_5$	$b_5 = 0$
6	$\theta_6 = \theta_5$	$b_6 = 0$
7	$\theta_7 = \theta_4$	$b_7 = 0$
8	$\theta_8 = \theta_3$	$b_8 = 0$
9	$\theta_9 = \theta_2$	$b_9 = 0$
output polarizer	$\theta_p = \theta_1 \pm 90°$	$b_p = 0$

Table I

STAGE	ROTATION ANGLE	COMPENSATOR RETARDATION (radians)
1	$\theta_1 \rightarrow -\theta_1$	$b_1 \rightarrow \pi$
2	$\theta_2 = \theta_2$	$b_2 \rightarrow \pi$
3	$\theta_3 \rightarrow -\theta_3$	$b_3 \rightarrow \pi$
4	$\theta_4 = \theta_4$	$b_4 \rightarrow \pi$
5	$\theta_5 \rightarrow -\theta_5$	$b_5 \rightarrow \pi$
6	$\theta_6 = \theta_5$	$b_6 \rightarrow \pi$
7	$\theta_7 \rightarrow -\theta_4$	$b_7 \rightarrow \pi$
8	$\theta_8 = \theta_3$	$b_8 \rightarrow \pi$
9	$\theta_9 \rightarrow -\theta_2$	$b_9 \rightarrow \pi$
output polarizer	$\theta_p = \theta_1 \pm 90°$	$b_p = 0$

Table II

Our goal will again be to obtain a network having the symmetry shown in Fig. 4b. We begin by stating a theorem. Asterisks denote complex conjugates.

Theorem

If the C_i of the desired transmittance are chosen so that $C_0 = C_n^*$, $C_1 = C_{n-1}^*$, $C_2 = C_{n-2}^*$, $C_3 = C_{n-3}^*$, $\cdots$ etc, then the resulting lossless birefringent networks have $\theta_1 = -\theta_p + 90°$, $\theta_2 = \theta_n$, $\theta_3 = \theta_{n-1}$, $\theta_4 = \theta_{n-2}$, $\cdots$ etc, and $b_1 = b_n - \pi$, $b_2 = b_{n-1}$, $b_3 = b_{n-2}$, $b_4 = b_{n-3}$, $\cdots$ etc.

The proof of this theorem is similar to the proofs of Theorems 4b and 5b in Part III and hence will not be given here.

We will again use a network with $n = 9$ for illustration; the technique is applicable only when n is odd. If the C_i satisfy the requirements listed above, the resulting networks will have the symmetry shown in Table III. We next apply the result of Section I by noting that $C(\omega)$ for the network remains unaltered if we change θ_8 to $-\theta_3$, b_8 to $b_2 + \pi$, b_7 to $b_3 + \pi$; θ_6 to $-\theta_5$, b_6 to $b_4 + \pi$, b_5 to $b_5 + \pi$; θ_4 to $-\theta_4$, b_4 to $b_4 + \pi$, b_3 to $b_3 + \pi$; and θ_2 to $-\theta_2$, b_2 to $b_2 + \pi$, b_1 to $b_1 + \pi$. In addition, b_p is changed to 0. This new network, whose θ_i and b_i are listed in Table IV, has the symmetry necessary for application of methods A and B, and hence the desired result has been obtained. For other odd values of n, the same technique can be applied.

Several items should be briefly mentioned at this point. The first is to note that when the C_i are complex, one begins manipulating the (n-1)th stage while when the C_i are real, one starts with the nth stage. The second point concerns our setting b_p to zero. This step is necessary if the input and output polarizers are to be the "mirror-images" of each other. The result of setting b_p to zero is that the transmittance of the double-pass network will be $(\exp ib_p) \cdot C(\omega)$ instead of the

STAGE	ROTATION ANGLE	COMPENSATOR RETARDATION (radians)
1	$\theta_1 = \theta_1$	$b_1 = b_1$
2	$\theta_2 = \theta_2$	$b_2 = b_2$
3	$\theta_3 = \theta_3$	$b_3 = b_3$
4	$\theta_4 = \theta_4$	$b_4 = b_4$
5	$\theta_5 = \theta_5$	$b_5 = b_5$
6	$\theta_6 = \theta_5$	$b_6 = b_4$
7	$\theta_7 = \theta_4$	$b_7 = b_3$
8	$\theta_8 = \theta_3$	$b_8 = b_2$
9	$\theta_9 = \theta_2$	$b_9 = b_1 + \pi$
output polarizer	$\theta_p = -\theta_1 + 90°$	$b_p = b_p$

Table III

STAGE	ROTATION ANGLE	COMPENSATOR RETARDATION (radians)
1	$\theta_1 = \theta_1$	$b_1 \rightarrow b_1 + \pi$
2	$\theta_2 \rightarrow -\theta_2$	$b_2 \rightarrow b_2 + \pi$
3	$\theta_3 = \theta_3$	$b_3 \rightarrow b_3 + \pi$
4	$\theta_4 \rightarrow -\theta_4$	$b_4 \rightarrow b_4 + \pi$
5	$\theta_5 = \theta_5$	$b_5 \rightarrow b_5 + \pi$
6	$\theta_6 \rightarrow -\theta_5$	$b_6 \rightarrow b_4 + \pi$
7	$\theta_7 = \theta_4$	$b_7 \rightarrow b_3 + \pi$
8	$\theta_8 \rightarrow -\theta_3$	$b_8 \rightarrow b_2 + \pi$
9	$\theta_9 = \theta_2$	$b_9 = b_1 + \pi$
output polarizer	$\theta_p = -\theta_1 + 90°$	$b_p = 0$

Table IV

desired $C(\omega)$. The difference is only a constant phase factor, which in most instances is unimportant. Furthermore, if C_0 is originally chosen to be real, $b_p = 0$ and the need for the final polarizer is automatically eliminated.

Finally, if the C_i satisfy $C_0 = -C_n^*$, $C_1 = -C_{n-1}^*$, $C_2 = -C_{n-2}^*$, $C_3 = -C_{n-3}^*$ ··· etc., the technique of this section is also applicable. This can be seen by noting that if we multiply such a $C(\omega)$ by the factor i, the new $C(\omega)$ satisfies the constraints of the theorem given in this section.

IV. DISCUSSION

We have seen in Sections II and III that if certain restrictions are satisfied by the C_i, double-pass synthesis procedures can be employed. An important question, then, is how severely these restrictions limit one in choosing a $C(\omega)$. In discussing this, it will be convenient to deal with $K(\omega)$ as well as $C(\omega)$. $K(\omega)$ is formed by multiplying $C(\omega)$ by $e^{i(n/2)a\omega}$ and therefore has the form

$$K(\omega) = C_0 e^{i(n/2)a\omega} + C_1 e^{i[(n/2) - 1]a\omega} + \dots + C_{n-1} e^{-i[(n/2) - 1]a\omega} + C_n e^{-i(n/2)a\omega} . \tag{8}$$

The usefulness of $K(\omega)$ stems from the fact that it is often real, whereas $C(\omega)$ is complex. In choosing a desired transmittance, it is often written first in the form of Eq. (8) and then converted to $C(\omega)$.

In terms of $K(\omega)$, the restrictions upon the C_i have the following effects:

(a) The restrictions $C_0 = -C_n$, $C_1 = -C_{n-1}$, $C_2 = -C_{n-2}$, $C_3 = -C_{n-3}$, ··· etc, which were necessary in Part IV of this series are equivalent to requiring that $K(\omega)$ be purely imaginary and have odd symmetry.

(b) The restrictions $C_0 = C_n$, $C_1 = C_{n-1}$, $C_2 = C_{n-2}$, $C_3 = C_{n-3}$, $\cdots$ etc. which were necessary in Section II of this paper are equivalent to requiring that $K(\omega)$ be real and have even symmetry.

(c) The restrictions $C_0 = C_n^*$, $C_1 = C_{n-1}^*$, $C_2 = C_{n-2}^*$, $C_3 = C_{n-3}^*$, $\cdots$ etc. which were necessary in Section III of this paper are equivalent to requiring that $K(\omega)$ be real. The symmetry of $K(\omega)$ is not restricted in any way. Thus these restrictions (particularly those of Section III) impose relatively little constraint upon the choice of desired amplitude transmittance.

Finally we note that the procedure of Section II can be considered to be a special case of the more general procedure of Section III.

ACKNOWLEDGMENT

The authors gratefully acknowledge stimulating discussions with R. B. Emmons.

FOOTNOTES

* This work was supported by the National Aeronautics and Space Administration under Contract NAS8-20570.

1. E. O. Ammann, J. Opt. Soc. Am. 56, 952 (1966).

2. S. E. Harris, E. O. Ammann, and I. C. Chang, J. Opt. Soc. Am. 54, 1267 (1964).

3. E. O. Ammann and J. M. Yarborough, J. Opt. Soc. Am. 56, (1966).

4. R. C. Jones, J. Opt. Soc. Am. 31, 488 (1941).

5. E. O. Ammann, J. Opt. Soc. Am. 56, 943 (1966).

CAPTIONS FOR FIGURES AND TABLES

Fig. 1 Basic configuration of birefringent network (4 stages) obtained from the synthesis procedure of Part I. F and S denote the "fast" and "slow" axes of the birefringent crystals.

Fig. 2 Basic configuration of birefringent network (4 stages) obtained from the synthesis procedure of Part V.

Fig. 3 Single stage of the network of Fig. 2. Components are a birefringent crystal and optical compensator.

Fig. 4 Network symmetry which is required in order for methods A and B (of Part IV of this series) to be applicable. (a) Lossless network without compensators, and (b) lossless network with compensators.

Table I Network symmetry which results for $n = 9$ when the (real) C_i are chosen to satisfy $C_0 = C_9$, $C_1 = C_8$, $C_2 = C_7$, $C_3 = C_6$, and $C_4 = C_5$.

Table II Network which is equivalent to that listed in Table I.

Table III Network symmetry which results for $n = 9$ when the (complex) C_i are chosen to satisfy $C_0 = C_9^*$, $C_1 = C_8^*$, $C_2 = C_7^*$, $C_3 = C_6^*$, and $C_4 = C_5^*$.

Table IV Network which is equivalent to that listed in Table III.

Appendix C

SYNTHESIS OF ELECTRO-OPTIC MODULATORS FOR AMPLITUDE MODULATION OF LIGHT

E. O. Ammann and J. M. Yarborough
Electronic Defense Laboratories
Sylvania Electronic Systems - Western Operation
Mountain View, California

to be submitted for publication

I. INTRODUCTION

Amplitude modulation of light using an electro-optic medium has been the subject of onsiderable investigation the past few years. Most of this work has centered on (1) studying romising electro-optic materials [1] - [8] and (2) finding suitable means for applying lectric fields to these materials. The latter work can be conveniently divided into investi- ations of cavity-type modulators [9] - [11] and traveling-wave modulators [12] - [17]. his work has resulted in several useful electro-optic materials and a variety of ingenious orms of amplitude modulators.

It is perhaps surprising, then, that all of these devices produce amplitude modulation in ssentially the same fashion as the simplified modulator of Fig. 1. That is, regardless of ie material used and the manner in which the modulating field is applied, the model of ig. 1 can be used to describe the essential modulation characteristics of virtually all xisting electro-optic amplitude modulators. (We have assumed, for simplicity, that ynchronism conditions are perfectly satisfied, that the medium is not naturally birefringent i the direction of light propagation, etc.)

The modulator model of Fig. 1 consists of an input polarizer, an electro-optic medium, quarter-wave plate, and an output polarizer. The birefringence of the electro-optic iedium is assumed to be directly proportional to the modulating signal, a condition which s satisfied exactly by Pockels-effect materials and approximately by Kerr-effect materials iased with a dc voltage. The modulator of Fig. 1 has an amplitude-transmission vs. pplied voltage characteristic

$$K(v) = \frac{(1+i)}{2\sqrt{2}} e^{i\frac{\pi}{2}\frac{v}{V_0}} + \frac{(1-i)}{2\sqrt{2}} e^{-i\frac{\pi}{2}\frac{v}{V_0}} = \cos\left(\frac{\pi}{2}\frac{v}{V_0} - 45°\right), \tag{1}$$

here V_0 is the half-wave retardation voltage.

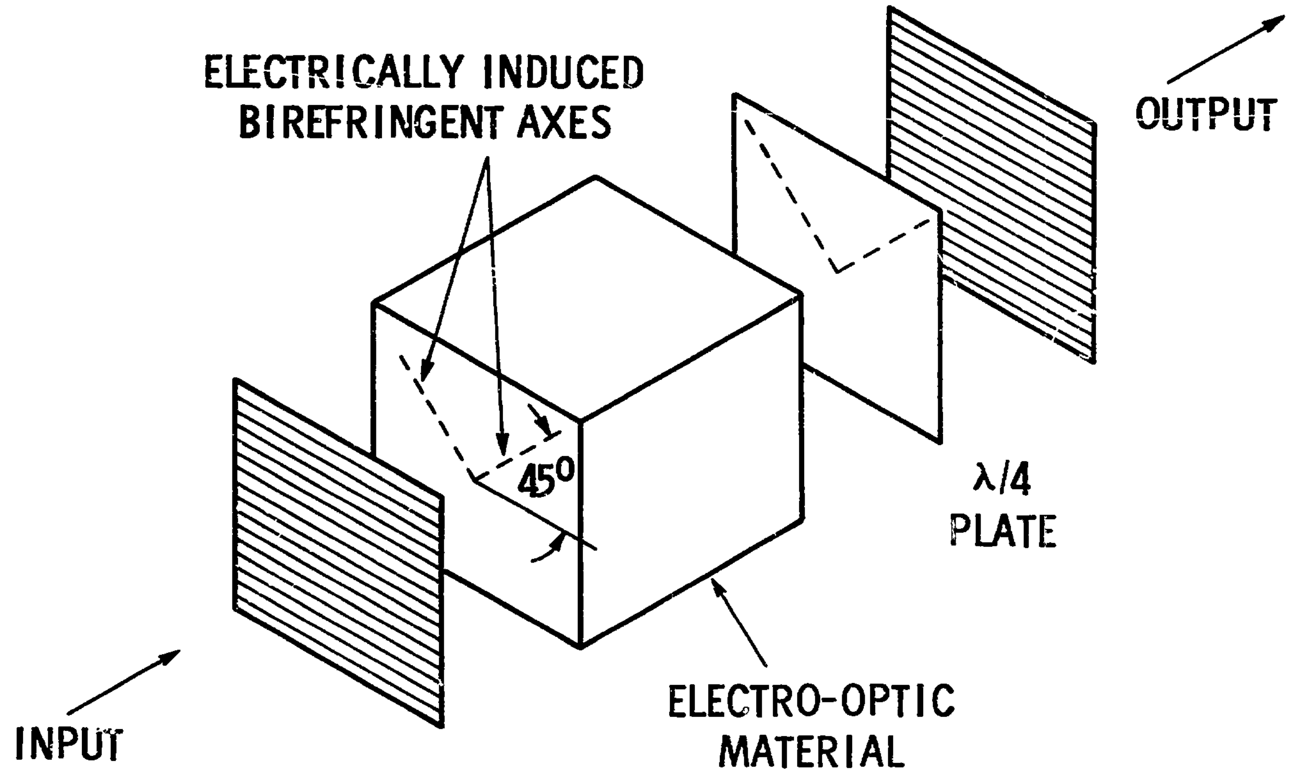
ELECTRICALLY INDUCED
BIREFRINGENT AXES
OUTPUT
45^0
λ/4
PLATE
INPUT
ELECTRO-OPTIC
MATERIAL

Figure 1

It is well known [18] - [19] that this K(v) is not the optimum characteristic for an amplitude modulator. The device of Fig. 1, and therefore existing amplitude modulators, have performance characteristics which depart from ideal. The result is that harmonics, intermodulation products, and other undesirable components are present in the modulator output. These distortion components are small when small depths of modulation are used, but their effects become more pronounced at greater modulation depths.

One of the purposes of this paper is to describe a synthesis procedure which allows the realization of amplitude modulators having an arbitrarily specifiable voltage transfer function. With this synthesis procedure it is possible to design modulators whose properties are tailored to the particular application at hand. The synthesized modulator (shown in Fig. 3) consists of a series of cascaded stages between an input and output polarizer. Each stage contains electro-optic material and an optical compensator [20] (wave-plate). The number of stages required depends upon the complexity of the desired voltage transfer function K(v). It should be emphasized that there is nothing new about any of the components which make up the synthesized modulator; **rather**, it is the arrangement of these standard components which results in a device whose characteristics can be arbitrarily prescribed.

This paper also discusses the transfer function of an ideal amplitude modulator and methods of approximating it. The ideal transfer function depends upon the type of detector employed to demodulate the signal. Two cases are considered: the use of (a) envelope detection, and (b) square-law detection. While it is possible in theory to synthesize a modulator having an ideal transfer function, it would contain an infinite number of stages. Hence in practice it is necessary to find suitable approximations to the ideal function which can be realized by modulators containing a finite number of stages. Several approximation techniques are described and compared on the basis of distortion present in the demodulated signal. Finally, modulator designs which correspond to these approximations are tabulated.

II. THE SYNTHESIS PROCEDURE

A. General

The procedure to be described for synthesizing amplitude modulators draws heavily upon the results given in a series of papers [21] - [26] dealing with birefringent network synthesis. Since several papers of this series are especially applicable, we will begin by mentioning their results and how they apply to the problem at hand.

Part I [21] of the series reported a procedure for synthesizing birefringent networks having a prescribed frequency transfer function $C(\omega)$. The desired transfer function is written as

$$C(\omega) = C_0 + C_1 e^{-i\alpha\omega} + C_2 e^{-i2\alpha\omega} + \ldots + C_n e^{-in\alpha\omega}, \tag{2}$$

where the number of terms employed is finite but arbitrary. $C(\omega)$ might typically be the complex Fourier series representation of a given function truncated after a certain number of terms. Any method, however, may be used to choose $C(\omega)$ as long as each C_i is real. Figure 2 shows the form of the network resulting from the synthesis procedure of Part I. The network consists of a series of identical naturally-birefringent crystals between an input and output polarizer. The "fast" and "slow" axes of the crystal are denoted by F and S, respectively. A network containing n crystals is necessary to realize a $C(\omega)$ having $n+1$ terms. For a given $C(\omega)$, the synthesis procedure is used to calculate the rotation angles (ϕ_i) of the crystals and the output polarizer.

Because the procedure of Part I requires that the C_i be real, it can be used only when $C(\omega)$ is Hermetian (i.e., the real part of $C(\omega)$ is even and the imaginary part is odd). Part V [26] describes a generalization of the synthesis procedure of Part I which allows the realization of $C(\omega)$ having complex C_i. An n - stage birefringent network is again required to produce a $C(\omega)$ having $n+1$ terms, but each stage now consists of a birefringent crystal and optical compensator. Such a network is shown in Fig. 3. The synthesis procedure of

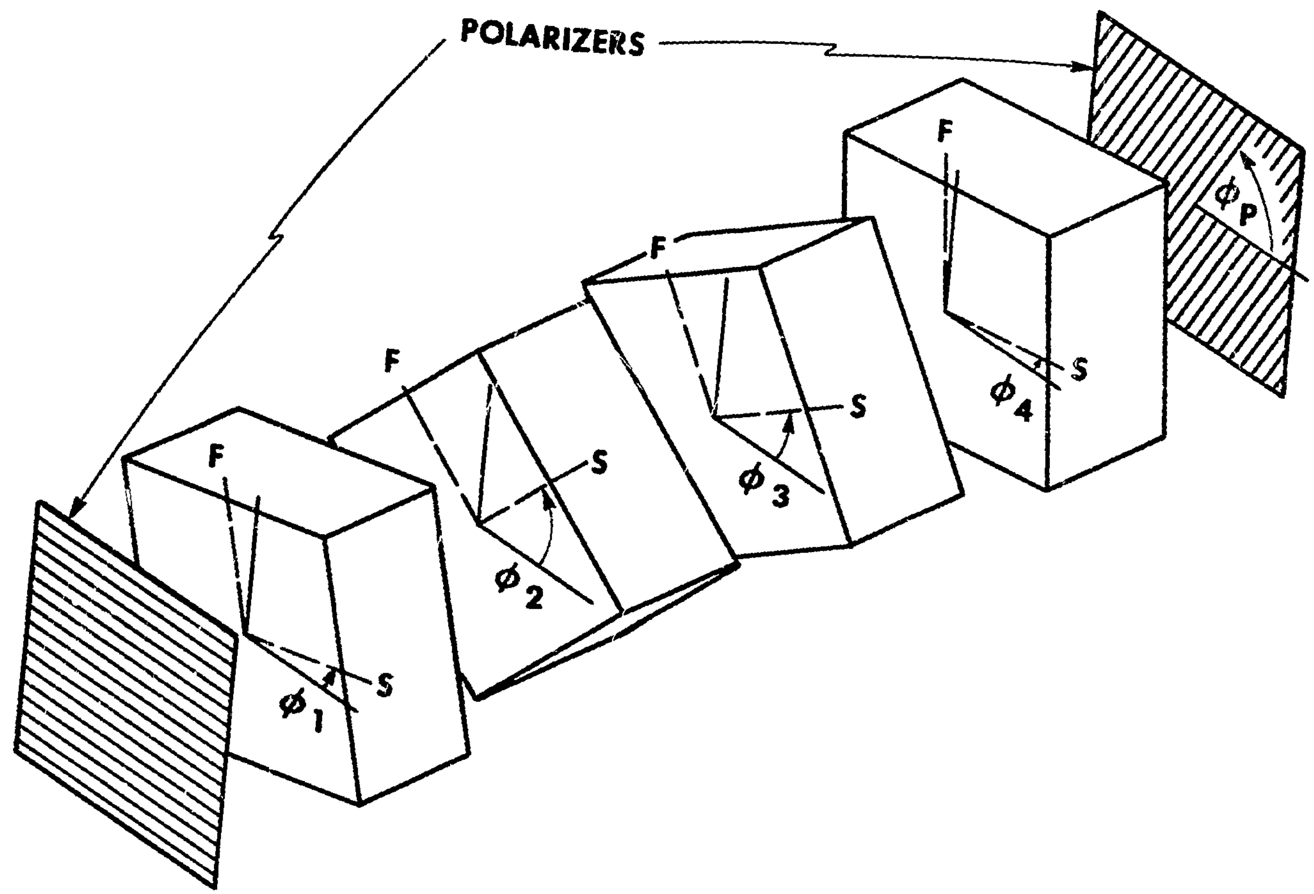

Figure 2

Part V determines the rotation angle of each crystal, the retardation introduced by each compensator, and the rotation angle of the output polarizer.

Recently it has been noted [25] that the techniques which were developed in Parts I-V [21] - [24], [26] for synthesizing optical networks composed of naturally-birefringent crystals can also be used, with very little modification, in the synthesis of networks composed of electro-optic crystals (or liquids). The two situations are, in fact, analogous. If a Pockels-effect material is used, the voltage applied to the electro-optic medium plays the same role that frequency does in naturally-birefringent materials. If a Kerr-effect material is used, frequency is replaced by the square of the voltage. This means that the same techniques which were developed to synthesize birefringent networks having arbitrary frequency transfer functions can be used to synthesize electro-optic networks having arbitrary transmission vs. applied voltage characteristics. In Ref. [25] it was shown that a procedure analogous to the synthesis procedure of Part I could be used to design electro-optic shutters with improved characteristics. In this paper we will see that a procedure analogous to the more general procedure of Part V can be used to synthesize amplitude modulators having specified modulation characteristics.

Since the modulator synthesis procedure is a direct analogy of the procedure described in Part V, only a brief discussion will be given. It is assumed in what follows that the reader is familiar with the material covered in Part V [26] and in Ref. [25].

The frequency-voltage analogy between a birefringent network and an electro-optic network can be understood in the following way. The basic building block of the birefringent networks of Parts I-V is the naturally birefringent crystal shown in Fig. 4. Light which enters the crystal with its electric field polarized in the F direction is operated upon by the frequency transfer function $e^{i\alpha\omega/2}$, while light polarized along S is operated upon by $e^{-i\alpha\omega/2}$. The quantity α is proportional to the crystal's birefringence and is given by

$$\alpha = L\,\Delta\eta/c,$$

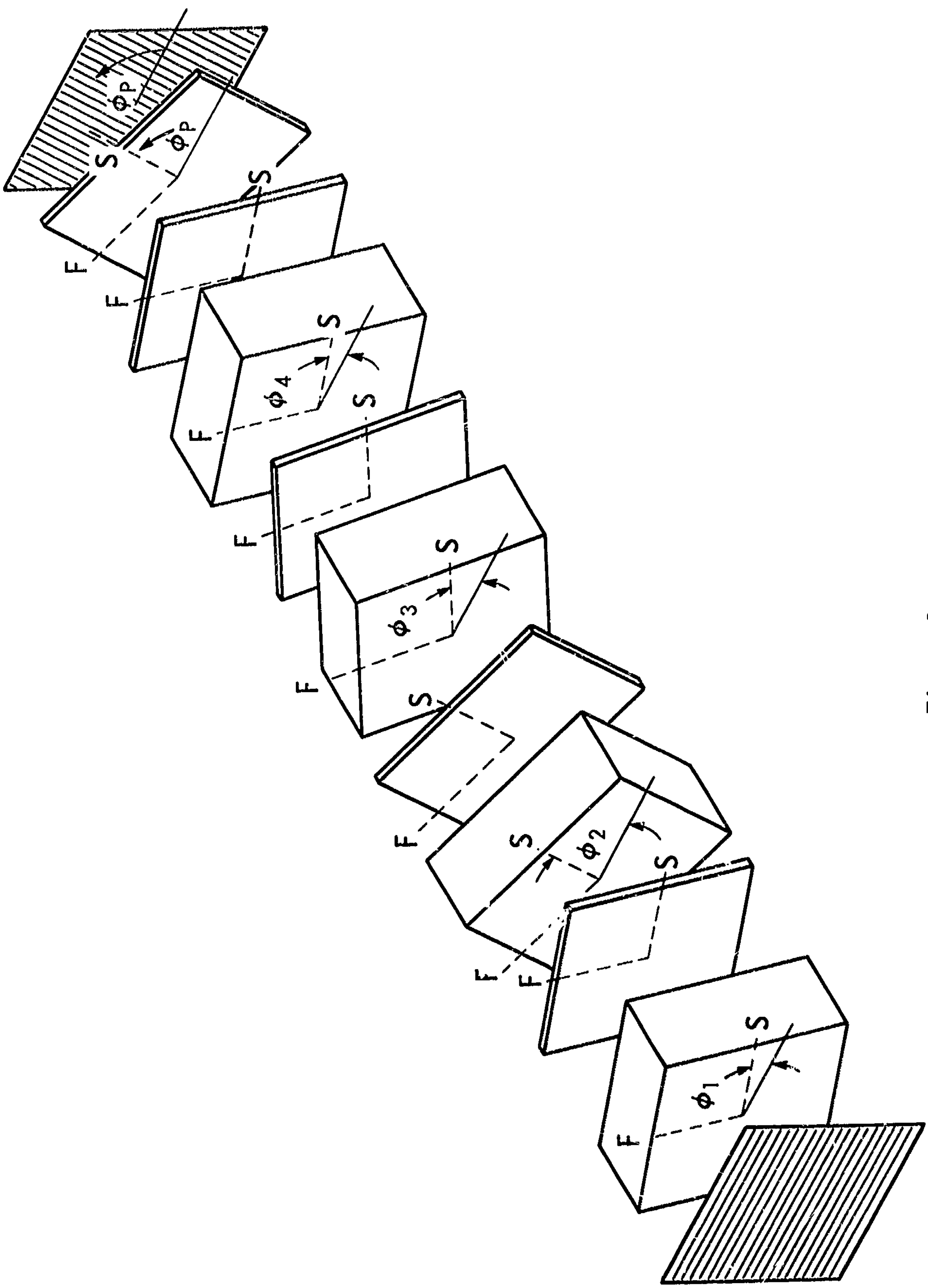

Figure 3

where L is the length of the crystal, $\Delta\eta$ is the difference between the crystal's extraordinary and ordinary indices of refraction, and c is the velocity of light in a vacuum.

Now suppose that the building block of Fig. 4 is an electro-optic cell, and that its birefringence is linearly proportional to the applied electric field. The F and S frequency transfer functions are again $e^{i\alpha\omega/2}$ and $e^{-i\alpha\omega/2}$. In this case, however, α is due to the applied electric field while in the previous case, α was due to the natural birefringence of the medium. Hence we can rewrite the F and S transfer functions of the electro-optic cell in the form $e^{i\frac{\pi}{2}\frac{v}{V_0}}$ and $e^{-i\frac{\pi}{2}\frac{v}{V_0}}$, where v is the voltage applied to the medium and V_0 is the voltage required to produce one-half wave (π radians) of retardation. In writing the F and S transfer functions of the electro-optic cell in this way, several simplifying assumptions have been made. Most important of these is that perfect synchronism exists between the modulating voltage and the transmitted light, and hence that transit-time effects are not a problem.

The transfer functions for the electro-optic cell are seen to depend upon v in exactly the same fashion as the transfer functions for the birefringent crystal depend upon frequency[1]. Thus the transfer function of a cell or series of cells varies with v in precisely the same fashion that the transfer function of a birefringent crystal or series of crystals varies with ω. Since we are able from Part V to synthesize a birefringent network with an arbitrary transmission vs. frequency characteristic, we are also able to synthesize an electro-optic modulator which has an arbitrary transmission vs. applied-voltage characteristic.

Using the analogy just discussed, the desired voltage transfer function for the modulator is written as

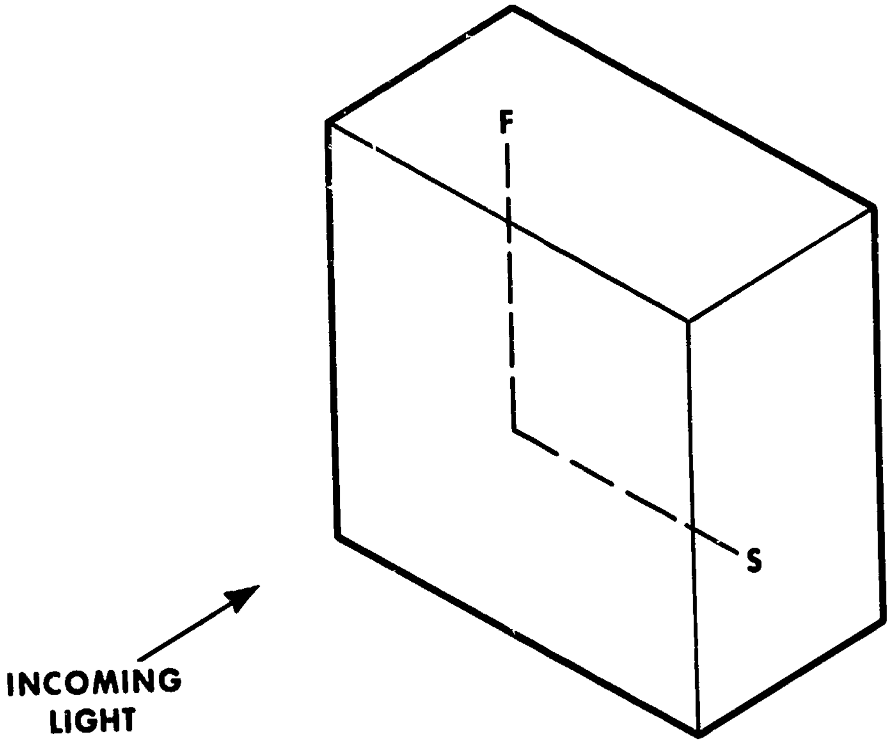

Figure 4

$$K(v) = C_0 e^{i \frac{n}{2} \pi \frac{v}{V_0}} + C_1 e^{i \frac{(n-2)}{2} \pi \frac{v}{V_0}} + C_2 e^{i \frac{(n-4)}{2} \pi \frac{v}{V_0}}$$

$$+ \dots + C_{n-2} e^{-i \frac{(n-4)}{2} \pi \frac{v}{V_0}} + C_{n-1} e^{-i \frac{(n-2)}{2} \pi \frac{v}{V_0}} + C_n e^{-i \frac{n}{2} \pi \frac{v}{V_0}} \tag{3}$$

The synthesized modulator has the general form shown in Fig. 3, with each stage composed of an electro-optic cell of half-wave voltage V_0 and an optical compensator. All cells must exhibit the same birefringence; hence (1) all cells must be identical, and (2) all cells must have the same signal applied to them. Note that the manner of applying the modulating field to the medium has not in any way bee.. restricted. Hence it is immaterial whether the modulating field is transverse or longitudinal, is applied by resonant structure or traveling-wave structure, as long as the induced birefringent axes are oriented as in Fig. 4.

B. Outline of Synthesis Procedure

The steps to be followed in synthesizing an amplitude modulator are summarized below:

(1) Choose the desired transmission vs. voltage characteristic $K(v)$ for the amplitude modulator and write it in the form of Eq. (3). The C_i may be complex.

(2) Multiply $K(v)$ by $e^{-i \frac{n}{2} \pi \frac{v}{V_0}}$, which gives

$$C(v) = e^{-i \frac{n}{2} \pi \frac{v}{V_0}} K(v) = C_0 + C_1 e^{-i \pi \frac{v}{V_0}} + C_2 e^{-i2 \pi \frac{v}{V_0}} + \dots$$

$$+ C_n e^{-in \pi \frac{v}{V_0}}. \tag{4}$$

(3) Follow steps (3) through (8) of Section II-C of Ref. [26]. This determines the rotation angle of each electro-optic cell, the delay introduced by each optical compensator, and the rotation angle of the output polarizer.

III. AMPLITUDE MODULATORS FOR USE WITH ENVELOPE DETECTORS

As mentioned earlier, the choice of an ideal characteristic for an amplitude modulator depends upon the properties of the detector used to demodulate the signal. In this section we discuss the ideal characteristic (and approximations to it) for an amplitude modulator which is used with an envelope detector. Although envelope detectors at optical frequencies are not presently available, this case is still of interest since optical heterodyne detection can be employed to shift the amplitude-modulated signal down in frequency to a range in which envelope detectors are available.

A. Ideal Modulator Characteristic

From conventional modulation theory, it is well known [27] that a linear modulator characteristic gives distortionless results when envelope detection is employed. Hence one possible[2] ideal voltage transfer function for an amplitude modulator is that shown in Fig. 5. Since an electro-optic amplitude modulator does not add energy to the carrier, the magnitude of the characteristic can not exceed unity. Note that v/V_0 (voltage applied to each cell/ the half-wave retardation voltage of each cell) is plotted along the abscissa. This normalized form of voltage is quite convenient and will be used throughout this paper.

Before proceeding further, let us establish performance criteria so that we may make quantitative comparisons of the modulators synthesized. There are a number of different criteria which could be employed, and hence our choice must be somewhat arbitrary. We will assume that a single-tone signal of the form

$$v = V \cos \omega_m t \tag{5}$$

is the modulating signal. Ideally then, the demodulated signal should be directly proportional to (5). That is, the amplitude of the fundamental (ω_m component) should be linearly proportional to V; furthermore there should be no harmonics present at $2\omega_m$, $3\omega_m$, etc. Hence as a measure of performance we will examine the detector output for (1) the deviation from linearity of the fundamental's amplitude, and (2) the amplitudes of the second and third harmonics.

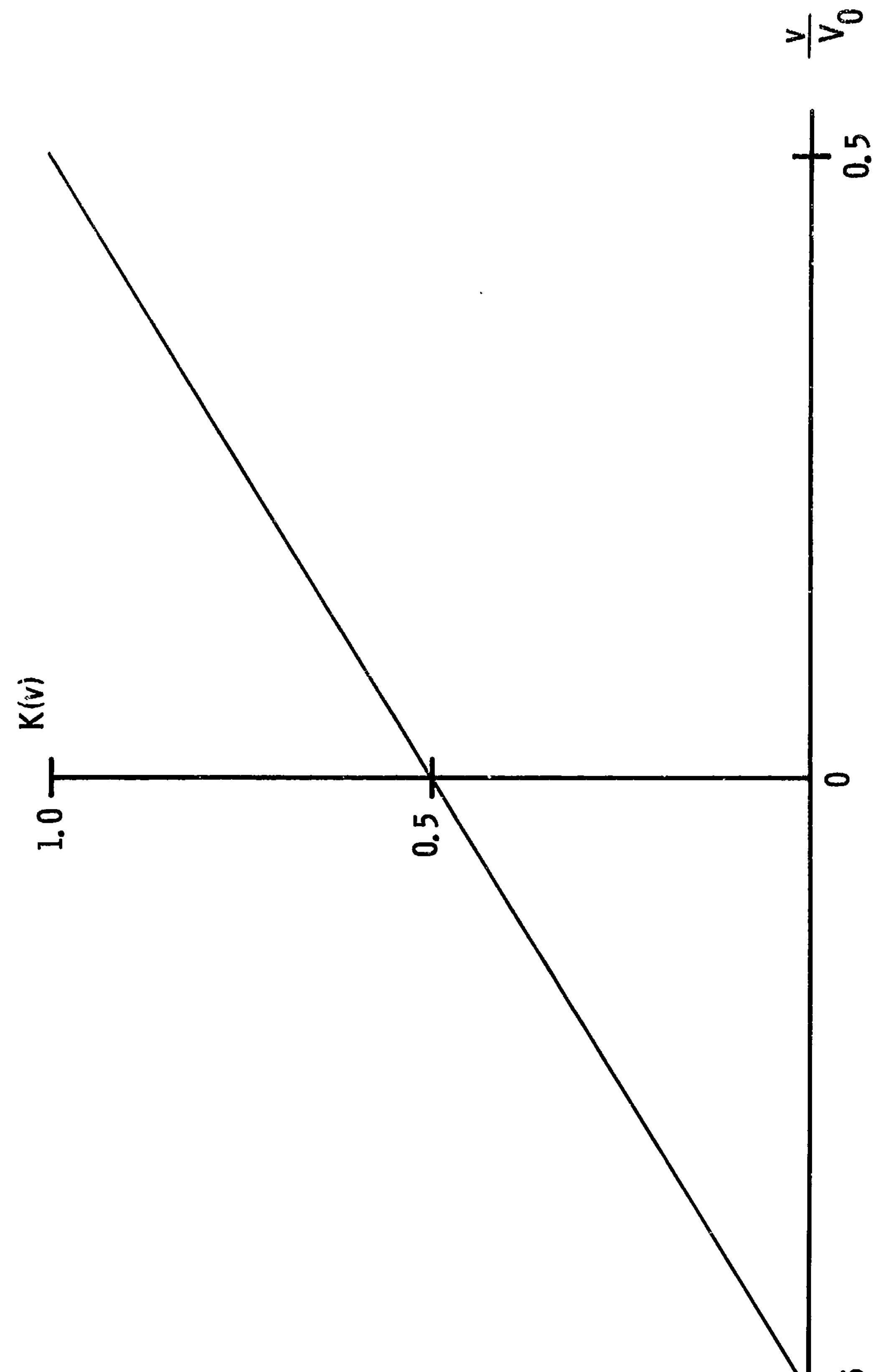

Figure 5

Using these criteria, let us establish that the characteristic of Fig. 5 is indeed an ideal characteristic. The analytic expression for the characteristic of Fig. 5 is

$$K(v) = \frac{1}{2} + \frac{v}{V_0}. \tag{6}$$

Assume that the incoming optical signal is of frequency ω, has an electric field of unity amplitude, and hence is given by

$$E_{in} = e^{i\omega t}. \tag{7}$$

The signal E_{out} leaving the modulator is $E_{in}K(v)$, and is therefore given by

$$E_{out} = \left(\frac{1}{2} + \frac{v}{V_0}\right) e^{i\omega t}.$$

Assuming that $v = V \cos \omega_m t$, we obtain

$$E_{out} = \left(\frac{1}{2} + \frac{V}{V_0} \cos \omega_m t\right) e^{i\omega t}, \tag{8}$$

the signal which impinges on the detector. The detector's output I_{out} is proportional to the envelope of E_{out}, which is just the term in parentheses (provided it remains non-negative). Thus the output is

$$I_{out} = k \left(\frac{1}{2} + \frac{V}{V_0} \cos \omega_m t\right), \tag{9}$$

where k is a constant of proportionality. We see that the detector output of Eq. (9) contains a fundamental whose amplitude is linearly proportional to V, and no higher harmonics. This satisfies our criteria for perfect modulator performance.

B. Formulas for Amplitudes of Fundamental and Harmonics

The modulators synthesized using the procedure of Section II will have voltage transfer functions of the form shown in Eq. (3). We derive here general expressions for the amplitudes of the fundamental and harmonics present in the detector output. The resulting expressions are functions of V/V_0, and contain the C_i as parameters. For this calculation and others later, it will be convenient to separately consider the cases of n odd and n even.

1. n odd

For n odd, expressions are derived for 1, 3, 5, 7, and 9 stage networks. From Eq. (3), the voltage transfer functions for these networks are seen to be

$$n = 1 \qquad K(v) = C_0 e^{i\frac{\pi}{2}\frac{v}{V_0}} + C_1 e^{-i\frac{\pi}{2}\frac{v}{V_0}}, \tag{10a}$$

$$n = 3 \qquad K(v) = C_0 e^{i\frac{3\pi}{2}\frac{v}{V_0}} + C_1 e^{i\frac{\pi}{2}\frac{v}{V_0}} + C_2 e^{-i\frac{\pi}{2}\frac{v}{V_0}} + C_3 e^{-i\frac{3\pi}{2}\frac{v}{V_0}}, \tag{10b}$$

$$n = 5 \qquad K(v) = C_0 e^{i\frac{5\pi}{2}\frac{v}{V_0}} + C_1 e^{i\frac{3\pi}{2}\frac{v}{V_0}} + C_2 e^{i\frac{\pi}{2}\frac{v}{V_0}} + C_3 e^{-i\frac{\pi}{2}\frac{v}{V_0}} + C_4 e^{-i\frac{3\pi}{2}\frac{v}{V_0}}$$
$$+ C_5 e^{-i\frac{5\pi}{2}\frac{v}{V_0}}, \tag{10c}$$

$$n = 7 \qquad K(v) = C_0 e^{i\frac{7\pi}{2}\frac{v}{V_0}} + C_1 e^{i\frac{5\pi}{2}\frac{v}{V_0}} + C_2 e^{i\frac{3\pi}{2}\frac{v}{V_0}} + C_3 e^{i\frac{\pi}{2}\frac{v}{V_0}} + C_4 e^{-i\frac{\pi}{2}\frac{v}{V_0}}$$
$$+ C_5 e^{-i\frac{3\pi}{2}\frac{v}{V_0}} + C_6 e^{-i\frac{5\pi}{2}\frac{v}{V_0}} + C_7 e^{-i\frac{7\pi}{2}\frac{v}{V_0}}, \tag{10d}$$

$$n = 9 \qquad K(v) = C_0 e^{i\frac{9\pi}{2}\frac{v}{V_0}} + C_1 e^{i\frac{7\pi}{2}\frac{v}{V_0}} + C_2 e^{i\frac{5\pi}{2}\frac{v}{V_o}} + C_3 e^{i\frac{3\pi}{2}\frac{v}{V_0}} + C_4 e^{i\frac{\pi}{2}\frac{v}{V_0}}$$
$$+ C_5 e^{-i\frac{\pi}{2}\frac{v}{V_0}} + C_6 e^{-i\frac{3\pi}{2}\frac{v}{V_0}} + C_7 e^{-i\frac{5\pi}{2}\frac{v}{V_0}} + C_8 e^{-i\frac{7\pi}{2}\frac{v}{V_0}} + C_9 e^{-i\frac{9\pi}{2}\frac{v}{V_0}} \tag{10e}$$

We will go through the details of the computation for n = 9 only. Results for n = 1, 3, 5, and 7 are obtained from the n = 9 results by setting appropriate C_i equal to zero and renumbering the remaining C_i.

At this point we will impose the requirement that our approximating $K(v)$ be real. If a complex $K(v)$ is used, the phase as well as the amplitude of the demodulated fundamental will depend upon V. Hence for the envelope detector case, a real $K(v)$ should be employed in order to avoid phase distortion. This means that in Eq. (10e), $C_0 = C_9^*$, $C_1 = C_8^*$, $C_2 = C_7^*$, $C_3 = C_6^*$, and $C_4 = C_5^*$. (Asterisks denote complex conjugate.) Using this fact, and letting

$$C_i = A_i + iB_i , \tag{11}$$

Eq. (10e) can be rewritten as

$$\begin{aligned} K(v) = 2 \Bigg[& A_0 \cos \frac{9\pi}{2}\frac{v}{V_0} + A_1 \cos \frac{7\pi}{2}\frac{v}{V_0} + A_2 \cos \frac{5\pi}{2}\frac{v}{V_0} + A_3 \cos \frac{3\pi}{2}\frac{v}{V_0} \\ & + A_4 \cos \frac{\pi}{2}\frac{v}{V_0} - B_0 \sin \frac{9\pi}{2}\frac{v}{V_0} - B_1 \sin \frac{7\pi}{2}\frac{v}{V_0} - B_2 \sin \frac{5\pi}{2}\frac{v}{V_0} \\ & - B_3 \sin \frac{3\pi}{2}\frac{v}{V_0} - B_4 \sin \frac{\pi}{2}\frac{v}{V_0} \Bigg] . \end{aligned} \tag{12}$$

If we assume that light incident upon the modulator is given by $e^{i\omega t}$, the light (E_{out}) leaving the modulator is given by Eq. (12) multiplied by $e^{i\omega t}$. Substituting $v = V \cos \omega_m t$, we obtain

$$\begin{aligned} E_{out} = 2 \Bigg[& A_0 \cos \left(\frac{9\pi}{2}\frac{V}{V_0} \cos \omega_m t\right) + A_1 \cos \left(\frac{7\pi}{2}\frac{V}{V_0} \cos \omega_m t\right) \\ & + A_2 \cos \left(\frac{5\pi}{2}\frac{V}{V_0} \cos \omega_m t\right) + A_3 \cos \left(\frac{3\pi}{2}\frac{V}{V_0} \cos \omega_m t\right) \\ & + A_4 \cos \left(\frac{\pi}{2}\frac{V}{V_0} \cos \omega_m t\right) - B_0 \sin \left(\frac{9\pi}{2}\frac{V}{V_0} \cos \omega_m t\right) \\ & - B_1 \sin \left(\frac{7\pi}{2}\frac{V}{V_0} \cos \omega_m t\right) - B_2 \sin \left(\frac{5\pi}{2}\frac{V}{V_0} \cos \omega_m t\right) \\ & - B_3 \sin \left(\frac{3\pi}{2}\frac{V}{V_0} \cos \omega_m t\right) - B_4 \sin \left(\frac{\pi}{2}\frac{V}{V_0} \cos \omega_m t\right) \Bigg] e^{i\omega t}. \end{aligned} \tag{13}$$

Using the standard expansions for cos (kcos θ) and sin (kcos θ), Eq. (13) becomes

$$
\begin{aligned}
E_{out} = \Bigg\{ & 2 \left[A_0 J_0 \left(\frac{9\pi V}{2 V_0}\right) + A_1 J_0 \left(\frac{7\pi V}{2 V_0}\right) + A_2 J_0 \left(\frac{5\pi V}{2 V_0}\right) \right. \\
& \left. + A_3 J_0 \left(\frac{3\pi V}{2 V_0}\right) + A_4 J_0 \left(\frac{\pi V}{2 V_0}\right) \right] \\
& - 4 \left[B_0 J_1 \left(\frac{9\pi V}{2 V_0}\right) + B_1 J_1 \left(\frac{7\pi V}{2 V_0}\right) + B_2 J_1 \left(\frac{5\pi V}{2 V_0}\right) \right. \\
& \left. + B_3 J_1 \left(\frac{3\pi V}{2 V_0}\right) + B_4 J_1 \left(\frac{\pi V}{2 V_0}\right) \right] \cos \omega_m t \\
& - 4 \left[A_0 J_2 \left(\frac{9\pi V}{2 V_0}\right) + A_1 J_2 \left(\frac{7\pi V}{2 V_0}\right) + A_2 J_2 \left(\frac{5\pi V}{2 V_0}\right) \right. \\
& \left. + A_3 J_2 \left(\frac{3\pi V}{2 V_0}\right) + A_4 J_2 \left(\frac{\pi V}{2 V_0}\right) \right] \cos 2\omega_m t \\
& + 4 \left[B_0 J_3 \left(\frac{9\pi V}{2 V_0}\right) + B_1 J_3 \left(\frac{7\pi V}{2 V_0}\right) + B_2 J_3 \left(\frac{5\pi V}{2 V_0}\right) \right. \\
& \left. + B_3 J_3 \left(\frac{3\pi V}{2 V_0}\right) + B_4 J_3 \left(\frac{\pi V}{2 V_0}\right) \right] \cos 3\omega_m t \\
& + \ldots \Bigg\} e^{i\omega t},
\end{aligned}
\tag{14}
$$

where J_n is a Bessel function of first kind and order n. As long as the bracketed term multiplying $e^{i\omega t}$ in (14) remains non-negative, the detector output I_{out} will be directly proportional to it. Hence we obtain the desired result,

$$
\begin{aligned}
I_{out}/k = 2 & \left[A_0 J_0 \left(\frac{9\pi V}{2 V_0}\right) + A_1 J_0 \left(\frac{7\pi V}{2 V_0}\right) + A_2 J_0 \left(\frac{5\pi V}{2 V_0}\right) \right. \\
& \left. + A_3 J_0 \left(\frac{3\pi V}{2 V_0}\right) + A_4 J_0 \left(\frac{\pi V}{2 V_0}\right) \right]
\end{aligned}
$$

$$- 4 \left[B_0 J_1 \left(\frac{9\pi}{2}\frac{V}{V_0}\right) + B_1 J_1 \left(\frac{7\pi}{2}\frac{V}{V_0}\right) + B_2 J_1 \left(\frac{5\pi}{2}\frac{V}{V_0}\right)\right.$$

$$\left. + B_3 J_1 \left(\frac{3\pi}{2}\frac{V}{V_0}\right) + B_4 J_1 \left(\frac{\pi}{2}\frac{V}{V_0}\right)\right] \cos \omega_m t$$

$$- 4 \left[A_0 J_2 \left(\frac{9\pi}{2}\frac{V}{V_0}\right) + A_1 J_2 \left(\frac{7\pi}{2}\frac{V}{V_0}\right) + A_2 J_2 \left(\frac{5\pi}{2}\frac{V}{V_0}\right)\right.$$

$$\left. + A_3 J_2 \left(\frac{3\pi}{2}\frac{V}{V_0}\right) + A_4 J_2 \left(\frac{\pi}{2}\frac{V}{V_0}\right)\right] \cos 2\omega_m t$$

$$+ 4 \left[B_0 J_3 \left(\frac{9\pi}{2}\frac{V}{V_0}\right) + B_1 J_3 \left(\frac{7\pi}{2}\frac{V}{V_0}\right) + B_2 J_3 \left(\frac{5\pi}{2}\frac{V}{V_0}\right)\right.$$

$$\left. + B_3 J_3 \left(\frac{3\pi}{2}\frac{V}{V_0}\right) + B_4 J_3 \left(\frac{\pi}{2}\frac{V}{V_0}\right)\right] \cos 3\omega_m t$$

$$+ \text{higher order harmonics.} \tag{15}$$

Equation (15) gives the dc, fundamental, second harmonic, and third harmonic components present in the envelope-detector output for $n = 9$. Note that the even harmonic amplitudes are determined by the B_i while the odd harmonic amplitudes depend upon the A_i.

2. n even

For n even, we will consider 2, 4, 6, 8, and 10 stage networks. The voltage transfer functions for these networks are given by

$$n = 2 \qquad K(v) = C_0 e^{i\frac{\pi v}{V_0}} + C_1 + C_2 e^{-i\frac{\pi v}{V_0}} \tag{16a}$$

$$n = 4 \qquad K(v) = C_0 e^{i\frac{2\pi v}{V_0}} + C_1 e^{i\frac{\pi v}{V_0}} + C_2 + C_3 e^{-i\frac{\pi v}{V_0}} + C_4 e^{-i\frac{2\pi v}{V_0}} \tag{16b}$$

$$n = 6 \qquad K(v) = C_0 e^{i\frac{3\pi v}{V_0}} + C_1 e^{i\frac{2\pi v}{V_0}} + C_2 e^{i\frac{\pi v}{V_0}} + C_3 + C_4 e^{-i\frac{\pi v}{V_0}}$$

$$+ C_5 e^{-i\frac{2\pi v}{V_0}} + C_6 e^{-i\frac{3\pi v}{V_0}} \tag{16c}$$

$$n = 8 \qquad K(v) = C_0 e^{i\frac{4\pi v}{V_0}} + C_1 e^{i\frac{3\pi v}{V_0}} + C_2 e^{i\frac{2\pi v}{V_0}} + C_3 e^{i\frac{\pi v}{V_0}} + C_4$$

$$+ C_5 e^{-i\frac{\pi v}{V_0}} + C_6 e^{-i\frac{2\pi v}{V_0}} + C_7 e^{-i\frac{3\pi v}{V_0}} + C_8 e^{-i\frac{4\pi v}{V_o}} \tag{16d}$$

$$n = 10 \qquad K(v) = C_0 e^{i\frac{5\pi v}{V_0}} + C_1 e^{i\frac{4\pi v}{V_0}} + C_2 e^{i\frac{3\pi v}{V_0}} + C_3 e^{i\frac{2\pi v}{V_0}} + C_4 e^{i\frac{\pi v}{V_0}}$$

$$+ C_5 + C_6 e^{-i\frac{\pi v}{V_0}} + C_7 e^{-i\frac{2\pi v}{V_0}} + C_8 e^{-i\frac{3\pi v}{V_0}} + C_9 e^{-i\frac{4\pi v}{V_0}}$$

$$+ C_{10} e^{-i\frac{5\pi v}{V_0}} \; . \tag{16e}$$

It will be sufficient to carry out the calculation only for $n = 10$; results for $n = 2$, 4, 6, and 8 can be obtained from the $n = 10$ results by setting appropriate C_i equal to zero and renumbering the remaining C_i.

The calculation proceeds similarly as for n odd. We first stipulate that $K(v)$ be real. This requires that the C_i of (16e) satisfy $C_0 = C_{10}^*$, $C_1 = C_9^*$, $C_2 = C_8^*$, $C_3 = C_7^*$, $C_4 = C_6^*$, and that C_5 be real. Again the substitution $v = V\cos\omega_m t$ is made, and standard expansions for $\cos(k\cos\theta)$ and $\sin(k\cos\theta)$ employed. The final result for $n = 10$ is

$$I_{out}/k = A_5 + 2\left[A_0 J_0\left(\frac{5\pi V}{V_0}\right) + A_1 J_0\left(\frac{4\pi V}{V_0}\right) + A_2 J_0\left(\frac{3\pi V}{V_0}\right)\right.$$

$$\left. + A_3 J_0\left(\frac{2\pi V}{V_0}\right) + A_4 J_0\left(\frac{\pi V}{V_0}\right)\right]$$

$$- 4 \left[B_0 J_1 \left(\frac{5\pi V}{V_0}\right) + B_1 J_1 \left(\frac{4\pi V}{V_0}\right) + B_2 J_1 \left(\frac{3\pi V}{V_0}\right) + B_3 J_1 \left(\frac{2\pi V}{V_0}\right) + B_4 J_1 \left(\frac{\pi V}{V_0}\right) \right] \cos \omega_m t$$

$$- 4 \left[A_0 J_2 \left(\frac{5\pi V}{V_0}\right) + A_1 J_2 \left(\frac{4\pi V}{V_0}\right) + A_2 J_2 \left(\frac{3\pi V}{V_0}\right) + A_3 J_2 \left(\frac{2\pi V}{V_0}\right) + A_4 J_2 \left(\frac{\pi V}{V_0}\right) \right] \cos 2\omega_m t$$

$$+ 4 \left[B_0 J_3 \left(\frac{5\pi V}{V_0}\right) + B_1 J_3 \left(\frac{4\pi V}{V_0}\right) + B_2 J_3 \left(\frac{3\pi V}{V_0}\right) + B_3 J_3 \left(\frac{2\pi V}{V_0}\right) + B_4 J_3 \left(\frac{\pi V}{V_0}\right) \right] \cos 3\omega_m t$$

+ higher order harmonics. (17)

C. Fourier Approximation to Ideal Characteristic

We are now ready to find approximations to the ideal characteristic of Fig. 5 which can be written in the form of Eq. (3). One obvious choice is to use the Fourier approximation to determine the C_i of Eq. (3). Since the $K(v)$ given by (10) and (16) are periodic, the ideal characteristic must also be periodic.

The symmetry of the ideal characteristic must be different for the cases of n odd and n even. For n odd, we will choose the ideal characteristic over one period to be that shown in Fig. 6a. This characteristic is, of course, only one of an infinite number of possibilities, and no claim is made that it is in any way optimum. It was chosen because it does not have any discontinuities and one might therefore hope that its Fourier series converges rapidly. For n even, the ideal characteristic of Fig. 6b will be used. It is identical to the characteristic of Fig. 6a over the region $-0.5 < v/V_0 < 1.5$, but differs over the remainder of its period.

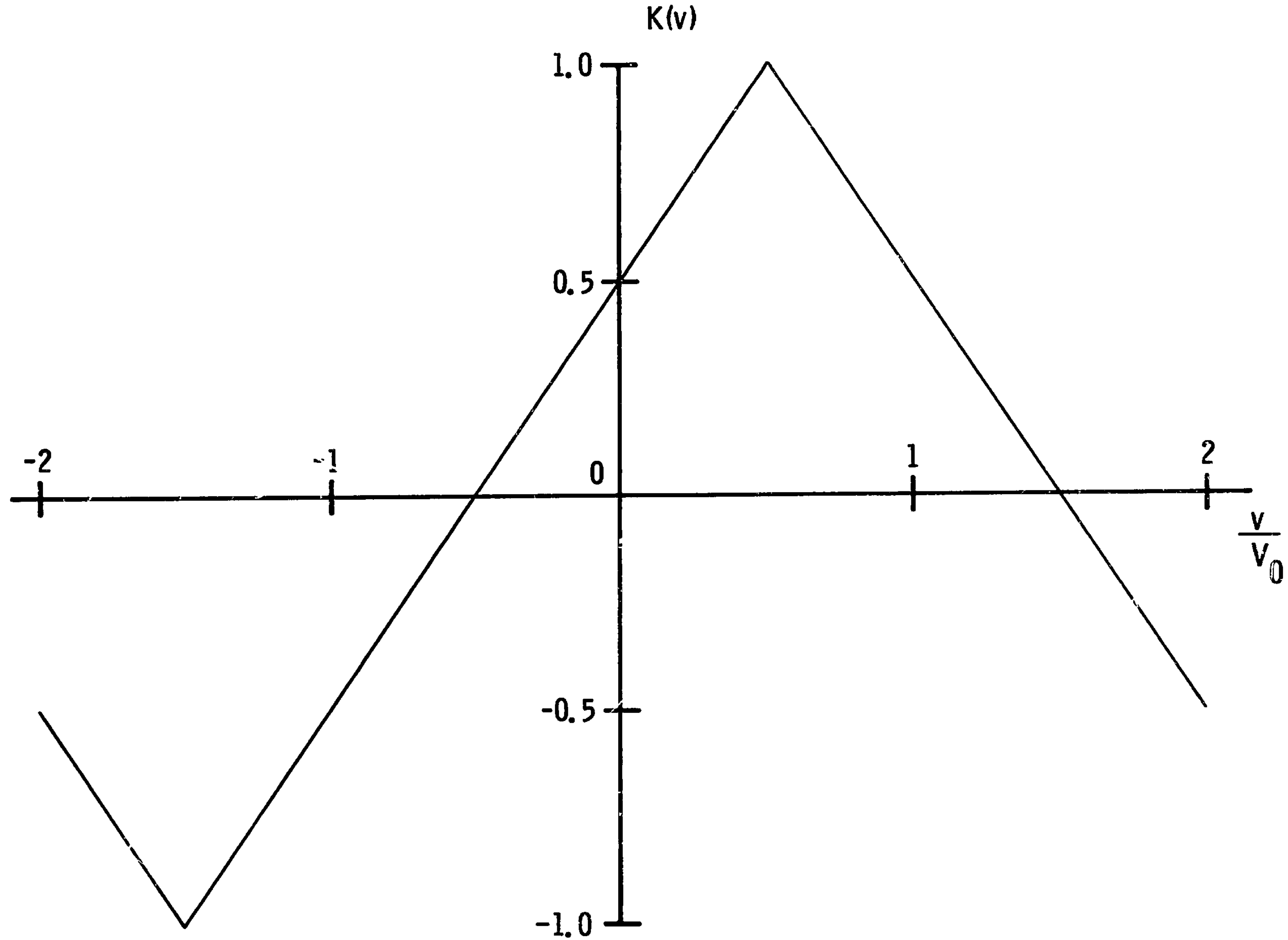

Figure 6a

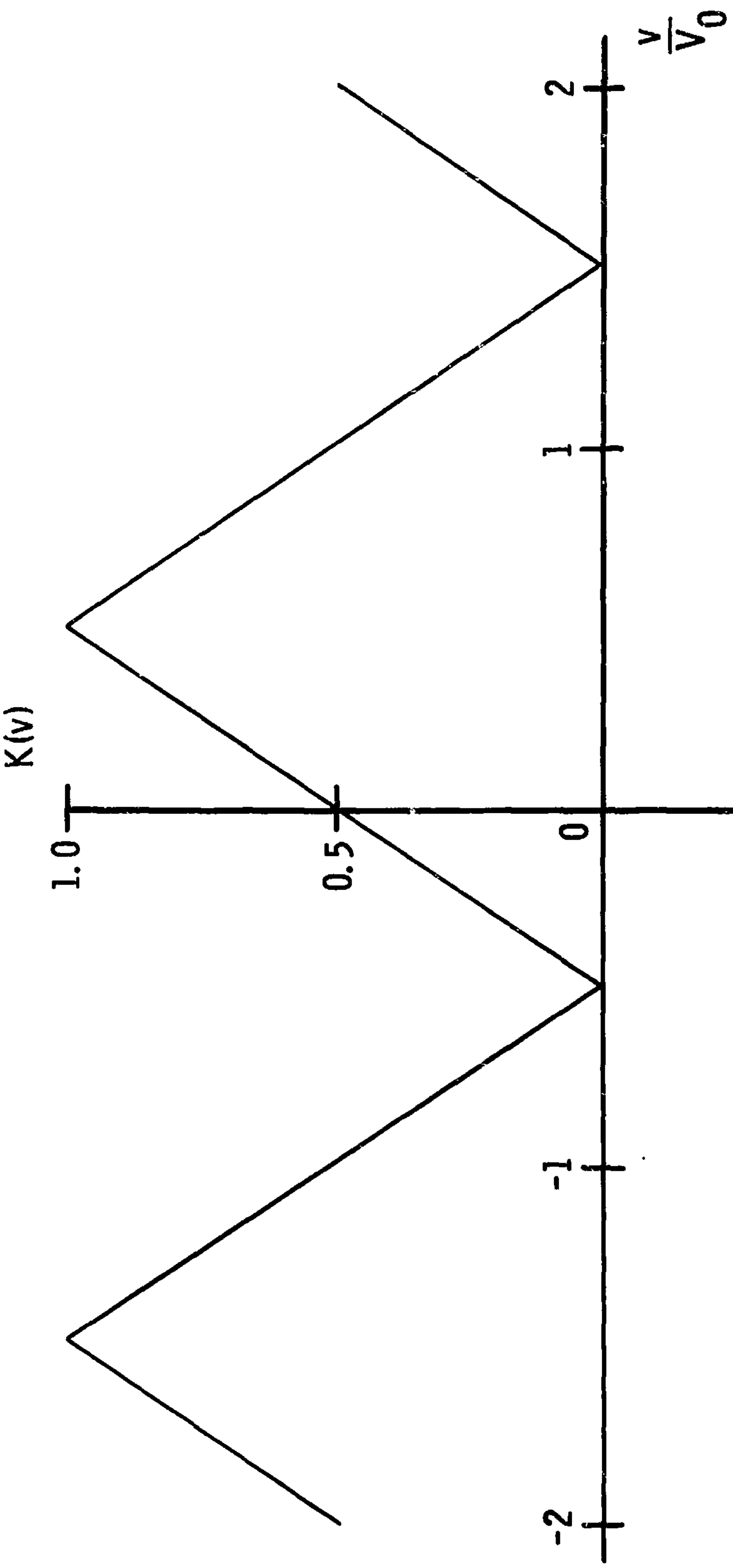

Figure 6b

1. n odd

The complex Fourier series was calculated for the ideal characteristic of Fig. 6a. The expression for K(v) for each value of n was found by truncating the series after an appropriate number of terms. Each truncated series was then normalized to have a maximum magnitude of unity. The resulting K(v) are

$$n = 1 \qquad K(v) = 0.353553(1-i)\,e^{i\frac{\pi}{2}\frac{v}{V_0}} + 0.353553(1+i)\,e^{-i\frac{\pi}{2}\frac{v}{V_0}}, \tag{18a}$$

$$n = 3 \qquad K(v) = -0.0353553(1+i)\,e^{i\frac{3\pi}{2}\frac{v}{V_0}} + 0.318198(1-i)\,e^{i\frac{\pi}{2}\frac{v}{V_0}} + 0.318198(1+i)\,e^{-i\frac{\pi}{2}\frac{v}{V_0}}$$
$$-0.0353553(1-i)\,e^{-i\frac{3\pi}{2}\frac{v}{V_0}}, \tag{18b}$$

$$n = 5 \qquad K(v) = -0.0122856(1-i)\,e^{i\frac{5\pi}{2}\frac{v}{V_0}} - 0.0341268(1+i)\,e^{i\frac{3\pi}{2}\frac{v}{V_0}} + 0.307141(1-i)\,e^{i\frac{\pi}{2}\frac{v}{V_0}}$$
$$+0.307141(1+i)\,e^{-i\frac{\pi}{2}\frac{v}{V_0}} - 0.0341268(1-i)\,e^{-i\frac{3\pi}{2}\frac{v}{V_0}}$$
$$-0.0122856(1+i)\,e^{-i\frac{5\pi}{2}\frac{v}{V_0}}, \tag{18c}$$

$$n = 7 \qquad K(v) = 0.0061589(1+i)\,e^{i\frac{7\pi}{2}\frac{v}{V_0}} - 0.0120716(1-i)\,e^{i\frac{5\pi}{2}\frac{v}{V_0}}$$
$$-0.0335323(1+i)\,e^{i\frac{3\pi}{2}\frac{v}{V_0}} + 0.301791(1-i)\,e^{i\frac{\pi}{2}\frac{v}{V_0}} + 0.301791(1+i)\,e^{-i\frac{\pi}{2}\frac{v}{V_0}}$$
$$-0.0335323(1-i)\,e^{-i\frac{3\pi}{2}\frac{v}{V_0}} - 0.0120716(1+i)\,e^{-i\frac{5\pi}{2}\frac{v}{V_0}} + 0.0061589(1-i)\,e^{-i\frac{7\pi}{2}\frac{v}{V_0}}$$

(18d)

$$n = 9 \qquad K(v) = 0.003687(1-i)\,e^{i\frac{9\pi}{2}\frac{v}{V_0}} + 0.006094(1+i)\,e^{i\frac{7\pi}{2}\frac{v}{V_0}} - 0.011945(1-i)\,e^{i\frac{5\pi}{2}\frac{v}{V_0}}$$

$$- 0.033182(1+i)\,e^{i\frac{3\pi}{2}\frac{v}{V_0}} + 0.298643(1-i)\,e^{i\frac{\pi}{2}\frac{v}{V_0}} + 0.298643(1+i)\,e^{-i\frac{\pi}{2}\frac{v}{V_0}}$$

$$- 0.033182(1-i)\,e^{-i\frac{3\pi}{2}\frac{v}{V_0}} - 0.011945(1+i)\,e^{-i\frac{5\pi}{2}\frac{v}{V_0}} + 0.006094(1-i)\,e^{-i\frac{7\pi}{2}\frac{v}{V_0}}$$

$$+ 0.003687(1+i)\,e^{-i\frac{9\pi}{2}\frac{v}{V_0}} . \qquad (18e)$$

These $K(v)$ are shown plotted in Fig. 7 over the portion of the characteristic which is of most interest, $-0.5 < v/V_0 < +0.5$. Solid curves are used for $n = 1, 3,$ and 5, and dotted curves for $n = 7$ and 9. The ideal characteristic is shown dashed. These conventions will be used throughout. The curve $n = 1$ corresponds to the conventional amplitude modulator of Fig. 1.

As expected, the approximation to the ideal $K(v)$ improves with increasing n. In general, for all n the approximation is better for $-0.5 < v/V_0 < 0$ than for $0 < v/V_0 < +0.5$. This might have been expected since there is a discontinuity in the slope of $K(v)$ at $v/V_0 = +0.5$, while there is none at $v/V_0 = -0.5$.

Of primary interest, however, is not how well the $K(v)$ of Eqs. (18) approximate the ideal $K(v)$, but rather how well the criteria established in Section IIIA are satisfied. To determine this for $n = 9$, we substitute the A_i and B_i of (18e) into Eq. (15). For the other values of n, the A_i and B_i are substituted into the appropriate equations derived from Eq. (15). This gives the information desired on the fundamental and harmonic amplitudes present in the demodulated signal.

The results are plotted in Fig. 8 where (a) the dc component, (b) the fundamental amplitude, (c) the second-harmonic magnitude, (d) the third harmonic magnitude, and (e) the deviation from linearity of the fundamental are shown as a function of V/V_0.

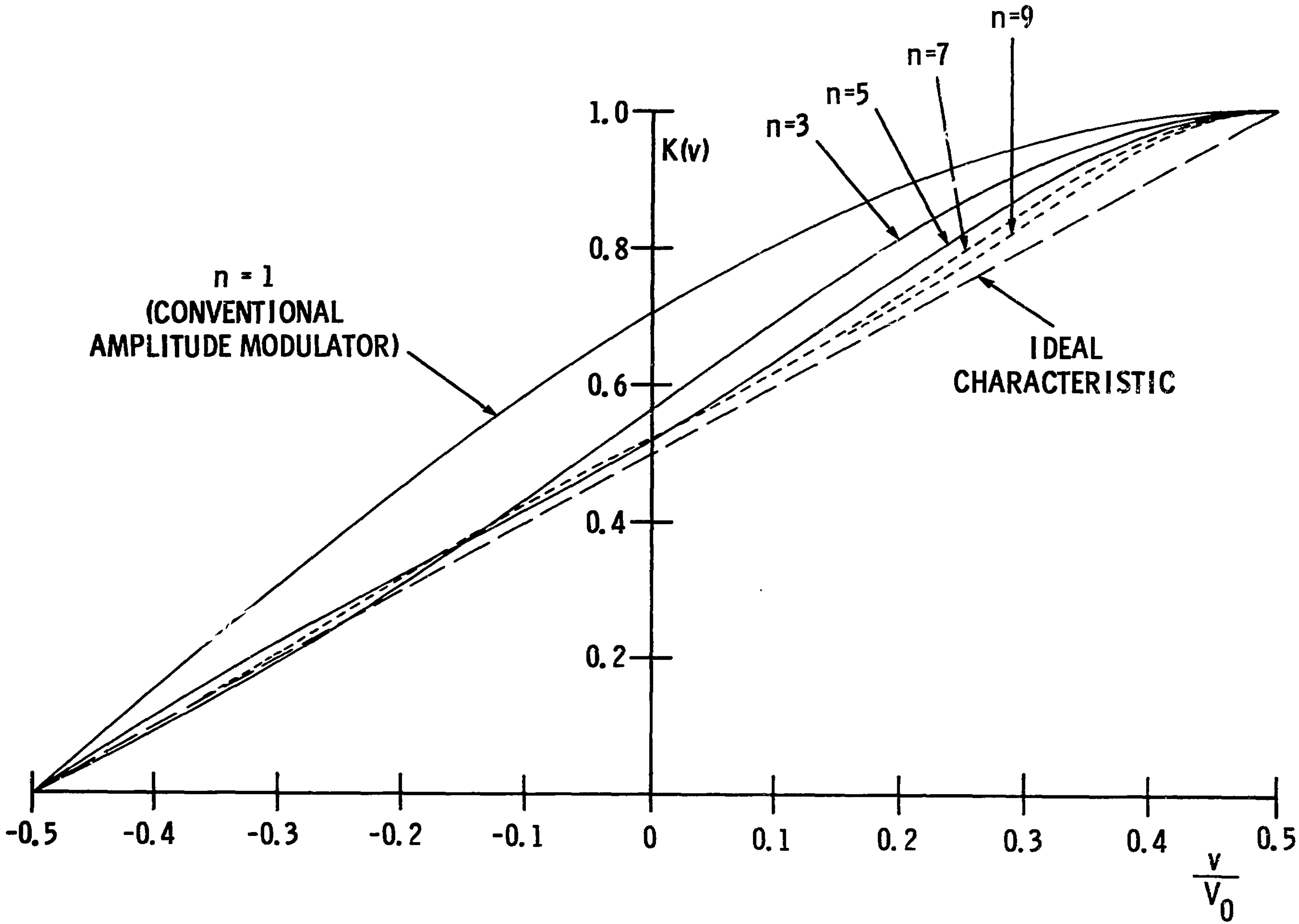

n=9
n=7
n=5
n=3
1.0
K(v)
0.8
0.6
0.4
0.2
n = 1
(CONVENTIONAL
AMPLITUDE MODULATOR)
IDEAL
CHARACTERISTIC
-0.5
-0.4
-0.3
-0.2
-0.1
0
0.1
0.2
0.3
0.4
0.5
v/V0

Figure 7

Graphs (a), (b), (c), and (d) are found from the appropriate terms of Eq. (15). The deviation from linearity of the fundamental is calculated in the following way. The slope of each curve of Fig. 8b is calculated at the origin. A straight line is then constructed for each curve by extrapolating this small-signal slope. The difference between each amplitude curve and its extrapolated straight line is termed the deviation from linearity. In Fig. 8e we plot the magnitude of this deviation.

The following results are seen from Fig. 8. The fundamental amplitude is approximately linear with V/V_0 for all values of n. Hence from Fig. 8b alone, it is difficult to compare modulator performance on the basis of linearity of fundamental. The deviation from linearity curves of Fig. 8e, however, give a clear comparison for various n. From Fig. 8e we see that in all cases, deviation from linearity increases with increasing depth of modulation, although not necessarily in a monotonic fashion. Furthermore, we see that while the deviation from linearity for $n = 5$ and 9 is less than for $n = 1$, it is greater for $n = 3$ and 7. Hence we conclude that with respect to deviation from linearity of the fundamental, systematic improvement is not obtained as one uses more stages.

The second harmonic magnitudes are shown in Fig. 8c. Here a fairly uniform improvement with increasing n is obtained. For example the second harmonic amplitude for $n = 7$ is less than that for $n = 1$ by an order of magnitude for all values of V/V_0.

The third harmonic magnitudes are plotted in Fig. 8d. The curves for the third harmonic magnitude are very similar in form to those of Fig. 8e which show deviation from linearity of the fundamental. The magnitude of the third harmonic is reduced for $n = 5$ and 9, but is greater for $n = 3$ and 7.

From the above results, we conclude that the technique of determining $K(v)$ by finding the complex Fourier series of the ideal characteristic of Fig. 6a did not prove to be satisfactory. While improvement was noted over conventional modulator performance for some values of n, poorer performance was obtained for others. One difficulty with this approach lies in the following. The C_i were chosen to approximate a certain voltage

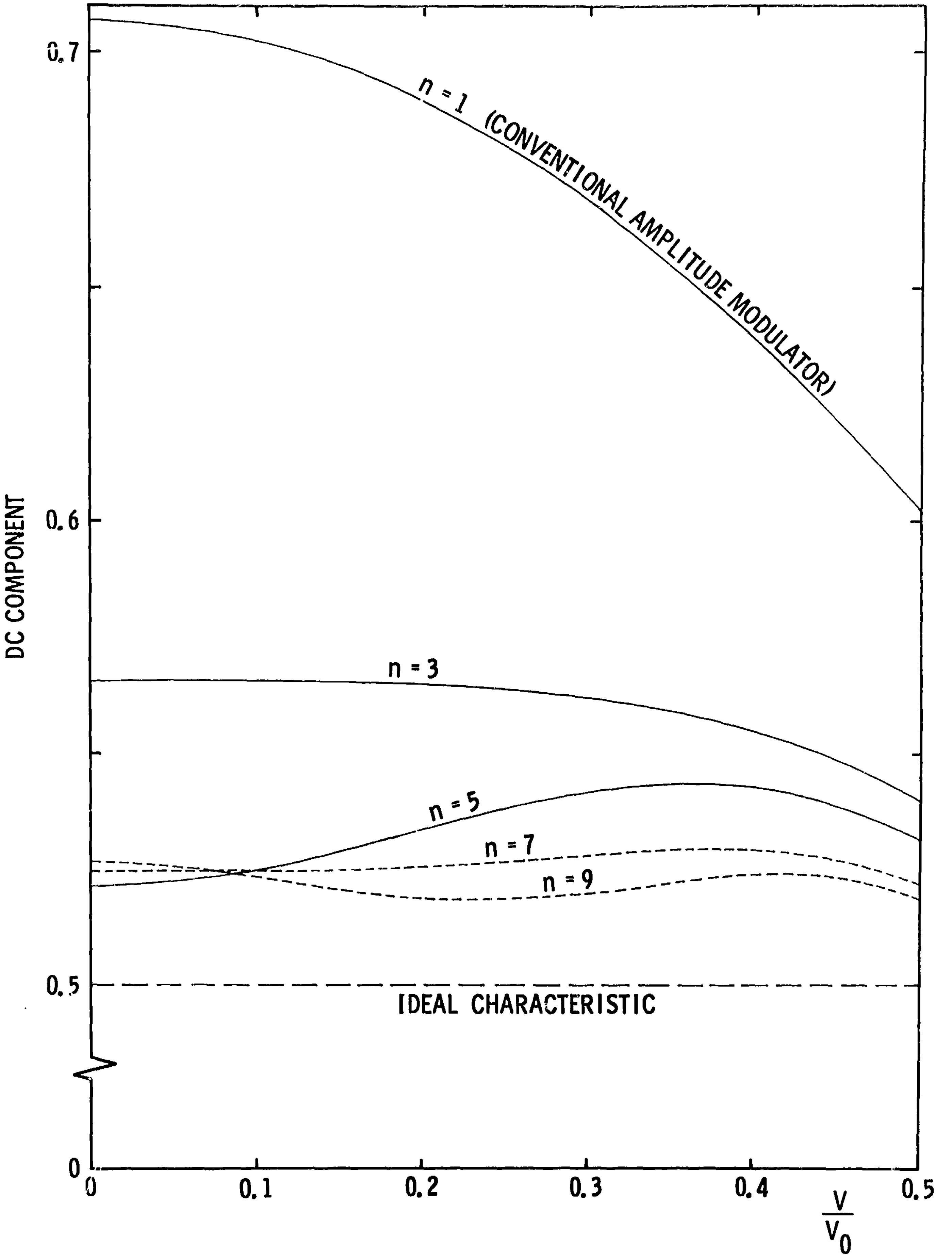

DC COMPONENT
0.7
0.6
0.5
0
n = 1 (CONVENTIONAL AMPLITUDE MODULATOR)
n = 3
n = 5
n = 7
n = 9
IDEAL CHARACTERISTIC
0
0.1
0.2
0.3
0.4
0.5
V/V0

Figure 8a

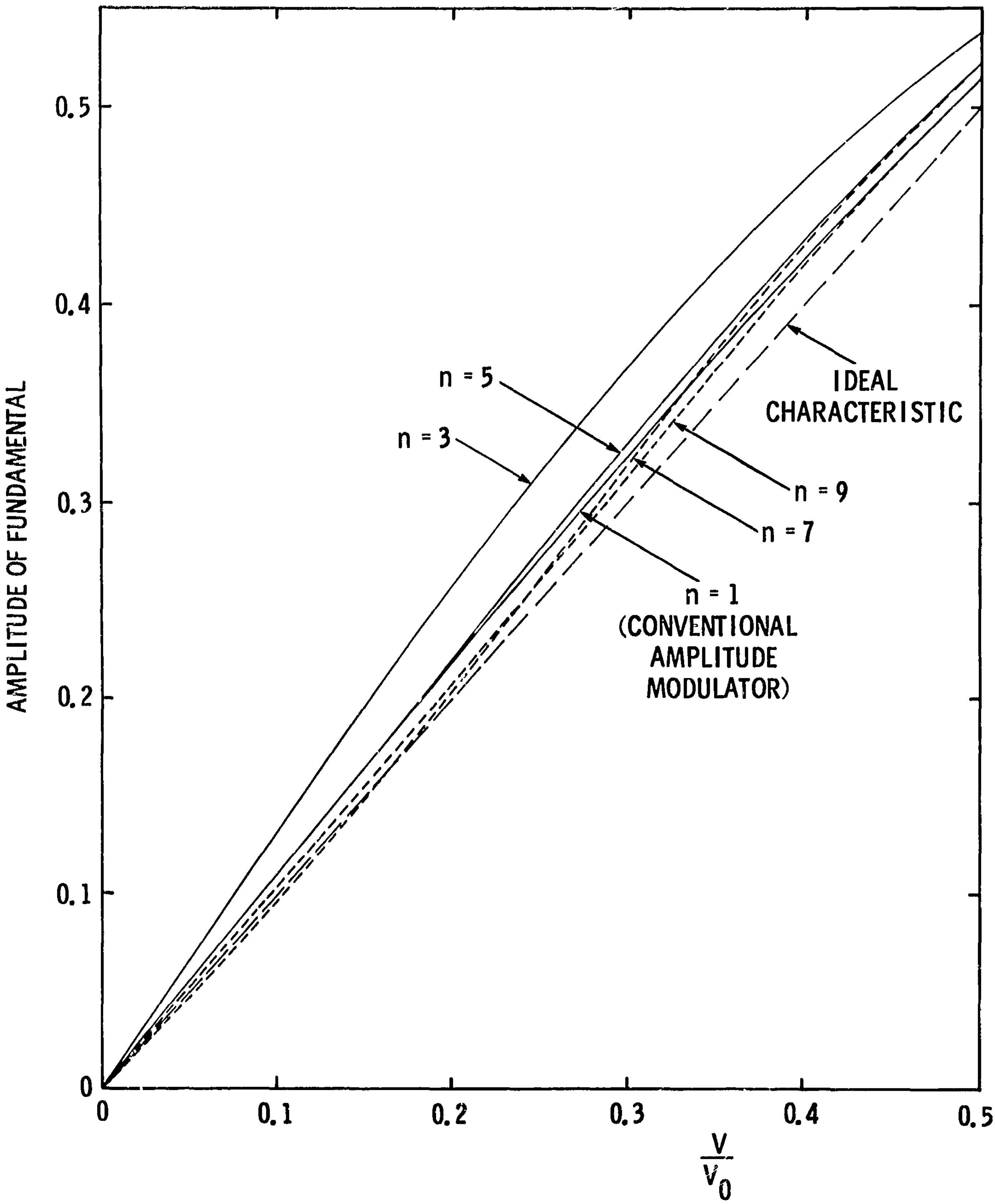
0.5
0.4
0.3
0.2
0.1
0
AMPLITUDE OF FUNDAMENTAL
n = 5
n = 3
IDEAL CHARACTERISTIC
n = 9
n = 7
n = 1 (CONVENTIONAL AMPLITUDE MODULATOR)
0
0.1
0.2
0.3
0.4
0.5
V/V0

Figure 8b

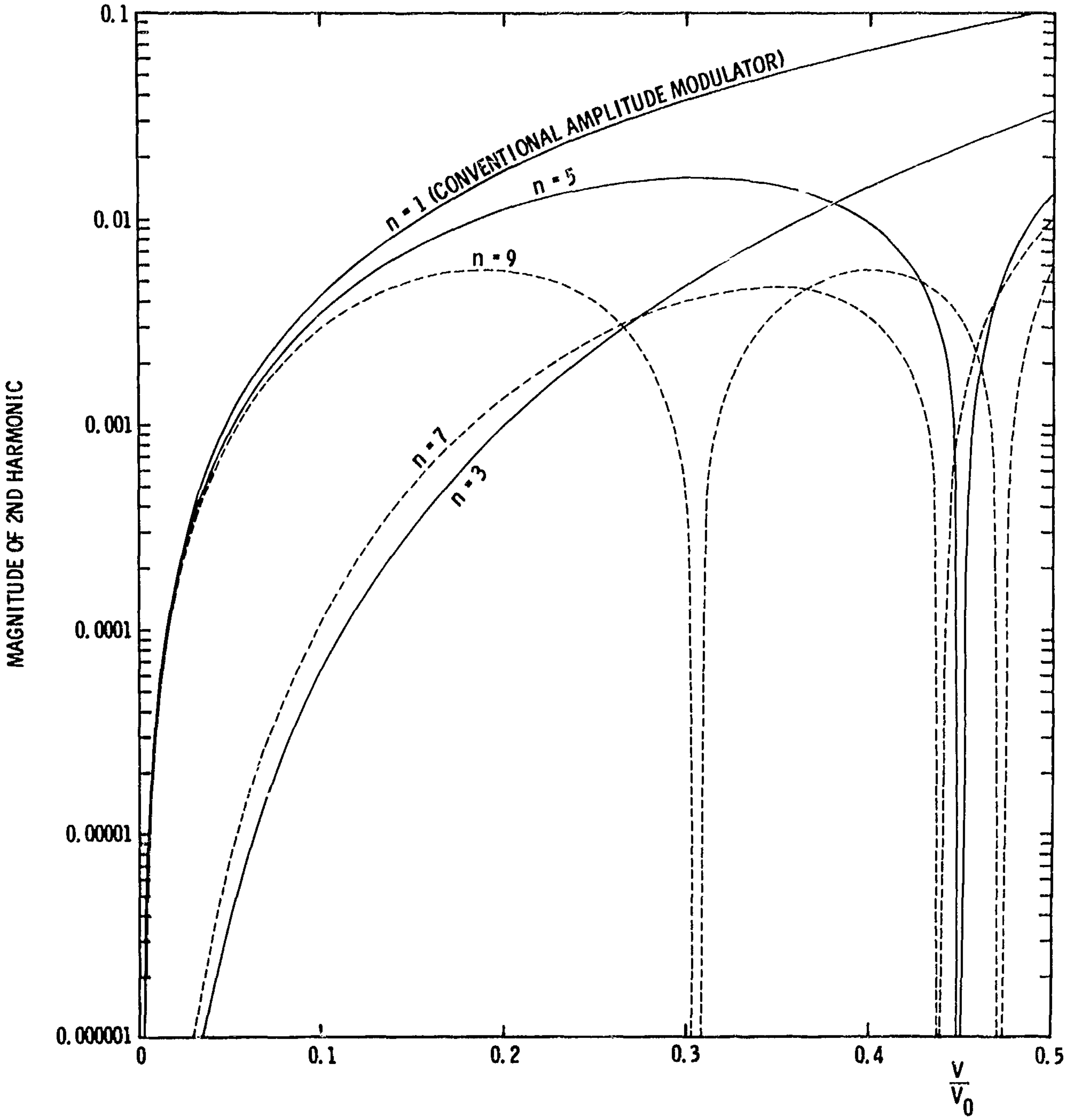

n = 1 (CONVENTIONAL AMPLITUDE MODULATOR)
n = 5
n = 9
n = 7
n = 3
MAGNITUDE OF 2ND HARMONIC
0.1
0.01
0.001
0.0001
0.00001
0.000001
0
0.1
0.2
0.3
0.4
0.5
$\frac{V}{V_0}$

Figure 8c

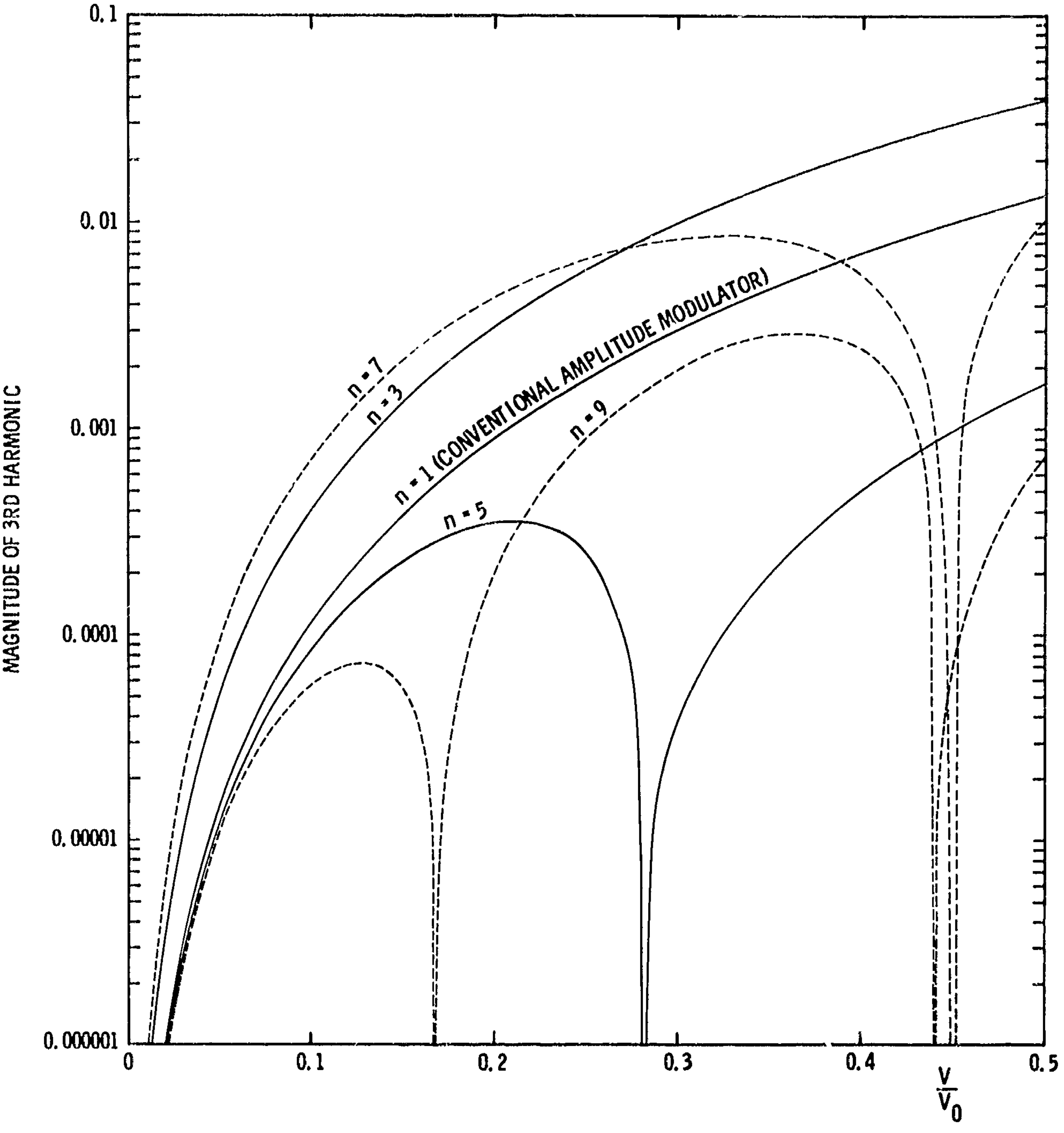

0.1
0.01
0.001
0.0001
0.00001
0.000001
MAGNITUDE OF 3RD HARMONIC
0
0.1
0.2
0.3
0.4
0.5
$\frac{V}{V_0}$
n = 7
n = 3
n = 1 (CONVENTIONAL AMPLITUDE MODULATOR)
n = 9
n = 5

Figure 8d

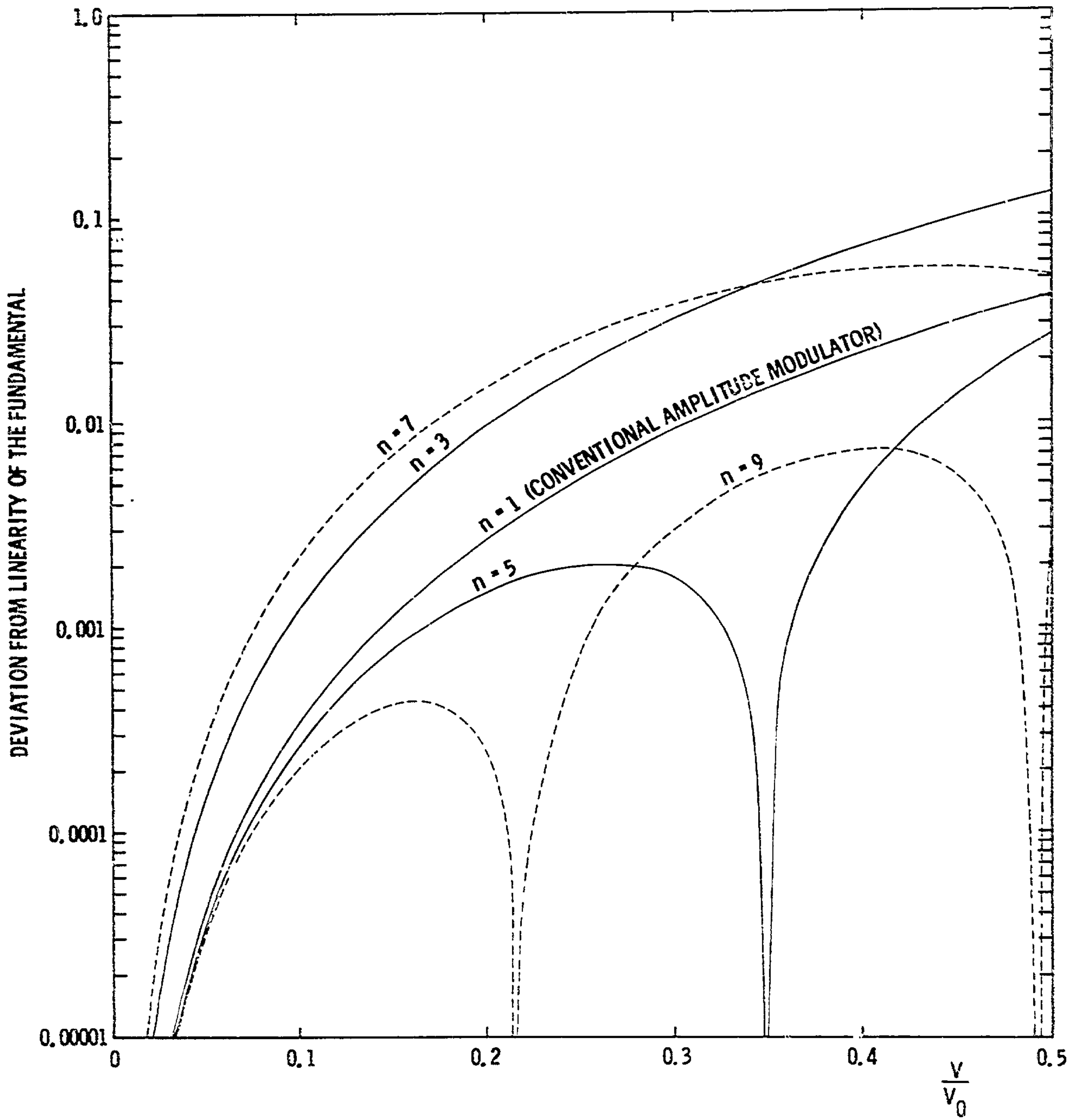
1.0
0.1
0.01
0.001
0.0001
0.00001
0
0.1
0.2
0.3
0.4
0.5
$\frac{V}{V_0}$
DEVIATION FROM LINEARITY OF THE FUNDAMENTAL
n = 7
n = 3
n = 1 (CONVENTIONAL AMPLITUDE MODULATOR)
n = 5
n = 9

Figure 8e

transfer function. Our ultimate concern, however, is not with how well this transfer function is approximated, but rather with modulator performance as measured by the amplitudes of the fundamental and harmonics present in the demodulated signal. Thus it is more desirable to choose the C_i by some technique which directly optimizes the modulator properties of interest. In the following section, this approach is employed to determine the C_i of the modulator transfer function.

2. n even

Since the Fourier approximation technique did not prove satisfactory for n odd, the equivalent calculation for n even was not performed.

D. Maximally-linear Approximation to Ideal Characteristic

1. n odd

Equation (15) gives the dc, fundamental, second harmonic, and third harmonic components present in the demodulated output for $n = 9$. This is a general expression which is valid for any choice of C_i. Consider now the portion of Eq. (15) which gives the amplitude of the fundamental.

$$\begin{aligned}\text{amplitude of fundamental} = -4 \Bigg[& B_0 J_1\left(\frac{9\pi V}{2V_0}\right) + B_1 J_1\left(\frac{7\pi V}{2V_0}\right) + B_2 J_1\left(\frac{5\pi V}{2V_0}\right) + B_3 J_1\left(\frac{3\pi V}{2V_0}\right) \\ & + B_4 J_1\left(\frac{\pi V}{2V_0}\right)\Bigg] \qquad (19)\end{aligned}$$

If we write each Bessel function of (19) in series form, we obtain

$$\begin{aligned}\text{amplitude of fundamental} = -4 \Bigg[& \frac{\pi}{4}\frac{V}{V_0}(B_4 + 3B_3 + 5B_2 + 7B_1 + 9B_0) - \frac{\pi^3}{128}\left(\frac{V}{V_0}\right)^3 \\ & (B_4 + 3^3B_3 + 5^3B_2 + 7^3B_1 + 9^3B_0) + \frac{\pi^5}{12,288}\left(\frac{V}{V_0}\right)^5 \\ & (B_4 + 3^5B_3 + 5^5B_2 + 7^5B_1 + 9^5B_0) - \frac{\pi^7}{2,359,296}\left(\frac{V}{V_0}\right)^7 \\ & (B_4 + 3^7B_3 + 5^7B_2 + 7^7B_1 + 9^7B_0) + \frac{\pi^9}{754,974,720}\left(\frac{V}{V_0}\right)^9 \\ & (B_4 + 3^9B_3 + 5^9B_2 + 7^9B_1 + 9^9B_0) - \dots\Bigg] \qquad (20)\end{aligned}$$

Since ideally the amplitude of the fundamental is directly proportional to V/V_0, the V/V_0 term of (20) is the desired portion of the output while the $(V/V_0)^3$, $(V/V_0)^5$, $(V/V_0)^7$, etc. terms represent distortion. Hence we will choose the B_i so as to eliminate as many of these distortion terms as possible.

In order to make the coefficient of the $(V/V_0)^3$ term be zero, the B_i must satisfy

$$B_4 + 3^3 B_3 + 5^3 B_2 + 7^3 B_1 + 9^3 B_0 = 0. \tag{21a}$$

Similarly, if the B_i satisfy

$$B_4 + 3^5 B_3 + 5^5 B_2 + 7^5 B_1 + 9^5 B_0 = 0, \tag{21b}$$

the coefficient of the $(V/V_0)^5$ term will be zero. And finally if the coefficients of the $(V/V_0)^7$ and $(V/V_0)^9$ terms are to be zero, the B_i must satisfy

$$B_4 + 3^7 B_3 + 5^7 B_2 + 7^7 B_1 + 9^7 B_0 = 0, \tag{21c}$$

and

$$B_4 + 3^9 B_3 + 5^9 B_2 + 7^9 B_1 + 9^9 B_0 = 0. \tag{21d}$$

Since we are free to choose five B_i (B_0, B_1, B_2, B_3, and B_4), we are able to make four coefficients of (20) become zero. The first remaining nonzero distortion term is $(V/V_0)^{11}$, and hence we call this method of determining the B_i a maximally-linear approximation.

In Eqs. (21a), (21b), (21c), and (21d) we have four simultaneous linear equations. Solving them, we obtain

$$\begin{aligned} B_3 &= -2/27 \quad B_4, \\ B_2 &= 2/175 \quad B_4, \\ B_1 &= -1/686 \quad B_4, \\ B_0 &= 1/10,206 \quad B_4. \qquad\qquad n = 9 \end{aligned} \tag{22}$$

The results we have just derived are for the case $n = 9$. For the case $n = 7$, $K(v)$ is given by (10d) and an expression similar to Eq. (20) can be derived for the amplitude of the fundamental. Since one less B coefficient is available, we are able to force one less distortion term to zero. For $n = 7$, the equations obtained by requiring that the coefficients of the $(V/V_0)^3$, $(V/V_0)^5$, and $(V/V_0)^7$ terms be zero are

$$B_3 + 3^3 B_2 + 5^3 B_1 + 7^3 B_0 = 0, \tag{23a}$$

$$B_3 + 3^5 B_2 + 5^5 B_1 + 7^5 B_0 = 0, \tag{23b}$$

$$B_3 + 3^7 B_2 + 5^7 B_1 + 7^7 B_0 = 0. \tag{23c}$$

The solutions for the B_i are

$$\begin{aligned} B_2 &= -1/15 \quad B_3, \\ B_1 &= 1/125 \quad B_3, \\ B_0 &= -1/1715\ B_3. \qquad\qquad n = 7 \end{aligned} \tag{24}$$

Correspondingly, for $n = 5$ we are able to make $(V/V_0)^3$ and $(V/V_0)^5$ terms be zero, while for $n = 3$ we can make only the $(V/V_0)^3$ term be zero. The solutions for the B_i for these last two cases are

$$\begin{aligned} B_1 &= -1/18 \quad B_2, \\ B_0 &= 1/250 \quad B_2, \qquad\qquad n = 5 \end{aligned} \tag{25}$$

and

$$B_0 = -1/27 \quad B_1. \qquad\qquad n = 3 \tag{26}$$

We have thus determined relative values for the B_i for $n = 3, 5, 7,$ and 9 by eliminating as many higher-order terms as possible from the series expansion of the amplitude of the fundamental. Since the A_i are not present in the expression for the fundamental, they remain to be determined. The A_i are present in expressions for the dc, second harmonic, fourth harmonic, etc. components of the output (see Eq. (15)), and hence can be chosen to optimize one of these. Our choice will be to pick the A_i to minimize the amplitude of the second harmonic.

We again return to the expression of Eq. (15) for $n = 9$. From (15), the amplitude of the second harmonic is seen to be

$$\text{second harmonic amplitude} = -4\left[A_0 J_2\left(\frac{9\pi V}{2V_0}\right) + A_1 J_2\left(\frac{7\pi V}{2V_0}\right) + A_2 J_2\left(\frac{5\pi V}{2V_0}\right) + A_3 J_2\left(\frac{3\pi V}{2V_0}\right) + A_4 J_2\left(\frac{\pi V}{2V_0}\right)\right]. \tag{27}$$

If we rewrite each Bessel function in series form, (27) becomes

$$\begin{aligned}\text{second harmonic amplitude} = -4\Bigg[& \frac{\pi^2}{32}\left(\frac{V}{V_0}\right)^2\left(A_4 + 3^2A_3 + 5^2A_2 + 7^2A_1 + 9^2A_0\right) \\ & - \frac{\pi^4}{1536}\left(\frac{V}{V_0}\right)^4\left(A_4 + 3^4A_3 + 5^4A_2 + 7^4A_1 + 9^4A_0\right) \\ & + \frac{\pi^6}{196,608}\left(\frac{V}{V_0}\right)^6\left(A_4 + 3^6A_3 + 5^6A_2 + 7^6A_1 + 9^6A_0\right) \\ & - \frac{\pi^8}{47,185,920}\left(\frac{V}{V_0}\right)^8\left(A_4 + 3^8A_3 + 5^8A_2 + 7^8A_1 + 9^8A_0\right) \\ & + \dots\Bigg]\end{aligned} \tag{28}$$

We can make the $(V/V_0)^2$, $(V/V_0)^4$, $(V/V_0)^6$, and $(V/V_0)^8$ terms go to zero by requiring that

$$A_4 + 3^2A_3 + 5^2A_2 + 7^2A_1 + 9^2A_0 = 0, \tag{29a}$$

$$A_4 + 3^4A_3 + 5^4A_2 + 7^4A_1 + 9^4A_0 = 0, \tag{29b}$$

$$A_4 + 3^6A_3 + 5^6A_2 + 7^6A_1 + 9^6A_0 = 0, \tag{29c}$$

$$A_4 + 3^8A_3 + 5^8A_2 + 7^8A_1 + 9^8A_0 = 0. \tag{29d}$$

Solving these four simultaneous linear equations, we obtain

$$A_3 = -\ 2/9 \quad A_4,$$

$$A_2 = \quad 2/35 \quad A_4,$$

$$A_1 = -\ 1/98 \quad A_4,$$

$$A_0 = \quad 1/1134\ A_4. \qquad\qquad n = 9 \qquad\qquad (30)$$

Proceeding as before, we find for $n = 3, 5,$ and 7 that

$$A_2 = -\ 1/5 \quad A_3,$$

$$A_1 = \quad 1/25 \quad A_3,$$

$$A_0 = -1/245 \quad A_3. \qquad\qquad n = 7 \qquad\qquad (31)$$

$$A_1 = -\ 1/6 \quad A_2,$$

$$A_0 = \quad 1/50 \quad A_2. \qquad\qquad n = 5 \qquad\qquad (32)$$

$$A_0 = -\ 1/9 \quad A_1. \qquad\qquad n = 3 \qquad\qquad (33)$$

Two additional constraints must now be applied in order to obtain absolute values for the A_i and B_i. Consider the $n = 9$ case again. We have obtained values for the B_i in terms of B_4, and values for the A_i in terms of A_4. So far, however, the size of B_4 relative to A_4 has not been determined. In order to make this choice, we observe the following. All calculations performed thus far have assumed that the depth of modulation never exceeds 100%. That is, we have assumed that a value of v is never reached for which $K(v)$ is negative. This means, for example, that for the ideal characteristic of Fig. 5, v/V_0 is never less than $-1/2$. **Thus we would hope that the K(v) which we obtain for the maximally-linear case would be roughly comparable to the characteristic of Fig. 5. We would like for K(v=0) to be** approximately 0.5, and we would further hope that K(v) would be unity and zero for approximately equal positive and negative values of v. By setting $B_4 = -A_4$, we attempt to force this behavior. For from (10e) we recall that B_4 and A_4 are the amplitudes of the $e^{i\frac{\pi}{2}\frac{v}{V_0}}$ and $e^{-i\frac{\pi}{2}\frac{v}{V_0}}$ terms in K(v), and hence the above choice gives

$$C_4 e^{i\frac{\pi}{2}\frac{v}{V_0}} + C_4^* e^{-i\frac{\pi}{2}\frac{v}{V_0}} = 2A_4 \cos\left(\frac{\pi}{2}\frac{v}{V_0} - \frac{\pi}{2}\right) .$$

Thus the first Fourier component of K(v) is a cosine curve which is maximum at $v/V_0 = 1/2$ and zero at $v/V_0 = -1/2$. To summarize then, by making $B_4 = -A_4$ we attempt to make the general shape of K(v) comparable to that of the ideal K(v) of Fig. 6a. The detailed shape will be determined by the other A_i and B_i given in Eqs. (22) and (30).

We now have for the n = 9 case,

$$\begin{aligned} K(v) = A_4 \Bigg[& \left(\frac{1}{1134} - \frac{i}{10,206}\right) e^{i\frac{9\pi v}{2V_0}} - \left(\frac{1}{98} - \frac{i}{686}\right) e^{i\frac{7\pi v}{2V_0}} \\ & + \left(\frac{2}{35} - \frac{2i}{175}\right) e^{i\frac{5\pi v}{2V_0}} - \left(\frac{2}{9} - \frac{2i}{27}\right) e^{i\frac{3\pi v}{2V_0}} \\ & + (1-i)\, e^{i\frac{\pi}{2}\frac{v}{V_0}} + (1+i)\, e^{-i\frac{\pi}{2}\frac{v}{V_0}} - \left(\frac{2}{9} + \frac{2i}{27}\right) e^{-i\frac{3\pi v}{2V_0}} \\ & + \left(\frac{2}{35} + \frac{2i}{175}\right) e^{-i\frac{5\pi v}{2V_0}} - \left(\frac{1}{98} + \frac{i}{686}\right) e^{-i\frac{7\pi v}{2V_0}} \\ & + \left(\frac{1}{1134} + \frac{i}{10,206}\right) e^{-i\frac{9\pi v}{2V_0}} . \end{aligned} \tag{34}$$

Our final task is to choose A_4 so that the maximum magnitude of (34) is unity. Doing this we obtain

$$
\begin{aligned}
n = 9 \qquad K(v) = {} & (0.000274 - i0.000030)\, e^{i\frac{9\pi v}{2V_0}} - (0.003179 - i0.000454)\, e^{i\frac{7\pi v}{2V_0}} \\
& + (0.017806 - i0.003561)\, e^{i\frac{5\pi v}{2V_0}} - (0.069248 - i0.023082)\, e^{i\frac{3\pi v}{2V_0}} \\
& + (0.311616 - i0.311616)\, e^{i\frac{\pi v}{2V_0}} + (0.311616 + i0.311616)\, e^{-i\frac{\pi v}{2V_0}} \\
& - (0.069248 + i0.023082)\, e^{-i\frac{3\pi v}{2V_0}} + (0.017806 + i0.003561)\, e^{-i\frac{5\pi v}{2V_0}} \\
& - (0.003179 + i0.000454)\, e^{-i\frac{7\pi v}{2V_0}} + (0.000274 + i0.000030)\, e^{-i\frac{9\pi v}{2V_0}} .
\end{aligned}
\tag{35a}
$$

The final K(v) for n = 1, 3, 5, and 7 are similarly found to be

$$
\begin{aligned}
n = 7 \qquad K(v) = {} & - (0.001294 - i0.000184)\, e^{i\frac{7\pi v}{2V_0}} + (0.012683 - i0.002536)\, e^{i\frac{5\pi v}{2V_0}} \\
& - (0.063414 - i0.021138)\, e^{i\frac{3\pi v}{2V_0}} + (0.317074 - i0.317074)\, e^{i\frac{\pi v}{2V_0}} \\
& + (0.317074 + i0.317074)\, e^{-i\frac{\pi v}{2V_0}} - (0.063414 + i0.021138)\, e^{-i\frac{3\pi v}{2V_0}} \\
& + (0.012683 + i0.002536)\, e^{-i\frac{5\pi v}{2V_0}} - (0.001294 + i0.000184)\, e^{-i\frac{7\pi v}{2V_0}}
\end{aligned}
\tag{35b}
$$

$$n = 5 \qquad K(v) = (0.006489 - i0.001297)\, e^{i\frac{5\pi v}{2V_0}} - (0.054077 - i0.018025)\, e^{i\frac{3\pi v}{2V_0}}$$

$$+ (0.324465 - i0.324465)\, e^{i\frac{\pi v}{2V_0}} + (0.324465 + i0.324465)\, e^{-i\frac{\pi v}{2V_0}}$$

$$- (0.054077 + i0.018025)\, e^{-i\frac{3\pi v}{2V_0}} + (0.006489 + i0.001297)\, e^{-i\frac{5\pi v}{2V_0}} . \tag{35c}$$

$$n = 3 \qquad K(v) = - (0.037258 - i0.012419)\, e^{i\frac{3\pi v}{2V_0}} + (0.335330 - i0.335330)\, e^{i\frac{\pi v}{2V_0}}$$

$$+ (0.335330 + i0.335330)\, e^{-i\frac{\pi v}{2V_0}} - (0.037258 + i0.012419)\, e^{-i\frac{3\pi v}{2V_0}} . \tag{35d}$$

$$n = 1 \qquad K(v) = (0.353553 - i0.353553)\, e^{i\frac{\pi v}{2V_0}} + (0.353553 + i0.353553)\, e^{-i\frac{\pi v}{2V_0}} . \tag{35e}$$

We can now substitute the A_i and B_i of Eqs. (35) into Eq. (15) [or, in the cases of $n = 1$, 3, 5, and 7, into the appropriate expressions derived from (15)] to assess the modulator performance obtained using the maximally-linear approximation. The results are shown in Fig. 9 where (a) the dc component, (b) the first harmonic amplitude, (c) the second harmonic magnitude, (d) the 3rd harmonic magnitude, and (e) the deviation from linearity of the fundamental are plotted as a function of V/V_0. The case $n = 1$ again corresponds to a conventional amplitude modulator. Results for n even are also shown on Fig. 9, but for the present we will limit our remarks to the case of n odd.

Figures 9c, 9d, and 9e show that a substantial, uniform reduction in distortion occurs for increasing values of n. These results must be interpreted with care, however, for Fig. 9b shows that there is also a reduction in the amplitude of the fundamental. Hence as n increases, the reduction in distortion is accompanied by a reduction in the desired output.

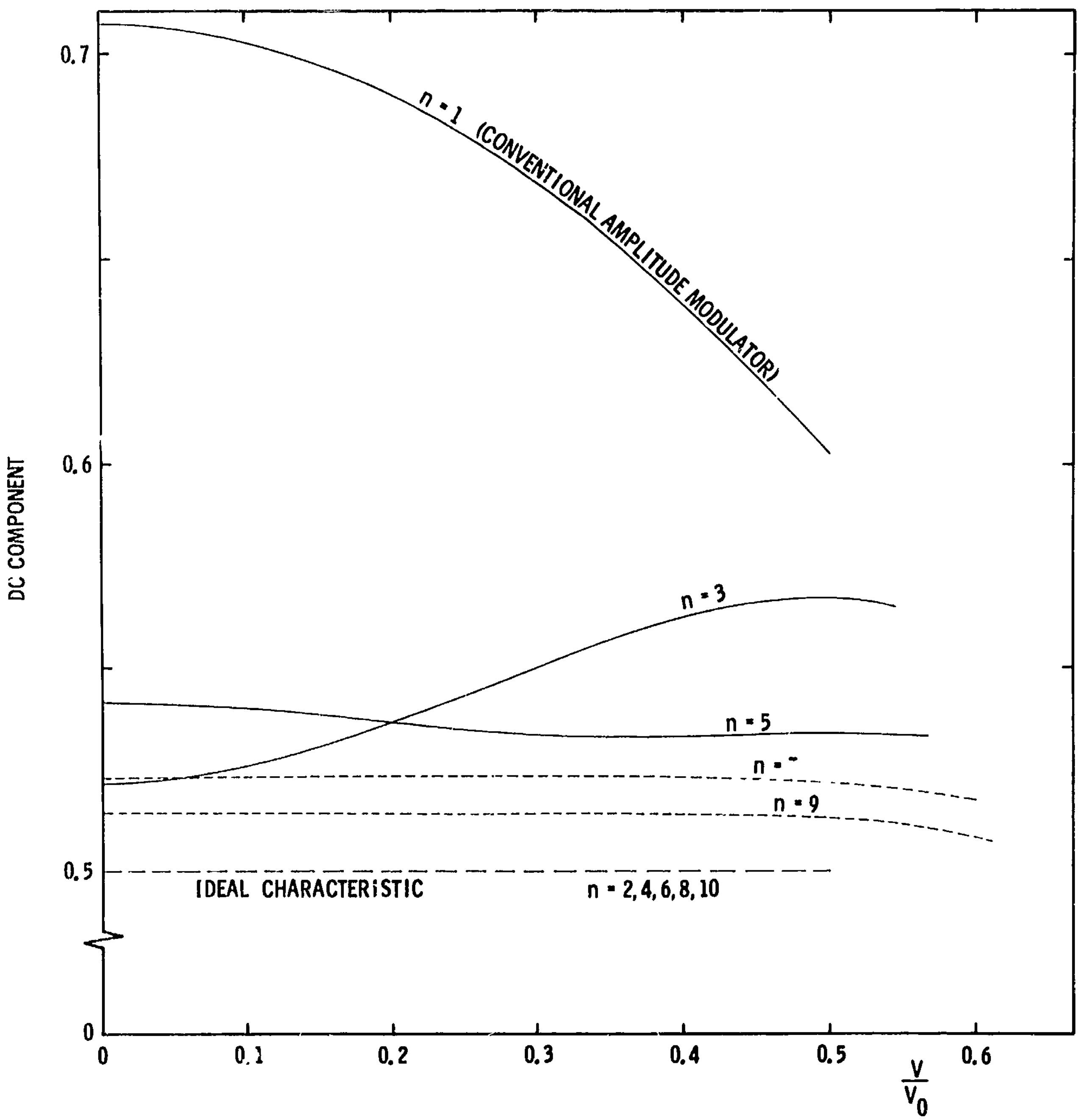
0.7
0.6
0.5
0
DC COMPONENT
n = 1 (CONVENTIONAL AMPLITUDE MODULATOR)
n = 3
n = 5
n = -
n = 9
IDEAL CHARACTERISTIC
n = 2, 4, 6, 8, 10
0
0.1
0.2
0.3
0.4
0.5
0.6
V/V0

Figure 9a

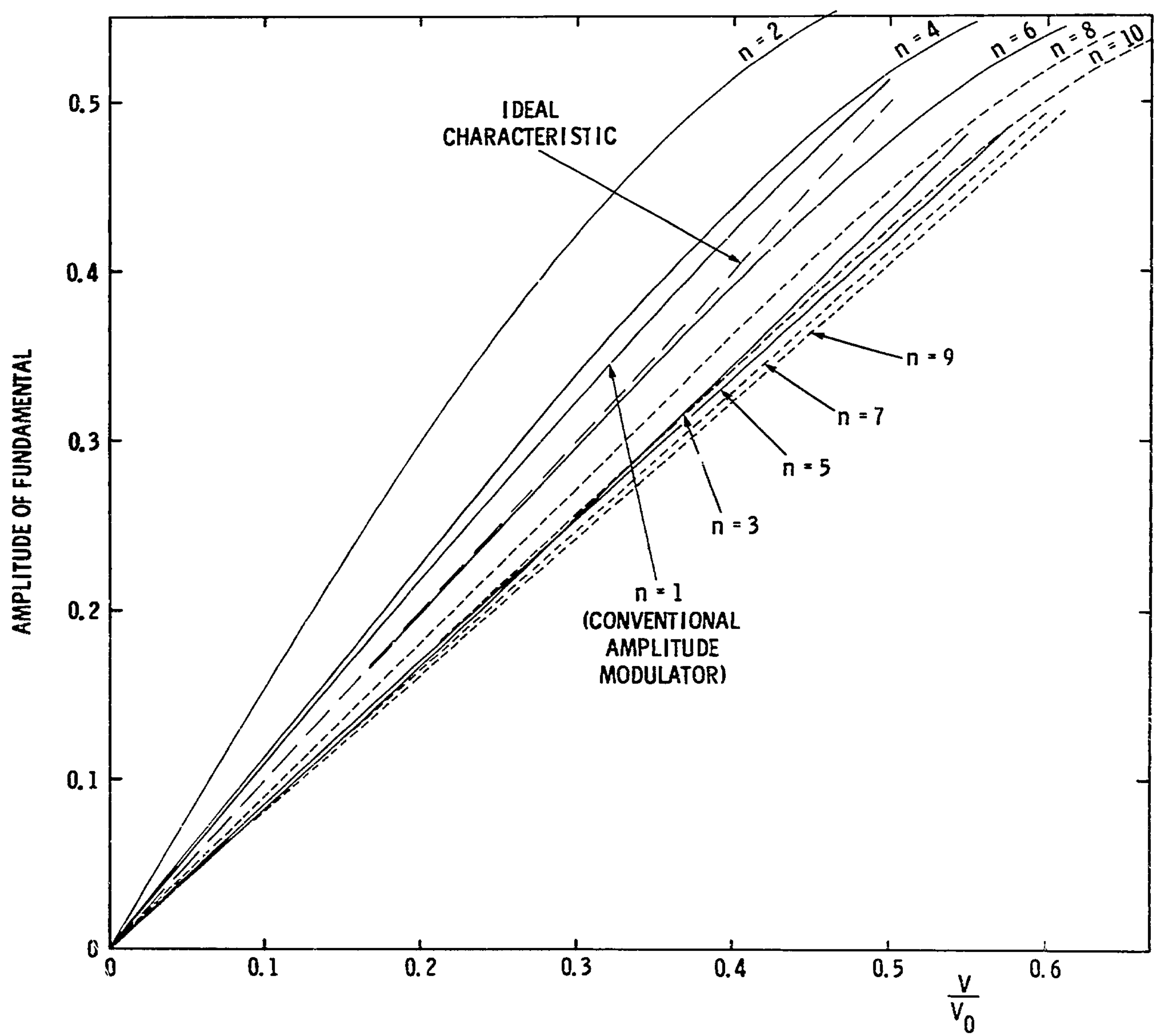

AMPLITUDE OF FUNDAMENTAL
0.5
0.4
0.3
0.2
0.1
0
0.1
0.2
0.3
0.4
0.5
0.6
$\frac{V}{V_0}$
IDEAL CHARACTERISTIC
n = 2
n = 4
n = 6
n = 8
n = 10
n = 9
n = 7
n = 5
n = 3
n = 1 (CONVENTIONAL AMPLITUDE MODULATOR)

Figure 9b

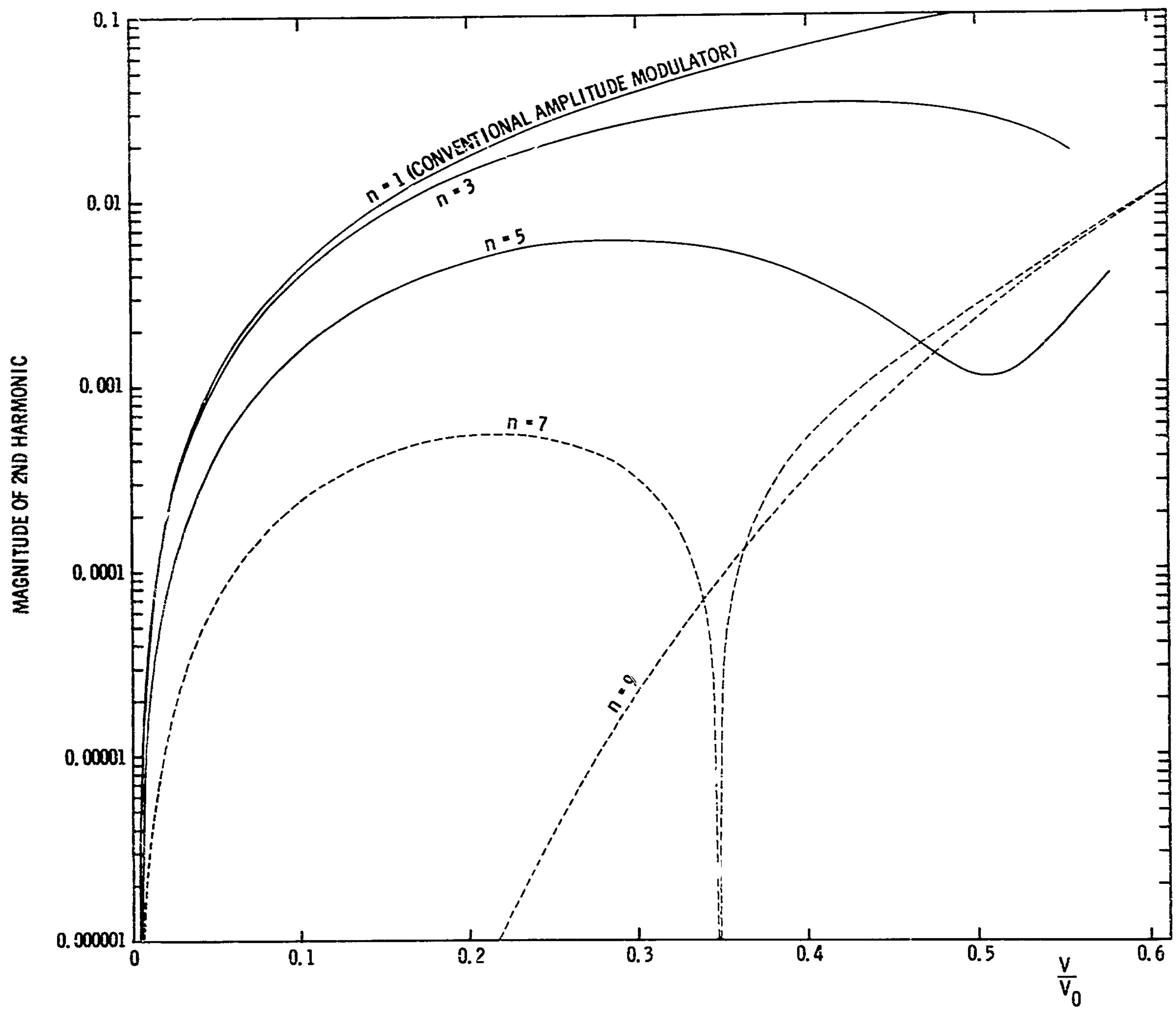
n = 1 (CONVENTIONAL AMPLITUDE MODULATOR)
n = 3
n = 5
n = 7
n = 9
MAGNITUDE OF 2ND HARMONIC
0.1
0.01
0.001
0.0001
0.00001
0.000001
0
0.1
0.2
0.3
0.4
0.5
0.6
$\frac{V}{V_0}$

Figure 9c

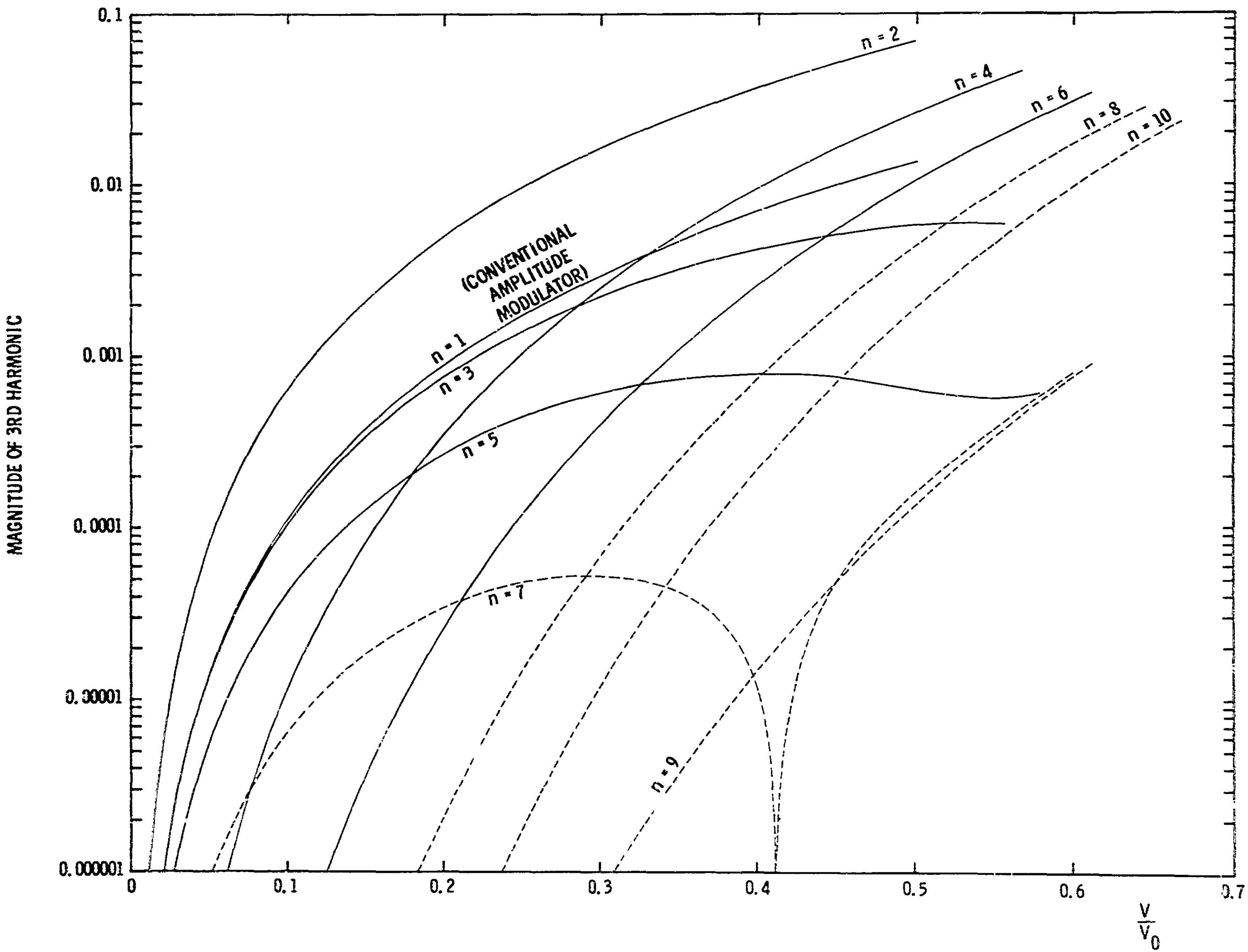
MAGNITUDE OF 3RD HARMONIC
0.1
0.01
0.001
0.0001
0.00001
0.000001
0
0.1
0.2
0.3
0.4
0.5
0.6
0.7
$\frac{V}{V_0}$
n = 1
(CONVENTIONAL AMPLITUDE MODULATOR)
n = 2
n = 3
n = 4
n = 5
n = 6
n = 7
n = 8
n = 9
n = 10

Figure 9d

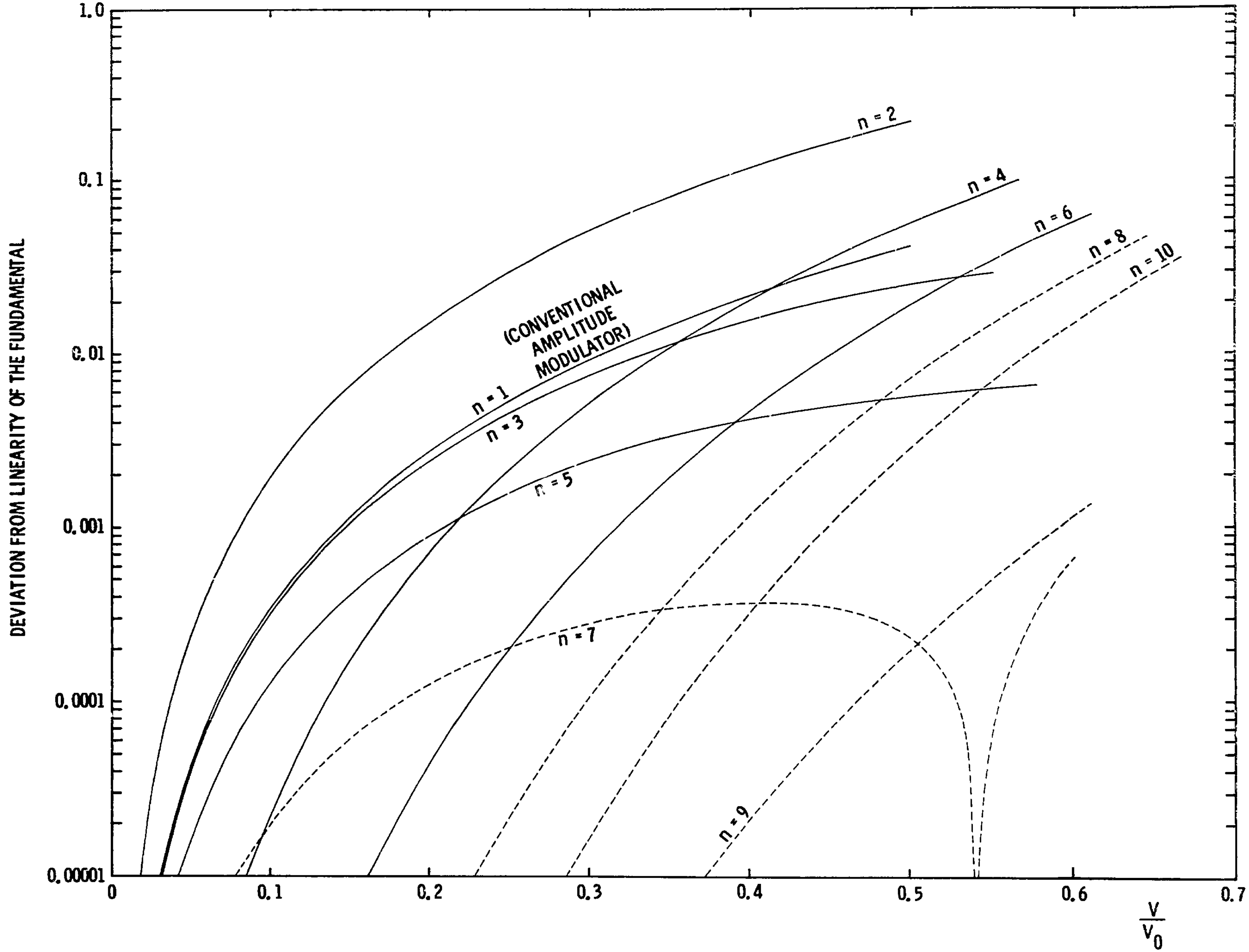

DEVIATION FROM LINEARITY OF THE FUNDAMENTAL
1.0
0.1
0.01
0.001
0.0001
0.00001
0
0.1
0.2
0.3
0.4
0.5
0.6
0.7
$\frac{V}{V_0}$
n = 1
n = 2
n = 3
n = 4
n = 5
n = 6
n = 7
n = 8
n = 9
n = 10
(CONVENTIONAL AMPLITUDE MODULATOR)

Figure 9e

A clearer picture of these results is given in Fig. 10 where (a) the deviation from linearity of the fundamental, and (b) the magnitude of the second harmonic are plotted vs. n for certain fixed values of the amplitude of the fundamental. Curves are given for fundamental amplitudes of 0.475 (which corresponds to a degree of modulation of roughly 90%), 0.4 (approximately 70%), 0.3 (approximately 50%), 0.2 (approximately 30%), and 0.1 (approximately 15%). Points representing odd values of n are connected by solid lines while points for even values of n are connected by dotted lines. Since the behavior of the third harmonic's magnitude was very similar to Fig. 10a, a separate graph was not plotted for it.

Figure 10a shows how distortion in the fundamental varies with n. It is seen that in going from a conventional modulator to a three stage modulator, the fundamental distortion does not improve, and in fact, becomes slightly worse. For $n = 5$, some improvement is noted while for $n = 7$ and 9, significant improvement is obtained. Similar results are obtained for the second harmonic magnitude.

We therefore conclude that for n odd, the maximally-linear approximation technique is only partially successful. For small values of n ($n \leq 5$), relatively little improvement is obtained while for larger values of n ($n \geq 7$), substantial improvement occurs. Thus the improvement increases with increasing values of n.

It is of some interest to know what a plot of K(v) looks like for the maximally-linear case. Figure 11 shows the K(v) of Eqs. (35) plotted as a function of v/V_0. We see that the K(v) are closely approaching a straight line with increasing n. Note that the slopes of the curves of Fig. 11 decrease somewhat with increasing n; this causes the slight decrease in the amplitude of the fundamental which was mentioned in the previous paragraph. It should also be noted that the value of v/V_0 at which K(v) becomes zero is slightly different for different values of n. The maximum voltage, therefore, which can be applied becomes somewhat greater as n is increased. In Fig. 9, the curves are plotted up to this maximum permissible voltage.

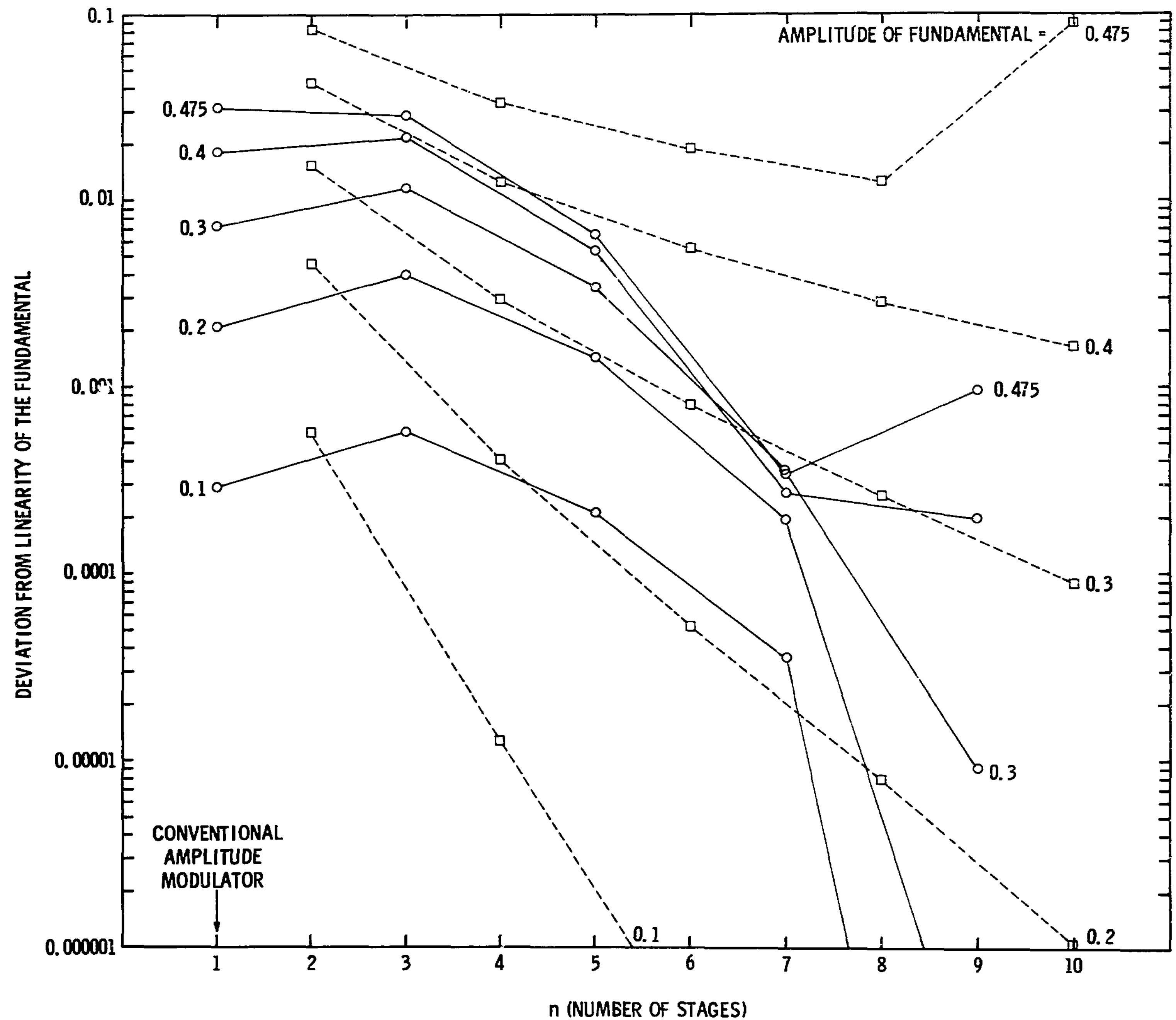
AMPLITUDE OF FUNDAMENTAL = 0.475
0.4
0.3
0.2
0.1
0.475
0.4
0.3
0.2
0.1
0.475
0.3
CONVENTIONAL AMPLITUDE MODULATOR
DEVIATION FROM LINEARITY OF THE FUNDAMENTAL
0.1
0.01
0.001
0.0001
0.00001
0.000001
1
2
3
4
5
6
7
8
9
10
n (NUMBER OF STAGES)

Figure 10a

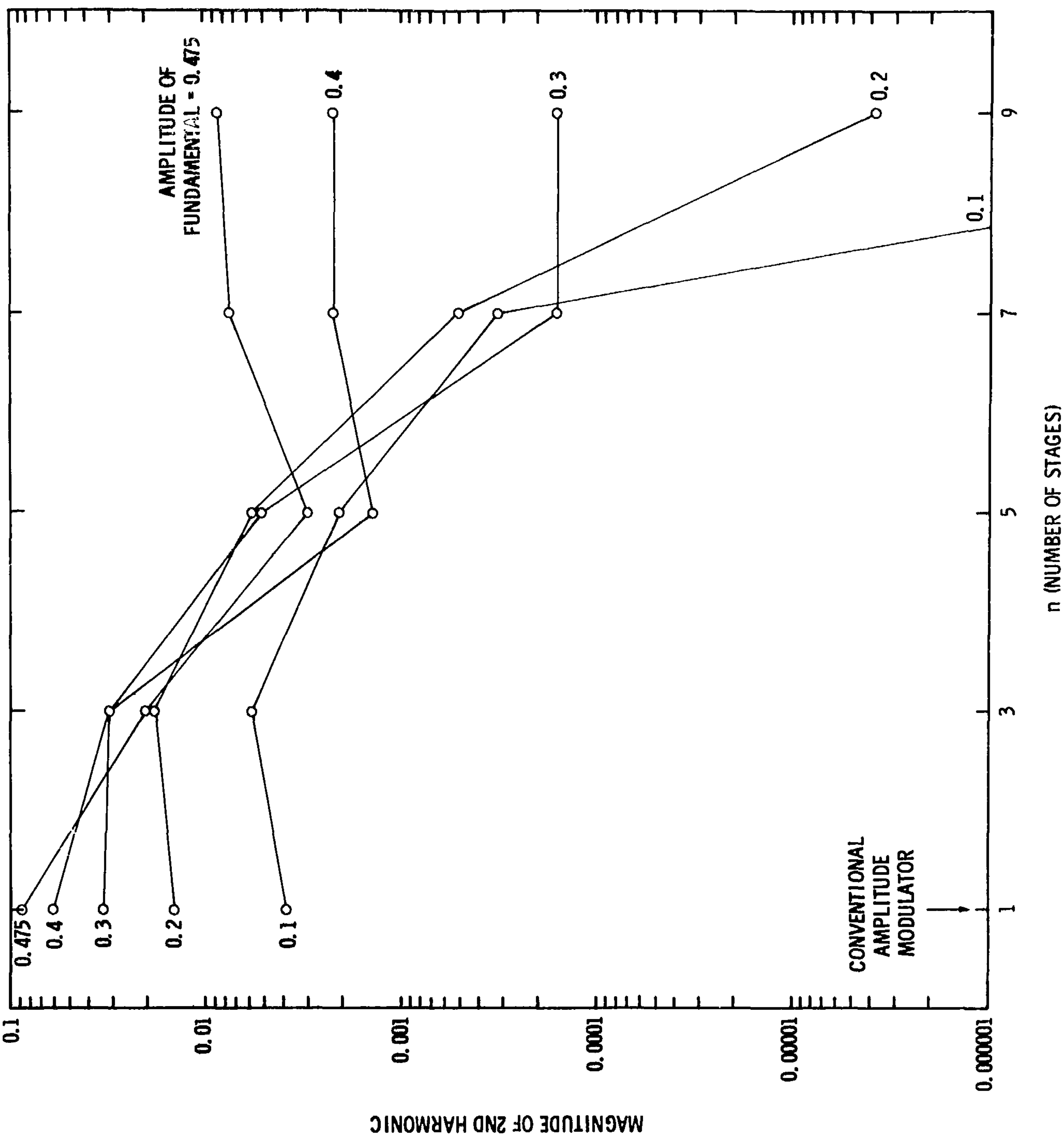

MAGNITUDE OF 2ND HARMONIC
0.1
0.01
0.001
0.0001
0.00001
0.000001
n (NUMBER OF STAGES)
1
3
5
7
9
CONVENTIONAL
AMPLITUDE
MODULATOR
AMPLITUDE OF
FUNDAMENTAL = 0.475
0.475
0.4
0.3
0.2
0.1

Figure 10b

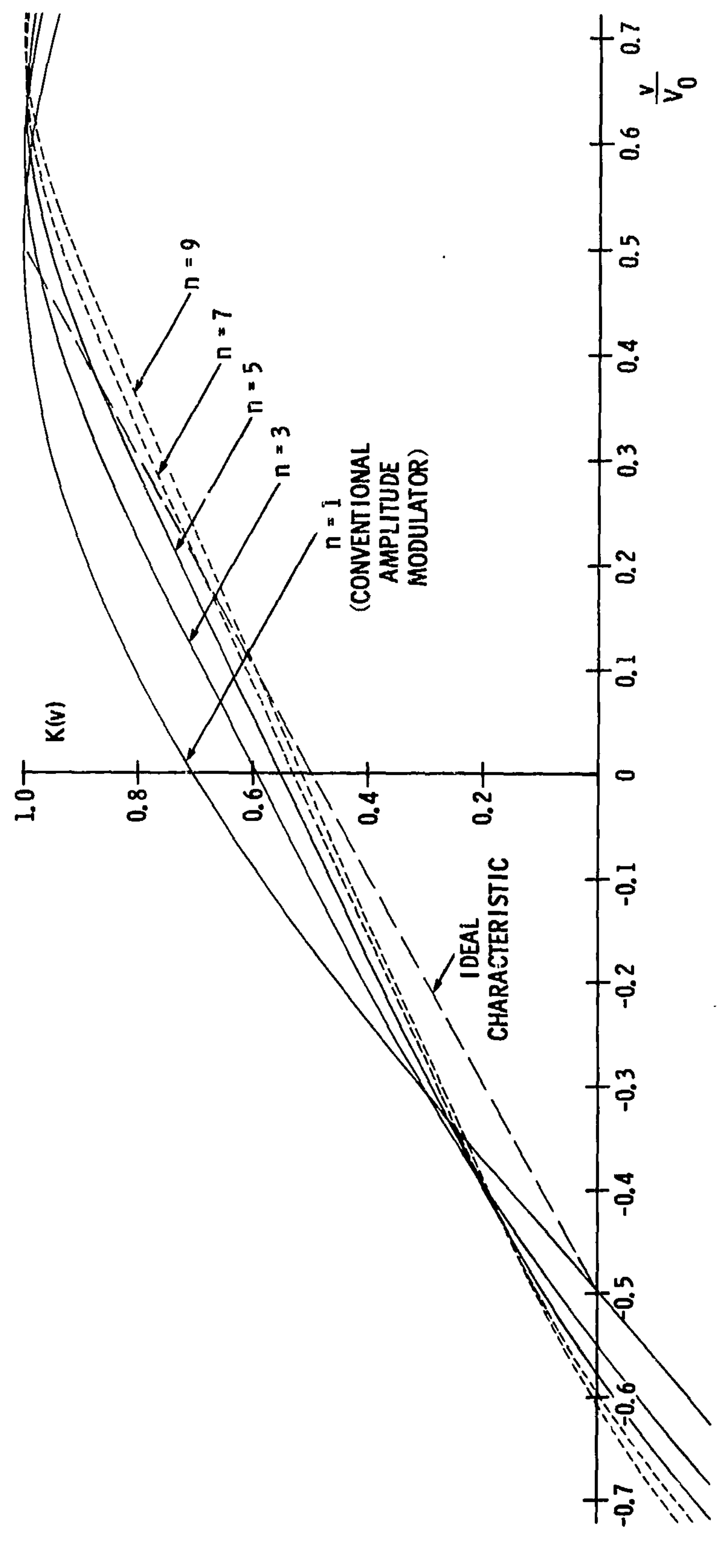
K(v)
1.0
0.8
0.6
0.4
0.2
-0.7
-0.6
-0.5
-0.4
-0.3
-0.2
-0.1
0
0.1
0.2
0.3
0.4
0.5
0.6
0.7
v/V0
n = 9
n = 7
n = 5
n = 3
n = 1
(CONVENTIONAL
AMPLITUDE
MODULATOR)
IDEAL
CHARACTERISTIC

Figure 11

The modulator designs which correspond to the $K(v)$ derived by using the maximally-linear technique are tabulated in Table I. These designs were found by applying the synthesis procedure of Section II to the $K(v)$ of Eqs. (35). The quantities listed in Table I are the rotation angle (θ_i) of each electro-optic cell, the retardation (b_i) introduced by each optical compensator, and the rotation angle (θ_p) of the output polarizer.

2. n even

An equivalent calculation can be carried out for modulators having an even number of stages. Although this calculation is similar in many respects to that just described for n odd, it is different in at least one important aspect – namely, modulators can be designed which produce no even harmonics in the demodulated output.

Let us restrict our attention to the $n = 10$ case. Equation (17) gives the demodulated output leaving the envelope detector for $n = 10$. The amplitude of the fundamental is given by

$$\text{amplitude of fundamental} = -4\left[B_0J_1\left(\frac{5\pi V}{V_0}\right) + B_1J_1\left(\frac{4\pi V}{V_0}\right) + B_2J_1\left(\frac{3\pi V}{V_0}\right) + B_3J_1\left(\frac{2\pi V}{V_0}\right) + B_4J_1\left(\frac{\pi V}{V_0}\right)\right]. \tag{36}$$

Writing each Bessel function in series form, we obtain

$$\begin{aligned}\text{amplitude of fundamental} = -4\Bigg[&\frac{\pi}{2}\frac{V}{V_0}(B_4 + 2B_3 + 3B_2 + 4B_1 + 5B_0)\\ &-\frac{\pi^3}{16}\left(\frac{V}{V_0}\right)^3(B_4 + 2^3B_3 + 3^3B_2 + 4^3B_1 + 5^3B_0)\\ &+\frac{\pi^5}{384}\left(\frac{V}{V_0}\right)^5(B_4 + 2^5B_3 + 3^5B_2 + 4^5B_1 + 5^5B_0)\\ &-\frac{\pi^7}{18,432}\left(\frac{V}{V_0}\right)^7(B_4 + 2^7B_3 + 3^7B_2 + 4^7B_1 + 5^7B_0)\\ &+\frac{\pi^9}{1,488,060}\left(\frac{V}{V_0}\right)^9(B_4 + 2^9B_3 + 3^9B_2 + 4^9B_1 + 5^9B_0) - \ldots\Bigg]\end{aligned} \tag{37}$$

	n=1	n=2	n=3	n=4	n=5	n=6	n=7	n=8	n=9	n=10
θ_1	45°00'	19°40'	4°46'	2°27'	0°45'	0°32'	0°07'	0°06'	0°01'	0°01'
b_1 (rad)	1.57	4.71	3.68	3.21	3.38	3.25	3.25	3.23	3.22	3.18
θ_2		39°19'	47°03'	19°06'	6°56'	5°02'	1°06'	1°09'	0°16'	0°13'
b_2 (rad)		1.57	4.56	4.64	3.60	3.24	3.31	3.24	3.24	3.19
θ_3			47°03'	38°51'	44°58'	23°57'	5°51'	6°12'	1°34'	1°19'
b_3 (rad)			0.54	4.64	4.50	4.50	3.57	3.22	3.30	3.19
θ_4				19°06'	44°58'	48°44'	34°29'	23°19'	6°23'	5°17'
b_4 (rad)				0.07	3.60	4.50	4.58	4.45	3.55	3.17
θ_5					6°56'	23°57'	34°29'	48°01'	33°46'	17°45'
b_5 (rad)					0.24	3.24	3.57	4.45	4.57	4.55
θ_6						5°02'	5°51'	23°19'	33°46'	38°04'
b_6 (rad)						0.11	3.31	3.22	3.55	4.55
θ_7							1°06'	6°12'	6°23'	17°45'
b_7 (rad)							0.11	3.24	3.30	3.17
θ_8								1°09'	1°34'	5°17'
b_8 (rad)								0.08	3.24	3.19
θ_9									0°16'	1°19'
b_9 (rad)									0.07	3.19

Table I

	n=1	n=2	n=3	n=4	n=5	n=6	n=7	n=8	n=9	n=10
θ_{10}										0°13'
b_{10} (rad)										0.04
θ_p	-45°00'	70°20'	85°14'	87°33'	89°15'	89°28'	89°53'	89°54'	89°59'	89°59'
b_p (rad)	0	1.57	3.46	4.71	0.20	1.57	3.28	4.71	0.11	1.57

Table I (Continued)

We can make the coefficients of the $(V/V_0)^3$, $(V/V_0)^5$, $(V/V_0)^7$, and $(V/V_0)^9$ terms be zero by setting

$$B_4 + 2^3 B_3 + 3^3 B_2 + 4^3 B_1 + 5^3 B_0 = 0, \tag{38a}$$

$$B_4 + 2^5 B_3 + 3^5 B_2 + 4^5 B_1 + 5^5 B_0 = 0, \tag{38b}$$

$$B_4 + 2^7 B_3 + 3^7 B_2 + 4^7 B_1 + 5^7 B_0 = 0, \tag{38c}$$

$$B_4 + 2^9 B_3 + 3^9 B_2 + 4^9 B_1 + 5^9 B_0 = 0. \tag{38d}$$

Solving these four equations, we obtain

$$\begin{aligned} B_3 &= -2/7 \; B_4, \\ B_2 &= 1/14 \; B_4, \\ B_1 &= -1/84 \; B_4, \\ B_0 &= 1/1050 \; B_4. \qquad n = 10 \end{aligned} \tag{39}$$

Similar calculations can be carried out for $n = 2, 4, 6,$ and 8. For these cases, we obtain

$$\begin{aligned} B_2 &= -1/4 \; B_3, \\ B_1 &= 1/21 \; B_3, \\ B_0 &= -1/224 \; B_3. \qquad n = 8 \end{aligned} \tag{40}$$

$$\begin{aligned} B_1 &= -1/5 \; B_2, \\ B_0 &= 1/45 \; B_2. \qquad n = 6 \end{aligned} \tag{41}$$

and

$$B_0 = -1/8 \; B_1. \qquad n = 4 \tag{42}$$

It is interesting to note that as far as the B_i are concerned, the $n = 10$ case is very similar to the $n = 9$ case. In both cases, we make the $(V/V_0)^3$, $(V/V_0)^5$, $(V/V_0)^7$, and $(V/V_0)^9$ terms be zero by appropriately choosing B_0, B_1, and B_2. As we are about to see, however, the two cases are quite different as far as the A_i are concerned.

For $n = 10$, we will set all A_i except A_5 equal to zero. As seen from Eq. (17) this will automatically make the amplitude of the second harmonic (and all other even harmonics) zero. It is important to note that we are able to do this and still have $K(v)$ assume the general form of the ideal function of Fig. 6b. The ideal function of Fig. 6b may be thought of as consisting of a constant term of 0.5 plus a triangular wave of odd symmetry. Hence, the A_i are not required (except for A_5) and the ideal $K(v)$ can be approximated by a $K(v)$ consisting of a constant term plus sine terms. This was not possible in the case of the ideal function of Fig. 6a since both cosine and sine terms are needed to approximate it.

To conclude our determination of the $K(v)$ for n even, it is necessary only to set the constant term $C_{n/2}$ equal to 0.5 and to normalize the B_i so that $K(v)$ has a maximum value of $+1$. Doing this, we obtain

$$n = 10 \qquad K(v) = -i0.0002159\, e^{i\frac{5\pi v}{V_0}} + i0.0026996\, e^{i\frac{4\pi v}{V_0}} - i0.0161975\, e^{i\frac{3\pi v}{V_0}}$$

$$+ i0.0647900\, e^{i\frac{2\pi v}{V_0}} - i0.2267650\, e^{i\frac{\pi v}{V_0}} + 0.5$$

$$+ i0.2267650\, e^{-i\frac{\pi v}{V_0}} - i0.0647900\, e^{-i\frac{2\pi v}{V_0}} + i0.0161975\, e^{-i\frac{3\pi v}{V_0}}$$

$$- i0.0026996\, e^{-i\frac{4\pi v}{V_0}} + i0.0002159\, e^{-i\frac{5\pi v}{V_0}}, \qquad (43a)$$

$$n = 8 \qquad K(v) = i0.0010318\, e^{i\frac{4\pi v}{V_0}} - i0.0110064\, e^{i\frac{3\pi v}{V_0}} + i0.0577835\, e^{i\frac{2\pi v}{V_0}}$$

$$- i0.2311339\, e^{i\frac{\pi v}{V_0}} + 0.5 + i0.2311339\, e^{-i\frac{\pi v}{V_0}}$$

$$- i0.0577835\, e^{-i\frac{2\pi v}{V_0}} + i0.0110064\, e^{-i\frac{3\pi v}{V_0}} - i0.0010318\, e^{-i\frac{4\pi v}{V_0}}, \tag{43b}$$

$$n = 6 \qquad K(v) = - i0.0052498\, e^{i\frac{3\pi v}{V_0}} + i0.0472481\, e^{i\frac{2\pi v}{V_0}} - i0.2362406\, e^{i\frac{\pi v}{V_0}}$$

$$+ 0.5 + i0.2362406\, e^{-i\frac{\pi v}{V_0}} - i0.0472481\, e^{-i\frac{2\pi v}{V_0}}$$

$$+ i0.0052498\, e^{-i\frac{3\pi v}{V_0}}, \tag{43c}$$

$$n = 4 \qquad K(v) = i0.0303643\, e^{i\frac{2\pi v}{V_0}} - i0.2429150\, e^{i\frac{\pi v}{V_0}} + 0.5$$

$$+ i0.2429150\, e^{-i\frac{\pi v}{V_0}} - i0.0303643\, e^{-i\frac{2\pi v}{V_0}}, \tag{43d}$$

$$n = 2 \qquad K(v) = - i0.2500000\, e^{i\frac{\pi v}{V_0}} + 0.5 + i0.2500000\, e^{-i\frac{\pi v}{V_0}}. \tag{43e}$$

Figure 12 shows these $K(v)$ plotted as a function of v/V_0. Solid lines are used for $n = 2$, 4, and 6, dotted lines for $n = 8$ and 10, and a dashed line for the ideal characteristic. The performance of the modulators corresponding to these $K(v)$ is evaluated by substituting the A_i and B_i of (43a) into (17), and the A_i and B_i of (43b) - (43e) into the corresponding equations derived from (17). The results are shown in Fig. 9a through 9e.

Since all A_i except $A_{n/2}$ were chosen to be zero, the dc component of the output is constant with a value of 0.5. For the same reason, the magnitude of the second harmonic is zero for all n even. The deviation from linearity of the fundamental and the magnitude of

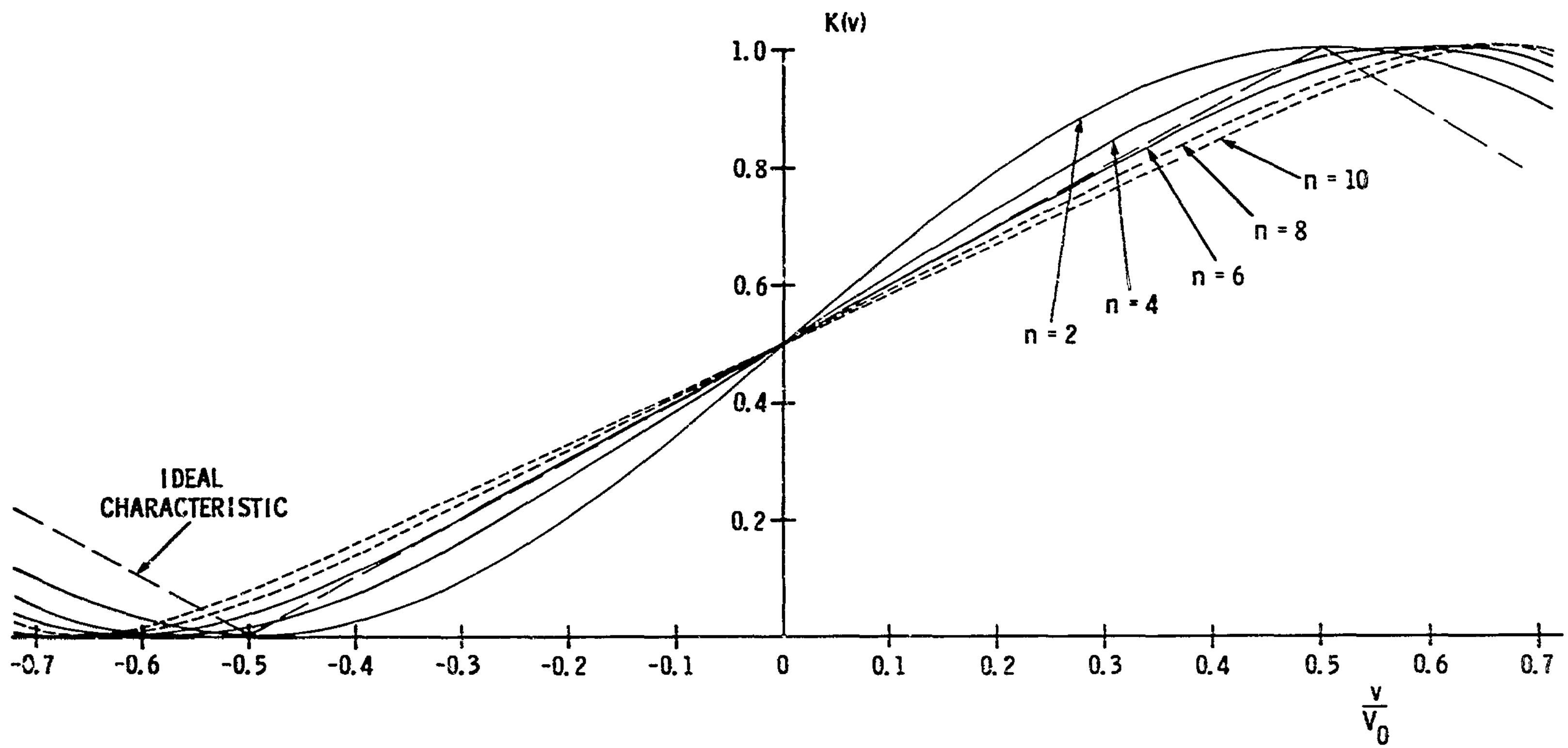
K(v)
1.0
0.8
0.6
0.4
0.2
-0.7
-0.6
-0.5
-0.4
-0.3
-0.2
-0.1
0
0.1
0.2
0.3
0.4
0.5
0.6
0.7
v/V0
IDEAL CHARACTERISTIC
n = 2
n = 4
n = 6
n = 8
n = 10

Figure 12

the third harmonic, seen in Figs. 9d and 9e, again behave in very similar fashion to each other. These figures show that the maximally-linear approximation is, in general, less successful for n even than for n odd. For example, there is more fundamental and third harmonic distortion present for $n = 10$ than for $n = 9$ for all values of v/V_0. In some cases, the n even networks produce less distortion than the n odd networks for small values of v/V_0, but for larger values of v/V_0 the n even networks are consistantly inferior in performance.

In order to obtain the entire picture, however, the variation of the fundamental amplitude with n must also be considered. This is shown in Fig. 9a, where it is seen that the fundamental amplitude does not fall off nearly as much with increasing n when n is even as when n is odd. However, as can be seen from Fig. 10a where fundamental distortion is plotted vs. n for constant values of the fundamental amplitude, the modulators having n even are still inferior to those with n odd.

To summarize then, the maximally-linear approximation technique is perhaps less successful for n even than for n odd. For n even, an advantage is obtained in that the second, fourth, sixth, etc. harmonics are zero. If the elimination of even harmonics is of prime importance, the n even case may well be the solution. The distortion present in the odd harmonics of the output, however, is worse for n even than for n odd.

IV. AMPLITUDE MODULATORS FOR USE WITH SQUARE-LAW DETECTORS

In this section we consider the ideal characteristic and methods for its approximation for an amplitude modulator to be used with a square-law detector. This case is probably of greater general interest than the envelope-detector case since various square-law detectors are available and widely used.

A. Ideal Modulator Characteristic

In Section III it was seen that for the envelope-detector case, one possible ideal characteristic is

$$K(v) = \left(\frac{1}{2} + \frac{v}{V_0}\right) .$$

It is not difficult to see, then, that for the square-law case the corresponding ideal characteristic is

$$K(v) = \left(\frac{1}{2} + \frac{v}{V_0}\right)^{1/2} . \tag{44}$$

To verify that the $K(v)$ of (44) is indeed an ideal modulator transfer function, assume that an optical signal $e^{i\omega t}$ enters a modulator having such a $K(v)$. The signal E_{out} leaving the modulator is given by

$$E_{out} = \left(\frac{1}{2} + \frac{v}{V_0}\right)^{1/2} e^{i\omega t} . \tag{45}$$

If we assume that the modulating signal v has the form $v = V \cos \omega_m t$, Eq. (45) becomes

$$E_{out} = \left(\frac{1}{2} + \frac{V}{V_0} \cos \omega_m t\right)^{1/2} e^{i\omega t} , \tag{46}$$

the signal which is incident upon the detector. The detector output I_{out} is given by $kE_{out}E^*_{out}$, which using (46) gives

$$I_{out} = k \left(\frac{1}{2} + \frac{V}{V_0} \cos \omega_m t\right) . \tag{47}$$

As noted before, this satisfies perfectly the criteria which we have selected for modulator performance, namely that the detector output contain a fundamental whose amplitude is linearly proportional to V, and no higher harmonics. The ideal characteristic of Eq. (44) is plotted in Fig. 13. Finally, it should be noted that just as there were an infinite number of possible ideal characteristics (of various slopes) for the envelope-detector case, there are likewise an infinite number of possibilities for the square-law case.

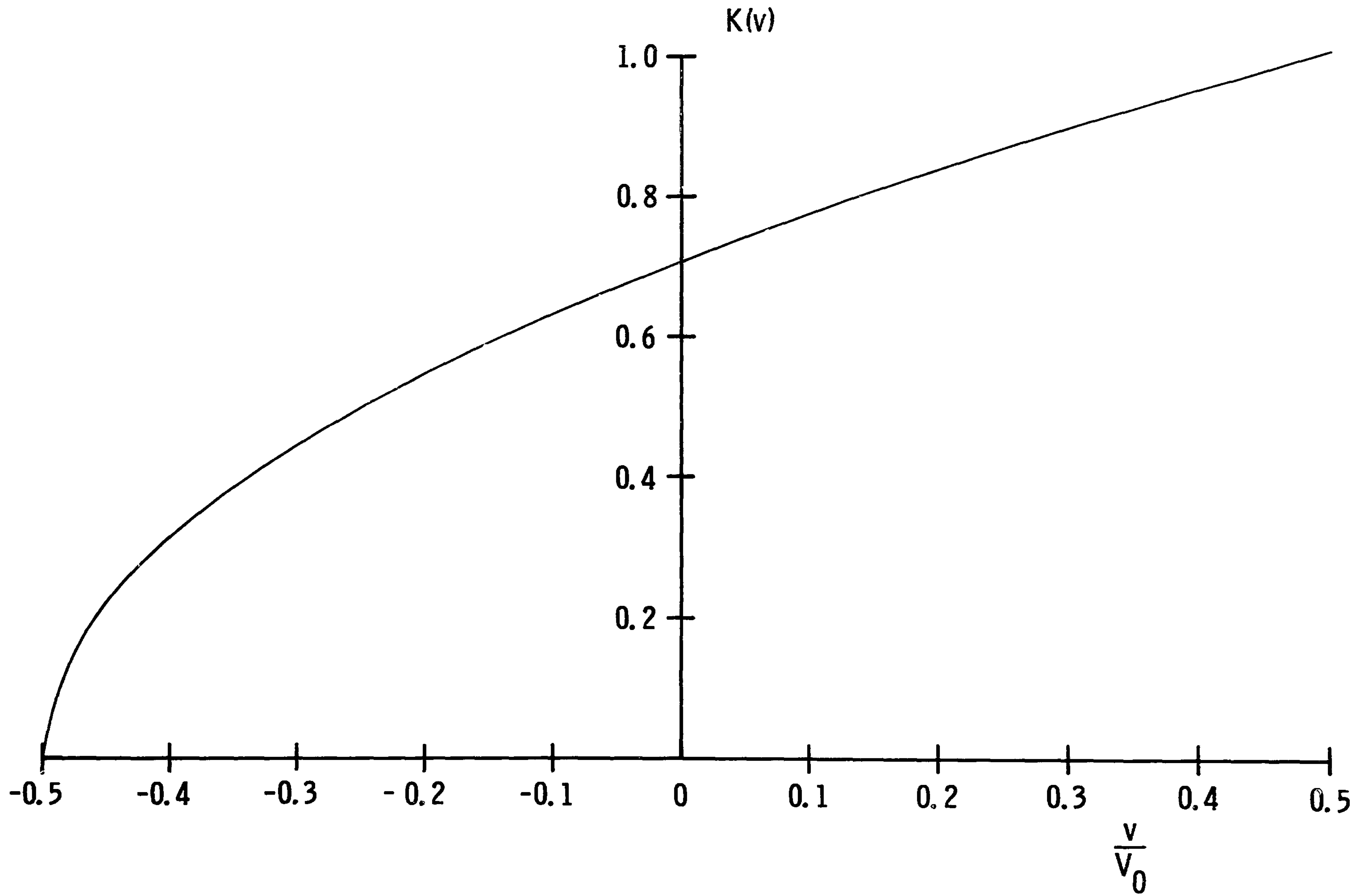

Figure 13

For the square-law case, we will consider only n odd. The previous section showed it to be more useful than n even in almost all respects. The sole exception was in elimination of even harmonics, where by proper choice of the A_i, a modulator with n even could be designed to produce no even harmonics. However as we will see, even this potential advantage is not present in the square-law case, since the even harmonic amplitudes are now functions of the A_i and B_i rather than the A_i alone.

B. Formulas for Amplitudes of Fundamental and Harmonics

We now derive general expressions for the amplitudes of the fundamental and harmonics present in the detector output. The voltage transfer functions for 1, 3, 5, 7, and 9 stage networks are again given by Eqs. (10). The details of the computation will be given for $n = 9$ only, since results for $n = 1, 3, 5,$ and 7 are derivable from the $n = 9$ case.

We again impose the requirement that $K(v)$ be real. This condition was necessary in the envelope-detector case to ensure that the phase of the demodulated fundamental did not depend upon V; it is not necessary, however, in the square-law case. Hence the decision to restrict $K(v)$ to being real is admittedly an arbitrary one, made primarily for convenience. An additional incentive is provided, however, by the work of Ammann and Yarborough [28]. They have shown that if $K(v)$ is real, a modification of the synthesis procedure of Part V can be used which results in a modulator containing only half as many stages as normally required.

With this restriction, $K(v)$ for $n = 9$ becomes

$$K(v) = C_0 e^{i\frac{9\pi v}{2V_0}} + C_1 e^{i\frac{7\pi v}{2V_0}} + C_2 e^{i\frac{5\pi v}{2V_0}} + C_3 e^{i\frac{3\pi v}{2V_0}} + C_4 e^{i\frac{\pi v}{2V_0}}$$

$$+ C_4^* e^{-i\frac{\pi v}{2V_0}} + C_3^* e^{-i\frac{3\pi v}{2V_0}} + C_2^* e^{-i\frac{5\pi v}{2V_0}} + C_1^* e^{-i\frac{7\pi v}{2V_0}} + C_0^* e^{-i\frac{9\pi v}{2V_0}} \tag{48}$$

The square-law detector output is given by

$$I_{out} = k\ K(v)\,K^*(v)\ E_{in}E_{in}^*,$$

which for the E_{in} of Eq. (7) gives

$$I_{out} = k\ K(v)\,K^*(v). \tag{49}$$

Substituting (48) into (49) gives

$$
\begin{aligned}
I_{out}/k = K(v)\,K^*(v) = 2\ &\left[C_0C_0^* + C_1C_1^* + C_2C_2^* + C_3C_3^* + C_4C_4^*\right] \\
&+ e^{i\frac{\pi v}{V_0}}\left[2(C_0C_1^* + C_1C_2^* + C_2C_3^* + C_3C_4^*) + C_4C_4\right] \\
&+ e^{-i\frac{\pi v}{V_0}}\left[2(C_0^*C_1 + C_1^*C_2 + C_2^*C_3 + C_3^*C_4) + C_4^*C_4^*\right] \\
&+ e^{i\frac{2\pi v}{V_0}}\left[2(C_0C_2^* + C_1C_3^* + C_2C_4^* + C_3C_4)\right] \\
&+ e^{-i\frac{2\pi v}{V_0}}\left[2(C_0^*C_2 + C_1^*C_3 + C_2^*C_4 + C_3^*C_4^*)\right] \\
&+ e^{i\frac{3\pi v}{V_0}}\left[2(C_0C_3^* + C_1C_4^* + C_2C_4) + C_3C_3\right] \\
&+ e^{-i\frac{3\pi v}{V_0}}\left[2(C_0^*C_3 + C_1^*C_4 + C_2^*C_4^*) + C_3^*C_3^*\right] \\
&+ e^{i\frac{4\pi v}{V_0}}\left[2(C_0C_4^* + C_1C_4 + C_2C_3)\right]
\end{aligned}
$$

$$+ e^{-i\frac{4\pi v}{V_0}} \left[2(C_0^* C_4 + C_1^* C_4^* + C_2^* C_3^*) \right]$$

$$+ e^{i\frac{5\pi v}{V_0}} \left[2(C_0 C_4 + C_1 C_3) + C_2 C_2 \right]$$

$$+ e^{-i\frac{5\pi v}{V_0}} \left[2(C_0^* C_4^* + C_1^* C_3^*) + C_2^* C_2^* \right]$$

$$+ e^{i\frac{6\pi v}{V_0}} \left[2(C_0 C_3 + C_1 C_2) \right] + e^{-i\frac{6\pi v}{V_0}} \left[2(C_0^* C_3^* + C_1^* C_2^*) \right]$$

$$+ e^{i\frac{7\pi v}{V_0}} \left[2C_0 C_2 + C_1 C_1 \right] + e^{-i\frac{7\pi v}{V_0}} \left[2C_0^* C_2^* + C_1^* C_1^* \right]$$

$$+ e^{i\frac{8\pi v}{V_0}} \left[2C_0 C_1 \right] + e^{-i\frac{8\pi v}{V_0}} \left[2C_0^* C_1^* \right]$$

$$+ e^{i\frac{9\pi v}{V_0}} \left[C_0 C_0 \right] + e^{-i\frac{9\pi v}{V_0}} \left[C_0^* C_0^* \right] \quad . \tag{50}$$

Letting $C_i = A_i + iB_i$, we obtain

$$I_{out}/k = 2 \left[A_0^2 + A_1^2 + A_2^2 + A_3^2 + A_4^2 + B_0^2 + B_1^2 + B_2^2 + B_3^2 + B_4^2 \right]$$

$$+ 2\cos \frac{\pi v}{V_0} \left[A_4^2 - B_4^2 + 2(A_0 A_1 + B_0 B_1 + A_1 A_2 + B_1 B_2 + A_2 A_3 + B_2 B_3 + A_3 A_4 + B_3 B_4) \right]$$

$$- 2\sin \frac{\pi v}{V_0} \left[2(-A_0 B_1 + A_1 B_0 - A_1 B_2 + A_2 B_1 - A_2 B_3 + A_3 B_2 - A_3 B_4 + A_4 B_3 + A_4 B_4) \right]$$

$$+ 2\cos \frac{2\pi v}{V_0} \left[2(A_0 A_2 + B_0 B_2 + A_1 A_3 + B_1 B_3 + A_2 A_4 + B_2 B_4 + A_3 A_4 - B_3 B_4) \right]$$

$$- 2\sin \frac{2\pi v}{V_0} \left[2(-A_0 B_2 + A_2 B_0 - A_1 B_3 + A_3 B_1 - A_2 B_4 + A_4 B_2 + A_3 B_4 + A_4 B_3) \right]$$

$$+ \; 2\cos\frac{3\pi v}{V_0}\left[A_3^2 - B_3^2 + 2(A_0A_3 + B_0B_3 + A_1A_4 + B_1B_4 + A_2A_4 - B_2B_4)\right]$$

$$- \; 2\sin\frac{3\pi v}{V_0}\left[2(-A_0B_3 + A_3B_0 - A_1B_4 + A_4B_1 + A_2B_4 + A_4B_2 + A_3B_3)\right]$$

$$+ \; 2\cos\frac{4\pi v}{V_0}\left[2(A_0A_4 + B_0B_4 + A_1A_4 - B_1B_4 + A_2A_3 - B_2B_3)\right]$$

$$- \; 2\sin\frac{4\pi v}{V_0}\left[2(-A_0B_4 + A_4B_0 + A_1B_4 + B_1A_4 + A_2B_3 + A_3B_2)\right]$$

$$+ \; 2\cos\frac{5\pi v}{V_0}\left[A_2^2 - B_2^2 + 2(A_0A_4 - B_0B_4 + A_1A_3 - B_1B_3)\right]$$

$$- \; 2\sin\frac{5\pi v}{V_0}\left[2(A_0B_4 + A_4B_0 + A_1B_3 + A_3B_1 + A_2B_2)\right]$$

$$+ \; 2\cos\frac{6\pi v}{V_0}\left[2(A_0A_3 - B_0B_3 + A_1A_2 - B_1B_2)\right]$$

$$- \; 2\sin\frac{6\pi v}{V_0}\left[2(A_0B_3 + A_3B_0 + A_1B_2 + A_2B_1)\right]$$

$$+ \; 2\cos\frac{7\pi v}{V_0}\left[A_1^2 - B_1^2 + 2(A_0A_2 - B_0B_2)\right] - 2\sin\frac{7\pi v}{V_0}\left[2(A_0B_2 + A_2B_0 + A_1B_1)\right]$$

$$+ \; 2\cos\frac{8\pi v}{V_0}\left[2(A_0A_1 - B_0B_1)\right] - 2\sin\frac{8\pi v}{V_0}\left[2(A_0B_1 + A_1B_0)\right]$$

$$+ \; 2\cos\frac{9\pi v}{V_0}\left[A_0^2 - B_0^2\right] - 2\sin\frac{9\pi v}{V_0}\left[2A_0B_0\right] \quad . \tag{51}$$

For convenience we will designate the bracketed terms in (51) by $\mathcal{A}_0$, $\mathcal{A}_1$, $\mathcal{B}_1$, $\mathcal{A}_2$, $\mathcal{B}_2$, $\mathcal{A}_3$, $\mathcal{B}_3$, $\mathcal{A}_4$, $\mathcal{B}_4$, $\mathcal{A}_5$, $\mathcal{B}_5$, $\mathcal{A}_6$, $\mathcal{B}_6$, $\mathcal{A}_7$, $\mathcal{B}_7$, $\mathcal{A}_8$, $\mathcal{B}_8$, $\mathcal{A}_9$, and $\mathcal{B}_9$ respectively. Equation (51) then becomes

$$I_{out}/k = 2\,\mathcal{A}_0 + 2\,\mathcal{A}_1\cos\frac{\pi v}{V_0} - 2\,\mathcal{B}_1\sin\frac{\pi v}{V_0} + 2\,\mathcal{A}_2\cos\frac{2\pi v}{V_0}$$

$$- \; 2\,\mathcal{B}_2\sin\frac{2\pi v}{V_0} + 2\,\mathcal{A}_3\cos\frac{3\pi v}{V_0} - 2\,\mathcal{B}_3\sin\frac{3\pi v}{V_0} + 2\,\mathcal{A}_4\cos\frac{4\pi v}{V_0}$$

$$- 2\mathcal{B}_4 \sin\frac{4\pi v}{V_0} + 2\mathcal{A}_5 \cos\frac{5\pi v}{V_0} - 2\mathcal{B}_5 \sin\frac{5\pi v}{V_0} + 2\mathcal{A}_6 \cos\frac{6\pi v}{V_0}$$

$$- 2\mathcal{B}_6 \sin\frac{6\pi v}{V_0} + 2\mathcal{A}_7 \cos\frac{7\pi v}{V_0} - 2\mathcal{B}_7 \sin\frac{7\pi v}{V_0} + 2\mathcal{A}_8 \cos\frac{8\pi v}{V_0}$$

$$- 2\mathcal{B}_8 \sin\frac{8\pi v}{V_0} + 2\mathcal{A}_9 \cos\frac{9\pi v}{V_0} - 2\mathcal{B}_9 \sin\frac{9\pi v}{V_0}\ . \tag{52}$$

If we now let $v = V\cos\omega_m t$ and expand the $\cos(\cos\theta)$ and $\sin(\cos\theta)$ terms which result, the desired expression is obtained for $n = 9$.

$$\begin{aligned}
I_{out}/k = {} & 2\Big[\mathcal{A}_0 + \mathcal{A}_1 J_0\left(\tfrac{\pi V}{V_0}\right) + \mathcal{A}_2 J_0\left(\tfrac{2\pi V}{V_0}\right) + \mathcal{A}_3 J_0\left(\tfrac{3\pi V}{V_0}\right) + \mathcal{A}_4 J_0\left(\tfrac{4\pi V}{V_0}\right) \\
& + \mathcal{A}_5 J_0\left(\tfrac{5\pi V}{V_0}\right) + \mathcal{A}_6 J_0\left(\tfrac{6\pi V}{V_0}\right) + \mathcal{A}_7 J_0\left(\tfrac{7\pi V}{V_0}\right) + \mathcal{A}_8 J_0\left(\tfrac{8\pi V}{V_0}\right) + \mathcal{A}_9 J_0\left(\tfrac{9\pi V}{V_0}\right)\Big] \\
& - 4\Big[\mathcal{B}_1 J_1\left(\tfrac{\pi V}{V_0}\right) + \mathcal{B}_2 J_1\left(\tfrac{2\pi V}{V_0}\right) + \mathcal{B}_3 J_1\left(\tfrac{3\pi V}{V_0}\right) + \mathcal{B}_4 J_1\left(\tfrac{4\pi V}{V_0}\right) + \mathcal{B}_5 J_1\left(\tfrac{5\pi V}{V_0}\right) \\
& + \mathcal{B}_6 J_1\left(\tfrac{6\pi V}{V_0}\right) + \mathcal{B}_7 J_1\left(\tfrac{7\pi V}{V_0}\right) + \mathcal{B}_8 J_1\left(\tfrac{8\pi V}{V_0}\right) + \mathcal{B}_9 J_1\left(\tfrac{9\pi V}{V_0}\right)\Big]\cos\omega_m t \\
& - 4\Big[\mathcal{A}_1 J_2\left(\tfrac{\pi V}{V_0}\right) + \mathcal{A}_2 J_2\left(\tfrac{2\pi V}{V_0}\right) + \mathcal{A}_3 J_2\left(\tfrac{3\pi V}{V_0}\right) + \mathcal{A}_4 J_2\left(\tfrac{4\pi V}{V_0}\right) + \mathcal{A}_5 J_2\left(\tfrac{5\pi V}{V_0}\right) \\
& + \mathcal{A}_6 J_2\left(\tfrac{6\pi V}{V_0}\right) + \mathcal{A}_7 J_2\left(\tfrac{7\pi V}{V_0}\right) + \mathcal{A}_8 J_2\left(\tfrac{8\pi V}{V_0}\right) + \mathcal{A}_9 J_2\left(\tfrac{9\pi V}{V_0}\right)\Big]\cos 2\omega_m t \\
& + 4\Big[\mathcal{B}_1 J_3\left(\tfrac{\pi V}{V_0}\right) + \mathcal{B}_2 J_3\left(\tfrac{2\pi V}{V_0}\right) + \mathcal{B}_3 J_3\left(\tfrac{3\pi V}{V_0}\right) + \mathcal{B}_4 J_3\left(\tfrac{4\pi V}{V_0}\right) + \mathcal{B}_5 J_3\left(\tfrac{5\pi V}{V_0}\right) \\
& + \mathcal{B}_6 J_3\left(\tfrac{6\pi V}{V_0}\right) + \mathcal{B}_7 J_3\left(\tfrac{7\pi V}{V_0}\right) + \mathcal{B}_8 J_3\left(\tfrac{8\pi V}{V_0}\right) + \mathcal{B}_9 J_3\left(\tfrac{9\pi V}{V_0}\right)\Big]\cos 3\omega_m t \\
& + \text{higher order harmonics.}
\end{aligned} \tag{53}$$

From (53) we see that the amplitudes of the fundamental and harmonics are functions of both the A_i and B_i. This is in contrast to the envelope-detector case where even-harmonic amplitudes are functions of the A_i only, while odd harmonic amplitudes are functions of the B_i.

C. Fourier Approximation to Ideal Characteristic

One might again consider using the Fourier approximation to determine the C_i. This calculation was carried out for the ideal characteristic of Fig. 14 and the resulting A_i and B_i substituted into Eq. (53) (or, for the cases of $n = 1, 3, 5$, and 7, into equivalent expressions) to assess the modulators' performance. This approximation method again proved unsuccessful in yielding modulators with improved performance characteristics, and hence the results will be briefly summarized instead of presented in detail. The deviation from linearity of the fundamental was found to be greater for $n = 5$ and 9 than for $n = 1$, while for $n = 3$ and 7 the deviation from linearity was only slightly less than for $n = 1$. In addition since for $n = 1$ there is no second harmonic, the conventional modulator's performance is superior in this respect also. Therefore the conclusion is again reached that the Fourier method is not successful in designing improved amplitude modulators.

As mentioned earlier, the problem is probably at least partially due to the abrupt changes of slope of $K(v)$ which occur at $v/V_0 = -0.5$ and $+0.5$. In an attempt to verify this, another approach was tried. Instead of approximating the ideal $K(v)$ of Fig. 12, a new $K(v)$ was chosen which closely follows the $K(v)$ of Fig. 12 for $-0.45 < v/V_0 < 0.45$, but which deviates from it in such a fashion that abrupt slope changes are avoided in the vicinity of $v/V_0 = \pm 0.5$. Using graphical techniques, the Fourier coefficients for this new $K(v)$ were found and substituted into Eq. (53).

This technique resulted in a systematic, but fairly small, reduction in the deviation from linearity of the fundamental for $n = 1, 3, 5$, and 7. For $n = 9$, however, the deviation returned to essentially its $n = 1$ value. The second harmonic magnitudes decreased only slightly with increasing n. Thus although this technique was more successful than the regular Fourier approximation of the $K(v)$ of Fig. 12, it still leaves much to be desired. The improvements which it produces are not substantial enough, or sufficiently uniform with increasing n, to merit its use.

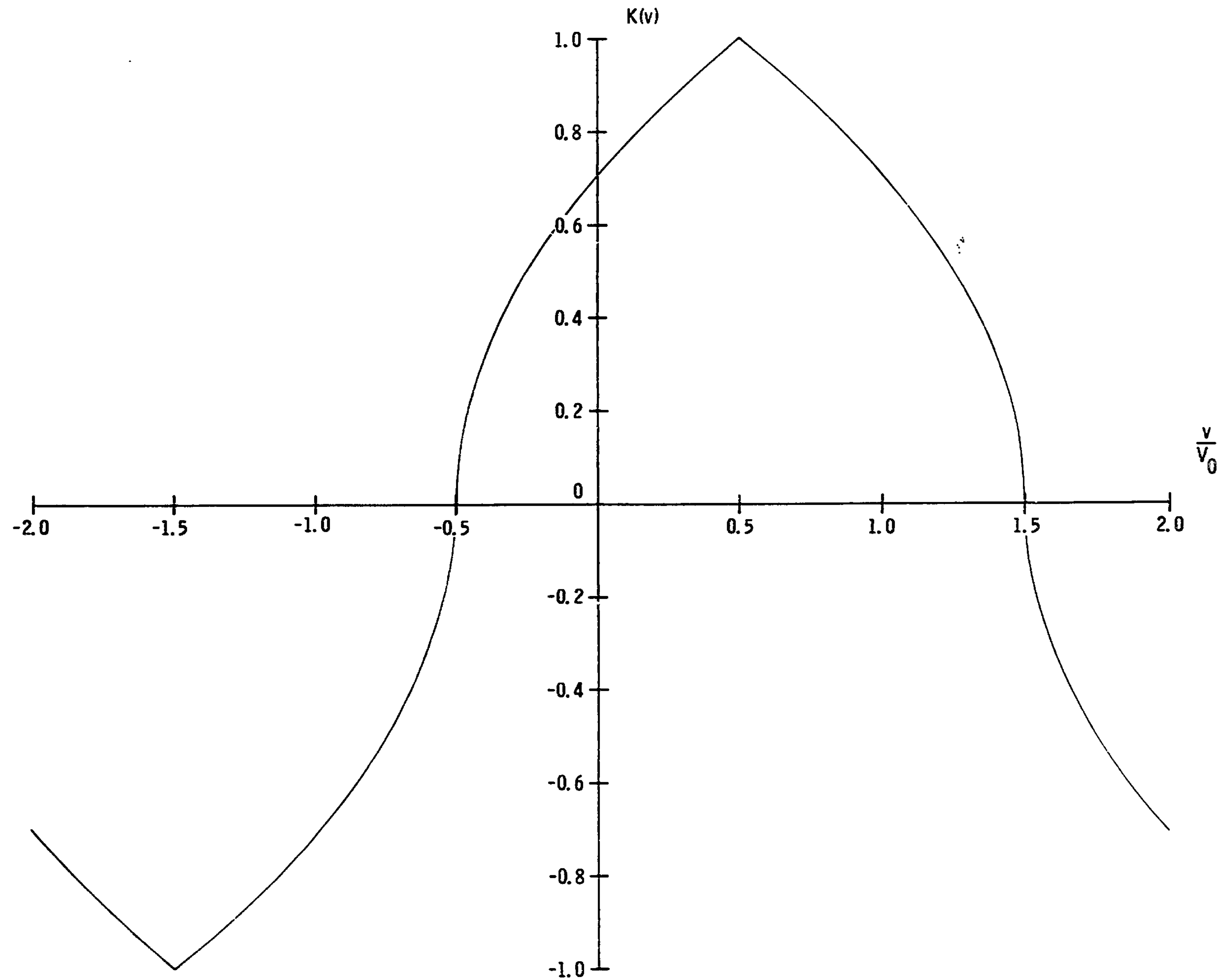

Figure 14

D. Maximally-linear Approximation to Ideal Characteristic

The approximation technique which proved most useful for the envelope-detector case is one in which the C_i were chosen to directly optimize the fundamental and second harmonic amplitudes. The goal was to minimize the second harmonic amplitude and to make the fundamental amplitude directly proportional to V, the amplitude of the modulating signal. We will now apply this same technique to the square-law detector case.

Equation (53) gives a general expression for the demodulated signal from a square-law detector. The amplitude of the fundamental is given by

$$\begin{aligned} \text{amplitude of fundamental} = -4 \Bigl[& \mathcal{B}_1 J_1\left(\frac{\pi V}{V_0}\right) + \mathcal{B}_2 J_1\left(\frac{2\pi V}{V_0}\right) + \mathcal{B}_3 J_1\left(\frac{3\pi V}{V_0}\right) + \mathcal{B}_4 J_1\left(\frac{4\pi V}{V_0}\right) \\ & + \mathcal{B}_5 J_1\left(\frac{5\pi V}{V_0}\right) + \mathcal{B}_6 J_1\left(\frac{6\pi V}{V_0}\right) + \mathcal{B}_7 J_1\left(\frac{7\pi V}{V_0}\right) + \mathcal{B}_8 J_1\left(\frac{8\pi V}{V_0}\right) \\ & + \mathcal{B}_9 J_1\left(\frac{9\pi V}{V_0}\right) \Bigr], \end{aligned} \tag{54}$$

while the amplitude of the second harmonic is given by

$$\begin{aligned} \text{second harmonic amplitude} = -4 \Bigl[& \mathcal{A}_1 J_2\left(\frac{\pi V}{V_0}\right) + \mathcal{A}_2 J_2\left(\frac{2\pi V}{V_0}\right) + \mathcal{A}_3 J_2\left(\frac{3\pi V}{V_0}\right) + \mathcal{A}_4 J_2\left(\frac{4\pi V}{V_0}\right) \\ & + \mathcal{A}_5 J_2\left(\frac{5\pi V}{V_0}\right) + \mathcal{A}_6 J_2\left(\frac{6\pi V}{V_0}\right) + \mathcal{A}_7 J_2\left(\frac{7\pi V}{V_0}\right) + \mathcal{A}_8 J_2\left(\frac{8\pi V}{V_0}\right) \\ & + \mathcal{A}_9 J_2\left(\frac{9\pi V}{V_0}\right) \Bigr]. \end{aligned} \tag{55}$$

It should be kept in mind that the $\mathcal{A}_i$ and $\mathcal{B}_i$ are functions of the A_i and B_i.

Writing each Bessel function of (54) and (55) in series form, we obtain

$$\begin{aligned} \text{amplitude of fundamental} = -4 \Bigl[& \frac{\pi}{2} \frac{V}{V_0} (\mathcal{B}_1 + 2\mathcal{B}_2 + 3\mathcal{B}_3 + 4\mathcal{B}_4 + 5\mathcal{B}_5 + 6\mathcal{B}_6 \\ & + 7\mathcal{B}_7 + 8\mathcal{B}_8 + 9\mathcal{B}_9) - \frac{\pi^3}{16}\left(\frac{V}{V_0}\right)^3 (\mathcal{B}_1 + 2^3\mathcal{B}_2 + 3^3\mathcal{B}_3 \end{aligned}$$

$$+ 4^3\mathcal{B}_4 + 5^3\mathcal{B}_5 + 6^3\mathcal{B}_6 + 7^3\mathcal{B}_7 + 8^3\mathcal{B}_8 + 9^3\mathcal{B}_9)$$

$$+ \frac{\pi^5}{384}\left(\frac{V}{V_0}\right)^5 (\mathcal{B}_1 + 2^5\mathcal{B}_2 + 3^5\mathcal{B}_3 + 4^5\mathcal{B}_4 + 5^5\mathcal{B}_5$$

$$+ 6^5\mathcal{B}_6 + 7^5\mathcal{B}_7 + 8^5\mathcal{B}_8 + 9^5\mathcal{B}_9) - \frac{\pi^7}{18,432}\left(\frac{V}{V_0}\right)^7 (\mathcal{B}_1 + 2^7\mathcal{B}_2$$

$$+ 3^7\mathcal{B}_3 + 4^7\mathcal{B}_4 + 5^7\mathcal{B}_5 + 6^7\mathcal{B}_6 + 7^7\mathcal{B}_7 + 8^7\mathcal{B}_8 + 9^7\mathcal{B}_9)$$

$$+ \frac{\pi^9}{1,474\ 560}\left(\frac{V}{V_0}\right)^9 (\mathcal{B}_1 + 2^9\mathcal{B}_2 + 3^9\mathcal{B}_3 + 4^9\mathcal{B}_4 + 5^9\mathcal{B}_5$$

$$+ 6^9\mathcal{B}_6 + 7^9\mathcal{B}_7 + 8^9\mathcal{B}_8 + 9^9\mathcal{B}_9) - \ldots\Bigg] , \qquad (56)$$

and

$$\text{second harmonic amplitude} = -4\left[\frac{\pi^2}{8}\left(\frac{V}{V_0}\right)^2 (a_1 + 2^2a_2 + 3^2a_3 + 4^2a_4 + 5^2a_5 + 6^2a_6\right.$$

$$+ 7^2a_7 + 8^2a_8 + 9^2a_9) - \frac{\pi^4}{96}\left(\frac{V}{V_0}\right)^4 (a_1 + 2^4a_2 + 3^4a_3$$

$$+ 4^4a_4 + 5^4a_5 + 6^4a_6 + 7^4a_7 + 8^4a_8 + 9^4a_9)$$

$$+ \frac{\pi^6}{3072}\left(\frac{V}{V_0}\right)^6 (a_1 + 2^6a_2 + 3^6a_3 + 4^6a_4 + 5^6a_5$$

$$+ 6^6a_6 + 7^6a_7 + 8^6a_8 + 9^6a_9) - \frac{\pi^8}{184,320}\left(\frac{V}{V_0}\right)^8 (a_1$$

$$+ 2^8a_2 + 3^8a_3 + 4^8a_4 + 5^8a_5 + 6^8a_6 + 7^8a_7 + 8^8a_8$$

$$+ 9^8 \mathcal{A}_9) + \frac{\pi^{10}}{8,847,360}\left(\frac{V}{V_0}\right)^{10} (\mathcal{A}_1 + 2^{10}\mathcal{A}_2 + 3^{10}\mathcal{A}_3$$

$$+ 4^{10}\mathcal{A}_4 + 5^{10}\mathcal{A}_5 + 6^{10}\mathcal{A}_6 + 7^{10}\mathcal{A}_7 + 8^{10}\mathcal{A}_8 + 9^{10}\mathcal{A}_9)$$

$$- \dots \Big] . \tag{57}$$

There are ten different A_i and B_i to be determined: A_0, A_1, A_2, A_3, A_4, B_0, B_1, B_2, B_3, and B_4. One of these is used up in normalizing K(v) to have a maximum magnitude of unity. Another will be fixed when we set $B_4 = - A_4$ in an attempt to make the general form of K(v) similar to that of the ideal function of Fig. 14. The remaining eight A_i and B_i can be chosen to make eight term coefficients in (56) and (57) be zero. The choice of which eight are made zero is arbitrary. Our choice will be the $(V/V_0)^3$, $(V/V_0)^5$, $(V/V_0)^7$, and $(V/V_0)^9$ terms in the fundamental amplitude and the $(V/V_0)^2$, $(V/V_0)^4$, $(V/V_0)^6$, and $(V/V_0)^8$ terms in the second harmonic amplitude.

The corresponding equations are

$$\mathcal{B}_1 + 2^3\mathcal{B}_2 + 3^3\mathcal{B}_3 + 4^3\mathcal{B}_4 + 5^3\mathcal{B}_5 + 6^3\mathcal{B}_6 + 7^3\mathcal{B}_7 + 8^3\mathcal{B}_8 + 9^3\mathcal{B}_9 = 0,$$

$$\mathcal{B}_1 + 2^5\mathcal{B}_2 + 3^5\mathcal{B}_3 + 4^5\mathcal{B}_4 + 5^5\mathcal{B}_5 + 6^5\mathcal{B}_6 + 7^5\mathcal{B}_7 + 8^5\mathcal{B}_8 + 9^5\mathcal{B}_9 = 0,$$

$$\mathcal{B}_1 + 2^7\mathcal{B}_2 + 3^7\mathcal{B}_3 + 4^7\mathcal{B}_4 + 5^7\mathcal{B}_5 + 6^7\mathcal{B}_6 + 7^7\mathcal{B}_7 + 8^7\mathcal{B}_8 + 9^7\mathcal{B}_9 = 0,$$

$$\mathcal{B}_1 + 2^9\mathcal{B}_2 + 3^9\mathcal{B}_3 + 4^9\mathcal{B}_4 + 5^9\mathcal{B}_5 + 6^9\mathcal{B}_6 + 7^9\mathcal{B}_7 + 8^9\mathcal{B}_8 + 9^9\mathcal{B}_9 = 0,$$

$$\mathcal{A}_1 + 2^2\mathcal{A}_2 + 3^2\mathcal{A}_3 + 4^2\mathcal{A}_4 + 5^2\mathcal{A}_5 + 6^2\mathcal{A}_6 + 7^2\mathcal{A}_7 + 8^2\mathcal{A}_8 + 9^2\mathcal{A}_9 = 0,$$

$$\mathcal{A}_1 + 2^4\mathcal{A}_2 + 3^4\mathcal{A}_3 + 4^4\mathcal{A}_4 + 5^4\mathcal{A}_5 + 6^4\mathcal{A}_6 + 7^4\mathcal{A}_7 + 8^4\mathcal{A}_8 + 9^4\mathcal{A}_9 = 0,$$

$$\mathcal{A}_1 + 2^6\mathcal{A}_2 + 3^6\mathcal{A}_3 + 4^6\mathcal{A}_4 + 5^6\mathcal{A}_5 + 6^6\mathcal{A}_6 + 7^6\mathcal{A}_7 + 8^6\mathcal{A}_8 + 9^6\mathcal{A}_9 = 0,$$

$$\mathcal{A}_1 + 2^8\mathcal{A}_2 + 3^8\mathcal{A}_3 + 4^8\mathcal{A}_4 + 5^8\mathcal{A}_5 + 6^8\mathcal{A}_6 + 7^8\mathcal{A}_7 + 8^8\mathcal{A}_8 + 9^8\mathcal{A}_9 = 0. \tag{58}$$

If we rewrite the above equations expressing the $\mathcal{a}_i$ and $\mathcal{B}_i$ in terms of the A_i and B_i, and if we let $B_4 = -A_4$, we obtain

$$- A_4^2 + 9A_4B_3 + 35A_4B_2 + 91A_4B_1 - 7A_4A_3 + 27A_3B_3 + 65A_3B_2 + 133A_3B_1$$
$$- 19A_4A_2 + 63A_2B_3 + 125A_2B_2 + 217A_2B_1 - 37A_4A_1 + 117A_1B_3 + 215A_1B_2$$
$$+ 343A_1B_1 + 189A_4B_0 + 243A_3B_0 + 351A_2B_0 + 513A_1B_0 - 61A_4A_0 + 189A_0B_3$$
$$+ 335A_0B_2 + 511A_0B_1 + 729A_0B_0 = 0, \tag{59a}$$

$$- A_4^2 + 33A_4B_3 + 275A_4B_2 + 1267A_4B_1 - 31A_4A_3 + 243A_3B_3 + 1025A_3B_2$$
$$+ 3157A_3B_1 - 211A_4A_2 + 1023A_2B_3 + 3125A_2B_2 + 7777A_2B_1 - 781A_4A_1$$
$$+ 3093A_1B_3 + 7775A_1B_2 + 16,807A_1B_1 + 4149A_4B_0 + 8019A_3B_0 + 16,839A_2B_0$$
$$+ 32,769A_1B_0 - 2101A_4A_0 + 7533A_0B_3 + 16,775A_0B_2 + 32,767A_0B_1$$
$$+ 59,049A_0B_0 = 0, \tag{59b}$$

$$- A_4^2 + 129A_4B_3 + 2315A_4B_2 + 18,571A_4B_1 - 127A_4A_3 + 2187A_3B_3 + 16,385A_3B_2$$
$$+ 78,253A_3B_1 - 2059A_4A_2 + 16,383A_2B_3 + 78,125A_2B_2 + 279,937A_2B_1$$
$$- 14,197A_4A_1 + 77,997A_1B_3 + 279,935A_1B_2 + 823,543A_1B_1 + 94,509A_4B_0$$
$$+ 282,123A_3B_0 + 823,671A_2B_0 + 2,097,153A_1B_0 - 61,741A_4A_0 + 277,749A_0B_3$$
$$+ 823,415A_0B_2 + 2,097,151A_0B_1 + 4,782,969A_0B_0 = 0, \tag{59c}$$

$$
\begin{aligned}
& - A_4^2 + 513A_4B_3 + 20,195A_4B_2 + 281,827A_4B_1 - 511A_4A_3 + 19,683A_3B_3 \\
& + 262,145A_3B_2 + 1,953,637A_3B_1 - 19,171A_4A_2 + 262,143A_2B_3 + 1,953,125A_2B_2 \\
& + 10,077,697A_2B_1 - 242,461A_4A_1 + 1,952,613A_1B_3 + 10,077,695A_1B_2 \\
& + 40,353,607A_1B_1 + 2,215,269A_4B_0 + 10,097,379A_3B_0 + 40,354,119A_2B_0 \\
& + 134,217,729A_1B_0 - 1,690,981A_4A_0 + 10,058,013A_0B_3 + 40,353,095A_0B_2 \\
& + 134,217,727A_0B_1 + 387,420,489A_0B_0 = 0,
\end{aligned}
\tag{59d}
$$

$$
\begin{aligned}
& 10A_4A_3 + 6A_4B_3 + 26A_4A_2 + 10A_4B_2 + 50A_4A_1 + 14A_4B_1 + 9A_3^2 - 9B_3^2 \\
& + 34A_3A_2 - 30B_3B_2 + 58A_3A_1 - 42B_3B_1 + 25A_2^2 - 25B_2^2 + 74A_2A_1 - 70B_2B_1 \\
& + 49A_1^2 - 49B_1^2 + 82A_4A_0 + 18A_4B_0 + 90A_3A_0 - 54B_3B_0 + 106A_2A_0 - 90B_2B_0 \\
& + 130A_1A_0 - 126B_1B_0 + 81A_0^2 - 81B_0^2 = 0,
\end{aligned}
\tag{59e}
$$

$$
\begin{aligned}
& 34A_4A_3 + 30A_4B_3 + 194A_4A_2 + 130A_4B_2 + 674A_4A_1 + 350A_4B_1 + 81A_3^2 \\
& - 81B_3^2 + 514A_3A_2 - 510B_3B_2 + 1282A_3A_1 - 1218B_3B_1 + 625A_2^2 - 625B_2^2 \\
& + 2594A_2A_1 - 2590B_2B_1 + 2401A_1^2 - 2401B_1^2 + 1762A_4A_0 + 738A_4B_0 \\
& + 2754A_3A_0 - 2430B_3B_0 + 4834A_2A_0 - 4770B_2B_0 + 8194A_1A_0 - 8190B_1B_0 \\
& + 6561A_0^2 - 6561B_0^2 = 0,
\end{aligned}
\tag{59f}
$$

$$130A_4A_3 + 126A_4B_3 + 1586A_4A_2 + 1330A_4B_2 + 9650A_4A_1 + 6734A_4B_1$$

$$+ 729A_3^2 - 729B_3^2 + 8194A_3A_2 - 8190B_3B_2 + 31,378A_3A_1 - 31,122B_3B_1$$

$$+ 15,625A_2^2 - 15,625B_2^2 + 93,314A_2A_1 - 93,310B_2B_1 + 117,649A_1^2$$

$$- 117,649B_1^2 + 39,442A_4A_0 + 23,058A_4B_0 + 94,770A_3A_0 - 91,854B_3B_0$$

$$+ 235,426A_2A_0 - 235,170B_2B_0 + 524,290A_1A_0 - 524,286B_1B_0 + 531,441A_0^2$$

$$- 531,441B_0^2 = 0, \tag{59g}$$

$$514A_4A_3 + 510A_4B_3 + 13,634A_4A_2 + 12,610A_4B_2 + 144,194A_4A_1$$

$$+ 117,950A_4B_1 + 6561A_3^2 - 6561B_3^2 + 131,074A_3A_2 - 131,070B_3B_2$$

$$+ 781,762A_3A_1 - 780,738B_3B_1 + 390,625A_2^2 - 390,625B_2^2 + 3,359,234A_2A_1$$

$$- 3,359,230B_2B_1 + 5,764,801A_1^2 - 5,764,801B_1^2 + 912,322A_4A_0 + 650,178A_4B_0$$

$$+ 3,372,354A_3A_0 - 3,346,110B_3B_0 + 11,530,114A_2A_0 - 11,529,090B_2B_0$$

$$+ 33,554,434A_1A_0 - 33,554,430B_1B_0 + 43,046,721A_0^2 - 43,046,721B_0^2 = 0. \tag{59h}$$

It is now necessary to solve these eight simultaneous equations for A_0, A_1, A_2, A_3, B_0, B_1, B_2, and B_3 in terms of A_4. In the linear detector case, the simultaneous equations were linear; in the square-law case, they are nonlinear and hence considerably more difficult to solve. Furthermore it is not known a priori whether real solutions for the A_i and B_i even exist.

The Eqs. (59) were solved by computer, and the A_i and B_i were found to have real solutions. These solutions are

$$
\begin{aligned}
A_3 &= -\,0.0864814\ A_4, \\
A_2 &= 0.0010356\ A_4, \\
A_1 &= 0.0025003\ A_4, \\
A_0 &= -\,0.0003848\ A_4, \\
B_3 &= 0.2232322\ A_4, \\
B_2 &= -\,0.0579300\ A_4, \\
B_1 &= 0.0099872\ A_4, \\
B_0 &= -\,0.0008140\ A_4. \qquad\qquad n = 9 \qquad\qquad (60)
\end{aligned}
$$

We now know the coefficients of $K(v)$ in terms of A_4. By normalizing $K(v)$ to have a maximum magnitude of unity, absolute values are obtained.

Similar calculations can be carried out for $n = 7$, 5, and 3. When $n = 7$, for example, three terms in the expression for the amplitude of the fundamental and three terms in the expression for the second harmonic amplitude can be set to zero. This requires the solution of six simultaneous nonlinear equations.

The final results for $K(v)$ using the maximally-linear approximation technique are

$$
\begin{aligned}
n = 9 \qquad K(v) = &-(0.000132 + i0.000280)e^{i\frac{9\pi v}{2V_0}} + (0.000859 + i0.003433)e^{i\frac{7\pi v}{2V_0}} \\
&+ (0.000356 - i0.019911)e^{i\frac{5\pi v}{2V_0}} - (0.029724 - i0.076727)e^{i\frac{3\pi v}{2V_0}} \\
&+ (0.343708 - i0.343708)e^{i\frac{\pi v}{2V_0}} + (0.343708 + i0.343708)e^{-i\frac{\pi v}{2V_0}}
\end{aligned}
$$

$$- (0.029724 + i0.076727)\, e^{-i\frac{3\pi v}{2V_0}} + (0.000356 + i0.019911)\, e^{-i\frac{5\pi v}{2V_0}}$$

$$+ (0.000859 - i0.003433)\, e^{-i\frac{7\pi v}{2V_0}} - (0.000132 - i0.000280)\, e^{-i\frac{9\pi v}{2V_0}}, \tag{61a}$$

n = 7

$$K(v) = (0.000250 + i0.001207)\, e^{i\frac{7\pi v}{2V_0}} + (0.000720 - i0.012645)\, e^{i\frac{5\pi v}{2V_0}}$$

$$- (0.027340 - i0.065522)\, e^{i\frac{3\pi v}{2V_0}} + (0.348012 - i0.348012)\, e^{i\frac{\pi v}{2V_0}}$$

$$+ (0.348012 + i0.348012)\, e^{-i\frac{\pi v}{2V_0}} - (0.027340 + i0.065522)\, e^{-i\frac{3\pi v}{2V_0}}$$

$$+ (0.000720 + i0.012645)\, e^{-i\frac{5\pi v}{2V_0}} + (0.000250 - i0.001207)\, e^{-i\frac{7\pi v}{2V_0}}, \tag{61b}$$

n = 5

$$K(v) = (0.000705 - i0.005565)\, e^{i\frac{5\pi v}{2V_0}} - (0.023582 - i0.050766)\, e^{i\frac{3\pi v}{2V_0}}$$

$$+ (0.351045 - i0.351045)\, e^{i\frac{\pi v}{2V_0}} + (0.351045 + i0.351045)\, e^{-i\frac{\pi v}{2V_0}}$$

$$- (0.023582 + i0.050766)\, e^{-i\frac{3\pi v}{2V_0}} + (0.000705 + i0.005565)\, e^{-i\frac{5\pi v}{2V_0}}, \tag{61c}$$

n = 3

$$K(v) = - (0.016675 - i0.030586)\, e^{i\frac{3\pi v}{2V_0}} + (0.352987 - i0.352987)\, e^{i\frac{\pi v}{2V_0}}$$

$$+ (0.352987 + i0.352987)\, e^{-i\frac{\pi v}{2V_0}} - (0.016675 + i0.030586)\, e^{-i\frac{3\pi v}{2V_0}}, \tag{61d}$$

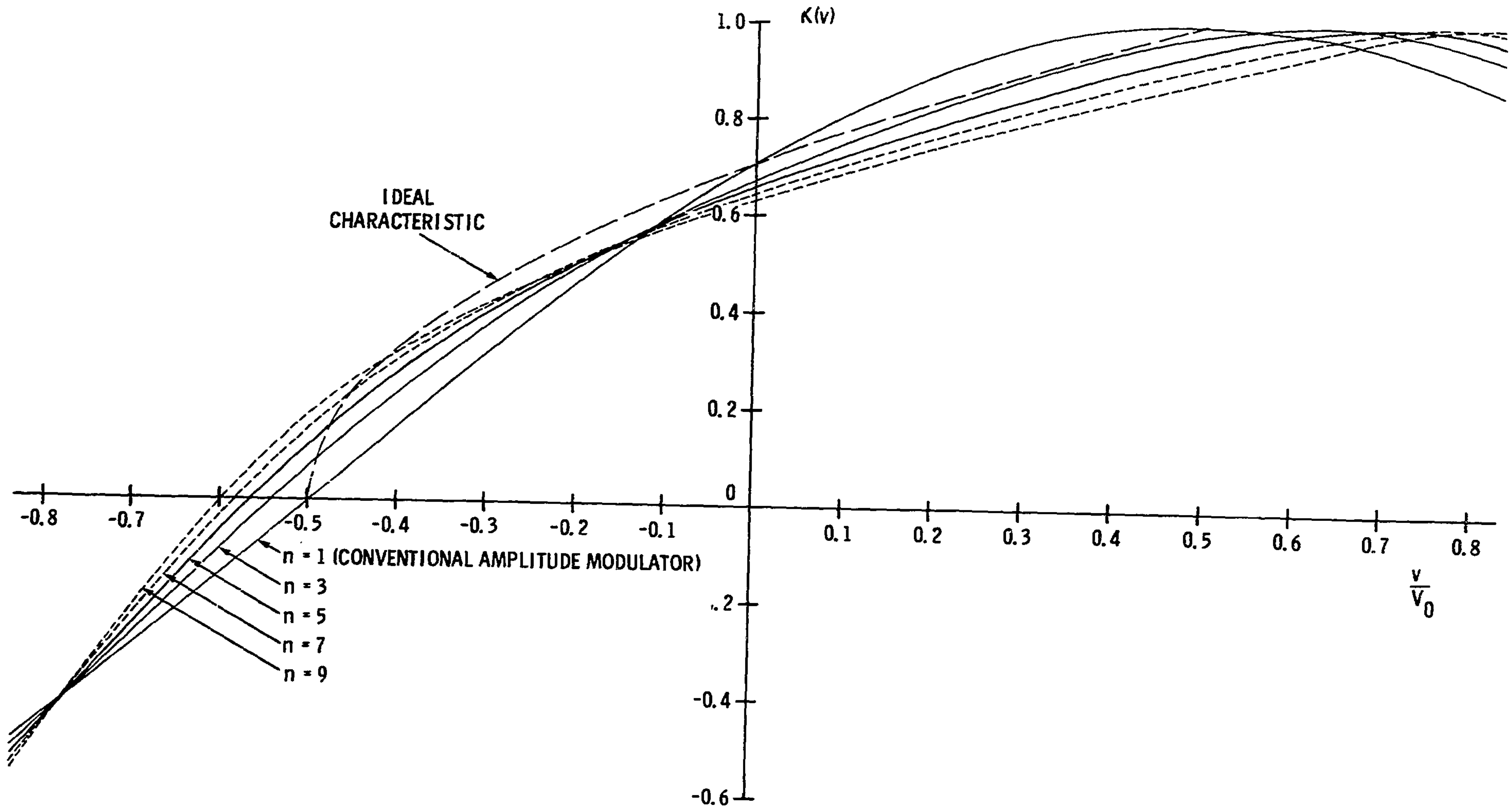
K(v)
1.0
0.8
0.6
0.4
0.2
0
.2
-0.4
-0.6
-0.8
-0.7
-0.5
-0.4
-0.3
-0.2
-0.1
0.1
0.2
0.3
0.4
0.5
0.6
0.7
0.8
v/V0
IDEAL CHARACTERISTIC
n = 1 (CONVENTIONAL AMPLITUDE MODULATOR)
n = 3
n = 5
n = 7
n = 9

Figure 15

$$n = 1 \qquad K(v) = (0.353553 - i0.353553)e^{i\frac{\pi}{2}\frac{v}{V_0}} + (0.353553 + i0.353553)e^{-i\frac{\pi}{2}\frac{v}{V_0}}. \tag{61c}$$

The K(v) of (63) are plotted in Fig. 15 together with the ideal characteristic of Eq. (44). The performance of the modulators corresponding to these K(v) is evaluated by substituting the A_i and B_i of Eqs. (61) into Eq. (53) (or, for $n \neq 9$, into comparable expressions). The results are shown in Fig. 16.

From Fig. 16e, the deviation from linearity of the fundamental is seen to decrease substantially with increasing n. Similar behavior is shown in Fig. 16d for the magnitude of the third harmonic. Figure 16c shows the results obtained for the second harmonic magnitude. Here it should be recalled that for n = 1, no second harmonic is present and hence the synthesized modulators are inferior to a conventional modulator in this respect. Finally the amplitude of the fundamental is shown plotted in Fig. 16b. It is seen that the decrease in fundamental amplitude is even more pronounced in the square-law detector case than in the envelope-detector case. Thus it is important that constant fundamental-amplitude curves similar to those of Fig. 10 be plotted to show more accurately the improvement obtained.

Such curves are shown in Fig. 17 where (a) the deviation from linearity of the fundamental and (b) the magnitude of the second harmonic are plotted as a function of n for various fixed values of fundamental amplitude. From Fig. 17a it is seen that substantial uniform improvement in fundamental linearity is obtained for increasing values of n in spite of the fall-off in fundamental amplitude. The greatest improvement is obtained in going from 1 to 3 stages, with slightly less improvement from 3 to 5, and so forth. That is, the improvement obtained from additional stages is greatest for small n and decreases with increasing n.

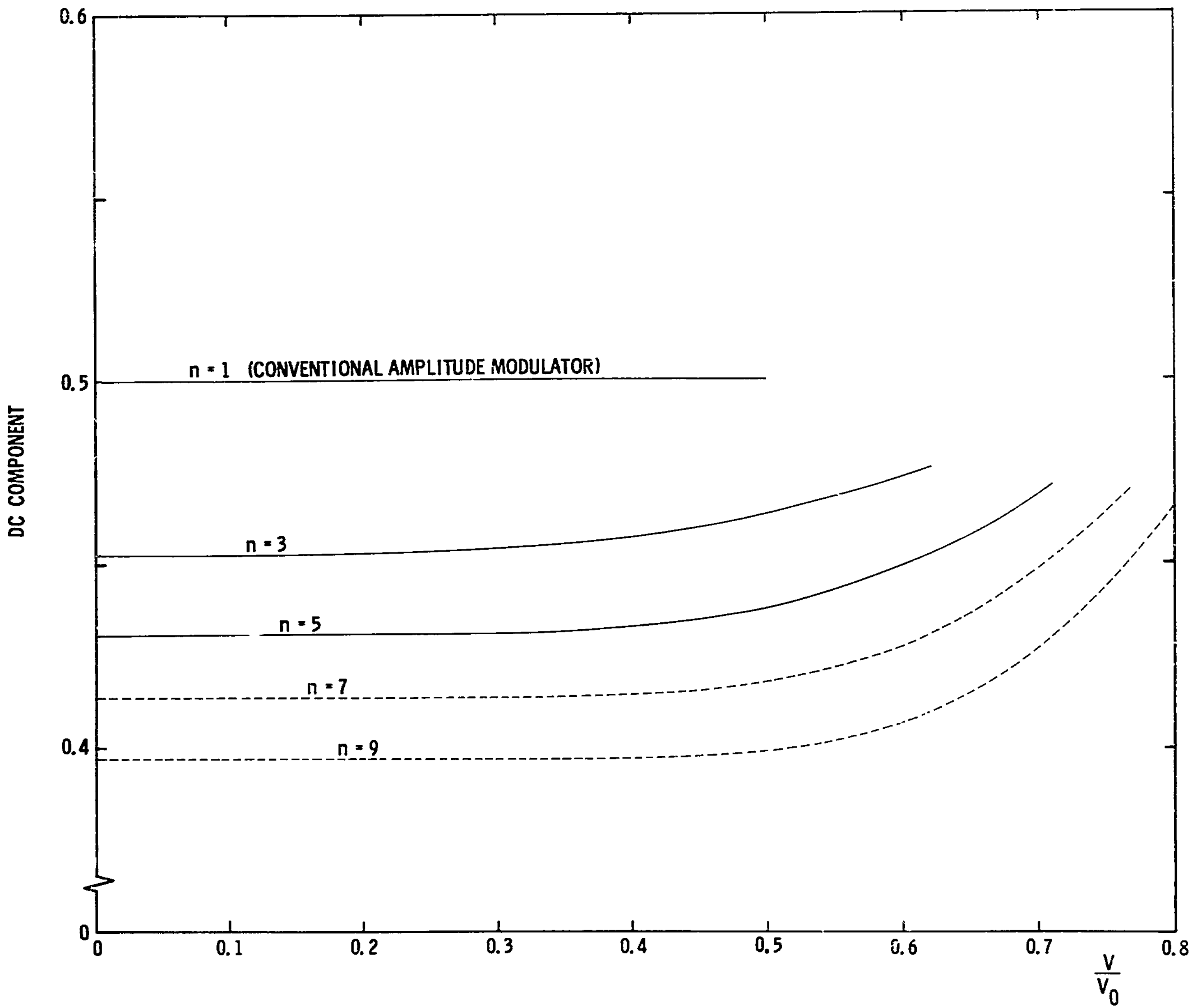

0.6
0.5
0.4
0
DC COMPONENT
n = 1 (CONVENTIONAL AMPLITUDE MODULATOR)
n = 3
n = 5
n = 7
n = 9
0
0.1
0.2
0.3
0.4
0.5
0.6
0.7
0.8
$\frac{V}{V_0}$

Figure 16a

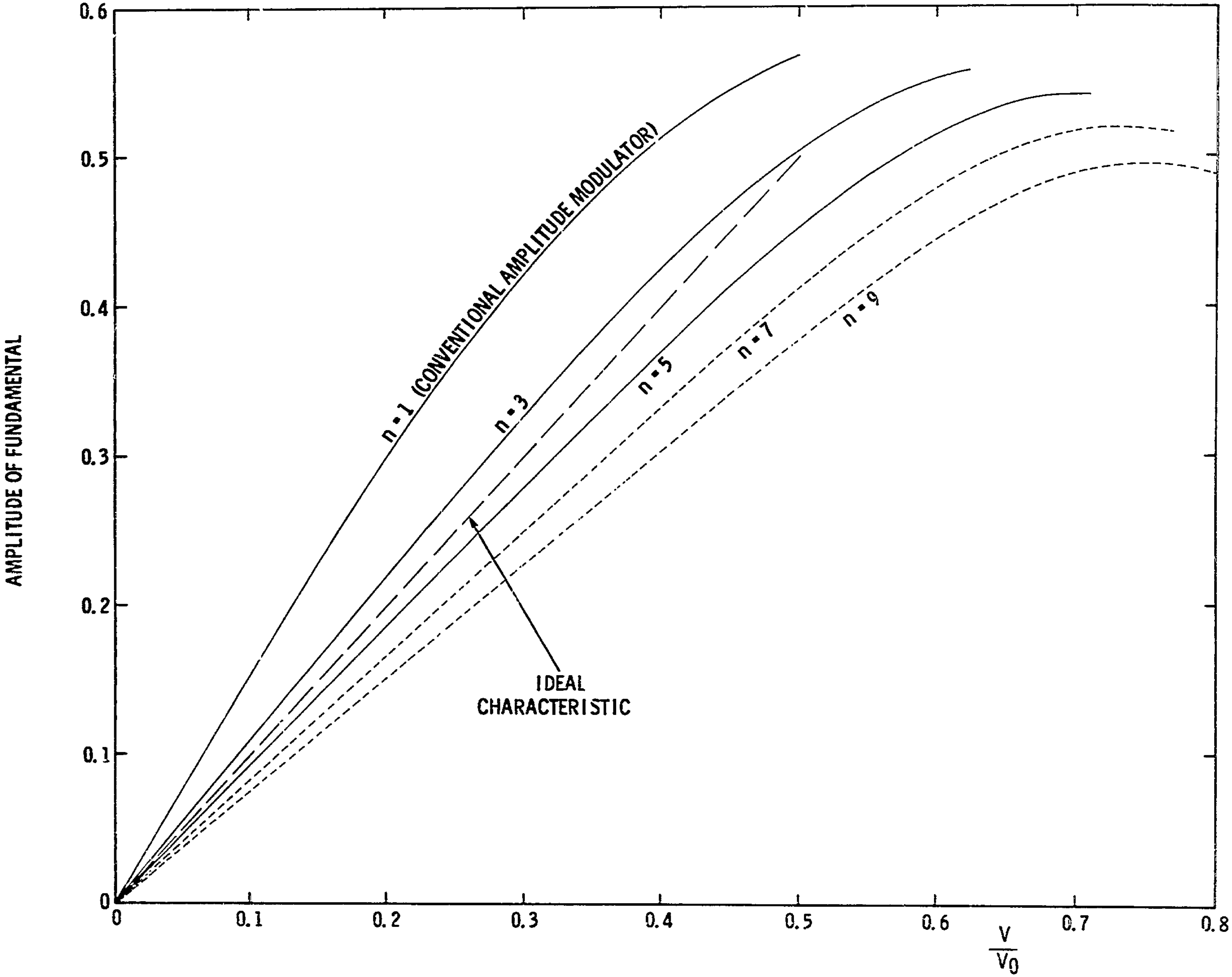
AMPLITUDE OF FUNDAMENTAL
0.6
0.5
0.4
0.3
0.2
0.1
0
0.1
0.2
0.3
0.4
0.5
0.6
0.7
0.8
$\frac{V}{V_0}$
n = 1 (CONVENTIONAL AMPLITUDE MODULATOR)
n = 3
n = 5
n = 7
n = 9
IDEAL CHARACTERISTIC

Figure 16b

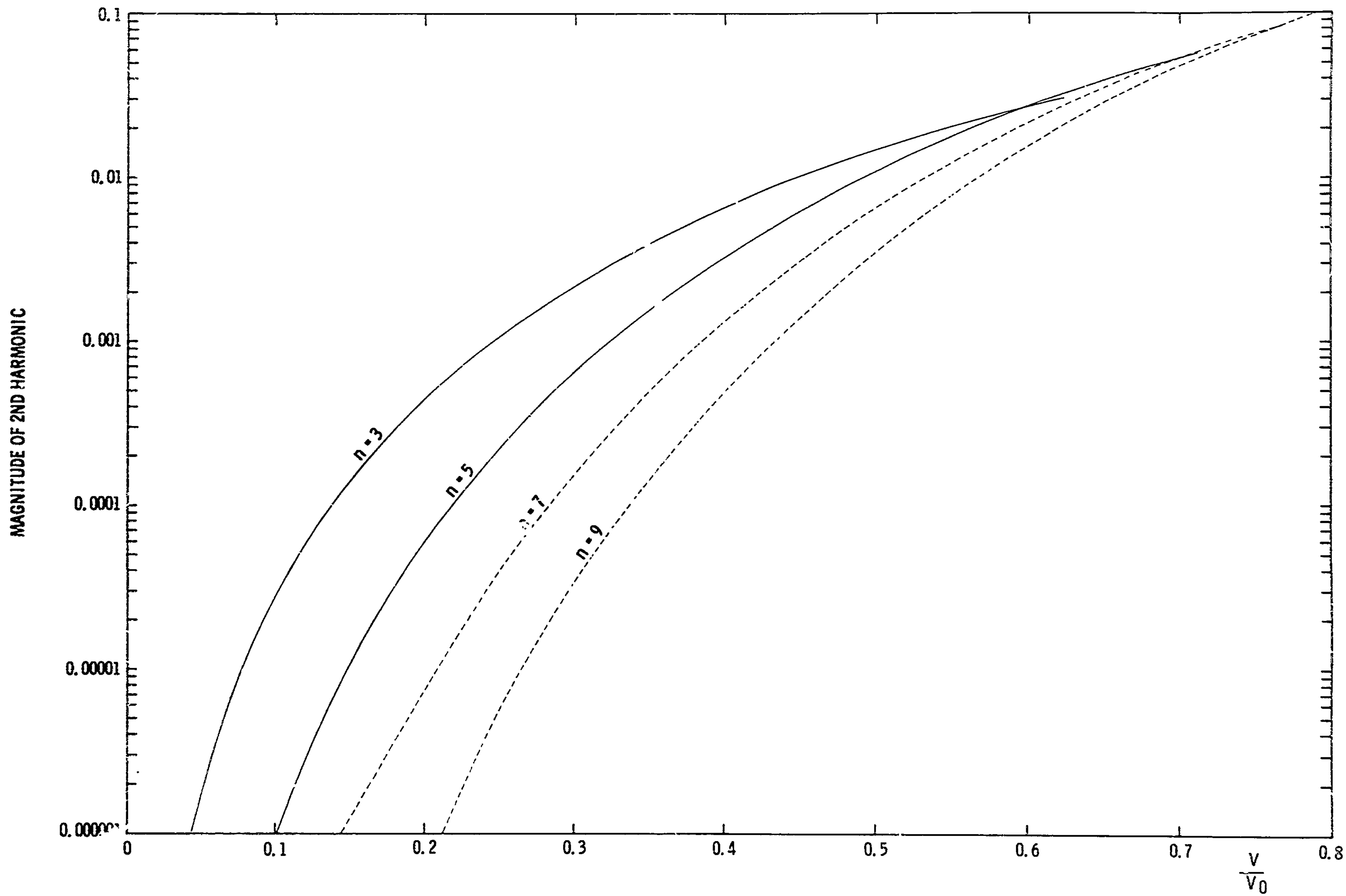
MAGNITUDE OF 2ND HARMONIC
0.1
0.01
0.001
0.0001
0.00001
0
0.1
0.2
0.3
0.4
0.5
0.6
0.7
0.8
V/V0
n = 3
n = 5
n = 9

Figure 16c

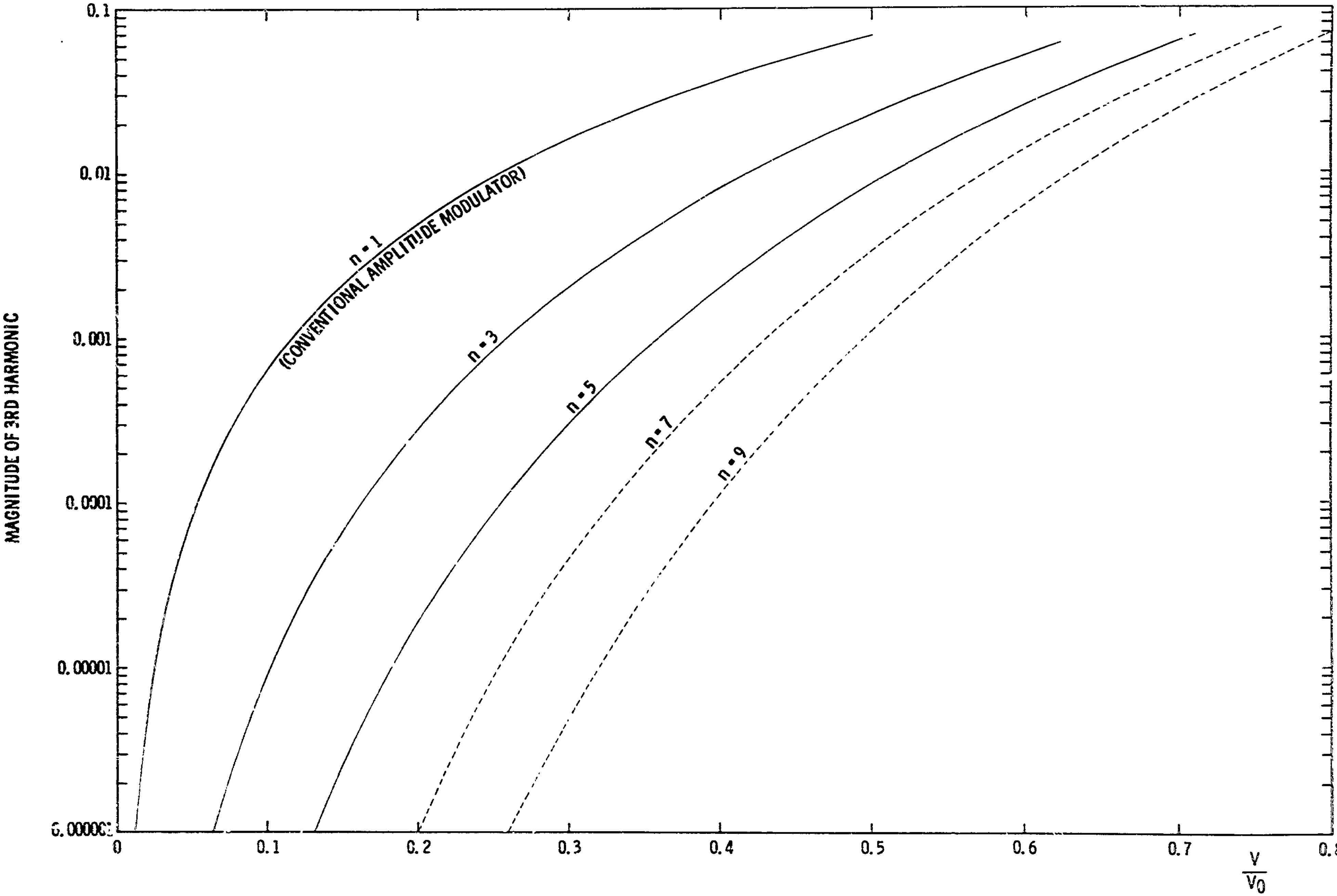
MAGNITUDE OF 3RD HARMONIC
0.1
0.01
0.001
0.0001
0.00001
0.000001
0
0.1
0.2
0.3
0.4
0.5
0.6
0.7
0.8
$\frac{V}{V_0}$
n = 1
(CONVENTIONAL AMPLITUDE MODULATOR)
n = 3
n = 5
n = 7
n = 9

Figure 16d

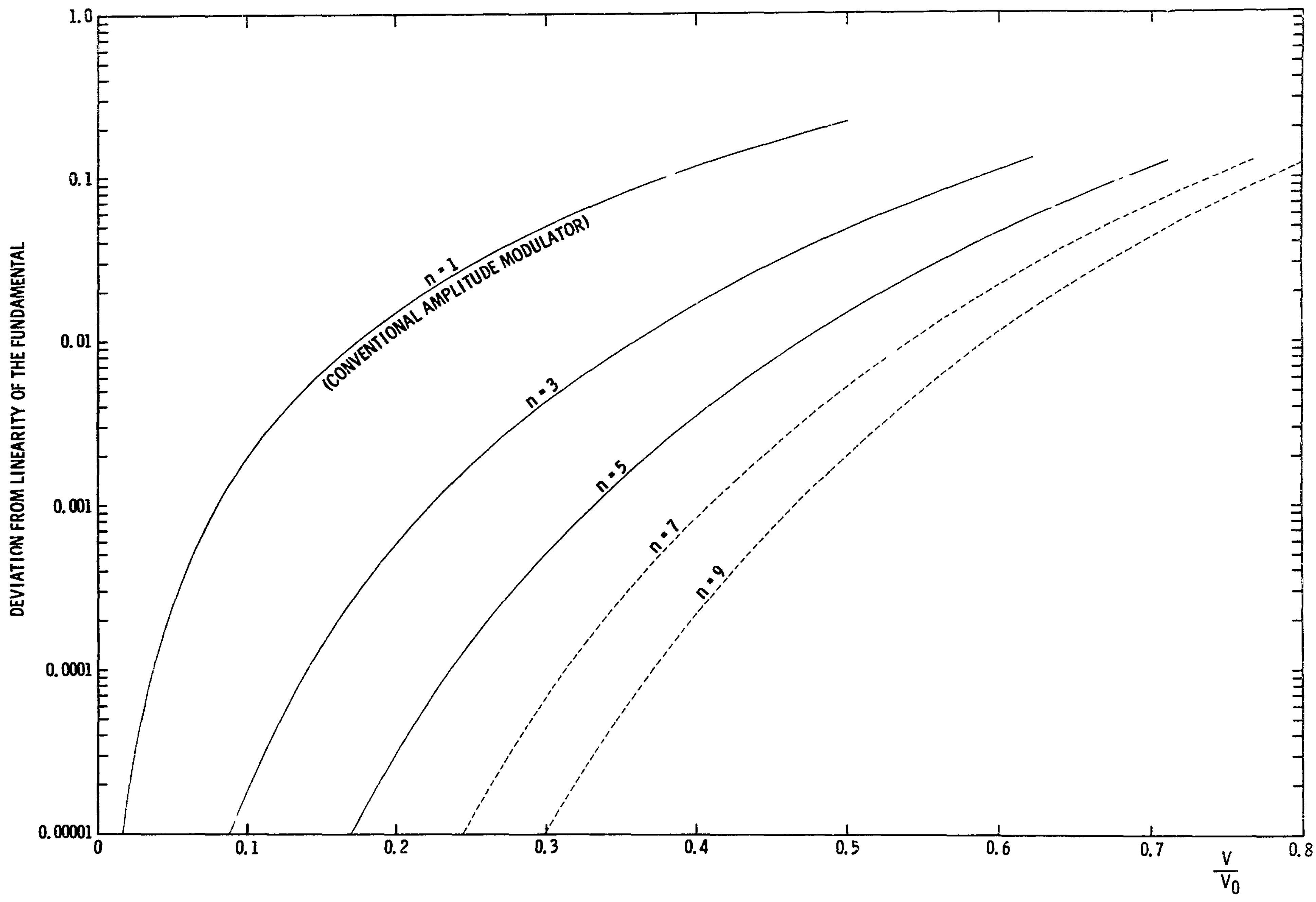
DEVIATION FROM LINEARITY OF THE FUNDAMENTAL
1.0
0.1
0.01
0.001
0.0001
0.00001
0
0.1
0.2
0.3
0.4
0.5
0.6
0.7
0.8
$\frac{V}{V_0}$
n = 1
(CONVENTIONAL AMPLITUDE MODULATOR)
n = 3
n = 5
n = 7
n = 9

Figure 16e

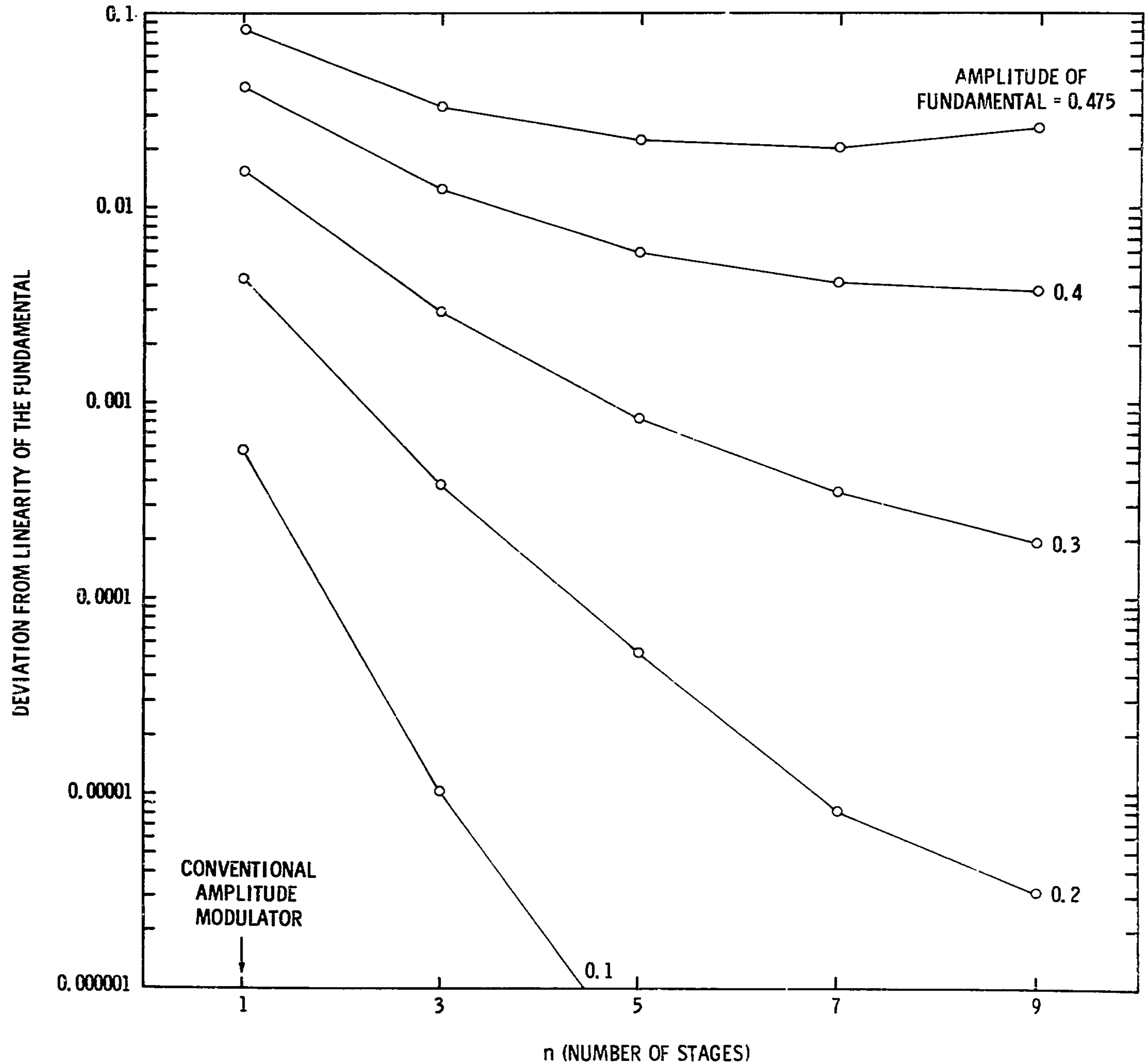
0.1
0.01
0.001
0.0001
0.00001
0.000001
DEVIATION FROM LINEARITY OF THE FUNDAMENTAL
AMPLITUDE OF
FUNDAMENTAL = 0.475
0.4
0.3
0.2
0.1
CONVENTIONAL
AMPLITUDE
MODULATOR
1
3
5
7
9
n (NUMBER OF STAGES)

Figure 17a

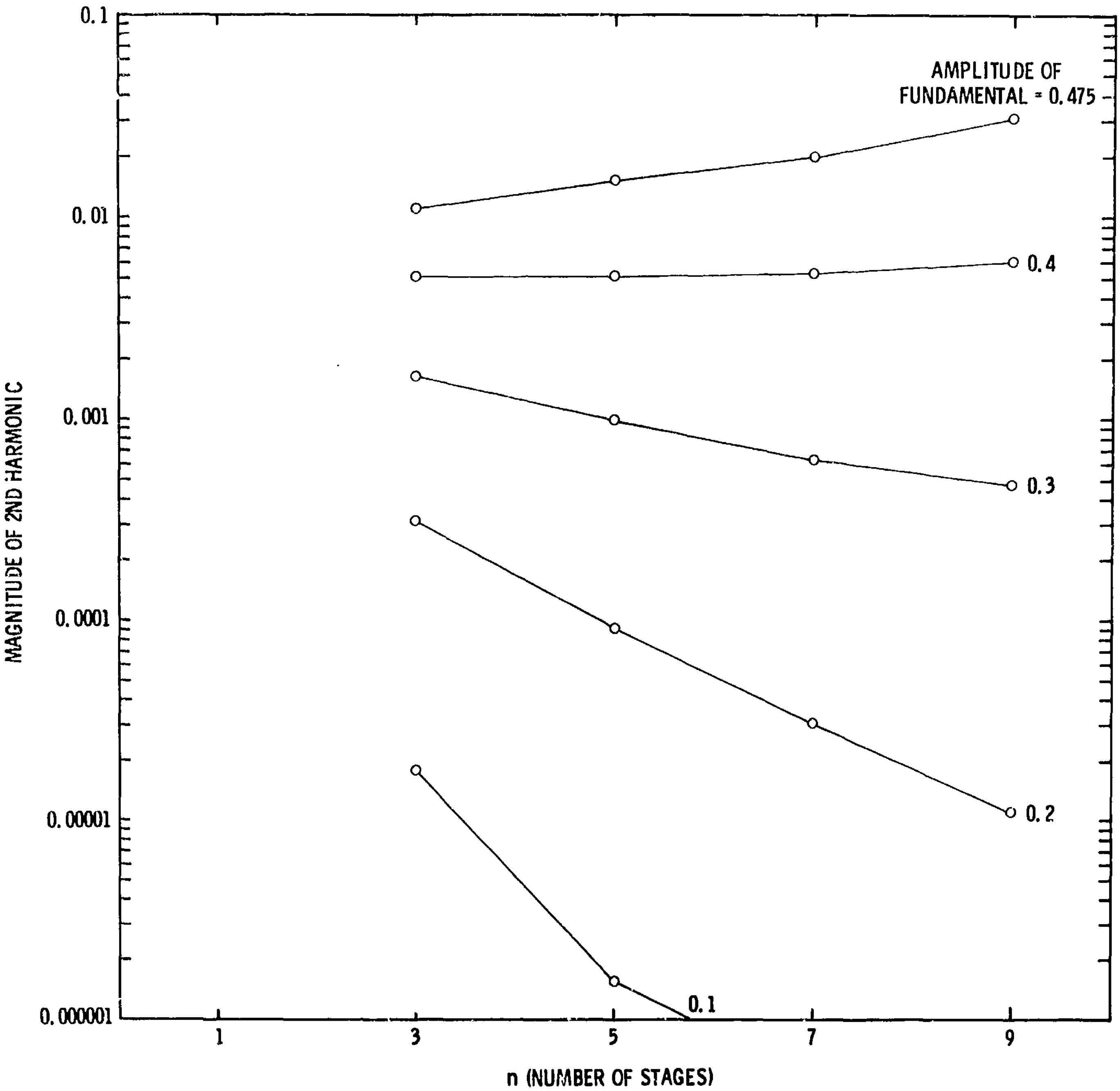

0.1
0.01
0.001
0.0001
0.00001
0.000001
MAGNITUDE OF 2ND HARMONIC
AMPLITUDE OF
FUNDAMENTAL = 0.475
0.4
0.3
0.2
0.1
1
3
5
7
9
n (NUMBER OF STAGES)

Figure 17b

For the square-law case, the maximally-linear approximation technique would have to be considered a qualified success. Fundamental distortion is uniformly reduced by increasing the number of stages, but second harmonic is present for $n = 3, 5, 7, 9, \ldots$ which is not present for $n = 1$. The modulator designs which correspond to the $K(v)$ of Eqs. (61) are listed in Table II for convenience.

V. SUMMARY AND CONCLUSIONS

A technique has been described which allows the synthesis of electro-optic amplitude modulators having arbitrary modulation characteristics. The technique is a direct analogy of the procedure of Ammann and Yarborough [26] for synthesizing naturally-birefringent networks. With the procedure of this paper, a voltage transfer function $K(v)$ of the form given in Eq. (3) can be realized by an electro-optic network of the form shown in Fig. 3. The synthesis procedure arranges standard components in a particular fashion to form a modulator having the required voltage transfer function.

The manner in which $K(v)$ is chosen is very important. If sufficient care is not taken in this choice, the performance of the synthesized modulator can easily be inferior to that obtained from the simple, conventional amplitude modulator of Fig. 1. Several techniques for choosing $K(v)$ were tried with varying degrees of success. The most satisfactory results were obtained when the C_i of $K(v)$ were chosen to directly optimize the modulator property (or properties) of greatest interest. This was done for two cases of interest: the design of a modulator for use with (a) an envelope detector, and (b) a square-law detector.

The modulator properties which were chosen (arbitrarily) for optimization in this paper were the following. The modulating signal v was assumed to be of the form, $v = V\cos \omega_m t$. The demodulated signal from the detector will in general contain a dc term, a fundamental, and harmonics. It was deemed desirable for the fundamental to be

	n=1	n=3	n=5	n=7	n=9
θ_1	45°00'	4°40'	0°31'	0°07'	0°02'
b_1 (rad)	1.57	2.95	2.89	2.94	2.99
θ_2		49°32'	5°10'	1°10'	0°19'
b_2 (rad)		4.52	2.80	2.86	2.93
θ_3		49°32'	38°21'	6°32'	1°50'
b_3 (rad)		6.09	4.57	2.73	2.84
θ_4			38°21'	37°41'	7°31'
b_4 (rad)			2.80	4.53	2.69
θ_5			5°10'	37°41'	36°51'
b_5 (rad)			6.04	2.73	4.50
θ_6				6°32'	36°51'
b_6 (rad)				2.86	2.69
θ_7				1°10'	7°31'
b_7 (rad)				6.08	2.84
θ_8					1°50'
b_8 (rad)					2.93
θ_9					0°19'
b_9 (rad)					6.13
θ_p	−45°00'	85°20'	89°29'	89°53'	89°58'
b_p (rad)	0	4.21	1.44	4.92	2.01

Table II

linearly proportional to V, and for the harmonics to be minimized. Hence modulator performance was measured by calculating the deviation from linearity of the fundamental and the amplitudes of the harmonics.

Best results were obtained for both the envelope and square-law detector cases by writing the fundamental and harmonic amplitudes as power series in V. The C_i were then chosen to eliminate as many nonlinear terms from the fundamental expression and as many low-order terms from the second harmonic expression as possible. The K(v) so derived do indeed give improved modulator performance (see Figs. 9, 10, 15, and 16); the modulator designs corresponding to these K(v) are tabulated in Tables I and II. However the improvement is, in some respects, less than might be hoped for. It is likely that still other approximation techniques will eventually be found which yield further improvement.

ACKNOWLEDGMENT

The authors are grateful to L. A. Drews, S. Barnard, B. Furst, and M. A. Wright for assistance with the computations.

FOOTNOTES

This work was supported by the National Aeronautics and Space Administration under Contract NAS8-20570.

1. To put it still more accurately, $\pi v/V_0$ plays the same role for the electro-optic cell that $\mathbf{a}\omega$ does for the birefringent crystal.

2. The linear characteristic may have any slope whatsoever, and hence there are an infinite number of possible ideal characteristics. We have chosen a characteristic with a slope of unity.

REFERENCES

[1] B. H. Billings, "The Electro-Optic Effect in Uniaxial Crystals of the Type XH_2PO_4. I. Theoretical," J. Opt. Soc. Am., vol. 39, pp. 797-801, October 1949; "The Electro-Optic Effect in Uniaxial Crystals of the Type XH_2PO_4. II. Experimental," J. Opt. Soc. Am., vol. 39, pp. 802-808, October 1949.

[2] F. Sterzer, D. J. Blattner, and S. F. Miniter, "Cuprous Chloride Light Modulators," J. Opt. Soc. Am., vol. 54, pp. 62-68, January 1964.

[3] J. E. Geusic, S. K. Kurtz, L. G. Van Uitert, and S. H. Wemple, "Electro-optic Properties of Some ABO_3 Perovskites in the Paraelectric Phase," Appl. Phys. Lett., vol. 4, pp. 141-143, April 15, 1964.

[4] S. M. Lee and S. M. Hauser, "Kerr Constant Evaluation of Organic Liquids and Solutions," Rev. Sci. Instr., vol. 35, pp. 1679-1681, December 1964.

[5] I. P. Kaminow, "Barium Titanate Light Phase Modulator," Appl. Phys. Lett., vol. 7, pp. 123-125, September 1, 1965; vol. 8, p. 54, January 15, 1966.

[6] C. J. Johnson, "Some Dielectric and Electro-optic Properties of $BaTi0_3$ Single Crystals," Appl. Phys. Lett., vol. 7, pp. 221-223, October 15, 1965.

[7] F. S. Chen, J. E. Geusic, S. K. Kurtz, J. G. Skinner, and S. H. Wemple, "Light Modulation and Beam Deflection with Potassium Tantalate-Niobate Crystals," J. Appl. Phys., vol. 37, pp. 388-398, January 1966.

[8] P. V. Lenzo, E. G. Spencer, and K. Nassau, "Electro-Optic Coefficients in Single-Domain Ferroelectric Lithium Niobate," J. Opt. Soc. Am., vol. 56, pp. 633-635, May 1966.

[9] I. P. Kaminow, "Microwave Modulation of the Electro-Optic Effect in KH_2PO_4," Phys. Rev. Lett., vol. 6, pp. 528-530, May 15, 1961.

[10] D. F. Holshouser, H. Von Foerster, and G. L. Clark, "Microwave Modulation of Light Using the Kerr Effect," J. Opt. Soc. Am., vol. 51, pp. 1360-1365, December 1961.

[11] R. H. Blumenthal, "Design of a Microwave-Frequency Light Modulator," Proc. IRE, vol. 50, pp. 452-456, April 1962.

[12] I. P. Kaminow, R. Kompfner, and W. H. Louisell, "Improvements in Light Modulators of the Traveling-Wave Type," IRE Trans. on Microwave Theory and Techniques, vol. MTT-10, pp. 311-313, September 1962.

[13] I. P. Kaminow and J. Liu, "Propagation Characteristics of Partially Loaded Two-Conductor Transmission Line for Broadband Light Modulators," Proc. IEEE, vol. 51, pp. 132-136, January 1963.

[14] W. W. Rigrod and I. P. Kaminow, "Wide-Band Microwave Light Modulation," Proc. IEEE, vol. 51, pp. 137-140, January 1963.

[15] M. DiDomenico, Jr. and L. K. Anderson, "Broadband Electro-Optic Traveling-Wave Light Modulators," Bell System Tech. J., vol. 42, pp. 2621-2678, November 1963.

[16] C. E. Enderby, "Wideband Optical Modulator," Proc. IEEE (Correspondence), vol. 52, pp. 981-982, August 1964.

[17] C. J. Peters, "Gigacycle-Bandwidth Coherent-Light Traveling-Wave Amplitude Modulator," Proc. IEEE, vol. 53, pp. 455-460, May 1965.

[18] J. E. Hopson, "Harmonic Structure of Modulated Light Beams," IEEE Trans. on Communication Systems, vol. CS-11, pp. 464-469, December 1963.

[19] G. Grau, "Verzerrungen bei der Amplitudenmodulation von Licht," Archiv der Elektrischen Übertragung, vol. 18, pp. 389-392, June 1964.

[20] H. G. Jerrard, "Optical Compensators for Measurement of Elliptical Polarization," J. Opt. Soc. Am., vol. 38, pp. 35-59, January 1948.

[21] S. E. Harris, E. O. Ammann, and I. C. Chang, "Optical Network Synthesis Using Birefringent Crystals. I. Synthesis of Lossless Networks of Equal-Length Crystals," J. Opt. Soc. Am., vol. 54, pp. 1267-1279, October 1964.

[22] E. O. Ammann and I. C. Chang, "Optical Network Synthesis Using Birefringent Crystals. II. Synthesis of Networks Containing One Crystal, Optical Compensator, and Polarizer per Stage," J. Opt. Soc. Am., vol. 55, pp. 835-841, July 1965.

[23] E. O. Ammann, "Optical Network Synthesis Using Birefringent Crystals. III. Some General Properties of Lossless Birefringent Networks," J. Opt. Soc. Am., vol. 56, pp. 943-951, July 1966.

[24] E. O. Ammann, "Optical Network Synthesis Using Birefringent Crystals. IV. Synthesis of Lossless Double-Pass Networks," J. Opt. Soc. Am., vol. 56, pp. 952-955, July 1966.

[25] E. O. Ammann, "Synthesis of Electro-Optic Shutters Having a Prescribed Transmission vs. Voltage Characteristic," J. Opt. Soc. Am., vol. 56, pp. 1081-1088, August 1966.

[26] E. O. Ammann and J. M. Yarborough, "Optical Network Synthesis Using Birefringent Crystals. V. Synthesis of Lossless Networks Containing Equal-Length Crystals and Compensators," J. Opt. Soc. Am., (to be published).

[27] See for example, T. S. Gray, "Applied Electronics," New York: John Wiley & Sons, Inc., 1956, p. 705.

[28] E. O. Ammann and J. M. Yarborough, "Optical Network Synthesis Using Birefringent Crystals. VI. Additional Techniques for the Synthesis of Lossless Double-Pass Networks," J. Opt. Soc. Am., (to be published).

CAPTIONS FOR FIGURES AND TABLES

Fig. 1 Model for conventional electro-optic amplitude modulators.

Fig. 2 Basic configuration for the birefringent network (4 stages) obtained from the synthesis procedure of Part I [21]. F and S denote the "fast" and "slow" axes of the birefringent crystals.

Fig. 3 Basic configuration of the birefringent network (4 stages) obtained from the synthesis procedure of Part V [26]; each stage contains a birefringent crystal and optical compensator. This also represents the basic configuration of the modulators obtained by the techniques of this paper; in this case each stage consists of an electro-optic cell and optical compensator.

Fig. 4 Naturally-birefringent crystal used as the basic "building block" of a birefringent network. This also represents an electro-optic cell used as the building block of an electro-optic network.

Fig. 5 Ideal voltage transfer function K(v) for an amplitude modulator which is followed by an envelope detector.

Fig. 6 Periodic ideal voltage transfer functions for an amplitude modulator having (a) n odd, and (b) n even.

Fig. 7 Fourier approximations to the ideal K(v) of Fig. 6a.

Fig. 8 Envelope detector output vs. V/V_0 when modulators having the K(v) of Fig. 7 are employed: (a) dc component of output; (b) amplitude of fundamental; (c) magnitude of second harmonic; (d) magnitude of third harmonic; and (e) deviation from linearity of fundamental.

Fig. 9 Envelope detector output vs. V/V_0 when modulators synthesized using the maximally-linear approximation are employed: (a) dc component of output; (b) amplitude of fundamental; (c) magnitude of second harmonic; (d) magnitude of third harmonic; and (e) deviation from linearity of fundamental. The magnitude of the second harmonic is zero for $n = 2, 4, 6, 8,$ and 10.

Fig. 10 Envelope detector output vs. n when modulators synthesized using the maximally-linear approximation are employed. Each curve represents a constant amplitude of the fundamental. Dotted lines connect points for which n is even while solid lines connect points for which n is odd. Shown are (a) deviation from linearity of fundamental, and (b) magnitude of second harmonic.

Fig. 11 K(v) obtained using the maximally-linear approximation (n odd, envelope detector)

Fig. 12 K(v) obtained using the maximally-linear approximation (n even, envelope detector)

Fig. 13 Ideal voltage transfer function K(v) for an amplitude modulator which is followed by a square-law detector.

Fig. 14 Periodic ideal voltage transfer function for an amplitude modulator having n odd.

Fig. 15 K(v) obtained using the maximally-linear approximation (n odd, square-law detector)

Fig. 16 Square-law detector output vs. V/V_0 when modulators having the K(v) of Fig. 15 are employed: (a) dc component of output; (b) amplitude of fundamental; (c) magnitude of second harmonic; (d) magnitude of third harmonic; and (e) deviation from linearity of fundamental. The magnitude of the second harmonic is zero for $n = 1$.

Fig. 17 Square-law detector output vs. n when modulators synthesized using the maximally-linear approximation are employed. Each curve represents a constant amplitude of the fundamental. Shown are (a) deviation from linearity of fundamental, and (b) magnitude of second harmonic. Dotted lines connect points for which n is even while solid lines connect points for which n is odd. For $n = 1$, the magnitude of the second harmonic is zero.

Appendix D

A COMPUTER PROGRAM FOR CALCULATING THE FOURIER SERIES COEFFICIENTS AN ARBITRARY IDEAL FUNCTION

A common method of choosing the C_i of Equation (2.1) is to make them the Fourier series coefficients of the ideal function. Since this calculation was repeated many times during the course of this work, a program was written so the coefficients could be calculated by computer. The computer language used in writing the program is FORTRAN (for a Control Data Corporation 3200 computer).

The program accomplishes the following things. For a given ideal function, the C_i are calculated for the cases n = 1, 2, 3, ... 20. In each case, the C_i are normalized so that the maximum value of $|C(\omega)|^2$ is unity. In addition, for each case the computer plots the magnitude of $C(\omega)$ over one period. It should be mentioned that the program can handle asymmetric as well as symmetric ideal functions; these result in complex values for the C_i. The only restriction is that the ideal function must be real.

The program is given below.

```
      PROGRAM FOURIER
      EXTERNAL FUNCT
      COMMON F(121)
      COMMON IORD,IFUNCT
      DIMENSION G(121),A(15),B(15),GRAND(121),X(121),SUM(121)
C     A AND B ARE FOURIER COEFFICIENTS
C     F(X)=A0+SUM(A(K)*COS(KX)+B(K)*SIN(KX)), K=1,KF FOR KF=1,N
C
  100 FORMAT(1H0,2HC(,I2,2H)=,F12.5,2X,F12.5,10X,F12.5)
  102 FORMAT(1H1)
  103 FORMAT(1H ,5(F8.5,2X,F12.5,4X))
  104 FORMAT(1H0)
  105 FORMAT(F14.7)
      N=10
      PI=3.1415927
      READ 105, EPS
      IORD=0
      IFUNCT=1
      DO 1 K=1,121
      X(K)=(K-61)*PI/60.
    1 F(K)=FUNCT(X(K))
      PRINT 103, (X(J),F(J),J=1,5)
      DO 2 I=1,23
      I5=I*5
    2 PRINT 103, X(I5+1),F(I5+1),X(I5+2),F(I5+2),X(I5+3),F(I5+3),X(I5+4
     1),F(I5+4),X(I5+5),F(I5+5)
      PRINT 103, X(121),F(121)
      CALL PLOT(0)
      ANS=SIMPSON(FUNCT,-PI,PI,EPS)
      A0=ANS/(2.*PI)
      PRINT 102
      K=0
      PRINT 100, K,A0
C     CALCULATE A(K), B(K), K=1,N
      DO 30 K=1,N
      IORD=K
      IFUNCT=1
      ANS=SIMPSON(FUNCT,-PI,PI,EPS)
      A(K)=ANS/PI
      IFUNCT=2
      ANS=SIMPSON(FUNCT,-PI,PI,EPS)
   30 B(K)=ANS/PI
C     PRINT A(K),B(K)
      DO 40 K=1,N
      C1=A(K)/2.
      C2=-B(K)/2.
   40 PRINT 100, K,C1,C2
C     FORM ARGUMENTS AND INITIALIZE SUMS
      DO 50 K=1,121
   50 SUM(K)=A0+A(1)*COS(X(K))+B(1)*SIN(X(K))
      DO 80 K=1,N
      PRINT 102
      IF(K.EQ.1)61,51
   51 DO 60 J=1,121
   60 SUM(J)=SUM(J)+A(K)*COS(K*X(J))+B(K)*SIN(K*X(J))
   61 SUMMAX=SUM(1)
```

```
      DO 62 J=2,121
   62 SUMMAX=AMAX1(SUM(J),SUMMAX)
      DO 63 J=1,121
   63 F(J)=SUM(J)/SUMMAX
      PRINT 103, (X(J),F(J),J=1,5)
      DO 70 I=1,23
      I5=I*5
   70 PRINT 103, X(I5+1),F(I5+1),X(I5+2),F(I5+2),X(I5+3),F(I5+3),X(I5+4
     1),F(I5+4),X(I5+5),F(I5+5)
      PRINT 103, X(121),F(121)
      PRINT 104
      DO 74 I=1,K
      I1=K-I+1
      I2=I-1
      C1=A(I1)/(2.*SUMMAX)
      C2=-B(I1)/(2.*SUMMAX)
   74 PRINT 100, I2,C1,C2
      C1=A0/SUMMAX
      PRINT 100, K,C1
      DO 75 I=1,K
      C1=A(I)/(2.*SUMMAX)
      C2= B(I)/(2.*SUMMAX)
      I1=K+I
   75 PRINT 100, I1,C1,C2
      CALL PLOT(K)
   80 CONTINUE
      STOP
      END
```

```
      FUNCTION FUNCT(X)
      COMMON G(121)
      COMMON N,IFUNCT
      PI=3.1415927
      TPI=2./P
      IF(X.LT.(-PI))100,1
    1 IF(X.LT.(-3.*PI/4.))10,20
   10 F=-SQRT(2.5+TPI*X)
      GO TO 91
   20 IF(X.LT.(-PI/4.))30,40
   30 F=-SQRT(-.5-TPI*X)
      GO TO 91
   40 IF(X.LT.PI/4.)50,60
   50 F=SQRT(.5+TPI*X)
      GO TO 91
   60 IF(X.LT.(3.*PI/4.))70,80
   70 F=SQRT(1.5-TPI*X)
      GO TO 91
   80 IF(X.LE.PI)90,100
   90 F=-SQRT(-1.5+TPI*X)
   91 IF(IFUNCT.EQ.1)92,93
   92 FUNCT=F*COS(N*X)
      RETURN
   93 IF(IFUNCT.EQ.2)94,95
   94 FUNCT=F*SIN(N*X)
      RETURN
   95 PRINT 96,IFUNCT
   96 FORMAT(1H0,7HIFUNCT=,I3)
      CALL ABNORMAL
  100 PRINT 101, X
  101 FORMAT(1H0,2HX=,F14.7)
      CALL ABNORMAL
      END
```

```
      FUNCTION SIMPSON(F,A1,B,E)
      EXTERNAL F
      DIMENSION DX(30),EPSP(30),X2(30),X3(30),F2(30),F3(30),F4(30)
      DIMENSION FMP(30),FBP(30),EST2(30),EST3(30),PVAL(30,3)
      DIMENSION RTRN(30)
      INTEGER RTRN
      A=A1
      EPS=E
      LVL=0
      MLVL=0
      ABSAR=0.0
      EST=0.0
      DA=B-A
      FA=F(A)
      FM= 4.0*F((A+B)/2.0)
      FB=F(B)
   10 LVL=LVL+1
      MLVL=LVL
      DX(LVL)=DA/3.0
      SX=DX(LVL)/6.0
      F1=4.0*F(A+DX(LVL)/2.0)
      X2(LVL)=A+DX(LVL)
      F2(LVL)=F(X2(LVL))
      X3(LVL)=X2(LVL)+DX(LVL)
      F3(LVL)=F(X3(LVL))
      EPSP(LVL)=EPS
      F4(LVL)=4.0*F(X3(LVL)+DX(LVL)/2.0)
      FMP(LVL)=FM
      EST1=(FA+F1+F2(LVL))*SX
      FBP(LVL)=FB
      EST2(LVL)=(F2(LVL)+F3(LVL)+FM)*SX
      EST3(LVL)=(F3(LVL)+F4(LVL)+FB)*SX
      SUM=EST1+EST2(LVL)+EST3(LVL)
      ABSAR=ABSAR-ABS(EST)+ABS(EST1)+ABS(EST2(LVL))+ABS(EST3(LVL))
      IF(ABS(EST-SUM).LE. EPSP(LVL)*ABSAR)20,15
   15 IF(LVL .LT. 30)30,21
   20 IF(MLVL.LT.4)15,21
   21 LVL=LVL-1
      I=RTRN(LVL)
      PVAL(LVL,I)=SUM
      GO TO (40,50,60),I
   30 RTRN(LVL)=1
      DA=DX(LVL)
      FM=F1
      FB=F2(LVL)
      EPS=EPSP(LVL)/1.7
      EST=EST1
      GO TO 10
   40 RTRN(LVL)=2
      DA= DX(LVL)
      FA=F2(LVL)
      FM=FMP(LVL)
      FB=F3(LVL)
      EPS=EPSP(LVL)/1.7
      EST=EST2(LVL)
      A=X2(LVL)
```

```
      GO TO 10
   50 RTRN(LVL)=3
      DA=DX(LVL)
      FA=F3(LVL)
      FM=F4(LVL)
      FB=FBP(LVL)
      EPS=EPSP(LVL)/1.7
      EST=EST3(LVL)
      A=X3(LVL)
      GO TO 10
   60 SUM=PVAL(LVL,1)+PVAL(LVL,2)+PVAL(LVL,3)
      IF(LVL.GT. 1)20,70
   70 SIMPSON=SUM
      RETURN
      END
```

```
      SUBROUTINE PLOT (N)
      COMMON  F(121)
      DIMENSION  LINE (121)
      CONST=1.09
      IBLNK=60606060B
      IAST=54606060B
      II=31606060B
      IDASH=40606060B
      IPLUS=20606060B
      WRITE (61,10) N
   10 FORMAT (7H1 PLOT ,I2)
      DO 20 I=1,121
      LINE(I)=IBLNK
   20 CONTINUE
      LINE(61)=II
      LINE(58)=01606060B
      LINE(59)=33606060B
      LINE(60)=01606060B
   21 DO  23 I=1,121
      IF(F(I).GT.1.11)22,23
   22 F(I)=-99.9
   23 CONTINUE
   25 DO 40 I=1,121
      IF(F(I).GT.CONST)26,40
   26 LINE(I)=IAST
      F(I)=-99.9
   40 CONTINUE
      WRITE(61,50) (LINE(I),I=1,121)
   50 FORMAT(1H ,5X,121A1)
      CONST=CONST-.02
      IF(CONST.LE.-0.01)51,60
   51 IF(CONST.LT.-.02)90,52
   52 DO 53 I=1,121
      LINE(I)=IDASH
   53 CONTINUE
      DO 54 I=1,121,15
      LINE(I)=IPLUS
   54 CONTINUE
      GO TO 25
   60 DO 61 I=1,121
      LINE(I)=IBLNK
   61 CONTINUE
      LINE(61)=II
      IF(CONST.LT..995.AND.CONST.GT..985)98,99
   98 LINE(58)=01606060B
      LINE(59)=33606060B
      LINE(60)=00606060B
      GO TO 25
   99 IF(CONST.LT..895.AND.CONST.GT..885)62,63
   62 LINE(59)=33606060B
      LINE(60)=11606060B
      GO TO 25
   63 IF(CONST.LT..795.AND.CONST.GT..785)64,65
   64 LINE(59)=33606060B
      LINE(60)=10606060B
      GO TO 25
```

```
 65  IF(CONST.LT..695.AND.CONST.GT..685)66,67
 66  LINE(59)=33606060B
     LINE(60)=07606060B
     GO TO 25
 67  IF(CONST.LT..595.AND.CONST.GT..585)68,69
 68  LINE(59)=33606060B
     LINE(60)=06606060B
     GO TO 25
 69  IF(CONST.LT..495.AND.CONST.GT..485)70,71
 70  LINE(59)=33606060B
     LINE(60)=05606060B
     GO TO 25
 71  IF(CONST.LT..395.AND.CONST.GT..385)72,73
 72  LINE(59)=33606060B
     LINE(60)=04606060B
     GO TO 25
 73  IF(CONST.LT..295.AND.CONST.GT..285)74,75
 74  LINE(59)=33606060B
     LINE(60)=03606060B
     GO TO 25
 75  IF(CONST.LT..195.AND.CONST.GT..185)76,77
 76  LINE(59)=33606060B
     LINE(60)=02606060B
     GO TO 25
 77  IF(CONST.LT..095.AND.CONST.GT..085)78,25
 78  LINE(59)=33606060B
     LINE(60)=01606060B
     GO TO 25
 90  CONTINUE
     WRITE(61,100)
100  FORMAT(1H ,3X,4H-180,11X,4H-135,11X,3H-90,12X,3H-45,14X,1H0,
    X13X,2H45,13X,2H90,13X,3H135,12X,3H180)
     WRITE(61,101)
101  FORMAT(1H1)
     WRITE (61,100)
     DO 120 I=1,121
     IF(F(I).LT.-1.11)110,120
110  F(I)=-99.9
120  CONTINUE
     DO 130 I=1,121
     LINE(I)=IDASH
130  CONTINUE
     DO 140 I=1,121,15
     LINE(I)=IPLUS
140  CONTINUE
     WRITE(61,50) (LINE(I),I=1,121)
     DO 150 I=1,121
     LINE(I)=IBLNK
150  CONTINUE
     LINE(61)=II
155  DO 180 I=1,121
     IF(F(I).GT.CONST)170,180
170  LINE(I)=IAST
     F(I)=-99.9
180  CONTINUE
     WRITE(61,50) (LINE(I),I=1,121)
```

```
      CONST=CONST-.02
      DO 190 I=1,121
      LINE(I)=IBLNK
  190 CONTINUE
      LINE(61)=II
  200 IF(CONST.LT.-.105.AND.CONST.GT.-.115)210,211
  210 LINE(60)=01606060B
      LINE(59)=33606060B
      LINE(58)=IDASH
      GO TO 155
  211 IF(CONST.LT.-.205.AND.CONST.GT.-.215)212,213
  212 LINE(60)=02606060B
      LINE(59)=33606060B
      LINE(58)=IDASH
      GO TO 155
  213 IF(CONST.LT.-.305.AND.CONST.GT.-.315)214,215
  214 LINE(60)=03606060B
      LINE(59)=33606060B
      LINE(58)=IDASH
      GO TO 155
  215 IF(CONST.LT.-.405.AND.CONST.GT.-.415)216,217
  216 LINE(60)=04606060B
      LINE(59)=33606060B
      LINE(58)=IDASH
      GO TO 155
  217 IF(CONST.LT.-.505.AND.CONST.GT.-.515)218,219
  218 LINE(60)=05606060B
      LINE(59)=33606060B
      LINE(58)=IDASH
      GO TO 155
  219 IF(CONST.LT.-.605.AND.CONST.GT.-.615)220,221
  220 LINE(60)=06606060B
      LINE(59)=33606060B
      LINE(58)=IDASH
      GO TO 155
  221 IF(CONST.LT.-.705.AND.CONST.GT.-.715)222,223
  222 LINE(60)=07606060B
      LINE(59)=33606060B
      LINE(58)=IDASH
      GO TO 155
  223 IF(CONST.LT.-.805.AND.CONST.GT.-.815)224,225
  224 LINE(60)=10606060B
      LINE(59)=33606060B
      LINE(58)=IDASH
      GO TO 155
  225 IF(CONST.LT.-.905.AND.CONST.GT.-.915)226,227
  226 LINE(60)=11606060B
      LINE(59)=33606060B
      LINE(58)=IDASH
      GO TO 155
  227 IF(CONST.LT.-1.005.AND.CONST.GT.-1.015)228,229
  228 LINE(60)=00606060B
      LINE(59)=33606060B
      LINE(58)=01606060B
      LINE(57)=IDASH
      GO TO 155
```

```
229 IF(CONST.LT.-1.105.AND.CONST.GT.-1.115)230,231
230 LINE(60)=01606060B
    LINE(59)=33606060B
    LINE(58)=01606060B
    LINE(57)=IDASH
    GO TO 155
231 IF(CONST.LE.-1.13)132,155
132 RETURN
    END
```

Appendix E

A COMPUTER PROGRAM FOR THE SYNTHESIS OF LOSSLESS NETWORKS CONTAINING EQUAL-LENGTH CRYSTALS AND COMPENSATORS

This Appendix gives a computer program written for performing the synthesis procedure of Appendix A. The computer language used is FORTRAN (for a Control Data Corporation 3200 computer). The desired C_i are the inputs to the program. The computer calculates the rotation angle θ_i and compensator delay b_i for each stage of the network. Having calculated the θ_i and b_i, the computer then calculates the $C(\omega)$ which is obtained from them as a check.

The program is given below.

```
      PROGRAM SYNTHES
C
C     PROGRAM FINDS THE RELATIVE CRYSTAL ANGLES AND RETARDATIONS
C     FOR AN OPTICAL FILTER WITH N CRYSTALS EACH FOLLOWED BY
C     AN OPTICAL COMPENSATOR
C
      TYPE COMPLEX (4) CMPLX,CONJ
      TYPE COMPLEX (4) C,F,A,R,D,RR,RI
      TYPE COMPLEX (4) CTMP
      INTEGER ABRTN
      REAL IO
      COMMON N,C(17),IO,F(17),A(33),R(32),D(17)
      DIMENSION RR(16),RI(16)
C
C     C IS ARRAY OF GIVEN COMPLEX COEFFICIENTS
C     IO IS MAXIMUM VALUE OF FUNCTION
C     A IS ARRAY OF X POLYNOMIAL COEFFICIENTS
C
C     FORMAT STATEMENTS
  101 FORMAT(1H0,10HC(I), I=0,,I3)
  102 FORMAT(1H0,3HIO=,F14.7)
  103 FORMAT(1H0,10HA(I), I=1,,I3)
  104 FORMAT(1H0,9HROOTS ARE)
  105 FORMAT(1H0,10HD(I), I=0,,I3)
  106 FORMAT(1H0,14HNO INVERSE FOR,I3,8H TH ROOT)
  107 FORMAT(1H0,22HCONJUGATE INVERSES ARE)
  108 FORMAT(1H0,21HNORMALIZED D(I), I=0,,I3)
C
      EPS=1.0E-02
C
C     GET COEFFICIENTS OF FILTER TRANSFER FUNCTION
    1 CALL READC
      IF(N.EQ.0)41,2
    2 N1=N+1
C
C     PRINT C ARRAY
C
      PRINT 101, N
      CALL PRNTC(N1,C,2)
      PRINT 102, IO
C
C     COMPUTE F(I)
C
      DO 10 I=1,N1
      F(I)=CMPLX(0.,0.)
      I1=I-1
      NJ=N1-I1
      DO 5 J=1,NJ
      JI=I1+J
    5 F(I)=F(I)+C(J)*CONJ(C(JI))
   10 CONTINUE
C
C     COMPUTE A(I)
C
      M=2*N
      M1=M+1
```

```
      DO 20 I=1,N
      I1=N1-I+1
      A(I)=-CONJ(F(I1))
      NI=NI+1
   20 A(NI)=-F(I+1)
      A(N1)=I0*I0-F(1)
      A0=CREAL(A(N1))
C
C     PRINT A ARRAY
C
      PRINT 103, M1
      CALL PRNTC(M1,A,2)
C
C     FIND ROOTS
C
      CALL POLYROOT(M,A,1.0E-05,R,ABRTN)
      IF(ABRTN.EQ.0)30,40
C     FORM AND FIND CONJUGATE INVERSES
   30 J=1
      DO 35 I=1,M
      TMP=CNORM(R(I))**2
      IF(TMP.EQ.0.)35,31
   31 RR(J)=R(I)
      RI(J)=1./CONJ(R(I))
      I1=I+1
      DO 33 K=I,M
      CREJ=CREAL(RI(J))
      CREK=CREAL(R(K))
      CIMJ=CIMAG(RI(J))
      CIMK=CIMAG(R(K))
      IF(CREJ.EQ.0.0)32,3223
 3223 IF(ABS((CREJ-CREK)/CREJ).LE.EPS.OR.ABS(CREJ-CREK).LE.EPS)32,33
   32 IF(CIMJ.EQ.0.0)34,3425
 3425 IF(ABS((CIMJ-CIMK)/CIMJ).LE.EPS.OR.ABS(CIMJ-CIMK).LE.EPS)34,33
   33 CONTINUE
      PRINT 106, J
      DO 500 I=1,M
      P=CREAL(R(I))
      Q=CIMAG(R(I))
      CTMP=1./CONJ(R(I))
      X=CREAL(CTMP)
      Y=CIMAG(CTMP)
  500 PRINT 501, P,Q,X,Y
  501 FORMAT(1H0,2(E14.7,2X,E14.7,5X))
      GO TO 40
   34 R(K)=CMPLX(0.,0.)
      R(I)=CMPLX(0.,0.)
      J=J+1
   35 CONTINUE
C
C     PRINT ROOTS
C
      PRINT 104
      CALL PRNTC(N,RR,1)
      PRINT 107
      CALL PRNTC(N,RI,1)
```

```
C
C     COMPUTE COEFFICIENTS USING FIRST N ROOTS
C
      CALL COEFF(N,RR,D)
C
C     PRINT D ARRAY
C
      PRINT 105, N
      CALL PRNTC(N1,D,2)
C
C     NORMALIZE COEFFICIENTS
C
      SUM=0.
      DO 36 I=1,N1
   36 SUM=SUM+CNORM(D(I))**2
      Q=SQRT(A0/SUM)
      DO 37 I=1,N1
   37 D(I)=D(I)*Q
C
C     PRINT NORMALIZED D ARRAY
C
      PRINT 108, N
      CALL PRNTC(N1,D,2)
C
C     COMPUTE ANGLES AND PHASE SHIFTS USING FIRST N ROOTS
C
      CALL ANGLES
   40 CONTINUE
      GO TO 1
   41 CONTINUE
      STOP
      END
```

```
      SUBROUTINE READC
      TYPE COMPLEX (4) CMPLX,CONJ
      TYPE COMPLEX (4) C,F,A,R,D
      COMMON N,C(17),IO,F(17),A(33),R(32),D(17)
      REAL IO
      DIMENSION I(40)
      DIMENSION P(2,17)
C
C     READ COEFFICIENTS SYMBOLICALLY AND PRINT
C
      READ 1, M
    1 FORMAT((8I10))
C     M IS NUMBER OF WORDS
      IF(M.EQ.0)7,10
   10 READ 2, (I(J), J=1,M)
    2 FORMAT(20A4)
      PRINT 3
    3 FORMAT(1H1,16HCOEFFICIENTS ARE)
      PRINT 4, (I(J), J=1,M)
    4 FORMAT(1H0,32A4)
C
C     DEFINE COEFFICIENTS
C
      READ 1, N
C
C     N IS NUMBER OF CRYSTALS
C
C     READ COEFFICIENTS
      N1=N+1
      READ 5, (P(1,J),P(2,J), J=1,N1)
    5 FORMAT((4E20.10))
      DO 6 J=1,N1
    6 C(J)=CMPLX(P(1,J),P(2,J))
      READ 5, IO
      RETURN
    7 N=0
      RETURN
      END
```

```
      SUBROUTINE PRNTC(N,P,M)
      DIMENSION P(2,33)
      GO TO (1,2), M
    1 PRINT 101, (P(1,I),P(2,I), I=1,N)
  101 FORMAT(1H0,2(E13.6,2X,E13.6,5X))
      RETURN
    2 PRINT 102, (P(1,I),P(2,I), I=1,N)
  102 FORMAT(1H0,4(E13.6,2X,E13.6,4X)/)
      RETURN
      END
```

```
FUNCTION CONJ(C)
TYPE COMPLEX (4) CMPLX,CONJ
TYPE COMPLEX (4) C
CONJ=CMPLX(CREAL(C),-CIMAG(C))
RETURN
END
```

```
      SUBROUTINE POLYROOT(M,C,EPS,R,ABRTN)
C     PROGRAM FINDS ROOTS OF POLYNOMIAL WITH COMPLEX COEFFICIENTS C(I)
C     AND WITH DEGREE M LEQ 32
C     M IS DEGREE OF POLYNOMIAL
C     C(I) IS LIST OF COEFFICIENTS
C     C MUST BE DECLARED COMPLEX
C     C(1) IS COEFFICIENT OF HIGH-ORDER TERM
C     EPS IS DESIRED RELATIVE ERROR IN ROOTS
C     R IS LIST OF REAL AND COMPLEX ROOTS, MUST BE DECLARED COMPLEX
C     ABRTN IS ABNORMAL RETURN FLAG, =1 FOR NO CONVERGENCE
      TYPE COMPLEX (4) ROOT,R,C,F,GUESS,CONJ
      INTEGER ABRTN
      DIMENSION C(33),R(32)
      J=1
      N=M
      N1=N+1
    5 CALL FINDROOT(N,C,EPS,ROOT,ABRTN)
      IF(ABRTN.EQ.0)10,100
   10 TEST=CIMAG(ROOT)
      IF(TEST.EQ.0.)20,50
C     REAL ROOT
   20 N=N-1
      N1=N+1
      R(J)=ROOT
      J=J+1
      DO 30 I=2,N1
   30 C(I)=C(I)+ROOT*C(I-1)
      IF(N.EQ.0)100,40
   40 IF(N.EQ.1)80,5
C     COMPLEX ROOT
   50 CALL FVAL(N,C,ROOT,F)
      F1=CNORM(F)
      R(J)=ROOT
      J=J+1
      N=N-1
      N1=N+1
      DO 51 I=2,N1
   51 C(I)=C(I)+ROOT*C(I-1)
      GUESS=CONJ(ROOT)
      CALL FVAL(N,C,GUESS,F)
      F2=CNORM(F)
      IF(F2.LE.F1)52,40
   52 ROOT=GUESS
      GO TO 20
C     LAST LINEAR FACTOR
   80 R(J)=-C(2)/C(1)
  100 CONTINUE
      RETURN
      END
```

```
      SUBROUTINE FINDROOT(N,C,EPS,ROOT,ABRTN)
C     S/R FINDS ROOT OF POLYNOMIAL USING TECHNIQUE BASED ON
C     D-ALEMBERT-S LEMMA
      TYPE COMPLEX (4) GUESS,POINT,F,ROOT,CMPLX,DFLR,DFLI,C
      INTEGER ABRTN
      DIMENSION POINT(4),FN(5),C(33)
C     INITIALIZE
      ABRTN=0
      GUESS=CMPLX(.1,.1)
C     GUESS IS CENTER POINT OF SQUARE WITH VERTICES POINT(I)
C     EVALUATE POLYNOMIAL AT GUESS
      CALL EVAL(N,C,GUESS,F)
      FN(1)=CNORM(F)
      DFLR=CMPLX(.5,0.)
      DFLI=CMPLX(0.,.5)
      I1=0
      I2=0
C     I1 INCREMENTS WHEN CENTER POINT IS MOVED, STEP SIZE REMAINS CONSTANT
C     I2 INCREMENTS WHEN STEP SIZE IS DECREASED, CENTER POINT REMAINS SAME
C
C     HAVE THERE BEEN FIVE ATTEMPTS WITH PRESENT STEP SIZE
C
   10 IF(I1.LT.5)20,30
C     NO, KEEP TRYING
   20 I1=I1+1
      IF(I1.LT.50)50,131
C
C     YES, HAS STEP SIZE EVER BEEN DECREASED-IF YES, KEEP ON TRYING
   30 IF(I2.GT.0)20,40
C
C     NO, INCREMENT STEP SIZE AND START AGAIN
   40 I1=1
      DFLR=8.*DFLR
      DFLI=8.*DFLI
C
C     COMPUTE POINTS
C
   50 POINT(1)=GUESS+DFLR
      POINT(2)=GUESS-DFLR
      POINT(3)=GUESS+DFLI
      POINT(4)=GUESS-DFLI
C
C     EVALUATE POLYNOMIAL AT POINT(I)
C
      DO 60 I=2,5
      CALL EVAL(N,C,POINT(I-1),F)
   60 FN(I)=CNORM(F)
      IF(I2.GT.10)101,70
C
C     ARE VALUES OF POLYNOMIAL ALL SMALL
C
   70 DO 80 I=1,5
      IF(FN(I).LE.10.)80,81
   80 CONTINUE
C     YES
      GO TO 101
```

```
C
C      NO, ARE VALUES OF POLYNOMIAL ALL CLOSE
C
   81 DO 100 I=1,5
      DO 90 J=1,5
      IF(ABS(FN(I)-FN(J)).LE.1.E-03)90,101
   90 CONTINUE
  100 CONTINUE
C
C      YES, HAS STEP SIZE EVER BEEN DECREASED
C      IF NOT, INCREMENT STEP SIZE
      IF(I2.GT.0)101,40
C      OTHERWISE, KEEP ON GOING
C      NO, IS GUESS A ROOT
C
  101 IF(FN(1).LE.1.E-10)102,103
C      YES
  102 ROOT=GUESS
      RETURN
C
C      NO,IS ANY POINT A ROOT
  103 DO 110 I=2,5
      IF(FN(I).LE.1.E-10)111,110
  110 CONTINUE
      GO TO 112
C      YES
  111 ROOT=POINT(I-1)
      RETURN
C
C      NO, COMPARE CENTER POINT WITH VERTICES
  112 DO 115 I=2,5
      IF(FN(1).LT.FN(I))115,123
  115 CONTINUE
C
C      ROOT LIES WITHIN PRESENT SQUARE, DECREASE STEP SIZE
      DELR=DELR/2.
      DELI=DELI/2.
C      IS STEP SIZE TOO SMALL
      A=CREAL(GUESS)
      IF(A.EQ.0.)116,117
  116 IF(CREAL(DELR).LE.EPS)118,121
  117 IF(ABS(CREAL(DELR)/A).LE.EPS)118,121
  118 A=CIMAG(GUESS)
      IF(A.EQ.0.)119,120
  119 IF(CREAL(DELR).LE.EPS)102,121
  120 IF(ABS(CREAL(DELR)/A).LE.EPS)102,121
C      NO, HAVE THERE BEEN TOO MANY ITERATIONS
  121 IF(I2.GT.50)131,122
C      NO
  122 I2=I2+1
      GO TO 50
C
C      ROOT LIES OUTSIDE PRESENT SQUARE, FIND MINIMUM POINT
C      FOR CENTER OF NEW SQUARE
  123 TEST=FN(2)
      J=1
```

```
      DO 130 I=3,5
      IF(TEST.LE.FN(I))130,124
  124 TEST=FN(I)
      J=I-1
  130 CONTINUE
      GUESS=POINT(J)
      FN(1)=FN(J+1)
      GO TO 10
C     YES, SET ABNORMAL RETURN
  131 ABRTN=1
      PRINT 132
  132 FORMAT(1H0,14HNO CONVERGENCE)
      ROOT=GUESS
      RETURN
      END
```

```
      SUBROUTINE EVAL(N,C,GUESS,F)
      TYPE COMPLEX(4) GUESS,F,C
      DIMENSION C(33)
      N1=N+1
      F=C(1)*GUESS+C(2)
      DO 10 I=3,N1
   10 F=F*GUESS+C(I)
      RETURN
      END
```

```
      SUBROUTINE COFFF(X,Y,M,A1,B1)
C     X, Y ARE REAL AND IMAGINARY PARTS OF THE ROOTS
C     M IS DEGREE OF POLYNOMIAL
C     A1, B1 ARE RESULTING COEFFICIENTS, REAL AND IMAGINARY PARTS,
C     BEGINNING WITH HIGH-ORDER TERM
      DIMENSION A1(25),B1(25),A2(25),B2(25),X(24),Y(24)
      M1=M+1
      A1(M1)=1.
      B1(M1)=0.
      A1(1)=X(1)*X(2)-Y(1)*Y(2)
      B1(1)=X(1)*Y(2)+X(2)*Y(1)
      A1(2)=-(X(1)+X(2))
      B1(2)=-(Y(1)+Y(2))
      IF(2-M)5,4,4
    5 DO 3 I=3, M
      A2(1)=-X(I)*A1(1)+Y(I)*B1(1)
      B2(1)=-X(I)*B1(1)-Y(I)*A1(1)
      L=I-1
      DO 1 J=2, L
      A2(J)=A1(J-1)-X(I)*A1(J)+Y(I)*B1(J)
    1 B2(J)=B1(J-1)-Y(I)*A1(J)-X(I)*B1(J)
      A2(I)=A1(I-1)-X(I)
      B2(I)=B1(I-1)-Y(I)
      DO 2 K=1, I
      A1(K)=A2(K)
    2 B1(K)=B2(K)
    3 CONTINUE
    4 DO 6 K=1,M1
      A2(K)=A1(K)
    6 B2(K)=B1(K)
      DO 7 K=1,M1
      J=M1+1-K
      A1(K)=A2(J)
    7 B1(K)=B2(J)
      RETURN
      END
```

```
      SUBROUTINE ANGLES
      COMMON N,C(17),IO,F(17),A(33),R(32),D(17)
      TYPE COMPLEX (4) CMPLX,CONJ
      TYPE COMPLEX (4) C,F,A,R,D,CP
      TYPE COMPLEX (4) FI,SI,AA,BB,CC,CTMP,FB,FS,FF,FM
      REAL IO
      REAL MU
      DIMENSION ITH(17),FMIN(17),SI(17),FI(17),TH(17),CP(17)
      DIMENSION AA(17,2),BB(2,2),CC(17,2),B(17)
      PI=3.1415927
      RATOD=180./PI
  100 FORMAT(1H0,13X,4HF(I),31X,4HS(I))
  101 FORMAT(1H0,2(F14.7,2X,F14.7,5X))
  102 FORMAT(1H1,43X,20HTHETA(I), B(I), I=1,,I3,12H  THETAP, BP)
  103 FORMAT(1H0,45X,I4,5H DEG ,F7.3,5H MIN ,5X,E14.7)
  104 FORMAT(1H0,3HMU=,F14.7)
  105 FORMAT(1H0,28HD(I) MULTIPLIED BY EXP(I*MU))
  106 FORMAT(1H0,13X,4HC(I),26X,15HCALCULATED C(I))
      N1=N+1
      M1=N1
      CTMP=D(M1)/C(M1)
      THP=ATAN(CNORM(CTMP))
      TH(M1)=THP
      B(M1)=ATAN2PI(-CIMAG(C(1)),CREAL(C(1)))
      COSB=COS(B(M1))
      SINB=SIN(B(M1))
      FB=CMPLX(COSB,SINB)
      A=ATAN2PI(CIMAG(CTMP),CREAL(CTMP))
      MU=B(M1)-A
      FM=CMPLX(COS(MU),SIN(MU))
      PRINT 104, MU
      DO 5 I=1,M1
    5 D(I)=D(I)*FM
      PRINT 105
      CALL PRNTC(M1,D,2)
      T1=THP*RATOD
      ITH(M1)=T1
      FMIN(M1)=ABS((T1-ITH(M1))*60.)
      SINP=SIN(THP)
      COSP=COS(THP)
      DO 10 I=1,M1
      FI(I)=C(I)*SINP*FB-D(I)*COSP
   10 SI(I)=C(I)*COSP*FB+D(I)*SINP
      PRINT 100
      DO 20 I=1,M1
      P=CREAL(FI(I))
      Q=CIMAG(FI(I))
      X=CREAL(SI(I))
      Y=CIMAG(SI(I))
   20 PRINT 101, P,Q,X,Y
   21 M1=M1-1
      IF(M1.EQ.0)70,22
   22 CTMP=FI(M1)/SI(M1+1)
      THP=ATAN(CNORM(CTMP))
      B(M1)=ATAN2PI(-CIMAG(CTMP),-CREAL(CTMP))
      IF(ABS(B(M1)-PI).LT.1.E-05)23,24
```

```
 23 B(M1)=0.
    THP=-THP
 24 TH(M1)=THP
    FB=CMPLX(COS(B(M1)),SIN(B(M1)))
    T1=THP*RATOD
    ITH(M1)=T1
    FMIN(M1)=ABS((T1-ITH(M1))*60.)
    IF(M1.EQ.1)21,25
 25 TF=CNORM(FI(M1))
    TS=CNORM(SI(M1+1))
    TMP=SQRT(TF*TF+TS*TS)
    DO 30 I=1,M1
    AA(I,1)=FI(I)
 30 AA(I,2)=SI(I+1)
    BB(1,1)=SI(M1+1)
    BB(2,1)=-FI(M1)
    BB(1,2)=CMPLX(0.,0.)
    BB(2,2)=BB(1,2)
    CALL MATMP(AA,M1,2,BB,2,1,CC)
    FS=CMPLX(CREAL(SI(M1+1))/TS,-CIMAG(SI(M1+1))/TS)
    DO 40 I=1,M1
 40 FI(I)=FS*CC(I,1)/TMP
    CTMP=CONJ(BB(1,1))
    BB(1,1)=CONJ(-BB(2,1))
    BB(2,1)=CTMP
    FF=FB*CONJ(FS)
    CALL MATMP(AA,M1,2,BB,2,1,CC)
    DO 50 I=1,N1
 50 SI(I)=FF*CC(I,1)/TMP
    PRINT 100
    DO 60 I=1,M1
    P=CREAL(FI(I))
    Q=CIMAG(FI(I))
    X=CREAL(SI(I))
    Y=CIMAG(SI(I))
    IF(I.EQ.1.AND.M1.EQ.2)51,60
 51 PP=P
 60 PRINT 101, P,Q,X,Y
    GO TO 21
 70 PRINT 102, N
    DO 80 I=1,N1
 80 PRINT 103,ITH(I),FMIN(I),B(I)
    P=PP
    IF(P.GT.0..AND.TH(1).GT.0.)81,82
 81 IO=-IO
    GO TO 84
 82 IF(P.LT.0..AND.TH(1).LT.0.)83,84
 83 IO=-IO
 84 CALL CINVERS(N,IO,TH,B,CP)
    PRINT 106
    DO 90 I=1,N1
    P=CREAL(C(I))
    Q=CIMAG(C(I))
    X=CREAL(CP(I))
    Y=CIMAG(CP(I))
 90 PRINT 101, P,Q,X,Y
```

```
      RETURN
      END
```

```
      SUBROUTINE MATMP(A,NRA,NCA,B,NRB,NCB,C)
      TYPE COMPLEX (4) A,B,C,CMPLX
      DIMENSION A(17,2),B(2,2),C(17,2)
      DO 2 I=1,NRA
      DO 2 K=1,NCB
      C(I,K)=CMPLX(0.,0.)
      DO 1 J=1,NCA
    1 C(I,K)=C(I,K)+A(I,J)*B(J,K)
    2 CONTINUE
      RETURN
      END
```

```
      SUBROUTINE CINVERS(N,IO,TH,B,C)
      REAL IO
      TYPE COMPLEX (4) FM,AA,BB,C,D,FB,CMPLX
      DIMENSION FM(32,30),TH(17),B(17),AA(34,1),BB(34,1),C(17),D(17)
  100 FORMAT(1H1,13HCHECK PROGRAM)
  101 FORMAT(1H0,10HD(K), K=0,,I3)
  102 FORMAT(1H0,60X,13X,4HF(I),31X,4HS(I))
  103 FORMAT(1H0,60X,2(F14.7,2X,F14.7,5X))
      PRINT 100
      N1=N+1
C     FIRST CRYSTAL
      I=1
      IM1=0
      SINT=SIN(TH(I))
      COST=COS(TH(I))
      FB=CMPLX(COS(B(I)),-SIN(B(I)))
      BB(1,1)=-SINT*IO
      BB(2,1)=FB*COST*IO
      PRINT 102
      P=CREAL(BB(1,1))
      Q=CIMAG(BB(1,1))
      X=CREAL(BB(2,1))
      Y=CIMAG(BB(2,1))
      PRINT 103, P,Q,X,Y
C     SECOND CRYSTAL
      I=I+1
      IF(I.LE.N)501,70
  501 IM1=I-1
      SINT=SIN(TH(I))
      COST=COS(TH(I))
      FB=CMPLX(COS(B(I)),-SIN(B(I)))
      DO 10 J=1,4
      DO 10 K=1,2
   10 FM(J,K)=CMPLX(0.,0.)
      FM(1,1)=CMPLX(COST,0.)
      FM(2,2)=CMPLX(-SINT,0.)
      FM(3,1)=FB*SINT
      FM(4,2)=FB*COST
      CALL MATMP1(FM,4,2,BB,2,1,AA)
      DO 20 J=1,4
   20 BB(J,1)=AA(J,1)
      PRINT 102
      DO 21 J=1,2
      J1=J+2
      P=CREAL(BB(J,1))
      Q=CIMAG(BB(J,1))
      X=CREAL(BB(J1,1))
      Y=CIMAG(BB(J1,1))
   21 PRINT 103, P,Q,X,Y
      I=I+1
      IF(I.LE.N)30,70
C     ITH CRYSTAL
   30 IP1=I+1
      IM1=I-1
      SINT=SIN(TH(I))
      COST=COS(TH(I))
```

```
      FB=CMPLX(COS(B(I)),-SIN(B(I)))
      I2=2*I
      I3=I2-2
      DO 40 J=1,I2
      DO 40 K=1,I3
   40 FM(J,K)=CMPLX(0.,0.)
      DO 50 J=1,IM1
      FM(J,J)=CMPLX(COST,0.)
      J1=J+1
      J2=IM1+J
      FM(J1,J2)=CMPLX(-SINT,0.)
      J1=I+J
      FM(J1,J)=FB*SINT
      J1=IP1+J
      J2=IM1+J
   50 FM(J1,J2)=FB*COST
      CALL MATMP1(FM,I2,I3,BB,I3,1,AA)
      DO 60 K=1,I2
   60 BB(K,1)=AA(K,1)
      PRINT 102
      DO 61 J=1,I
      J1=J+I
      P=CREAL(BB(J,1))
      Q=CIMAG(BB(J,1))
      X=CREAL(BB(J1,1))
      Y=CIMAG(BB(J1,1))
   61 PRINT 103, P,Q,X,Y
      I=I+1
      IF(I.LE.N)30,70
C     POLARIZER
   70 SINT=SIN(TH(N1))
      COST=COS(TH(N1))
      FB=CMPLX(COS(B(N1)),-SIN(B(N1)))
      N2=2*N+1
      DO 80 K=1,N
      NK=N2-K
   80 BB(NK+2,1)=BB(NK,1)
      BB(N1,1)=CMPLX(0.,0.)
      BB(N+2,1)=CMPLX(0.,0.)
      DO 90 K=1,N1
      NK=N1+K
      C(K)=FB*SINT*BB(K,1)+FB*COST*BB(NK,1)
   90 D(K)=-COST*BB(K,1)+SINT*BB(NK,1)
      PRINT 101, N
      CALL PRNTC(N1,D,2)
      RETURN
      END
```